FUNCTIONALIZATION OF HETEROCYCLES: A METAL CATALYZED APPROACH VIA ALLYLATION AND C-H ACTIVATION

A Dissertation
Submitted to the Graduate Faculty
of the
North Dakota State University
of Agriculture and Applied Science

By

Sandeepreddy Vemula

In Partial Fulfillment of the Requirements
for the Degree of
DOCTOR OF PHILOSOPHY

Major Department:
Chemistry and Biochemistry

October 2018

Fargo, North Dakota

North Dakota State University
Graduate School

Title

FUNCTIONALIZATION OF HETEROCYCLES: A METAL CATALYZED APPROACH VIA ALLYLATION AND C-H ACTIVATION

By

Sandeepreddy Vemula

The Supervisory Committee certifies that this ***disquisition*** complies with North Dakota State University's regulations and meets the accepted standards for the degree of

DOCTOR OF PHILOSOPHY

SUPERVISORY COMMITTEE:

Prof. Gregory R. Cook
Chair

Prof. Mukund P. Sibi

Prof. Pinjing Zhao

Prof. Dean Webster

Approved:

November 16, 2018
Date

Prof. Gregory R. Cook
Department Chair

ABSTRACT

The central core of many biologically active natural products and pharmaceuticals contain *N*-heterocycles, the installation of simple/complex functional groups using C-H/N-H functionalization methodologies has the potential to dramatically increase the efficiency of synthesis with respect to resources, time and overall steps to key intermediate/products. Transition metal-catalyzed functionalization of *N*-heterocycles proved as a powerful tool for the construction of C-C and C-heteroatom bonds. The work in this dissertation describes the development of palladium catalyzed allylation, and the transition metal catalyzed C-H activation for selective functionalization of electron deficient *N*-heterocycles.

Chapter 1 A thorough study highlighting the important developments made in transition metal catalyzed approaches for C-C and C-X bond forming reactions is discussed with a focus on allylation, directed indole C-2 substitution and vinylic C-H activation.

Chapter 2 describes the development of a selective Tsuji-Trost allylation reaction of electron deficient heterocycles. The key issues addressed in this chapter include an extensive investigation of mechanistic details, and factors influencing selectivity control of tautomerizable heteroarenes to form linear *N*-allylated products.

Chapter 3 describes the oxidative allylic C-H amidation reaction of *N*-heterocycles, an efficient and atom economic variant of traditional allylation. A simple protocol avoiding the use of expensive catalysts/ ligands or additives for allylation of *N*-heterocycles is demonstrated. Mechanistic investigation indicated the importance of Pd(II)/DMSO catalytic system for the allylic C-H activation, allowing for the efficient synthesis of π-allylpalladium chloride catalysts.

Chapter 4 describes a detailed investigation on the development of an unusual π-bond directed indole C-2 amidation. A mechanism-based reaction optimization, and comparison of

effectiveness of both Pd and Ni catalyst system indicated the effectiveness of $NiCl_2$ for the π-bond directed indole C-2 substitution. Mechanistic studies also shed light on the dual role of solvent system (DCE: DMSO), acting both as ligand (DMSO) and as an oxidant (DCE) for the regeneration of active Ni(II) catalyst.

Chapter 5 describes the development of a ruthenium catalyst system for the synthesis of fused quinazolinones *via* vinylic C-H/amide N-H bond activation/alkyne annulation. This chapter also describes the utilization of quinazoline core as a masked pyridine template for the synthesis highly substituted pyridines via amide alcoholysis.

ACKNOWLEDGEMENTS

I would like to first thank Professor Gregory R. Cook for accepting me into your research group. Nothing of this would have been possible without your support and guidance throughout my stay in NDSU. You provided a work conditions composed of the right mix of freedom and flexibility, and the need for results and progress. I thank you for your patience and for encouraging me to remain in my doctoral studies through difficult times. I could not have asked for a better experience in graduate school, and I want you to know that I will forever appreciate all the time and effort you invested for me to reach this point. Thanks again!

I would also like to thank Prof. Mukund P. Sibi, Prof. Pinjing Zhao and Prof. Dean Webster for being in my committee and helping in many ways to direct my research in the right path. A special thanks to Prof. Sibi for being there for me, whenever I needed any help. I have learned a lot from you and it was always a pleasure discussing with you in combined group meetings. Your passion for science and genuine interest in my progress inspired me to give the best in graduate school.

I cannot proceed further without thanking Dr. Dinesh Kumar. You truly are the leader, who kept me motivated, and pushed my limits introducing to various aspects of chemistry. Much of what has been accomplished could not have been without your help and guidance. You are a great friend, mentor, and coworker. I will surely miss both personal and scientific discussions with you.

I would like to thank all the supporting staff in the Department of Chemistry and Biochemistry for their help and support. A special thanks to Dr. Angel Ugrinov for his patience and help in solving X-ray crystal structures and helping with GCMS and HRMS. I would also like to thank Dr. John Bagu and Daniel Wanner for training me and helping me with NMR studies. I

am grateful to Wendy Leach, Linda Stoetzer, Dionna Martel, Amy Kain, Tina Exner, and Cole Larsen for their continuous help and for taking care of all my administrative requirements.

I would also like to acknowledge NSF-ND EPSCoR for providing me with doctoral dissertation assistantship, and college of science, NDSU for providing multiple travel grants for attending conferences.

I also like to thank past and present members of the Cook group. A special thanks to Michael Chhoun for being the best coworker in the lab and training me in lifting weights. I wish you nothing but success as you continue your career. I also extend my thanks to past and present members of Sibi group, Zhao group and Siva group for all their help, be it letting me borrow chemicals or answering all my questions, and for creating a healthy, competitive work environment.

Life in graduate school would have been stressful without the support from my friends. A special thanks to Chandu, Eric, Rajith, Nandini, Naveen, Dayananda, and Sunil for all the professional and personal support.

Most importantly, I'd like to thank my family and close friends for your unconditional love and support. My parents, sister and brother in law have always believed in me and encouraged in each and every step of my life. A special thanks to my wife (Anusha), you are my greatest gift, and meeting you was the best thing happened in my life. There's nothing comparable to the love and devotion that you guys have given me.

DEDICATION

To my parents

without whose love and support this would never have been possible

TABLE OF CONTENTS

LIST OF TABLES

LIST OF FIGURES

LIST OF SCHEMES

LIST OF ABBREVIATIONS

Å.....Angstrom

Ac.....Acetyl

Acac .....Acetylacetanato

Ar .....Aryl

Bn.....Benzyl

BINAP.....2-2’-Bis(diphenylphosphino)-1,1’-binaphthyl

n-Bu.....*normal*-Butyl

t-Bu .....*tertiary*-Butyl

Bz .....Benzoyl

Calcd .....Calculated

cod.....1,5-cyclooctadiene

coe .....cyclooctene

CO .....Carbon monoxide

Cp.....cyclopentadienyl

Cp* .....pentamethylcyclopentadienyl

Dba.....dibenzylideneacetone

DBU .....Diazabicyclo[5.4.0]undec-7-ene

DG.....Directing group

DMA .....N,N-dimethylacetamide

DMSO .....Dimethyl sulfoxide

DPPP .....1,3-bis(diphenylphosphino)propane

dr .....Diasteromeric ratio

EDG .....electron donating group

ee .....Enantiomeric excess

Equiv .....Equivalent

Et .....Ethyl

EtOAc .....ethyl acetate

Et_2O.....diethylether

EWG .....Electron-withdrawing group

GC .....Gas chromatography

GC/MS .....Gas chromatography/mass spectrometry

HRMS .....High resolution mass spectrometry

h.....Hours

HCl .....Hydrochloric acid

Hz .....Hertz

IMes .....1,3-bis(2,4,6-trimethylphenyl)imidazole-2-ylidene

IPr.....1,3-bis(2,6-triisopropylphenyl)imidazole-2-ylidene

J.....Coupling constants (in NMR)

L .....Ligand

m.....*meta*

M .....Metal

Me .....Methyl

MeO .....Methoxy

MeOH .....Methanol

mL .....millilitre

mol .....Moles

Mol.Wt .....Molecular weight

NHC .....N-heterocyclic carbene

NMR .....Nuclear magnetic resonance

NMP .....*N*-Methylpyrrolidine

Nu.....Nucleophile

o.....*ortho*

OTf.....Triflate

p.....*para*

Ph .....Phenyl

PivOH .....pivalic acid

ppm .....Parts per million

rt .....Room temperature

Temp .....Temperature

t-BuOK.....Potassium *tert*-butoxide

THF .....Tetrahydrofuran

TLC .....Thin layer chromatography

UV.....Ultraviolet

CHAPTER 1. TRANSITION METAL CATALYZED FUNCTIONALIZATION OF TAUTOMERIZABLE *N*-HETEROCYCLES

1.1. Introduction

Heterocycles make-up over half of all known organic compounds.[1] Quinazoline-4(3*H*)-ones represent a unique class of heterocycles that has attracted considerable attention due to their wide occurrence in natural products and biologically active compounds (Figure 1).[2–5] They exhibit a wide range of biological and pharmacological activities including but not limited to antibacterial,[6] antimalarial,[7] antidiabetic,[8,9] antiallergic,[2] and antifungal[10] properties. The selective functionalization of these heteroarenes can potentially generate lead molecules for the early drug development.

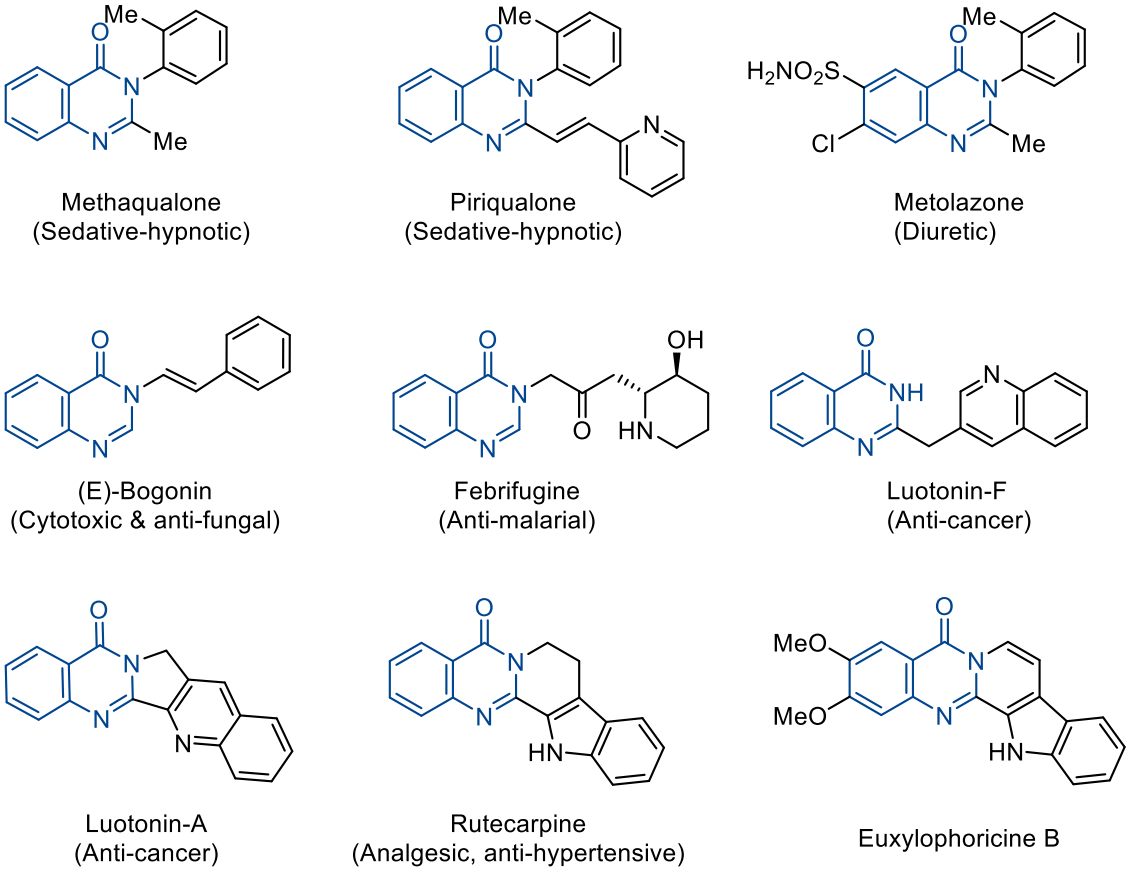

Figure 1.1: Selected biologically active quinazolinones

Given this reality, it is of no surprise that there is an immense interest among synthetic chemists and significant efforts have been put forth in the development of new and efficient reaction methodologies towards their structural elaboration.[11–16] The development of new methodology in synthetic organic chemistry has the potential to address many crucial challenges involved in terms of reactivity and selectivity. In general, functionalization or synthetic modifications can be categorized mainly in to three classes (Scheme 1.1).

1. Classical approaches of functional group interconversion
2. Cross-coupling reaction
3. C-H bond functionalization

Since the inception of organic chemistry, classical approaches to functionalize organic compounds consisted of transforming pre-existing functional groups into the desired chemical functions. These approaches tend to solve many regio- and/or chemoselectivity issues by using the impressive catalogue of organic reactions and a well-designed synthetic route. However, several transformations are generally needed for the synthesis of pre-functionalized starting materials. This has prompted researchers to investigate more atom and step economical alternatives such as transition metal catalyzed cross-coupling reactions and further advancement with C-H activation reactions (Scheme 1.1).[17–19]

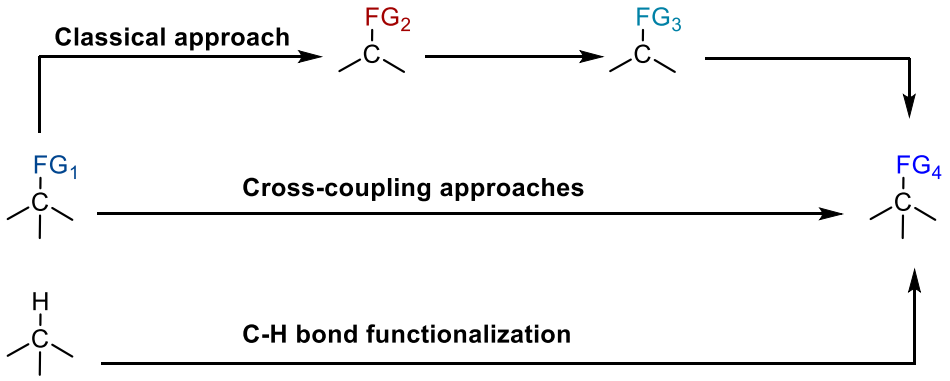

Scheme 1.1: Overview of different approaches to functionalize organic compounds

Since, the prime focus of this thesis is built upon the functionalization of *N*-heterocycles using transition metal catalysts, we will focus our discussion on transition metal catalysts and their utilization in cross-coupling reactions. Although there has been a vast literature to selectively functionalize these heterocycles, for conceptual simplicity and in line with the context of work done, only four different approaches (*vide infra*) with which *N*-heterocycle functionalization have been achieved will be discussed.

1. Palladium catalyzed allylic substitution/amination by leaving group approach
2. Palladium catalyzed allylic substitution/amination by C-H oxidation
3. Transition metal catalyzed indole C-2 amidation
4. Ruthenium catalyzed directed C-H activation/annulation

1.2. Transition metal catalysis for functionalization

Over the past few decades, transition metal catalysis has witnessed a rapid and comprehensive development. Especially in 1972, an important discovery in the area of cross-coupling was reported, using organic halides and Grignard reagents, for generating C-C bonds by using nickel or palladium-based catalysts, which is named Tamao-Kumada-Corriu coupling reaction.[20,21] Subsequently, a myriad development of this powerful synthetic transformation such as Sonagashira coupling,[22] Negishi coupling,[23] Stille coupling,[24] Suzuki-Miyaura coupling,[25] Tsuji-Trost allylation[26,27] has been witnessed during the last decades. Indeed, use of transition metal complexes allowed new disconnections for synthetic chemists to access molecular complexity in a rapid, convenient and selective manner. Notably, palladium-catalyzed cross-coupling emerged as a powerful tool for carbon-carbon or carbon-heteroatom bond formation. Due to their significant contribution on homogenous metal catalyzed cross coupling reactions in organic synthesis, Richard F. Heck, Ei-ichi Negishi and Akira Suzuki were awarded the 2010

Nobel Prize.[28] Although the foundation of these cross-coupling reactions was laid in 1960's, constant evolving of scope, selectivity and predictability of the products have made them the most widely used reactions both in academia and industry. A simplified mechanism for Pd-catalyzed cross-coupling reactions are shown in Scheme 1.2. Traditionally, cross-coupling reactions require preoxidized coupling partners, undergoing oxidative addition in the first step of the catalytic cycle forming a Pd(II) intermediate.[17]

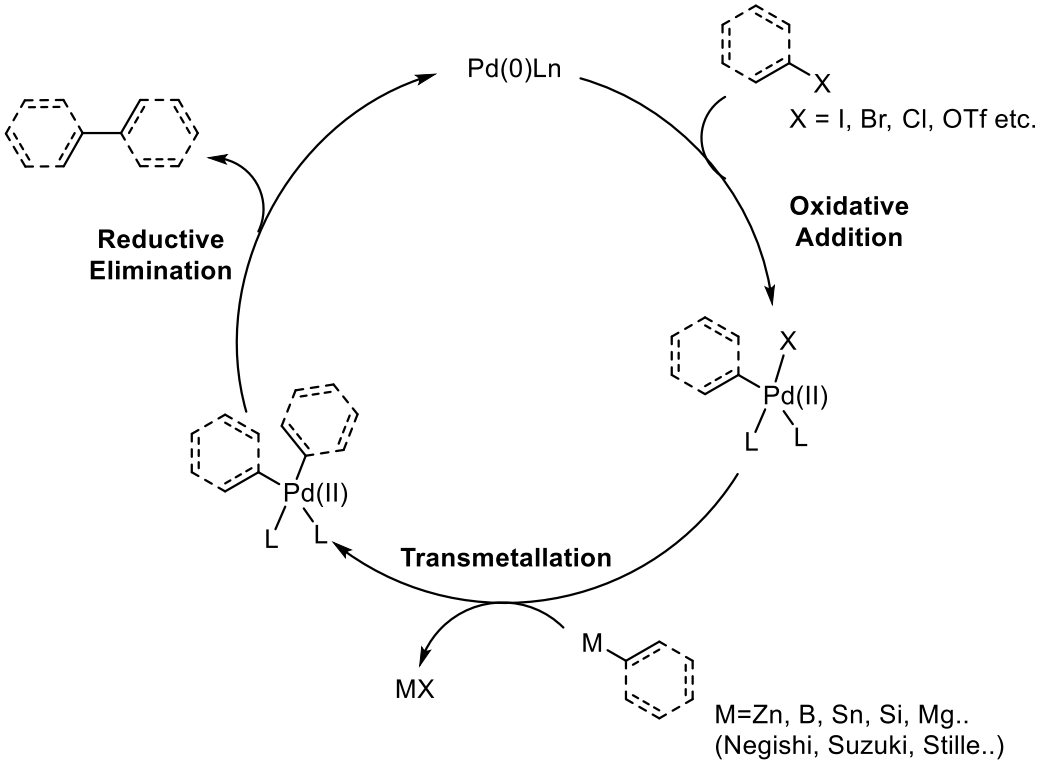

Scheme 1.2: General catalytic cycle for Pd-catalyzed cross-coupling reactions

The first step, oxidative addition is the case for most of the transition metal catalyzed C-C or C-X cross coupling reactions. Although mechanistically different from traditional cross coupling reactions, Tsuji-Trost reaction or palladium catalyzed allylation, is also one of this type of reactions which utilizes oxidized substrates for the formation of C-C and C-X bonds with even introduction of chirality.[29] This palladium catalyzed cross coupling of allyl electrophiles (most commonly allyl acetates, halides, and carbonates) with nucleophiles (β-dicarbonyls, enamines, and

enolates) has been widely utilized in the literature for various selective functionalizations (Scheme 1.3).

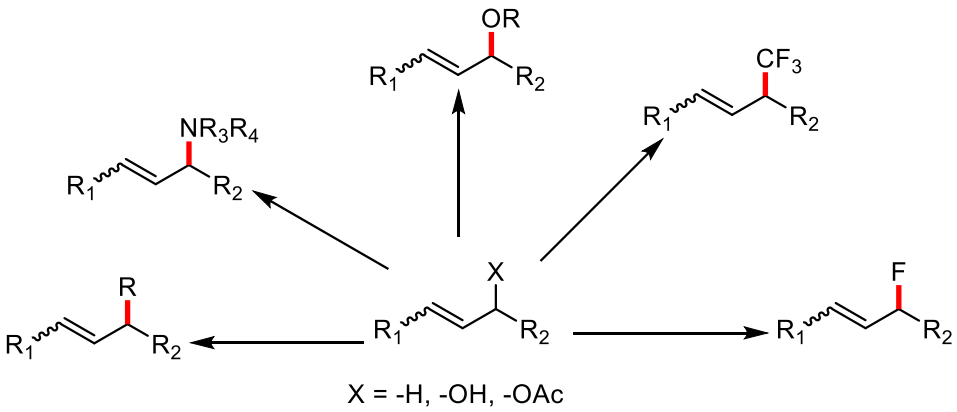

Scheme 1.3: Convergent transformations from allylic substitution

1.3. Tsuji-Trost allylation/ palladium catalyzed allylic substitution

1.3.1. Early discovery/ C-C bond formation

Wacker process to produce acetaldehyde by the oxidation of ethylene using $PdCl_2$ and $CuCl_2$ in aqueous HCl is the first example of palladium catalyzed reaction under homogenous conditions.[30] Tsuji's understanding and extension of the Wacker process led to the discovery of one of the widely used palladium catalyzed C-C and C-X bond forming reaction.[31] The reaction mechanism for the Wacker process can be explained in two steps, first step being the formation of oxypalladium intermediate **1.01** via a nucleophilic attack of H_2O on ethylene complexed with palladium. And, the second step follows by elimination of Pd(0) and a hydride shift forming carbon-oxygen bond to give acetaldehyde (Scheme 1.4). Tsuji envisioned that since, the reaction occurs by nucleophilic attack on ethylene complexed with palladium, any suitable nucleophile can potentially attack on this palladium intermediate to generate new C-C and C-X bonds.[31]

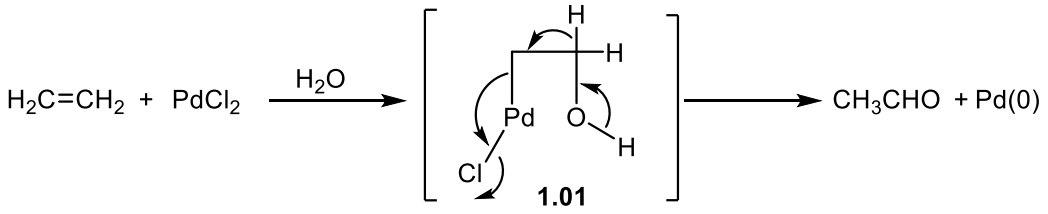

Scheme 1.4: Mechanism of acetaldehyde formation by Wacker process

In fact, his hypothesis was found successful when soft nucleophiles such as malonate or acetoacetate were employed under similar conditions to form C-C bonds. By increasing the olefinic chain length by one carbon from ethylene to allyl group Tsuji and coworkers were able to isolate a stable π-allylchloride complex (**1.02)**. This stochiometric complex was then coupled with sodium salt of diethyl malonate (**1.03**) to form carbon-carbon bond with precipitation of black Pd metal representing the first example of Tsuji-Trost allylation reaction. For the initial few years, the reaction remained stochiometric in palladium whereupon catalytic version was discovered and extensively employed by Tsuji, Trost and many others (Scheme 1.4).[32] The key to the development of catalytic conditions was the utilization of oxidized allyl reagents with a leaving group as the reacting partner rather than olefin.[33]

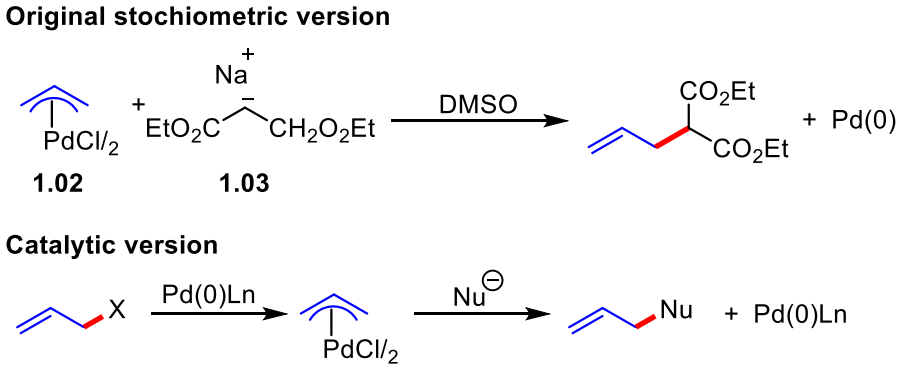

Scheme 1.4: Development of the Tsuji-Trost allylation

Since the development of catalytic conditions, it is one of the highly utilized and useful reaction in organic synthesis, as it not only forms a C-C and/or C-X bond but also leaves a pendent

olefin functionality. The olefin (C=C) functional group is an extremely versatile functional group capable of undergoing a multitude of synthetic transformations. Scheme 1.5 depicts some of the important transformations, which can be achieved by simple modification to the olefinic functionality. This diverse reactivity makes their incorporation in a given synthetic intermediate desirable. Furthermore, olefins are often considered as "latent" functional groups as their reactivity requires specific conditions or catalysts for activation, which are highly beneficial when performing multi-step synthesis.[32]

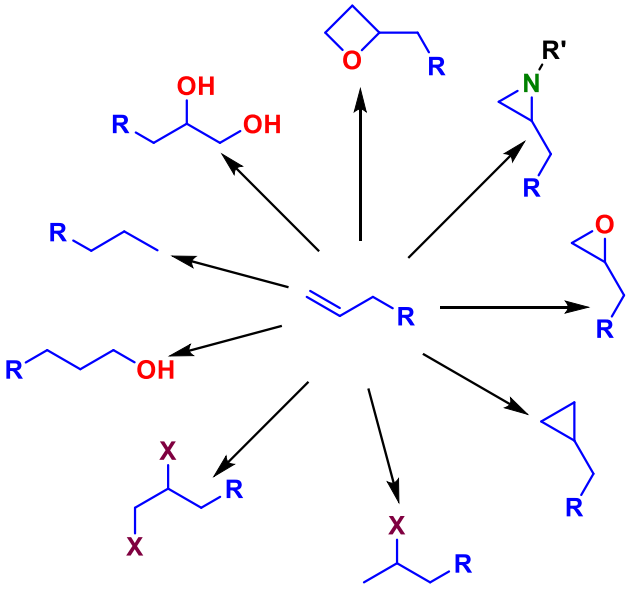

Scheme 1.5: Inherent use of pendent olefin of the allyl functionality

1.3.2. Mechanistic understanding of allylic alkylation

1.3.2.1. Catalytic cycle

The allylic alkylation reaction has been the object of numerous investigations, from the scope to the mechanism of the catalytic cycle. The generally accepted mechanism of palladium-catalyzed allylic substitution is shown in Scheme 1.6. An allylic substrate initially binds to a Pd(0) active catalyst forming a η^2 -complex, followed by an oxidative addition leading to an intermediate (η^3 -allyl)Pd(II) complex with the leaving group as counterion. Structurally, the π-allyl palladium

intermediate is a square planar 16-electron complex consisting of ligands and a coordinated allyl unit. Different possible configurations of the allyl ligand are possible when the allyl moiety is substituted: the *syn,syn* and *syn,anti* and *anti,anti* (based on the substituent at C2 position). The π-allyl intermediate resulting from an *E*-olefin electrophile typically prefers the *syn,syn* configuration, whereas in a cyclic system, the π-allyl is locked in the *anti,anti* configuration. Nucleophile then attacks at C1 or C3 of allyl termini generating an unstable Pd(0)-olefin complex which readily releases the final product regenerating Pd(0) for another catalytic cycle. [27,34]

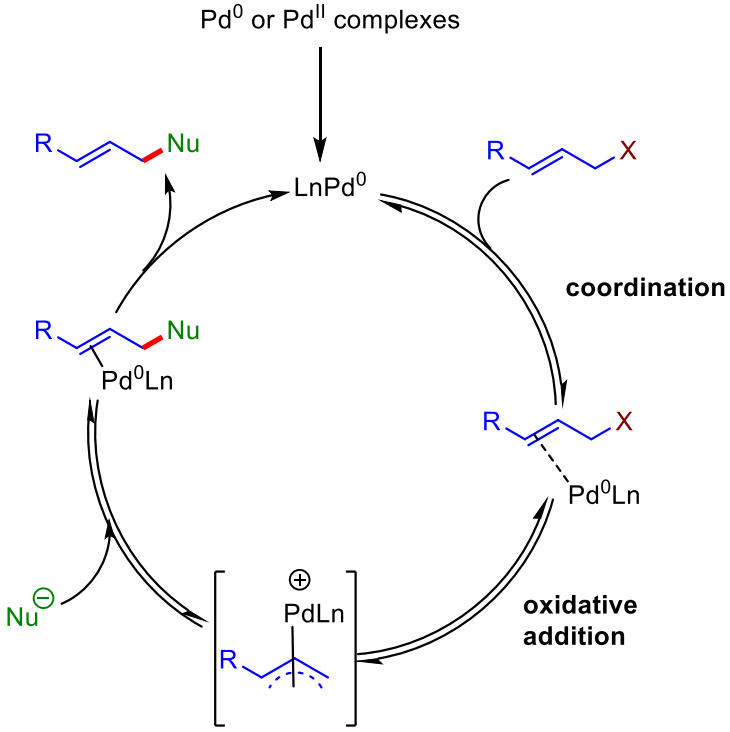

Scheme 1.6: Catalytic cycle in Palladium catalyzed allylic alkylation

The oxidative addition of allyl electrophiles to Pd proceed with inversion, involving π-complexation with palladium followed by intramolecular nucleophilic displacement of a leaving group. It is now well understood that after π-complexation Tsuji-Trost reaction proceed *via* two mechanistic pathways depending on the mode of attack of nucleophile on π-allylpalladium intermediate. Soft or stabilized nucleophiles attack directly on the olefinic carbon of π-

allylpalladium intermediate, where as hard or unstabilized nucleophiles coordinate to palladium center followed by transfer to the allylic carbon.[35]

1.3.2.2. Regioselectivity in Tsuji-Trost allylation

When the transiently formed π-allyl Pd-complex is unsymmetrically substituted the issue of site-selectivity comes into play. In the case of unsymmetrical substrates such as **1.04** or **1.05**, the intermediate (η^3 -allyl)palladium(II) complex formed after ionization can be attacked by nucleophiles at both termini of the allylic system, posing the problem of regioselectivity. It is generally accepted that in Pd-catalyzed allylic alkylation, the regioselectivity is influenced by opposing steric and electronic effects. Steric factors will direct the nucleophilic attack to the less hindered allylic terminus to minimize steric interactions with the nucleophile, yielding a linear product, rather than the branched isomer (Scheme 1.7). By contrast, electronic factors tend to favor the attack at the more electropositive carbon, usually the more substituted terminus.[29,36]

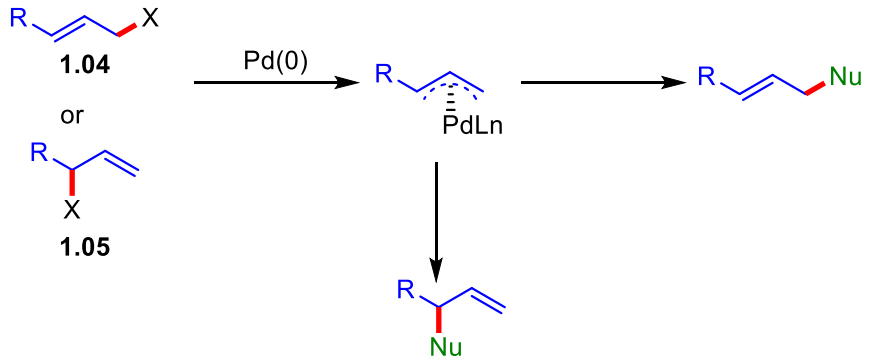

Scheme 1.7: Regiochemical outcome in Tsuji-Trost reaction

In general, it is difficult to rationalize the regiochemical outcome of nucleophilic attack on allyl complexes since steric effects are often superimposed with electronic effects. There are several other factors also that influence the regioselectivity of the reaction such as steric and electronic effects of the nucleophiles, nature of the metal, the ligands, solvent, the nature of the leaving group, and the presence of additives. Moreover, regioselectivity is also known to be

sensitive to the regiochemical memory of the position of the leaving group, the preferred configuration and to dynamic exchange in the (η^3 - allyl)Pd intermediate.[35]

1.3.3. Allyl alcohols in the Tsuji-Trost reaction

The leaving group ability of various allylic compounds has also been extensively studied, and a general reactivity scale was established. Typically, halogens found to be best leaving groups, followed by carbonates, acetates, and finally alcohols. The utilization of allylic alcohols directly as allylating partner in the Tsuji–Trost type coupling manifolds would be beneficial, because they are readily available, are not as toxic as their halogenated counterparts and are often trivial to synthesize. Furthermore, the formation of a new C–C bond via the condensation of an alcohol with a C–H bond is topologically obvious. Additionally, the generation of water as the only byproduct renders this reaction step and atom economic (Scheme 1.8).

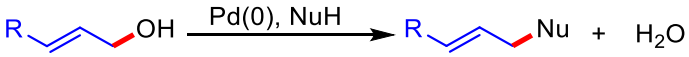

Scheme 1.8: Allylic alcohols in Tsuji-Trost reaction

Because of the strong C-O bond, and ability of hydroxide as a poor leaving group the oxidative addition of allyl alcohols to palladium catalyst is difficult. As a result, a variety of strategies have been employed to activate allyl alcohols towards cross-coupling reaction. Most common methods to activate alcohols include but not limited to the use of Lewis acids[37–39] or Bronsted acids[40–42] and bases as activators or *in situ* generation of carbonates via use of CO_2 as a reversible activator. Although, these activators have been widely used in the literature, they still suffer with issues like use of stoichiometric amounts in case of Lewis acids, the scope of reaction is limited to weakly basic nucleophiles in case of Bronsted acids and bases and use of specialized reaction conditions for using CO_2 as an activator. To avoid the use of these specialized reaction conditions we have developed a simple and efficient palladium catalyzed allylation of *N*-

heterocycles using allyl alcohol in renewable dimethyl carbonate as the solvent. Chapter 2 provides a detailed discussion on our approach for the development of this green protocol and a conclusive mechanistic detail for the selective *N*-allylation of tautomerizable heterocycles.

1.4. Palladium catalyzed allylic C-H activation

Allylic C-H alkylation reaction, an exemplary of the activating group category of C-H activation has been known for more than 50 years; it was initially developed as a two-step process, stoichiometric in palladium, by Tsuji and Trost in the 1960s (Scheme 1.9). They reported an initial C-H cleavage, effected by a palladium(II) salt generating π-allylpalladium intermediate.[43] The π-allylpalladium intermediate was then subsequently attacked by a nucleophile, forming an allylic C-C bond.[33]

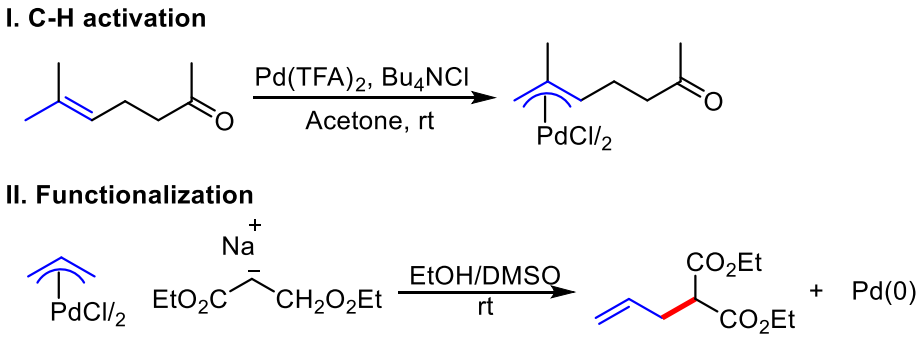

Scheme 1.9: Stochiometric allylic C-H alkylation

Despite a strong precedence in stoichiometric reactions, it was not until last decade, there was a considerable progress in the development of catalytic reactions. This is in part due to the ease of utilization of allyl substrates with different leaving groups, such as acetates, halides, carbonates, and phosphonates in allylic substitution reaction, which is famously called Tsuji-Trost reaction (Scheme 1.10).[27,33] The reaction is very well explored and tolerated a wide range of nucleophiles, such as *β*-carbonyls, enamines, and enolates etc. The success of this reaction is attributed to the fact that it generally displays a high level of chemo-, and regio- and

stereoselectivity.[44] However, despite the overwhelming success of the classical Tsuji-Trost reaction, the atom efficiency of the overall transformation is hampered by the necessity of a leaving group.[45]

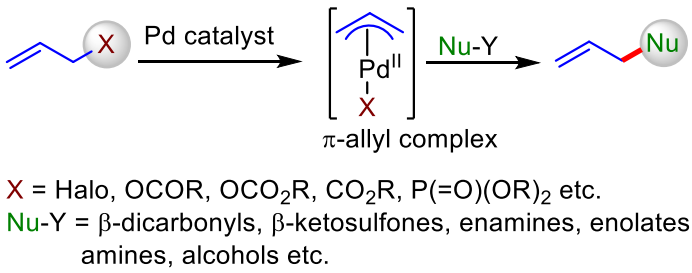

Scheme 1.10: Palladium catalyzed allylation or classical Tsuji-Trost allylation

To increase the atom efficiency, and to make use of the inherent reactivity of allylic C-H bonds there has been a considerable research over the past few decades to develop a catalytic version of the early palladium catalyzed allylation reactions. The fundamental difference between both the reactions is the nature of active catalyst, while the Pd catalyst is in zero (0) oxidation state is active catalyst in traditional allylation, Pd catalysts in +2 oxidation state is active catalyst in allylic C-H reactions. Re-oxidation of Pd(0) generated in the latter case to Pd(II) is essential for the development of catalytic reaction (Scheme 1.11).[31]

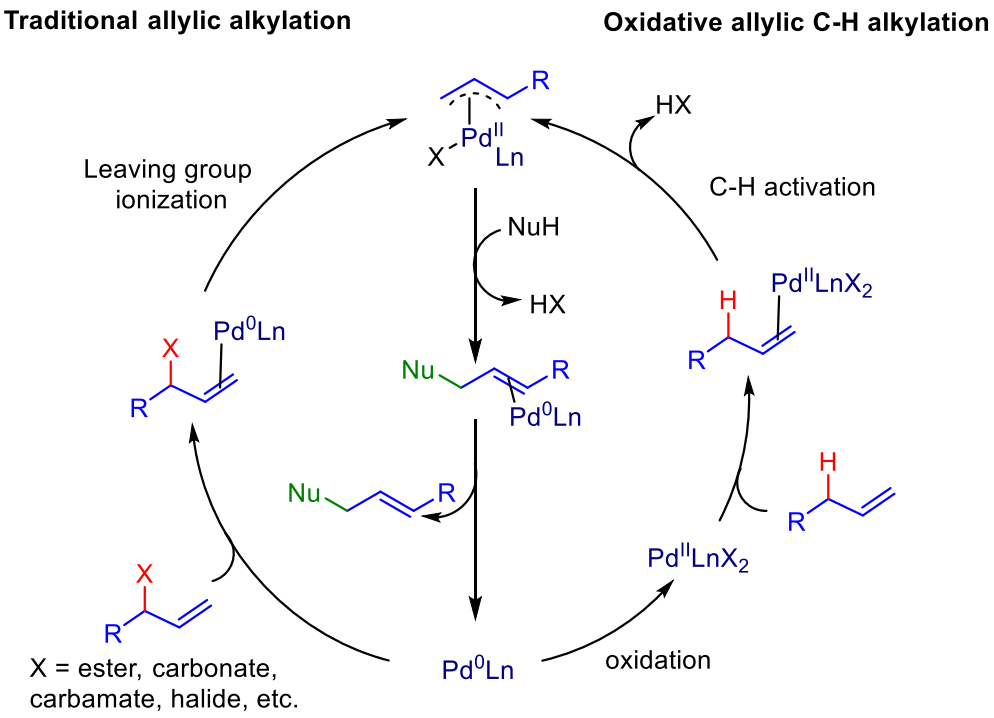

Scheme 1.11: Mechanistic differences between Tsuji-Trost allylation and allylic C-H activation

1.4.1. Allylic acetoxylation: development of catalytic allylic C-H activation reactions

After initial studies on the stochiometric palladium allylic oxidation reactions, Tsuji[46] and Mcmurray[47] independently revealed that using a stochiometric oxidant, the Pd(0) catalyst could be reoxidized to the active Pd(II) catalyst (Scheme 1.12) allowing the reaction proceed in catalytic palladium salts. Although a groundbreaking discovery, there has been not much follow up literature on the utilization of oxidants for catalytic allylic C-H oxidations.

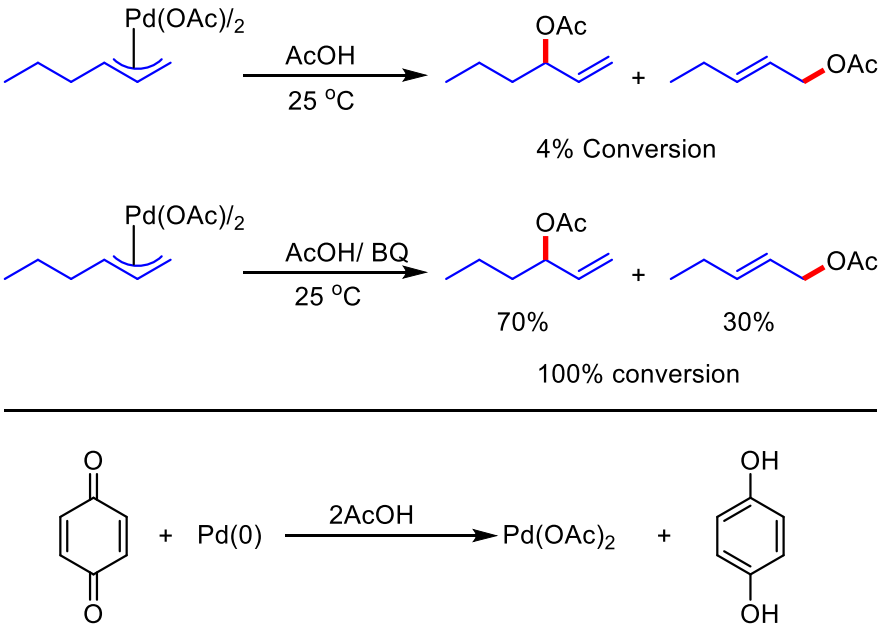

Scheme 1.12: Benzoquinone (BQ) role in regeneration of active Pd(II) catalyst

More recently, reports from White and coworkers led to a surge in development of catalytic systems for the selective allylic oxidation of terminal olefins. They reported a $Pd(OAc)_2$/BQ catalytic system for the selective formation of allylic acetates employing a DMSO-acetic acid solvent system.[48] In their initial studies they found the importance of sulfoxide ligation for the selective formation allylic products compared to Wacker products (Scheme 1.13). White group has also shown that depending on the ligation of sulfoxide ligands, mono *vs* bis ligation, regioselectivity of acetoxylation can be switched from linear to branched isomers respectively.

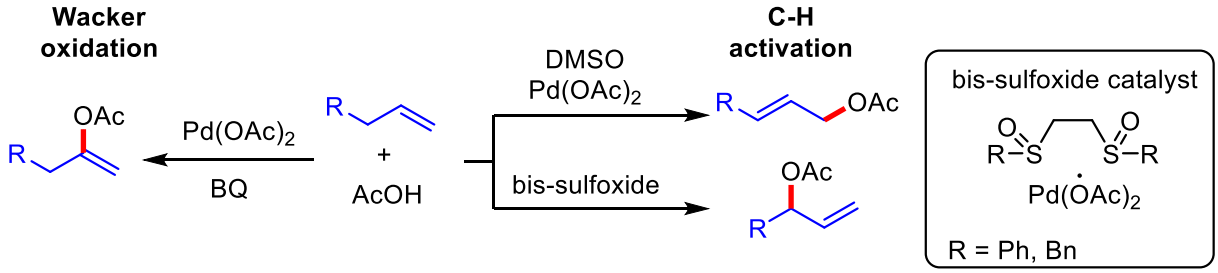

Scheme 1.13: Effect of sulfoxide ligands in Pd-catalyzed allylic oxidation

1.4.2. Palladium catalyzed allylic C-H oxidative C-C bond formation

Although there has been a tremendous development in allylic C-H acetoxylation[48–52] and esterification[53] reactions, not until recently allylic C-H alkylation reactions were developed. The fundamental challenge of combining three dissimilar steps-electrophilic C-H cleavage, nucleophilic functionalization, and oxidation regeneration of Pd(II)- in the reaction medium and identifying conditions where each of these steps does not interfere with each other's led to a gap in the literature for the development of catalytic allylic C-H alkylation reactions. In 2008, White and coworkers,[54] Shi and coworkers,[55] after extensive studies independently reported a similar sulfoxide ligated palladium catalyst for the first allylic C-H oxidative C-C bond forming reaction between olefins and carbon nucleophiles (Scheme 1.14). White and coworkers developed an intermolecular allylic C-H alkylation using stabilized carbon nucleophiles. During their investigation they found that addition of benzoquinone inhibits the reaction rather than regeneration of Pd(II). Careful control studies indicated that benzoquinone is incompatible with carbon nucleophiles, oxidizing them directly in a Michael reaction,[56] leading them to identify a more sterically hindered 2,6-dimethylbenzoquinone as an oxidant, which increased the overall research on allylic C-H oxidation reactions.[54] In a seminal work, Shi and coworkers reported both intra and intermolecular allylic C-H alkylation reactions using similar bissulfoxide catalyst. The success of their reaction was realized by the utilization of both BQ and O_2 gas balloon as the oxidants. Since then, there has been a great interest among the researchers for the development of allylic C-H alkylation reactions with various carbon centered nucleophiles.[57] More recently asymmetric allylic C-H alkylation has also been realized by Trost and co-workers by a specially designed ligand systems.[58–61] Since this thesis is focused on allylic C-H amination further excellent studies on allylic C-H alkylations will not be discussed. The discussion and the early development

of allylic C-H amination will be focused in chapter 3, followed by our approach and results in the development of selective *N*-allylation via an efficient Pd(II)-DMSO system.

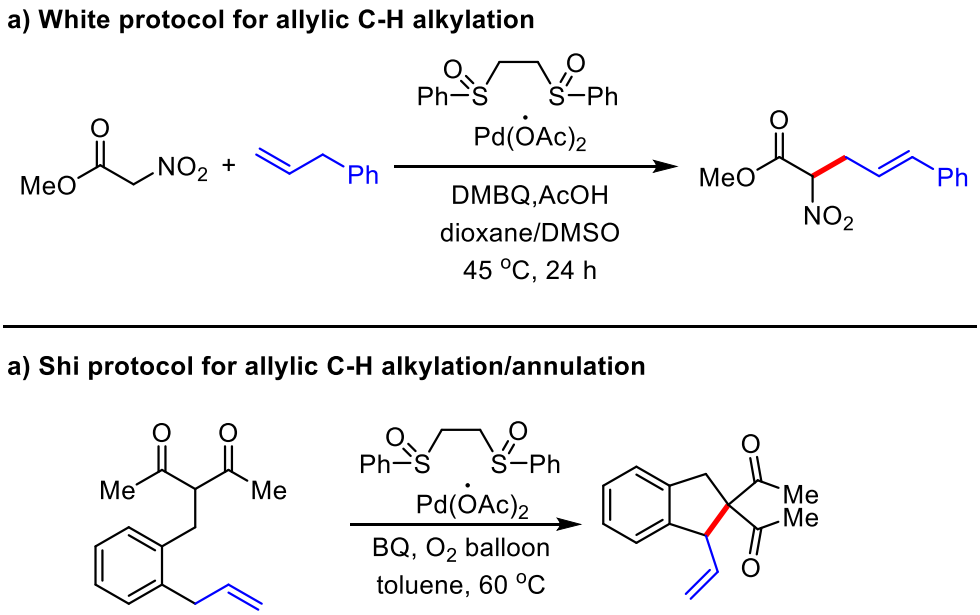

Scheme 1.14: Palladium catalyzed allylic C-H oxidative alkylation reaction

1.5. Directed indole C-2 functionalization

1.5.1. C-H activation for indole C-2 functionalization

The C-2 position of indole is the subject of numerous functionalizations, one of the reason being the site is most prone to metalation. Formation of C-C and C-X bonds have been studied extensively, and to date aryl, alkenyl, alkynyl, alkyl groups, cyanation and amine groups are successfully introduced at C-2 position.[62] For most of these reactions, directing groups on N-1 was critical to achieve high selectivity. A variety of auxiliaries such as acetyl derivatives, phosphonate, sulfonyl, pyridine, and pyrimidine have been employed as directing groups, where the 2-pyrimidine group has emerged as one of the most versatile and robust auxiliary for the selective C-2 carbon-carbon bond formation (Scheme 1.15).

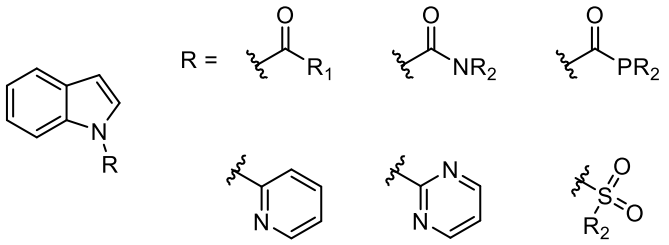

Scheme 1.15: Directing groups employed for Indole C-2 functionalization

1.5.2. Transition metal catalyzed directed dehydrogentative cross-coupling for C-C bond formation at indole C-2 position

1.5.2.1. Directing group on N-1 of indole

Carbon-carbon bond forming reactions constitute a major part in organic synthesis and is perhaps the most important transformation in organic chemistry. Many traditional approaches for the synthesis of C-2 substituted indoles involved cross-coupling of preoxidized indole substrate, which often require multistep synthesis. On the other hand, last few decades have seen utilization of various transition metals for the effective functionalization of indole cross-coupling reactions involving C-H bond activation. One of the earliest report by Fagnou and coworkers highlighted the importance of pivaloyl directing group in dehydrogentative cross-coupling for the C-2 arylation of indole (Scheme 1.16) albeit utilizing 60 equiv of benzene as the reacting partner.[63]

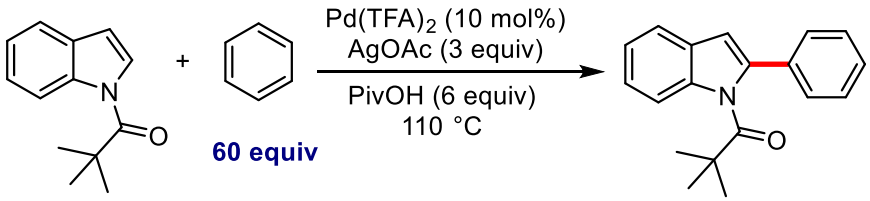

Scheme 1.16: Directing group strategy for indole C-2 arylation

Since then, there has been a tremendous progress on the dehydrogenative cross-coupling of indole with arenes, aryl halides and pseudo halides for selective C-2 and C-3 functionalization. In 2012, a seminal report from Miura *et al* [64] and You *et al* [65] reported the first dehydrogenative cross-coupling of indole with 1,3-azoles and pyridine *N*-oxide respectively with good yields albeit

at higher temperature (Scheme 1.17). Both methods have utilized pyrimidine substitution on indole as the directing group for selective C-2 arylation reactions.

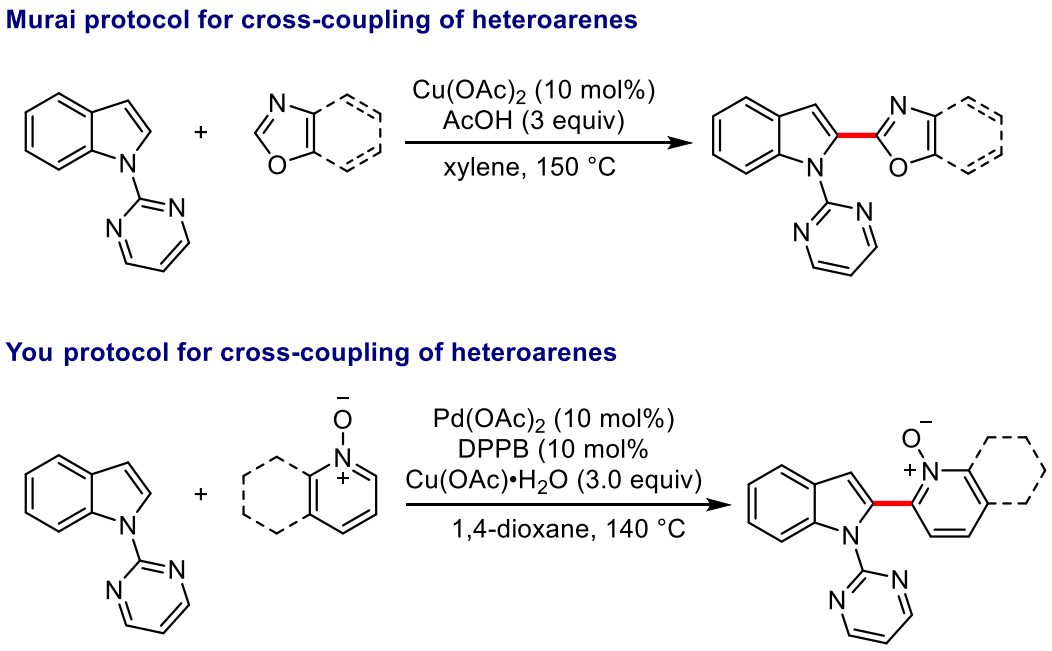

Scheme 1.17: Directed C(heteroatom)-C(heteroatom) bond formation

With the success of directed cross dehydrogenative couplings of indoles with arene compounds, similar strategy was also employed for alkenylation and alkylation reactions. Both alkynes and alkenes were used as coupling partners for the synthesis of 2-alkenylated and 2-alkylated indoles. Carretero and coworkers reported the use of 2-pyridylsulfonyl auxiliary for the C-2 alkenylation at indole C-2 with an olefin coupling partner to yield corresponding 2-alkenylindoles with a high functional group tolerance in excellent yields (Scheme 1.18).[66]

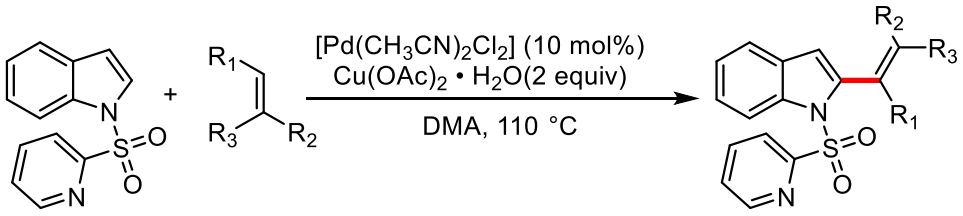

Scheme 1.18: Directing group strategy for indole C-2 alkenylation

Sha and co-workers developed an alternative rhodium catalyzed approach, utilizing a non-*N*-heterocyclic directing group, namely *o*-hydroxy and *o*-amino aryls for oxidative alkenylation employing α, β-unsaturated carbonyl compounds (Scheme 1.19).[67]

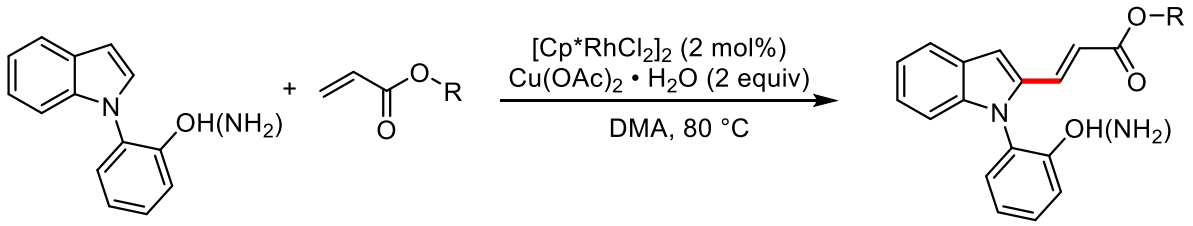

Scheme 1.19: *o*-Hydroxy- or *o*-aminoaryl-directed alkenylation.

Interestingly, when the carbonyl directing groups (acetyl or benzoyl) were employed along with Ir catalysts, α, β-unsaturated carbonyl compounds were successfully coupled with indole to form linear or branched alkyl indoles respectively (Scheme 1.20).[68]

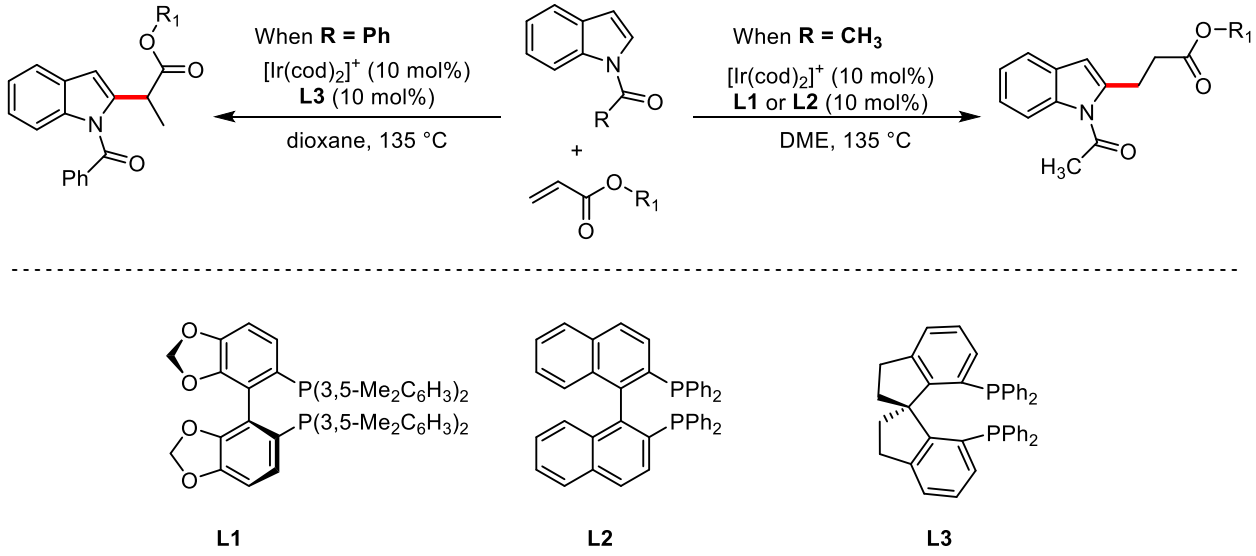

Scheme 1.20: Ir-catalyzed synthesis of 2-alkyl indoles

1.5.2.2. Directing group on C-3 of indole

Inspired by the ability of carboxyl and amine groups of tryptophan to direct C-2 functionalization of indoles with preoxidized substrates, Yoshikai and coworkers utilized an imine functionality (PMP = *p*-methoxyphenyl) on the C-3 position of indole to mediate C-H activation

at C-2 position. Subsequent alkylation or alkenylation was carried out in the presence of an iron-NHC catalyst. Depending on the identity of the coupling partner involved, two distinct products were formed. If alkynes were used, 2-alkenyl-3-formyl indoles were formed after acidic workup, whereas alkenes furnished 2-alkyl-3-formyl indoles. (Scheme 1.21). Although, directing groups on C-3 position can potentially direct C-2 functionalization as effectively as N-1 directing groups, there has been not much literature reported for cross-dehydrogenative coupling. During our investigation on palladium catalyzed allylic C-H oxidative amidation, we found that allyl group at C-3 position was able to direct C-2 amidation. Chapter 4 of this thesis will discuss about directed C-2 amination, and our approach to the development and mechanistic details of selective C-2 functionalization.[69,70]

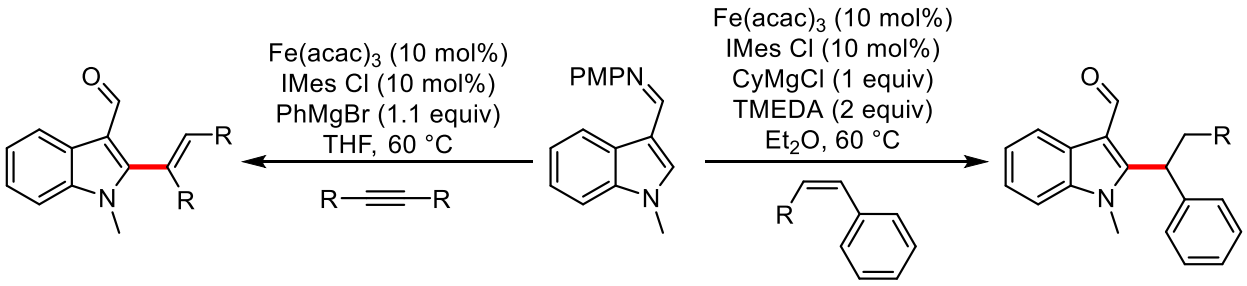

Scheme 1.21: Iron-NHC catalyzed C-2 alkenylation and alkylation

1.6. Ruthenium catalyzed directed C-H activation/annulation

1.6.1. Initial development/hydroarylation

The field of C-H bond activation chemistry emerged in the 1970s; however, Murai and coworkers reported the first synthetically useful catalytic functionalization for carbon-carbon bond formation in 1993. They have employed aromatic ketone as the directing group for hydroarylation of alkenes in the presence of a ruthenium catalyst. It was proposed that carbonyl group of aromatic ketone acts as a directing group for C-H activation by ruthenium complexes to form a 5-membered hydrometallacycle intermediate. This initial catalytic C-H bond functionalization of aromatic

ketone led to the significant development of atom-economical and sustainable processes for C-C and C-X bond forming reactions (Scheme 1.22).[71]

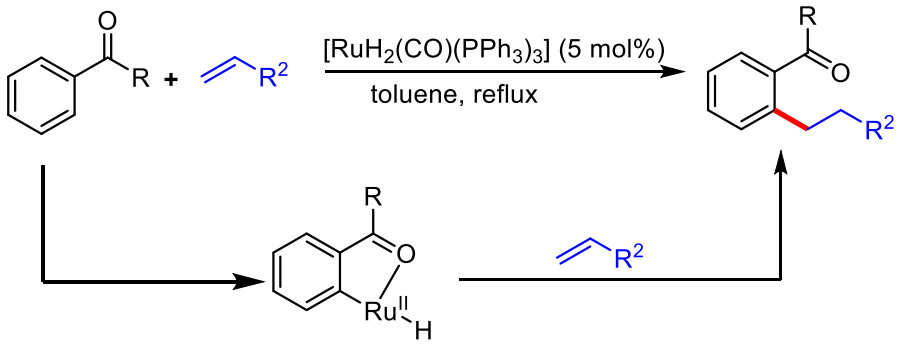

Scheme 1.22: Ruthenium catalyzed Murai hydroarylation

Murai in the year 1995, reported a carbonyl directed hydroarylation of alkynes with α-tetralones in the presence of ruthenium catalyst. Although the reaction was found to be very effective, good stereoselectivity was not achieved. To address the issues of selectivity in hydroarylation reactions, base promoted, chelation assisted transition metal catalyzed reactions have been developed. Various directing groups such as carbonyl compounds, amides, carbamates, sulfoxides, and pyridine-based compounds are employed in the hydroarylation of alkynes (Scheme 1.23).[72,73]

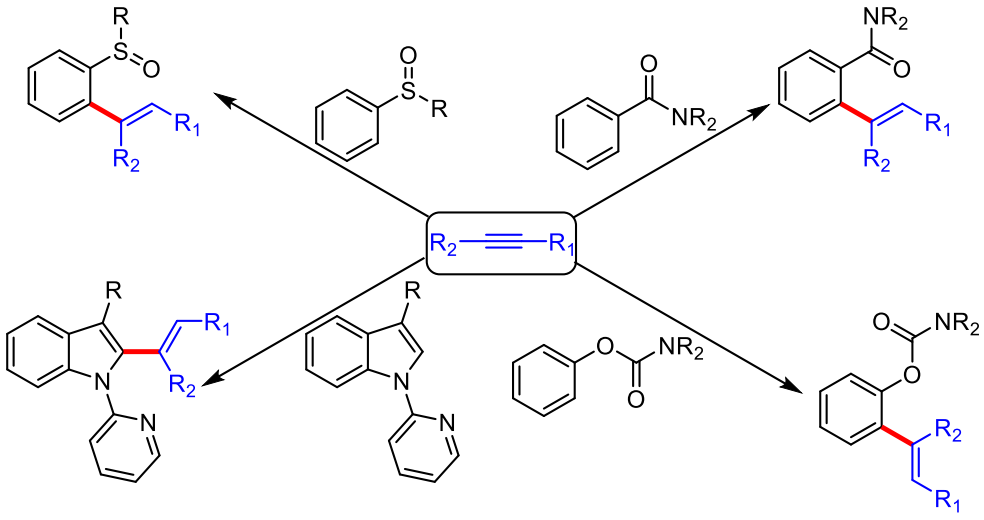

Scheme 1.23: Ruthenium catalyzed chelation assisted hydroarylation

1.6.2. Annulation reactions with alkynes

Directed *ortho*-C-H bond activation usually forms a stable five membered cyclometallated intermediate upon deprotonation. This cyclometallated intermediate can undergo a 1,2-insertion with alkynes to form a seven-membered metal-alkenyl intermediate. If the reaction is acidic in nature, the seven-membered metal complex abstracts the proton forming hydroarylated product, where as in basic or oxidative reaction conditions the complex cyclizes to generally form a five or six membered ring (Scheme 1.24).[73,74]

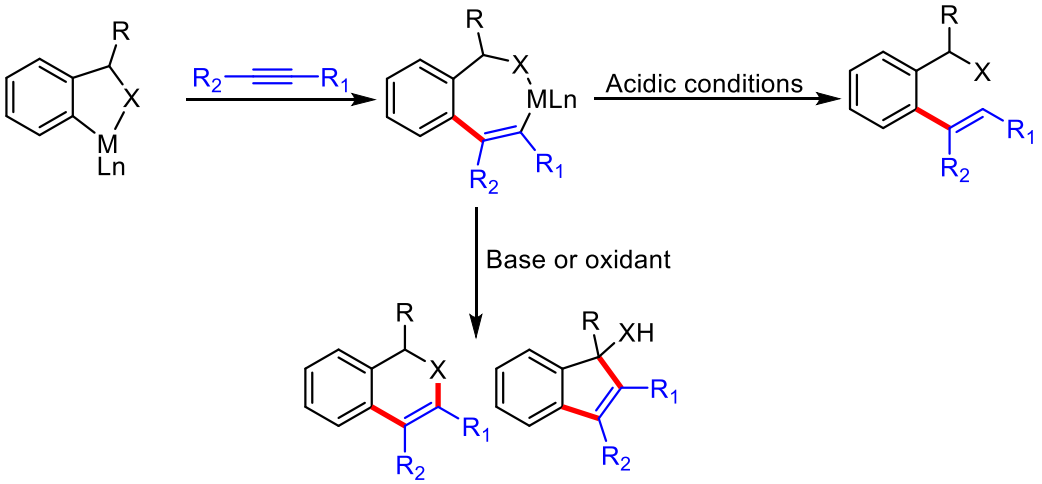

Scheme 1.24: Annulated product formation *via* ruthenium catalyzed *ortho*-C-H activation

With the initial reports from Fagnou and coworkers[75] for the annulation reaction to form indoles with Rh-catalyst, there has been much progress for the development of annulated products *via* C-H/N-H bond activation. But it was in 2011, Ackerman and coworkers succeeded in inserting disubstituted alkynes in to arene C-H bond for the formation of isoquinolone derivatives employing a cheaper ruthenium catalyst under oxidative conditions. The regioselective reaction involves the functionalization of both *ortho*-C-H bond of arene and N-H bonds of amide directing group forming isoquinolone derivatives at 100 °C (Scheme 1.25). Mechanistic studies suggested an irreversible C-H/N-H bond protonation by acetate ligand of $Cu(OAc)_2$ to form a five membered

ruthenacycle. 1,2-insertion of alkynes to ruthenacycle gives a seven-membered ruthenium-alkenyl intermediate. Subsequent C-N reductive elimination releases annulated product followed by reoxidation of the ruthenium(0) intermediate for the regeneration of the active catalyst (Scheme 1.25).[76]

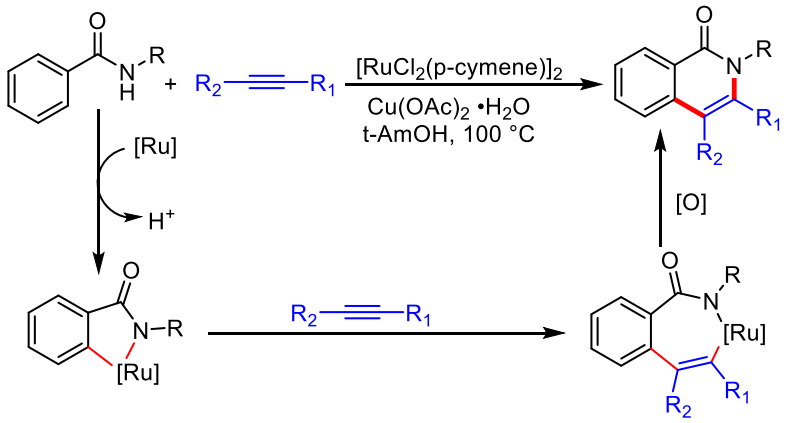

Scheme 1.25: Isoquinolone synthesis *via* C-H/N-H bond activation under Ru-catalysis

The same ruthenium catalytic system was also applied to acrylamides to generate 2-pyridones *via* vinylic sp^2 C-H, amide N-H activation and subsequent annulation with alkynes with excellent yields (Scheme 1.26). This methodology is a great improvement from a similar rhodium catalytic system as it uses inexpensive ruthenium catalyst, only 1 equiv of $Cu(OAc)_2 \cdot H_2O$ as oxidant and lower temperatures. This reaction is also extended to use unsymmetrical arylalkyl and dialkyl acetylenes leading to regioselective annulations.[77]

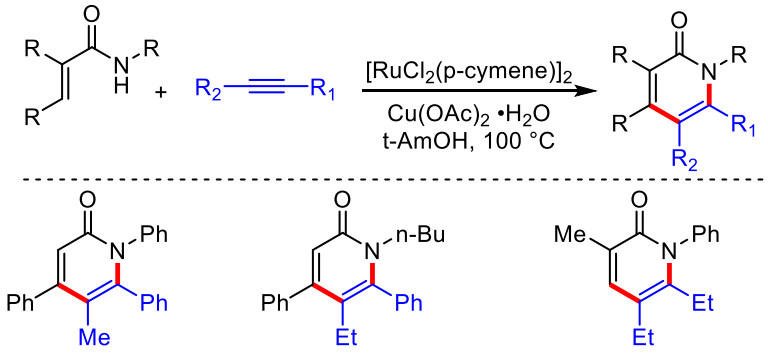

Scheme 1.26: Ruthenium catalyzed oxidative annulation *via* C-H/N-H activation

With the literature precedent and increasing interest in the development of annulation reactions under ruthenium catalysis, and our ongoing research to synthesize quinazoline based bio active molecules we also explored a ruthenium catalyzed (4+2) annulation reaction of styryl quinazolinones. Chapter 5 of this thesis will be focused on our approach to the development of alkyne annulation reaction *via* sp^2 and sp^3 C-H/ amide N-H bond activation.

1.7. Conclusions and research goals

While not comprehensive, this review summarizes some of the major developments in methods for the allylation and transition metal-catalyzed functionalization of aromatic and heteroaromatic C-H bonds. Palladium catalyzed allylation and transition metal catalyzed C–H bond functionalization constitutes an exciting class of chemical reactions that is enjoying resurgence in the current literature. The direct and selective functionalization of electron-deficient heterocycles, most notably tautomerizable heteroarenes, remains a synthetic challenge. This is substantiated by the fact that far more accounts of electron rich arenes continue to be reported in the literature. Due to the increasing demand for more direct synthetic methods which produce less waste and operate under more mild conditions, transition metal catalyzed approaches will surely continue to evolve at a rapid pace in the future. Following chapters in this thesis will describe our ideas and approach to further the development of effective heterocycle functionalization reactions which address some of the unmet challenges in their synthetic methodology.

1.8. References

(1) Park, Y.; Kim, Y.; Chang, S. Transition Metal-Catalyzed C–H Amination: Scope, Mechanism, and Applications. *Chem. Rev.* **2017**, *117* (13), 9247–9301.

(2) Wolfe, J. F.; Rathman, T. L.; Sleevi, M. C.; Campbell, J. A.; Greenwood, T. D. Synthesis and Anticonvulsant Activity of Some New 2-Substituted 3-Aryl-4(3H)-Quinazolinones. *J. Med. Chem.* **1990**, *33* (1), 161–166.

(3) Mhaske, S. B.; Argade, N. P. The Chemistry of Recently Isolated Naturally Occurring Quinazolinone Alkaloids. *Tetrahedron* **2006**, *62* (42), 9787–9826.

(4) Cagir, A.; Jones, S. H.; Gao, R.; Eisenhauer, B. M.; Hecht, S. M. Luotonin A. A Naturally Occurring Human DNA Topoisomerase I Poison. *J. Am. Chem. Soc.* **2003**, *125* (45), 13628–13629.

(5) Wang, S.; Fang, K.; Dong, G.; Chen, S.; Liu, N.; Miao, Z.; Yao, J.; Li, J.; Zhang, W.; Sheng, C. Scaffold Diversity Inspired by the Natural Product Evodiamine: Discovery of Highly Potent and Multitargeting Antitumor Agents. *J. Med. Chem.* **2015**, *58* (16), 6678–6696.

(6) Bouley, R.; Kumarasiri, M.; Peng, Z.; Otero, L. H.; Song, W.; Suckow, M. A.; Schroeder, V. A.; Wolter, W. R.; Lastochkin, E.; Antunes, N. T.; et al. Discovery of Antibiotic (E)-3-(3-Carboxyphenyl)-2-(4-Cyanostyryl)Quinazolin-4(3 H)-One. *J. Am. Chem. Soc.* **2015**, *137* (5), 1738–1741.

(7) Takaya, Y.; Tasaka, H.; Chiba, T.; Uwai, K.; Tanitsu, M. A.; Kim, H. S.; Wataya, Y.; Miura, M.; Takeshita, M.; Oshima, Y. New Type of Febrifugine Analogues, Bearing a Quinolizidine Moiety, Show Potent Antimalarial Activity against Plasmodium Malaria Parasite. *J. Med. Chem.* **1999**, *42* (16), 3163–3166.

(8) Malamas, M. S.; Millen, J. Quinazolineacetic Acids and Related Analogs as Aldose Reductase Inhibitors. *J. Med. Chem.* **1991**, *34* (4), 1492–1503.

(9) Peet, N. P.; Baugh, L. E.; Sunder, S.; Lewis, J. E.; Matthews, E. H.; Olberding, E. L.; Shah, D. N. 3-(LH-Tetrazol-5-Yl)-4(3H)-Quinazolinone Sodium Salt (MDL 427): A New Antiallergic Agent. *J. Med. Chem.* **1986**, *29* (11), 2403–2409.

(10) Liverton, N. J.; Armstrong, D. J.; Claremon, D. A.; Remy, D. C.; Baldvin, J. J.; Lynch, R. J.; Zhang, G.; Gould, R. J. Nonpeptide Glycoprotein IIb/IIIa Inhibitors: Substituted Quinazolinediones and Quinazolinones as Potent Fibrinogen Receptor Antagonists. *Bioorg. Med. Chem. Lett.* **1998**, *8* (5), 483–486.

(11) Liu, H.; Ko, S.-B.; Josien, H.; Curran, D. P. Selective N-Functionalization of 6-Substituted-2-Pyridones. *Tetrahedron Lett.* **1995**, *36* (49), 8917–8920.

(12) Fang, Y.-Q.; Bio, M. M.; Hansen, K. B.; Potter, M. S.; Clausen, A. Magnesium Coordination-Directed N -Selective Stereospecific Alkylation of 2-Pyridones, Carbamates, and Amides Using α-Halocarboxylic Acids. *J. Am. Chem. Soc.* **2010**, *132* (44), 15525–15527.

(13) Breugst, M.; Mayr, H. Ambident Reactivities of Pyridone Anions. *J. Am. Chem. Soc.* **2010**, *132* (43), 15380–15389.

(14) Kumar, D.; Vemula, S. R.; Cook, G. R. Highly Chemo- and Regioselective Allylic Substitution with Tautomerizable Heteroarenes. *Green Chem.* **2015**, *17* (8), 4300–4306.

(15) Kumar, D.; Vemula, S. R.; Cook, G. R. Merging C-H Bond Functionalization with Amide Alcoholysis: En Route to 2-Aminopyridines. *ACS Catal.* **2016**, *6* (6).

(16) Vemula, S. R.; Kumar, D.; Cook, G. R. Palladium-Catalyzed Allylic Amidation with N-Heterocycles via Sp^3 C-H Oxidation. *ACS Catal.* **2016**, *6* (8).

(17) Alberico, D.; Scott, M. E.; Lautens, M. Aryl−Aryl Bond Formation by Transition-Metal-Catalyzed Direct Arylation. *Chem. Rev.* **2007**, *107* (1), 174–238.

(18) Stuart, D. R.; Fagnou, K. The Catalytic Cross-Coupling of Unactivated Arenes. *Science.* **2007**, *316* (5828), 1172–1175.

(19) Satoh, T.; Miura, M. Catalytic Direct Arylation of Heteroaromatic Compounds. *Chem. Lett.* **2007**, *36* (2), 200–205.

(20) Tamao, K.; Sumitani, K.; Kumada, M. Selective Carbon-Carbon Bond Formation by Cross-Coupling of Grignard Reagents with Organic Halides. Catalysis by Nickel-Phosphine Complexes. *J. Am. Chem. Soc.* **1972**, *94* (12), 4374–4376.

(21) Corriu, R. J. P.; Masse, J. P. Activation of Grignard Reagents by Transition-Metal Complexes. A New and Simple Synthesis of Trans-Stilbenes and Polyphenyls. *J. Chem. Soc. Chem. Commun.* **1972**, No. 3, 144a.

(22) Sonogashira, K.; Tohda, Y.; Hagihara, N. A Convenient Synthesis of Acetylenes: Catalytic Substitutions of Acetylenic Hydrogen with Bromoalkenes, Iodoarenes and Bromopyridines. *Tetrahedron Lett.* **1975**, *16* (50), 4467–4470.

(23) King, A. O.; Okukado, N.; Negishi, E. Highly General Stereo-, Regio-, and Chemo-Selective Synthesis of Terminal and Internal Conjugated Enynes by the Pd-Catalysed Reaction of Alkynylzinc Reagents with Alkenyl Halides. *J. Chem. Soc. Chem. Commun.* **1977**, No. 19, 683.

(24) Milstein, D.; Stille, J. K. A General, Selective, and Facile Method for Ketone Synthesis from Acid Chlorides and Organotin Compounds Catalyzed by Palladium. *J. Am. Chem. Soc.* **1978**, *100* (11), 3636–3638.

(25) Miyaura, N.; Yamada, K.; Suzuki, A. A New Stereospecific Cross-Coupling by the Palladium-Catalyzed Reaction of 1-Alkenylboranes with 1-Alkenyl or 1-Alkynyl Halides. *Tetrahedron Lett.* **1979**, *20* (36), 3437–3440.

(26) Tsuji, J.; Kiji, J.; Imamura, S.; Morikawa, M.; Tsuji, J.; Kiji, J.; Imamura, S.; Morikawa, M. *Organic Syntheses by Means of Noble Metal Compounds. VIII.1 Catalytic Carbonylation of Allylic Compounds with Palladium Chloride*.

(27) Trost, B. M.; Fullerton, T. J. New Synthetic Reactions. Allylic Alkylation. *J. Am. Chem. Soc.* **1973**, *95* (1), 292–294.

(28) The Nobel Prize in Chemistry 2010 Was Awarded Jointly to Richard F. Heck, Ei-Ichi Negishi and Akira Suzuki "for Palladium-Catalyzed Cross Couplings in Organic Synthesis.

(29) Patil, M.; Thiel, W. Origin of Selectivity of Tsuji-Trost Allylic Alkylation of Lactones: Highly Ordered Transition States with Lithium-Containing Enolates. *Chem. - A Eur. J.* **2012**, *18* (33), 10408–10418.

(30) Smidt, J.; Hafner, W.; Jira, R.; Sieber, R.; Sedlmeier, J.; Sabel, A. The Oxidation of Olefins with Palladium Chloride Catalysts. *Angew. Chem. Int. Ed.* **1962**, *1* (2), 80–88.

(31) Tsuji, J. Dawn of Organopalladium Chemistry in the Early 1960s and a Retrospective Overview of the Research on Palladium-Catalyzed Reactions. *Tetrahedron* **2015**, *71* (37), 6330–6348.

(32) Trost, B. M. On Inventing Reactions for Atom Economy. *Acc. Chem. Res.* **2002**, *35* (9), 695–705.

(33) Tsuji, J.; Takahashi, H.; Morikawa, M. Organic Syntheses by Means of Noble Metal Compounds XVII. Reaction of π-Allylpalladium Chloride with Nucleophiles. *Tetrahedron Lett.* **1965**, *6* (49), 4387–4388.

(34) Trost, B. M.; Van Vranken, D. L. Asymmetric Transition Metal-Catalyzed Allylic Alkylations. *Chem. Rev.* **1996**, *96* (1), 395–422.

(35) Consiglio, G.; Waymouth, R. M. Enantioselective Homogeneous Catalysis Involving Transition-Metal-Allyl Intermediates. *Chem. Rev.* **1989**, *89* (1), 257–276.

(36) Schenck, T. G.; Bosnich, B. Homogeneous Catalysis. Transition-Metal-Catalyzed Claisen Rearrangements. *J. Am. Chem. Soc.* **1985**, *107* (7), 2058–2066.

(37) Tamaru, Y.; Horino, Y.; Araki, M.; Tanaka, S.; Kimura, M. Et3B-Promoted, Pd(0)-Catalyzed Allylation of Active Methylene Compounds with Allylic Alcohols. *Tetrahedron Lett.* **2000**, *41* (30), 5705–5709.

(38) Kimura, M.; Mukai, R.; Tanigawa, N.; Tanaka, S.; Tamaru, Y. Triethylborane as an Efficient Promoter for Palladium-Catalyzed Allylation of Active Methylene Compounds with Allyl Alcohols. *Tetrahedron* **2003**, *59* (39), 7767–7777.

(39) Masuyama, Y.; Takahara, J. P.; Kurusu, Y. Allylic Alcohols as Synthons of Allylic Carbanions. Palladium-Catalyzed Carbonyl Allylation by Allylic Alcohols with Tin Dichloride. *J. Am. Chem. Soc.* **1988**, *110* (13), 4473–4474.

(40) Manabe, K.; Kobayashi, S. Palladium-Catalyzed, Carboxylic Acid-Assisted Allylic Substitution of Carbon Nucleophiles with Allyl Alcohols as Allylating Agents in Water. *Org. Lett.* **2003**, *5* (18), 3241–3244.

(41) Tao, Z. L.; Zhang, W. Q.; Chen, D. F.; Adele, A.; Gong, L. Z. Pd-Catalyzed Asymmetric Allylic Alkylation of Pyrazol-5-Ones with Allylic Alcohols: The Role of the Chiral Phosphoric Acid in C-O Bond Cleavage and Stereocontrol. *J. Am. Chem. Soc.* **2013**, *135* (25), 9255–9258.

(42) Jiang, G.; List, B. Direct Asymmetric α-Allylation of Aldehydes with Simple Allylic Alcohols Enabled by the Concerted Action of Three Different Catalysts. *Angew. Chem. Int. Ed.* **2011**, *50* (40), 9471–9474.

(43) Trost, B. M.; Metzner, P. J. Reaction of Olefins with Palladium Trifluoroacetate. *J. Am. Chem. Soc.* **1980**, *102* (10), 3572–3577.

(44) Trost, B. M.; Crawley, M. L. Asymmetric Transition-Metal-Catalyzed Allylic Alkylations: Applications in Total Synthesis. *Chem. Rev.* **2003**, *103* (8), 2921–2944.

(45) Trost, B. The Atom Economy--a Search for Synthetic Efficiency. *Science.* **1991**, *254* (5037), 1471–1477.

(46) Tsuji, J.; Sakai, K.; Nagashima, H.; Shimizu, I. A Novel Synthetic Method for γ-Acetoxy-(E)-α,β-Unsaturated Esters by the Palladium Catalyzed Regio- and Stereoselective Acetoxylation of β,γ-Unsaturated Esters. *Tetrahedron Lett.* **1981**, *22* (2), 131–134.

(47) McMurry, J. E.; Kočotovský, P. A Method for the Palladium-Catalyzed Allylic Oxidation of Olefins. *Tetrahedron Lett.* **1984**, *25* (38), 4187–4190.

(48) Chen, M. S.; White, M. C. A Sulfoxide-Promoted, Catalytic Method for the Regioselective Synthesis of Allylic Acetates from Monosubstituted Olefins via C-H Oxidation. *J. Am. Chem. Soc.* **2004**, *126* (5), 1346–1347.

(49) Chen, M. S.; Prabagaran, N.; Labenz, N. A.; White, M. C. Serial Ligand Catalysis: A Highly Selective Allylic C-H Oxidation. *J. Am. Chem. Soc.* **2005**, *127* (19), 6970–6971.

(50) Delcamp, J. H.; White, M. C. Sequential Hydrocarbon Functionalization: Allylic C-H Oxidation/Vinylic C-H Arylation. *J. Am. Chem. Soc.* **2006**, *128* (47), 15076–15077.

(51) Campbell, A. N.; White, P. B.; Guzei, I. A.; Stahl, S. S. Allylic C-H Acetoxylation with a 4,5-Diazafluorenone-Ligated Palladium Catalyst: A Ligand-Based Strategy to Achieve Aerobic Catalytic Turnover. *J. Am. Chem. Soc.* **2010**, *132*(43), 15116–15119.

(52) Henderson, W. H.; Check, C. T.; Proust, N.; Stambuli, J. P. Allylic Oxidations of Terminal Olefins Using a Palladium Thioether Catalyst. *Org. Lett.* **2010**, *12*(4), 824–827.

(53) Qi, X.; Chen, P.; Liu, G. Advances and Challenges in Palladium-Catalyzed Intermolecular Selective Allylic C-H Functionalization of Alkenes. *Sci. China Chem*. **2015**,1249–1251.

(54) Young, A. J.; White, M. C. Catalytic Intermolecular Allylic C-H Alkylation. *J. Am. Chem. Soc*. **2008**, *130*(43) 14090–14091.

(55) Lin, S.; Song, C. X.; Cai, G. X.; Wang, W. H.; Shi, Z. J. Intra/Intermolecular Direct Allylic Alkylation via Pd(II)-Catalyzed Allylic C-H Activation. *J. Am. Chem. Soc*. **2008**, *130*(39), 12901–12903.

(56) Bloomer, J. L.; Damodaran, K. M. An Efficient Synthesis of Homogentisic Acid. *Synthesis.* **1980**, *1980* (02), 111–111.

(57) Engelin, C.; Jensen, T.; Rodriguez-Rodriguez, S.; Fristrup, P. Mechanistic Investigation of Palladium-Catalyzed Allylic C-H Activation. *ACS Catal.* **2013**, *3* (3), 294–302.

(58) Trost, B. M.; Mahapatra, S.; Hansen, M. Palladium-Catalyzed C-H Activation of N-Allyl Imines: Regioselective Allylic Alkylations to Deliver Substituted Aza-1,3-Dienes. *Angew. Chem. Int. Ed.* **2015**, *54* (20), 6032–6036.

(59) Trost, B. M.; Li, X. Pd-Catalyzed Asymmetric Allylic Alkylations via C–H Activation of N-Allyl Imines with Glycinates. *Chem. Sci.* **2017**, *8* (10), 6815–6821.

(60) Wang, P. S.; Liu, P.; Zhai, Y. J.; Lin, H. C.; Han, Z. Y.; Gong, L. Z. Asymmetric Allylic C-H Oxidation for the Synthesis of Chromans. *J. Am. Chem. Soc*. **2015**, *137*(40), 12732–12735.

(61) Trost, B. M.; Thaisrivongs, D. A.; Donckele, E. J. Palladium-Catalyzed Enantioselective Allylic Alkylations through C-H Activation. *Angew. Chemie Int. Ed.* **2013**, *52* (5), 1523–1526.

(62) Sandtorv, A. H. Transition Metal-Catalyzed C-H Activation of Indoles. *Adv. Synth. Catal.* **2015**, *357* (11), 2403–2435.

(63) Stuart, D. R.; Villemure, E.; Fagnou, K. Elements of Regiocontrol in Palladium-Catalyzed Oxidative Arene Cross-Coupling. *J. Am. Chem. Soc.* **2007**, *129* (40), 12072–12073.

(64) Nishino, M.; Hirano, K.; Satoh, T.; Miura, M. Copper-Mediated and Copper-Catalyzed Cross-Coupling of Indoles and 1,3-Azoles: Double C-H Activation. *Angew. Chemie Int. Ed.* **2012**, *51* (28), 6993–6997.

(65) Wang, Z.; Song, F.; Zhao, Y.; Huang, Y.; Yang, L.; Zhao, D.; Lan, J.; You, J. Elements of Regiocontrol in the Direct Heteroarylation of Indoles/Pyrroles: Synthesis of Bi- and Fused Polycyclic Heteroarenes by Twofold or Tandem Fourfold C-H Activation. *Chem. - A Eur. J.* **2012**, *18* (52), 16616–16620.

(66) García-Rubia, A.; Arrayás, R. G.; Carretero, J. C. Palladium(II)-Catalyzed Regioselective Direct C2 Alkenylation of Indoles and Pyrroles Assisted by the N -(2-Pyridyl)Sulfonyl Protecting Group. *Angew. Chemie Int. Ed.* **2009**, *48* (35), 6511–6515.

(67) Tang, C.-Y.; Tao, Y.; Wu, X.-Y.; Sha, F. Rhodium(III)-Catalyzed Direct C-2 Olefination of Unactivated Indoles Utilizing OH/NH_2 as Directing Group. *Adv. Synth. Catal.* **2014**, *356* (2–3), 609–615.

(68) Pan, S.; Ryu, N.; Shibata, T. Ir(I)-Catalyzed C–H Bond Alkylation of C2-Position of Indole with Alkenes: Selective Synthesis of Linear or Branched 2-Alkylindoles. *J. Am. Chem. Soc.* **2012**, *134* (42), 17474–17477.

(69) Wong, M. Y.; Yamakawa, T.; Yoshikai, N. Iron-Catalyzed Directed C2-Alkylation and Alkenylation of Indole with Vinylarenes and Alkynes. *Org. Lett.* **2015**, *17* (3), 442–445.

(70) Ding, Z.; Yoshikai, N. Cobalt-Catalyzed Intramolecular Olefin Hydroarylation Leading to Dihydropyrroloindoles and Tetrahydropyridoindoles. *Angew. Chemie Int. Ed.* **2013**, *52* (33), 8574–8578.

(71) Murai, S.; Kakiuchi, F.; Sekine, S.; Tanaka, Y.; Kamatani, A.; Sonoda, M.; Chatani, N. Efficient Catalytic Addition of Aromatic Carbon-Hydrogen Bonds to Olefins. *Nature* **1993**, *366* (6455), 529–531.

(72) Satoh, T.; Nishinaka, Y.; Miura, M.; Nomura, M. Iridium-Catalyzed Regioselective Reaction of 1-Naphthols with Alkynes at the Peri -Position. *Chem. Lett.* **1999**, *28* (7), 615–616.

(73) Hashimoto, Y.; Hirano, K.; Satoh, T.; Kakiuchi, F.; Miura, M. Ruthenium(II)-Catalyzed Regio- and Stereoselective Hydroarylation of Alkynes via Directed C–H Functionalization. *Org. Lett.* **2012**, *14* (8), 2058–2061.

(74) Liang, L.; Fu, S.; Lin, D.; Zhang, X.-Q.; Deng, Y.; Jiang, H.; Zeng, W. Ruthenium(II)-Catalyzed Direct Addition of Indole/Pyrrole C2–H Bonds to Alkynes. *J. Org. Chem.* **2014**, *79* (20), 9472–9480.

(75) Stuart, D. R.; Alsabeh, P.; Kuhn, M.; Fagnou, K. Rhodium(III)-Catalyzed Arene and Alkene C−H Bond Functionalization Leading to Indoles and Pyrroles. *J. Am. Chem. Soc.* **2010**, *132* (51), 18326–18339.

(76) Ackermann, L.; Lygin, A. V.; Hofmann, N. Ruthenium-Catalyzed Oxidative Annulation by Cleavage of C-H/N-H Bonds. *Angew. Chemie Int. Ed.* **2011**, *50*(28), 6379–6382.

(77) Ackermann, L.; Lygin, A. V.; Hofmann, N. Ruthenium-Catalyzed Oxidative Synthesis of 2-Pyridones through C-H/N-H Bond Functionalizations. *Org. Lett.* **2011**, *13* (12), 3278–3281.

CHAPTER 2. PALLADIUM CATALYZED TSUJI-TROST ALLYLATION OF ELECTRON DEFICIENT *N*-HETEROCYCLES

2.1. Introduction

The selective functionalization of heteroaryl systems with multiple reactive centers to generate highly functionalized compounds is a significant problem in the early drug development process to generate lead molecules.[1] Over the years, researchers have developed various strategies to selectively functionalize heterocycles to form C-C and C-X bonds. Among numerous developed methods, palladium catalyzed allylic substitution (Tsuji-Trost reaction) reaction is one of the powerful tool for the construction of C-C and C-X (N, O & S) bonds to obtain structural diversity.[2,3] The reaction was first reported by Tsuji and coworkers in 1965 using pre-formed (η^3-allyl)Pd complexes.[2] Thereafter, the reaction was further developed by Trost and coworkers by starting from alkenes and additional phosphine ligands.[3] Allyl substrates with a wide range of leaving groups (acetates, carbonates, halides, phosphonates, carboxylates etc.) can be utilized to form π-allylpalladium complexes, which can undergo nucleophilic substitution to form C-C/C-X bonds (Scheme 2.1).[4] A variety of nucleophiles can also be applied in the reaction, such as alkali metal enolates or heteroatom nucleophiles, but the most commonly used are soft stabilized carbon nucleophiles.

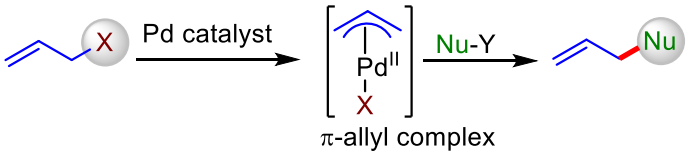

Scheme 2.1: Palladium catalyzed Tsuji-Trost allylation

2.2. Mechanism and catalytic cycle

Mechanistically, the Tsuji-Trost reaction proceeds by coordination of allylic substrate to palladium complex forming η^2-complex (Scheme 2.2). If the initial catalyst system is a Pd(II) complex, then it gets reduced *insitu* to Pd(0) active catalyst before the coordination to allylic substrate. Oxidative addition of allyl electrophiles to palladium catalyst forms a π-allylpalladium complex with the leaving group as counter ion. The nucleophile, then attacks on the π-allylpalladium complex, yielding a η^2-complex between Pd(0) and the newly formed product. In the final step, the product is released after dissociation from Pd(0), there by regenerating active catalyst for next catalytic cycle.

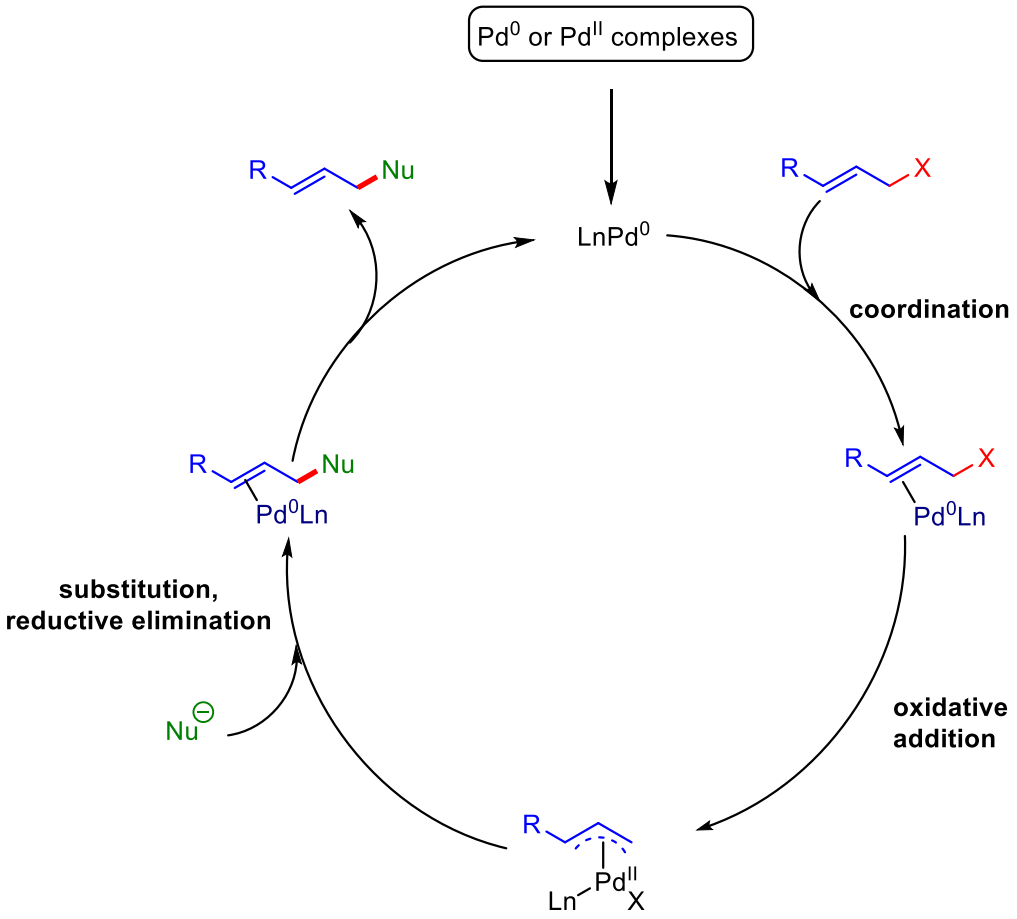

Scheme 2.2: Catalytic cycle for palladium catalyzed allylic substitution

2.2.1. Stereoselectivity in Tsuji-Trost allylation

After oxidative addition, and formation of π-allylpalladium complex, the nucleophilic substitution to π-allylpalladium complex can then proceed *via* two general routes, distinguished by the nature of the pronucleophiles (Scheme 2.3). Stabilized or "soft" nucleophiles, derived from conjugate acids with pKa < 25 attack directly at the allyl termini of the π-allylpalladium intermediate, with no prior coordination to the Pd-center leading to substitution with overall retention of the stereochemistry in the product. On the contrary, unstabilized or "hard" nucleophiles, derived from the conjugate acids with pKa > 25 coordinate to Pd-center of π-allylpalladium intermediate, leading to allylic substitution with the inversion of product stereochemistry. Thus, the net stereochemical outcome of Tsuji-Trost reaction is determined by nature and pKa of the nucleophile. And, since the pKa values are dependent on solvent and temperature, modifications to the reactions can alter the reactivity of the nucleophilic partners and there by selectivity of the overall reaction.

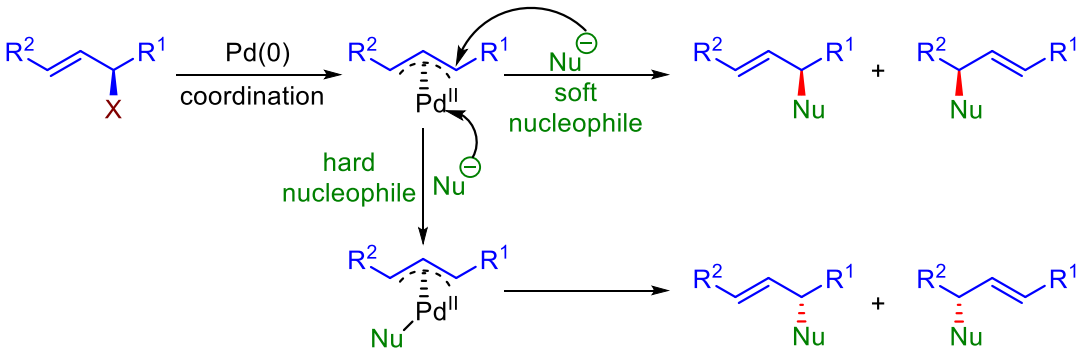

Scheme 2.3: Stereochemical outcome based on the nature of nucleophiles

2.2.2. Regioselectivity in Tsuji-Trost allylation

As shown in Scheme 2.3, when symmetrical allylic systems are employed, no regioselectivity issues occur. On the other hand, if the substitution on the allyl groups are different ($R^1 \neq R^2 \neq H$) the nucleophile can potentially attack at either end of the allyl group, forming product

as a mixture of regioisomers. In general, allylation occurs at less substituted center because of the steric effects, but the nature of R groups and reaction conditions (such as ligand, solvent and temperature) play an important role for the dominance of one product over the other possible products (Scheme 2.4).[5]

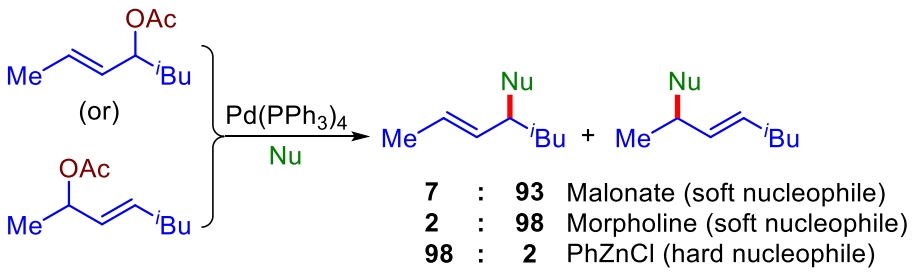

Scheme 2.4: Regioselectivity in Tsuji-Trost allylation

Malonate and morpholine being the soft nucleophiles, attack the unsymmetrical π-allyl complex at the less substituted carbon owing to steric factors. On the other hand, PhZnCl, being a hard nucleophile attacks on palladium in the π-allyl complex via transmetallation. Ligand and nucleophile then orient themselves to form the stable π-allyl complex considering the sterics and possible coordination. The phenyl group then attacks at the adjacent carbon to give the corresponding allylated product (Scheme 2.5)

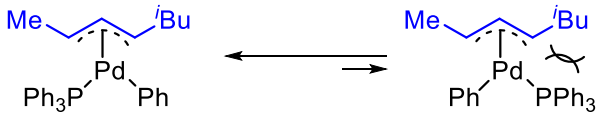

Scheme 2.5: Stability of π-allyl complex with hard nucleophiles

Controlling the regio- and chemoselectivty is an important consideration when developing a new methodology, whether it is for material or medicinal chemistry applications.[6] The issue becomes even more complicated when ambidentate nucleophiles with tautomeric equilibrium are employed.[7] Tautomerizable heteroarenes, such as 4-hydroxy quinazoline, or 2-hydroxy pyridine for example are a kind of organic molecules having multiple reactive centers, and depending on

the reaction conditions employed, can react at O-center or N-center leading to a mixtures of O- and N-substituted products. The quinazolinone scaffold, although found as a privileged core structure for a vast variety of drug candidates, displaying a wide spectrum of biological and pharmacological properties.[8–11] very limited examples have been documented till date for their selective functionalization. In our group continuous effort to develop new reaction methodology for functionalization of biologically active molecules, we chose to develop a selective allylation of these tautomerizable heteroarenes. We chose 4-hydroxy quinazoline as a model substrate, which when subjected to direct allylic substitution potentially can form at least three products *via* competitive reaction pathways (Scheme 2.6).

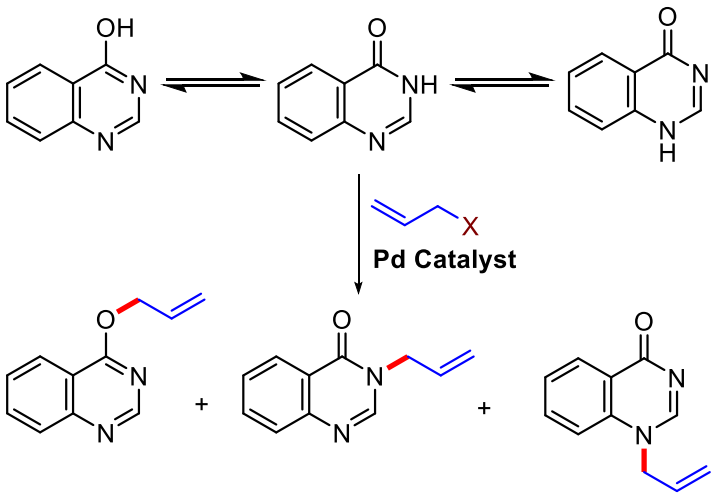

Scheme 2.6: Selectivity in Tsuji-Trost allylation of tautomerizable heteroarenes

Thus, we wanted to develop a simple and efficient catalytic system for selective allylation of quinazolinone and derivatives. The work described below aims to delineate the factors that control selectivity during Pd-catalyzed allylic substitution of tautomerizable heteroarenes in the context of allylating reagents, reaction conditions, and substrate scope. The work also offers a detailed mechanistic insight to rationalize selectivity and develop a generalized green allylation protocol.

2.3. Optimization of reaction conditions

2.3.1. Allyl reagent screening under neutral conditions

Aiming to develop a chemo and regioselective allylation of tautomerizable heteroarenes, we started our reaction optimization using 4-hydroxy quinazoline as a model substrate. We focused our initial investigation on the effects of leaving groups present on allyl substrates both under base free/neutral and basic conditions. Table 2.1 and Table 2.2 described below summarizes the effects of leaving group ionization on the palladium catalyzed allylation of hydroxy quinazoline. To begin with, a reaction of 4-hydroxy quinazoline **2.01a** with different allylating reagents **2.02**, in presence of $Pd(PPh_3)_4$ as catalyst was performed under base free conditions in toluene (Table 2.1). Not surprisingly, allylic substrates with easily ionizing groups afforded products in moderate to good yields (Table 2.1, entries 2-8). Allyl substrates with less ionizable leaving groups, such as chloride **2.02a**, phenyl ether **2.02i**, amine **2.02j**, isothiocyanate **2.02l**, cyanide **2.02p**, and hydrogen **2.02q** (Table 2.1, entries 1,9,10,12,16 and 17) proved ineffective. We were very glad to find that, in all the cases of the product formation, either formation of **2.03a$_2$** (amide-NH allylation) was exclusive or with a very high selectivity (Table 2.1, entries 6,11 and 13) towards **2.03a$_2$** was observed. In cases where **2.03a$_2$** was major product, a trace amounts of **2.03a$_1$** was also observed. Formation of 1-allyl quinazolin-4(3*H*)-one **2.03a$_3$** was not observed in any cases. Hydroxy group, which is considered as a weak leaving group surprisingly performed well providing product in comparable yields with its activated partners such as aceate and trifluoroacetate. Control reaction, in the absence of the Pd-catalyst yielded no product formation, indicating the neccessity of palladium complex for the allylic functionalization.

Table 2.1: Effect of allyl reagents under neutral conditions on the selectivity and allylation of **2.01a**

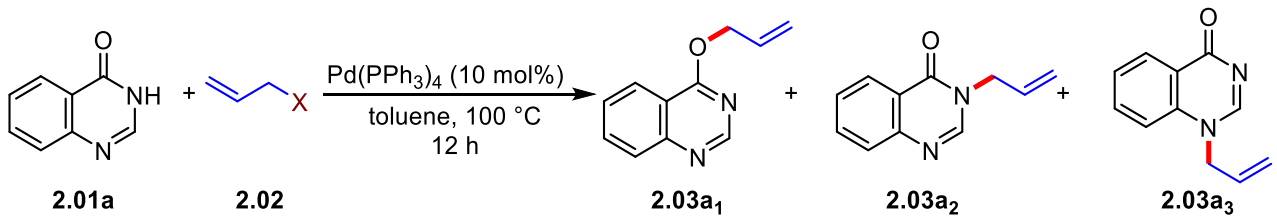

2.01a **2.02** **2.03a$_1$** **2.03a$_2$** **2.03a$_3$**

Entry	Allylating agent	Conversion (%)[a]			Yield (%)[b, c]
		2.03a$_1$	**2.03a$_2$**	**2.03a$_3$**	**2.03a$_2$**
1	**2.02a**; X = Cl	0	0	0	0
2	**2.02b**; X = Br	0	76	0	62
3	**2.02c**; X = I	0	81	0	68
4	**2.02d**; X = OH	0	82	0	70
5	**2.02e**; X = OAc	0	85	0	71
6	**2.02f**; X = $OCOCF_3$	3	85	0	72
7	**2.02g**; X = OCO_2Me	0	95	0	88
8	**2.02h**; X = $OP(O)(OEt)_2$	0	100	0	86
9	**2.02i**; X = OPh	0	0	0	0
10	**2.02j**; X = NH_2	0	0	0	0
11	**2.02k**; X = NCO	4	65	0	52
12	**2.02l**; X = NCS	0	0	0	0
13	**2.02m**; X = $NHCONH_2$	6	60	0	49
14	**2.02n**; X = SMe	0	26	0	15
15	**2.02o**; X = SO_2Me	0	38	0	25
16	**2.02p**; X = CN	0	0	0	0
17	**2.02q**; X = Ph	0	0	0	0

Reaction conditions: 2.01a (0.5 mmol) was treated with **2.02** (2 equiv, 1 mmol), $Pd(PPh_3)_4$ (10 mol %) in toluene (1 mL) at 100 °C for 12 h. [a]Based on GC-MS. [b]Isolated yield of **2.03a$_2$**. [c]No product formation was observed (**2.01a** was found intact) in absence of catalyst.

2.3.2. Allyl reagent screening under basic conditions

Addition of base was shown to have positive impacts in Tsuji-Trost allylation, both by increasing the leaving group ionization and by activation of nucleophile.[12] To examine the effect of base on chemoselectivity, the entire set of reactions shown in Table 2.1 were reinvestigated in the presence of K_2CO_3 (Table 2.2). No significant difference in the outcomes was observed with the exception that **2.02a**, **2.02i**, **2.02j**, and **2.02l**, which were ineffective without base, exhibited allylation to form **2.03a$_2$**. It is interesting to note the formation of **2.03a$_2$** with **2.02j** under basic conditions. This was likely formed through a nucleophilic ring-opening cascade by allylamine rather than ionization of the allyl group as the reaction in the absence of $Pd(PPh_3)_4$ also formed **2.03a$_2$** in appreciable yields. The inability of **2.02p**, and **2.02q** to form allylic substituted product with Pd(0) under neutral/basic conditions could be explained based on the inability of ionization of the allylic leaving to form a π-allylpalladium complex.

Most of the developed methods for Tsuji-Trost allylation employ pre-activated allyl substrates for a better leaving group (typically acetate or carbonate) ionization. A logical, greener and economical improvement would be to directly use allyl alcohols for increasing atom efficiency of the allylation reactions.[4,13] Allyl alcohols have been used in the literature even from early studies of Tsuji and coworkers,[14] however, the reported methods suffer from extended reaction times, high temperatures or lack of selectivity. Keeping in mind of all these difficulties, we were delighted to find allyl alcohol **2.02d** as a very effective allylating reagent for the allylation of **2.01a** and further studies have been conducted using **2.02d**.

Table 2.2: Effect of allyl reagents under basic conditions on the selectivity and allylation of **2.01a**

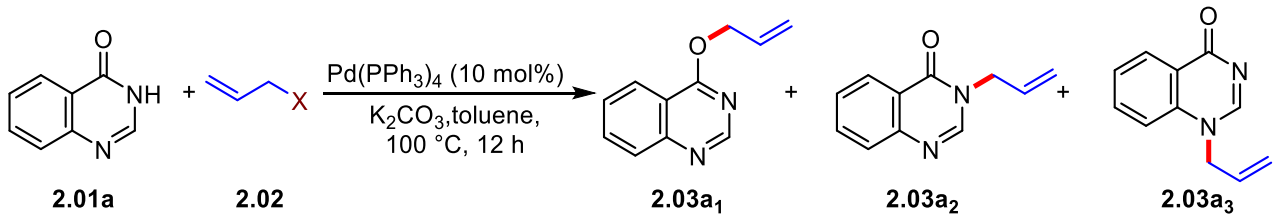

2.01a **2.02** **2.03a$_1$** **2.03a$_2$** **2.03a$_3$**

Entry	Allylating agent	Conversion (%)[a]			Yield (%)[b, c]
		2.03a$_1$	**2.03a$_2$**	**2.03a$_3$**	**2.03a$_2$**
1	**2.02a**; X = Cl	0	73	0	60
2	**2.02b**; X = Br	0	100	0	89
3	**2.02c**; X = I	0	100	0	88
4	**2.02d**; X = OH	0	92	0	79
5	**2.02e**; X = OAc	0	85	0	73
6	**2.02f**; X = $OCOCF_3$	3	92	0	79
7	**2.02g**; X = OCO_2Me	0	92	0	90
8	**2.02h**; X = $OP(O)(OEt)_2$	0	100	0	91
9	**2.02i**; X = OPh	6	88	0	74
10	**2.02j**; X = NH_2	0	25	0	12
11	**2.02k**; X = NCO	10	85	0	73
12	**2.02l**; X = NCS	0	97	0	81
13	**2.02m**; X = $NHCONH_2$	6	45	0	27
14	**2.02n**; X = SMe	0	38	0	24
15	**2.02o**; X = SO_2Me	0	51	0	37
16	**2.02p**; X = CN	0	0	0	0
17	**2.02q**; X = Ph	0	0	0	0

Reaction conditions: 2.01a (0.5 mmol) was treated with **2.02** (2 equiv, 1 mmol), $Pd(PPh_3)_4$ (10 mol %), K_2CO_3 (2.0 equiv, 1 mmol) in toluene (1 mL) at 100 °C for 12 h. [a]Based on GC-MS. [b]Isolated yield of **2.03a$_2$**. [c]No product formation was observed (**2.01a** was found intact) in absence of catalyst.

2.3.3. Effect of solvents on the tautomeric equilibrium

Tautomeric equilibrium is susceptible to various reaction conditions such as solvents, catalysts (metal salts), temperature, pH etc. which significantly affect the subsequent reaction outcomes.[15–17] To test whether the selectivity in the reaction of **2.01a** was vulnerable to changes in the tautomeric composition, the reaction of **2.01a** with allyl alcohol **2.02d** was performed in different solvents (Table 2.3) . No significant difference of the reaction media on selectivity was observed, however in solvents like MeOH, EtOH, TFE, and NO_2Me, the formation of **2.03a$_1$** was detected along with **2.03a$_2$**. The use of DMSO and DMC was found optimal, however DMC was chosen as the solvent of choice for further studies due of its favorable properties for sustainability (renewable, low toxicity and biodegradability).[18]

Table 2.3: Effect of solvents on the selectivity and allylation of **2.01a**

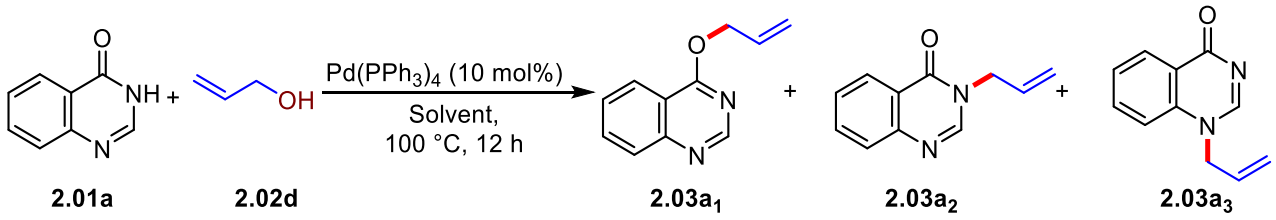

2.01a **2.02d** **2.03a$_1$** **2.03a$_2$** **2.03a$_3$**

Entry	Solvent	% Conversion[a]			Selectivity	Yield (%)[a]
		2.03a$_1$	**2.03a$_2$**	**2.03a$_3$**	**2.03a$_1$: 2.03a$_2$: 2.03a$_3$**	**2.03a$_2$**
1	MeOH	9	60	0	13 : 87 : 00	47
2	EtOH	5	90	0	05 : 95 : 00	78
3	TFE	2	97	0	02 : 98 : 00	81
4	1,4-Dioxane	0	97	0	00 : 100 : 00	84
5	THF	0	37	0	00 : 86 : 00	25
6	DMF	0	93	0	00 : 100 : 00	82
7	DMSO	0	96	0	00 : 100 : 00	85
8	PhMe	0	83	0	00 : 100 : 00	70
9	PhH	0	89	0	00 : 100 : 00	75
10	DCE	0	79	0	00 : 100 : 00	67
11	DMC	0	100	0	00 : 100 : 00	92
12	$MeNO_2$	5	46	0	09 : 91 : 00	29
13	MeCN	0	93	0	00 : 96 : 00	80

Reaction conditions: 2.01a (0.5 mmol) was treated with **2.02d** (2 equiv, 1 mmol) in various solvents (1 mL) at 100 °C in presence of $Pd(PPh_3)_4$ (10 mol%) for 12 h. [a]Based on GC-MS. [c]Isolated yield of **2.03a$_2$**.

2.3.4. Effect of palladium catalysts

A variety of transition metal-catalyzed allylic substitution are known, and the choice of metal and ligand can significantly affect the regioselectivity.[19–24] Thus, the reaction of **2.01a** with **2.02d** was investigated in the presence of different Pd catalysts (Table 2.4). The formation of **2.03a**$_2$ was observed with all Pd catalysts with varying yield, however $Pd(PPh_3)_4$ was found distinctly superior. Surprisingly, no effect of catalysts was observed on the overall selectivity towards product formation.

Table 2.4: Effect of palladium catalysts on selectivity and allylation of **2.01a**

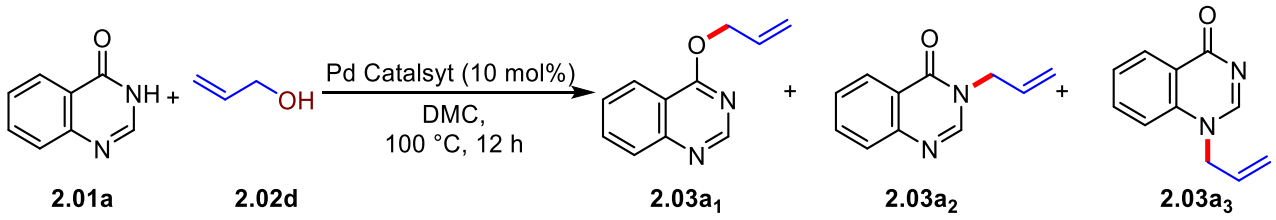

2.01a **2.02d** **2.03a$_1$** **2.03a$_2$** **2.03a$_3$**

Entry	Catalyst	% Conversion[a]			Yield (%)[b]
		2.03a$_1$	**2.03a$_2$**	**2.03a$_3$**	**2.03a$_2$**
1	$PdCl_2$	0	21	0	12
2	$Pd(OAc)_2$	0	18	0	10
3	$(PPh_3)_4Pd$	0	100	0	91
4	$(PPh_3)_2PdCl_2$	0	8	0	traces
5	$(TFA)_2Pd$	0	41	0	28
6	$[PdCl(C_3H_5)]_2$	0	40	0	28
7	$(C_6H_5CN)_2PdCl_2$	0	13	0	traces
8	$Pd_2(dba)_3$	0	12	0	traces
9	$Pd(dppf)Cl_2$	0	5	0	traces

Reaction conditions: 2.01a (0.5 mmol) was treated with **2.02d** (2 equiv, 1 mmol) in DMC (1 mL) at 100 °C in presence of different Pd-catalysts (10 mol%) for 12 h. [a]Based on GC-MS. [b]Isolated yield of **2.03a$_2$**.

2.3.5. Detailed optimization of all the reaction parameters

An overall extensive screening of the reaction parameters provided us with the utilization of 5 mol% of $Pd(PPh_3)_4$, 1.2 equiv of allyl alcohol in dimethyl carbonate at 100 °C for 12h as optimal conditions to yield **2.03b** as the sole product in 90% yield.

Table 2.5: Effect of different reaction parameters on the $Pd(PPh_3)_4$-catalyzed allylation of **2.01a** with **2.02da**.

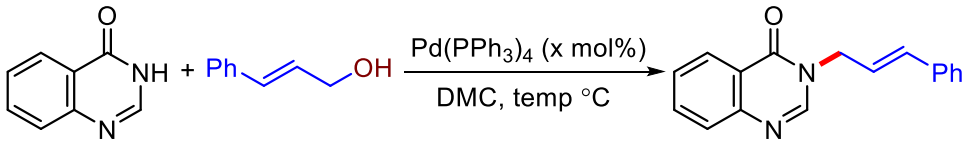

2.01a **2.02da** **2.03b**

Entry	catalyst (mol%)	equiv (**2.02da**)	Temp. (°C)	Time (h)	Yield (%)[a]
1	0.5	2	100	24	12
2	1	2	100	24	28
3	2.5	2	100	24	63
4	5.0	2	100	24	90
5	10	2	100	24	90
6	15	2	100	24	90
7	5.0	1	100	24	72
8	5.0	1.2	100	24	90
9	5.0	1.5	100	24	90
10	5.0	1.2	rt	24	traces
11	5.0	1.2	50	24	32
12	5.0	1.2	80	24	51
13	5.0	1.2	100	24	90
14	5.0	1.2	100	4	51
15	5.0	1.2	100	8	69
16	5.0	1.2	100	12	90
17	5.0	1.2	100	16	90

Reaction conditions: 2.01a (0.5 mmol) was treated with **2.02da** under different reaction conditions in DMC (1 mL). [a]Isolated yield of **2.03b**.

2.4. Mechanistic consideration

2.4.1. Intermolecular allyl migration

The predominant formation of **2.03a$_2$** irrespective of conditions tested (allylating reagent, base, solvent, catalyst, and ligand) increased our curiosity to investigate possible intramolecular allyl migration *via* intermediacy of **2.03a$_1$** and/or **2.03a$_3$**. Under catalysis, **2.03a$_1$**, **2.03a$_1$ or 2.03a$_3$** can potentially rearrange to form any one of the product depending on the parameters employed. To investigate allyl migration among the potential products, **2.03a$_1$**, **2.03a$_2$** and **2.03a$_3$** were prepared independently and subjected to optimized Pd(0) reaction conditions in DMC at 100 °C. A smooth conversion of **2.03a$_1$** into **2.03a$_2$** was observed, however **2.03a$_3$** failed to react (Scheme 2.7) under optimized reaction conditions. We also investigated other rearrangement pathways by which **2.03a$_1$** can be transformed to **2.03a$_2$** such as thermal or Lewis acid catalyzed [3,3]-sigmatropic rearrangement.[25,26] **2.03a$_1$**, when heated in DMC at 100 °C for 12 h with or without a Lewis acid [$In(OTf)_3$] did not produce any **2.03a$_2$**, ruling out the possibility of any sigmatropic rearrangements. On the contrary, addition of palladium catalyst to the reaction mixture containing **2.03a$_1$** formed product **2.03a$_2$** exclusively, indicating the exclusive role of the Pd-catalyst in allylic disposition from **2.03a$_1$** and its possible intermediacy in forming **2.03a$_2$**.[27,28]

Amine *N*-allylated compound **2.03a$_3$**, however did not undergo rearrangement to **2.03a$_2$** in all the conditions employed *viz* optimized palladium reaction conditions, thermal or Lewis acidic conditions for sigmatropic rearrangement, ruling out the intermediacy of **2.03a$_3$** in palladium catalyzed allylation of **2.03a$_2$**.

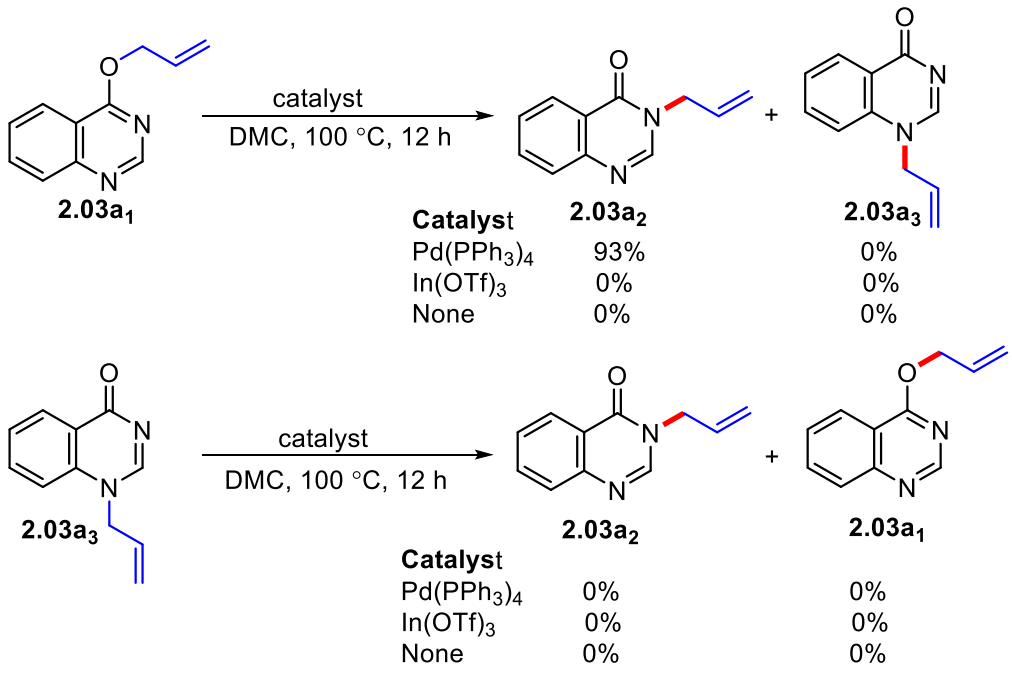

Scheme 2.7: Intermolecular allyl rearrangement from preformed **2.03a$_1$**, **2.03a$_3$** to **2.03a$_2$**

2.4.2. Plausible mechanistic pathways

To gain insight in to the possible mechanism of operation in our reaction condition, we have proposed different catalytic cycles as shown in Scheme 2.8 for the highly selective allylation of *N*-heterocycles with allyl alcohols. In all the cases, the first step is likely the coordination of $Pd(PPh_3)_4$ to allyl alcohols followed by oxidative addition of Pd(0) into the allylic alcohol to form an allylpalladium hydroxide intermediate (**A**). Nucleophilic attack on complex A can occur via three different pathways (Scheme 2.8). Path-A is the direct pathway, where in direct *N*-allylation of **2.01a** with loss of water would form the observed product **2.03a$_2$**. Alternatively, *O*-allylation could occur first to form **2.03a$_1$** as an intermediate (Path B). This could re-ionize to form bis allyl intermediate **B** that could produce the product **2.03a$_2$** (Path B-1). Alternatively, exogenous Pd(II) could catalyze a stepwise [3,3]-sigmatropic rearrangement to produce the final product (Path B-2). It should be noted that Path B-1 may be indistinguishable from Path A.

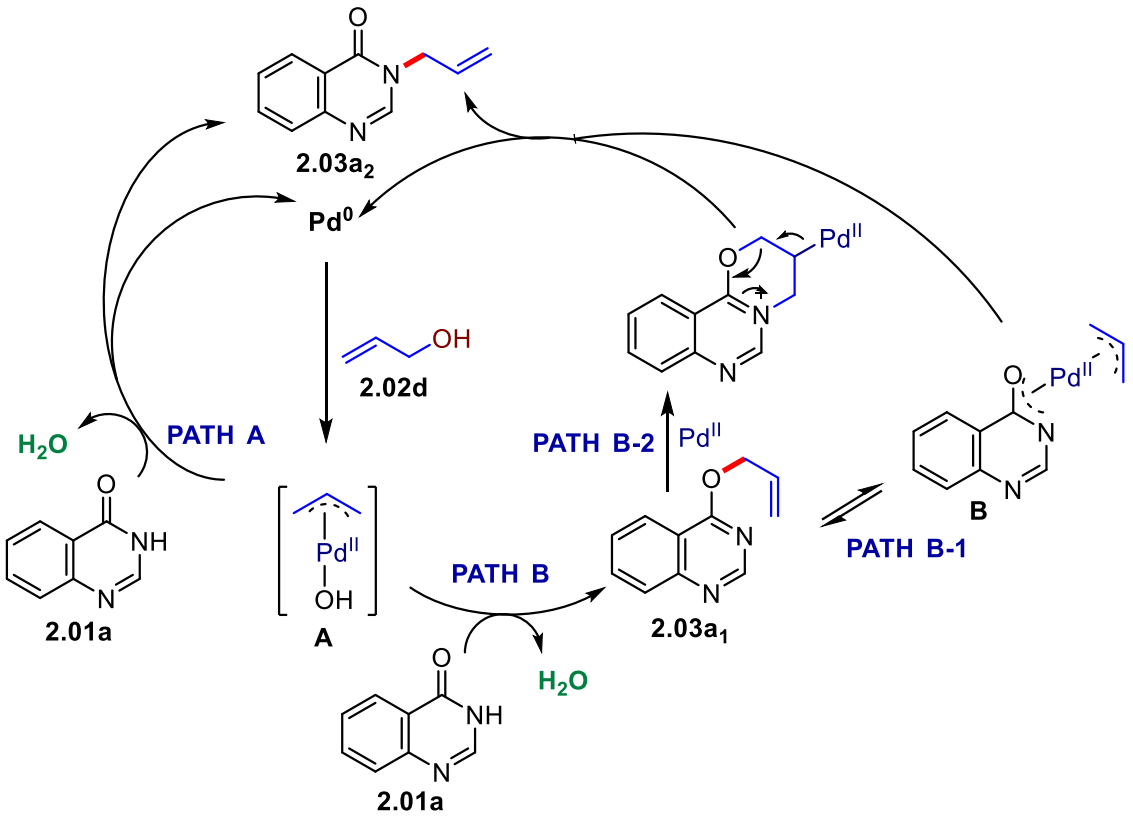

Scheme 2.8: Possible mechanistic pathways for the formation of **2.03a**$_2$

2.4.2.1. Control studies to validate pathways B-1 or B-2

To validate between two pathways, and to investigate allylic rearrangement between *O*-allylated product to *N*-allylated product, the crotyl product **2.04** was prepared and examined under the reaction conditions. If the rearrangement were to occur via Path B-1, a mixture of regioisomeric products would be expected. Alternatively, if the reaction proceeds through Path B-2, only the branched product would result. When **2.04** was subjected to optimized reaction conditions, we observed the formation of a mixture of regioisomers **2.05a** and **2.05b** (92:8; GC-MS) demonstrating the ionization pathway B-1 is operative, if the rearrangement were to happen (Scheme 2.9). But in optimized reaction conditions, we did not observe any branched product indicating that direct allylic substitution (Path-A) is the most plausible pathway for allylation of *N*-heterocycles with allyl alcohols.

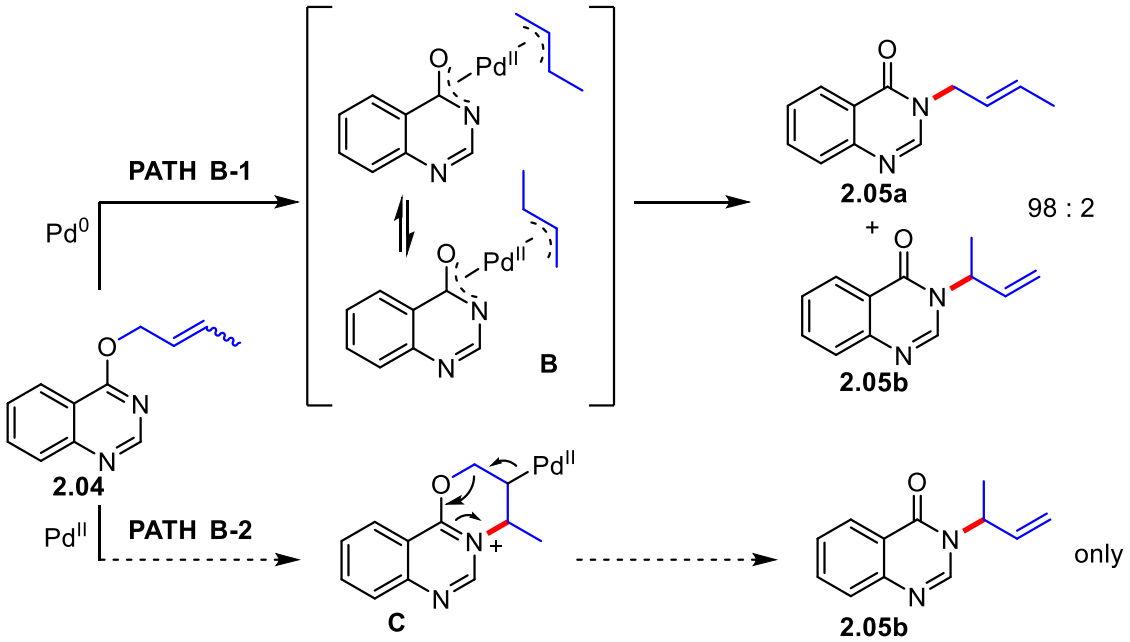

Scheme 2.9: Control studies to validate different pathways

2.5. Substrate scope: tautomerizable heterocycles

With optimization conditions in hand, and with establishing most possible mechanistic pathway, we started exploring the generality of the optimized methodology. The scope of tautomerizable heteroarenes was examined first. As summarized in Table 6, a wide range of 4-hydroxy quinazolines bearing alkyl, cycloalkyl, aryl, heteroaryl, and styryl moieties were reacted with cinnamyl alcohol **2da** affording excellent yield of *N*-allylated products (**2.03b-2.03p**). A wide range of functional groups involving both electron donating (-OMe, -NMe_2), electron withdrawing (-NO_2, -CN, -Cl, CF_3) and sensitive functional groups (-CHO, -COMe, -OCH_2O-) were tolerated well, validating the robustness of protocol. The applicability of this protocol was further extended to other biologically relevant tautomerizable heteroarenes. Compounds which are highly sensitive to tautomerization (**2.03q-2.03y**) were also tested under optimized condition. Gratifyingly, *N*-cinnamylation of these compounds also proceeded well with excellent yields.

Table 2.6: Cinnamylation of biologically relevant heteroarenes.

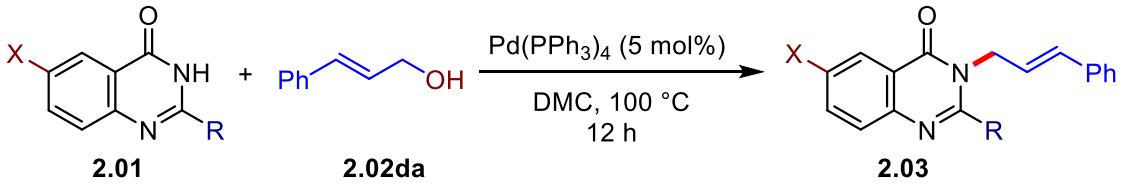

2.01 **2.02da** **2.03**

Heteroarenes	Products	Yield (%)[a]
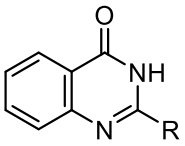	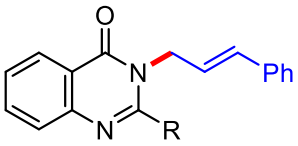	
2.01a: R = H	**2.03b**: R = H	90
2.01b: R = Me	**2.03c**: R = Me	91
2.01c: R = Cy	**2.03d**: R = Cy	85
2.01d: R = Ph	**2.03e**: R = Ph	88
2.01e: R = furyl	**2.03f**: R = furyl	84
2.01f: R = styryl	**2.03g**: R = styryl	72
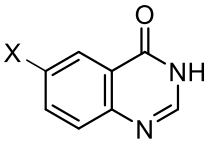	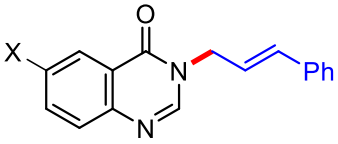	
2.01g: X = Cl	**2.03h**: X = Cl	84
2.01h: X = OMe	**2.03i**: X = OMe	90
2.01i: X = NO_2	**2.03j**: X = NO_2	82

Table 2.6: Cinnamylation of biologically relevant heteroarenes (continued).

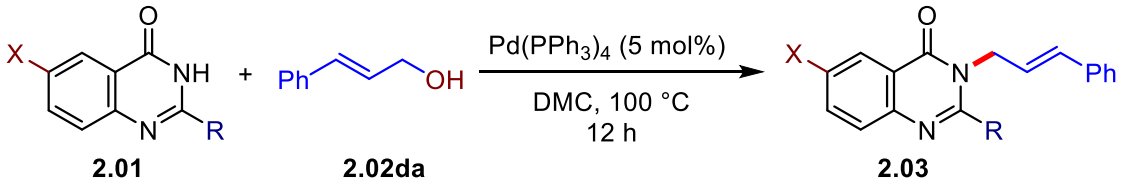

2.01 **2.02da** **2.03**

Heteroarenes	Products	Yield (%)[a]
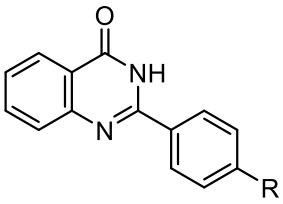	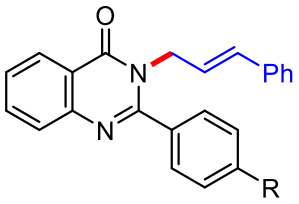	
2.01j: R = NMe_2	**2.03k**: R = NMe_2	85
2.01k: R = CF_3	**2.03l**: R = CF_3	86
2.01l: R = CN	**2.03m**: R = CN	85
2.01m: R = C(O)H	**2.03n**: R = C(O)H	90
2.01n: R = C(O)Me	**2.03o**: R = C(O)Me	85
2.01o: 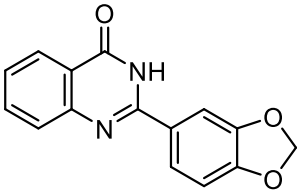	**2.03p:** 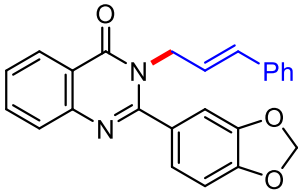	83
2.01p: 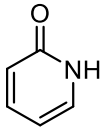	**2.03q:** 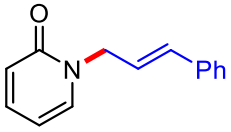	81
2.01q: 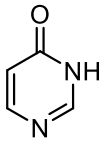	**2.03r:** 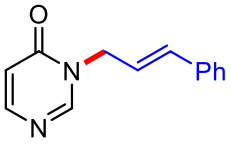	82
2.01r: 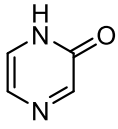	**2.03s:** 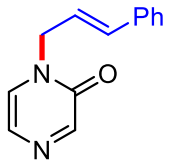	84

Table 2.6: Cinnamylation of biologically relevant heteroarenes (continued).

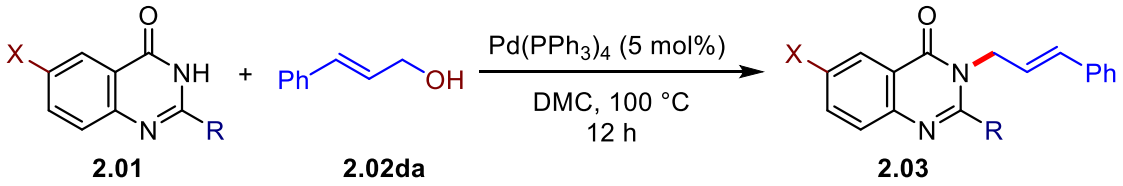

2.01 **2.02da** **2.03**

Heteroarenes	Products	Yield (%)[a]
2.01s: 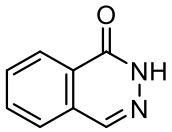	**2.03t:** 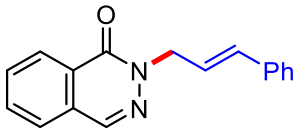	89
2.01t: 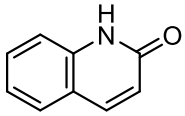	**2.03u:** 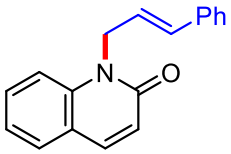	86
2.01u: 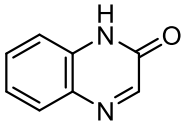	**2.03v:** 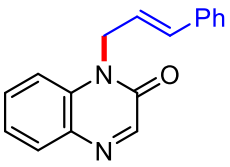	90
2.01v: 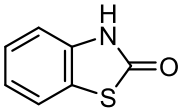	**2.03w:** 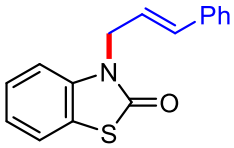	86
2.01w: 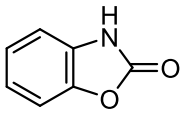	**2.03x:** 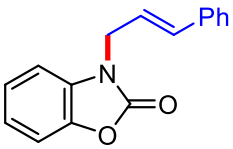	90
2.01x: 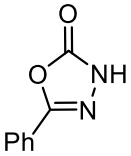	**2.03y:** 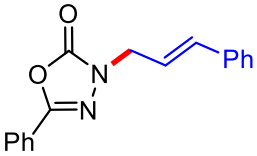	86

Reaction conditions: Tautomerizable heteroarenes (0.5 mmol) were treated with 2.02da (1.2 equiv, 0.6 mmol) in DMC (1 mL) at 100 °C in the presence of $Pd(PPh_3)_4$ (5 mol %) for 12 h. [a]Isolated yield.

2.6. Substrate scope: allyl alcohols

After the functionalization of heterocycles, we turned our attention towards the allylation of **2.01a** with a variety of allyl alcohols having either α-, β-, or γ-substitution. Our reaction conditions were found to be optimal even for substituted allyl alcohols producing the allylated products in excellent yields (Table 2.7).[29] With regards to regioselectivity, allylation with cinnamyl alcohol **2.02da** or 1-phenylprop-2-en-1-ol **2.02db** resulted in exclusive formation of the linear product (>99%; GC-MS) whereas a 94:6 isomeric ratio (linear: branched) was observed in the case of **2.02dc** or **2.02dd**. The reaction of **2.01a** with 2-butene-1,4-diol **2.02dh**, produced the dienamine **2.06d** in excellent yield. This could serve as model reaction for a generalized one-step synthesis of dienamines, alkenyl oxide/sulfide and conjugated dienes, a valuable synthon for pharmaceutical and materials applications. This methodology was found to be advantageous in terms of substrate scope, functional group tolerance and the use of additives or other promoters.[30–36]

Table 2.7: Pd-catalyzed reaction of **2.01a** with different allyl alcohols.

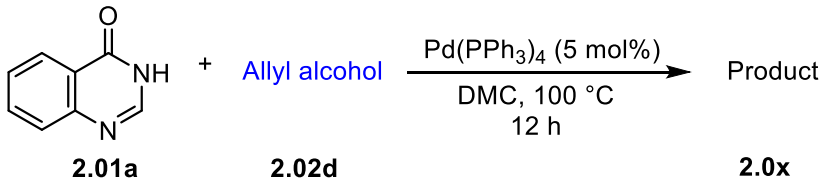

2.01a **2.02d** **2.0x**

Allyl alcohol	Product	Yield (%)[a]
2.02d; 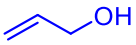	**2.03a2**: 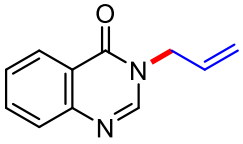	91
2.02da: 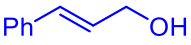	**2.03b**: 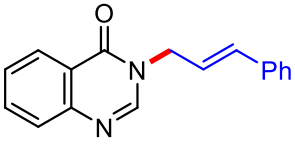	90
2.02db: 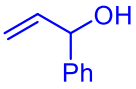	**2.03b**: 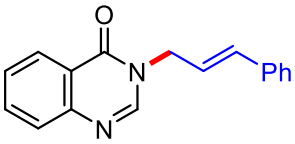	88
2.02dc: 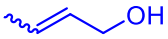	**2.05a**: 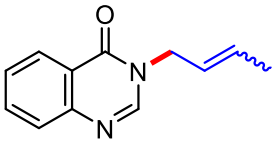	82[b]
2.02dd: 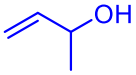	**2.05a**: 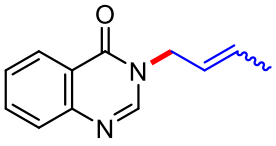	81[b]
2.02de: 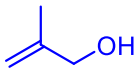	**2.06a**: 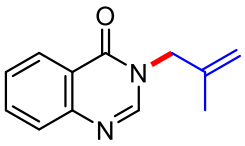	86
2.02df: 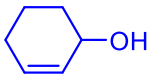	**2.06b**: 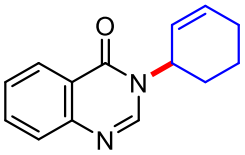	78

Table 2.7: Pd-catalyzed reaction of **2.01a** with different allyl alcohols (continued).

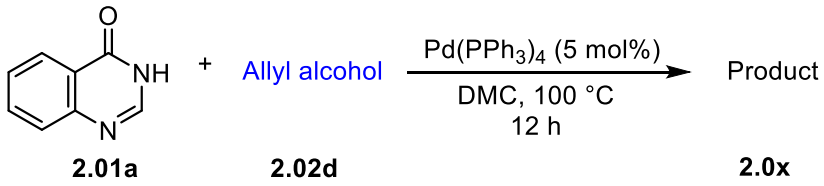

2.01a **2.02d** **2.0x**

Allyl alcohol	Product	Yield (%)[a]
2.02dg: 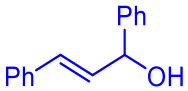	**2.06c**: 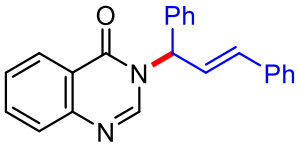	71
2.02dh: 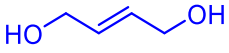	**2.06d**: 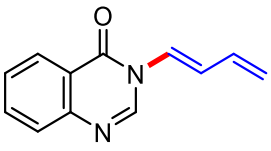	82

Reaction conditions: 2.01a (0.5 mmol) was treated with allyl alcohol (1-1.5 equiv) in DMC (1 mL) at 100 °C in the presence of $Pd(PPh_3)_4$ (5 mol %) for 12 h. [a]Isolated yield. [b]E/Z mixture (10:1). A small amount of the branched regioisomer (not shown) was also formed (94:6 linear: branched).

2.7. Conclusion

In conclusion, the present work reports the investigation of a wide range of allylating reagents, solvents, metal catalysts, and ligands for the chemo- and regioselective allylation of heteroarenes bearing multiple interconvertible nucleophilic sites. The process was developed as a generalized green protocol for allylation of biologically relevant heteroarenes with allyl alcohols using DMC as solvent with wide range of functional groups tolerance. The differential nucleophilicity of heteroarenes was examined through intermolecular competition studies involving two different heteroarenes and excellent selectivity was observed. Similarly, an excellent selectivity was observed during intermolecular competition involving two different allyl alcohols demonstrating the differential ability of allyl alcohols to form allylpalladium complexes and react with the nucleophile. The direct use of allyl alcohol as an allylating reagent, DMC as solvent, the lack of a requirement for additional additives/promoters, and the feasibility of scale up represent a

green protocol for the selective allylation of medicinally relevant tautomerizable *N*-heteroarenes and are an important addition to the tool box of medicinal chemists.

2.8. Experimental procedures

2.8.1. General information

Unless otherwise noted, all manipulations were carried out under a nitrogen atmosphere using standard Schlenk-line or glovebox techniques. All glassware was oven-dried for at least 1h prior to use. THF, toluene, ether, and hexane were degassed by purging with nitrogen for 45 min and dried with a solvent purification system (MBraun MB-SPS). DMF, dioxane, dimethoxyethane, dichloroethane, methanol, and ethanol were dried over activated 3 Å molecular sieves and degassed by purging with nitrogen. All commercially obtained reagents/solvents were purchased from Alfa Aesar®, Sigma-Aldrich®, Acros®, TCI America®, Mallinckrodt®, and Oakwood® Products, and used as received without further purification. TLC plates were visualized by exposure to ultraviolet light. Organic solutions were concentrated by rotary evaporation at ~10 torr. Flash column chromatography was performed with 32–63 microns silica gel. ^{1}H NMR spectra were obtained on a 400 MHz spectrometer, and chemical shifts were recorded relative to residual protiated solvent. ^{13}C NMR spectra were obtained at 100 MHz, and chemical shifts were recorded to the solvent resonance. Both ^{1}H and ^{13}C NMR chemical shifts were reported in parts per million downfield from tetramethylsilane (δ = 0 ppm). ^{19}F NMR spectra were obtained at 282.4 MHz, and all chemical shifts were reported in parts per million upfield of CF_3COOH (δ = -78.5 ppm). Coupling constants (J) are reported in hertz (Hz). Standard abbreviations indicating multiplicity were used as follows: s (singlet), br (broad), d (doublet), t (triplet), q (quartet) and m (multiplet). Data for ^{13}C NMR spectra are reported in terms of chemical shift (δ ppm). High-resolution mass spectra were obtained from a Bruker Daltronics BioTOF HRMS spectrometer.

2.8.2. Synthesis of standard materials of 2.03a$_1$, 2.03a$_2$, and 2.03a$_3$

2.8.2.1. Synthesis of 4-(allyloxy) quinazoline (2.03a$_1$)[37]

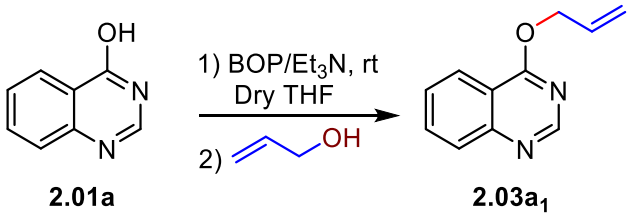

2.01a **2.03a$_1$**

In a glove box, to an oven dried 4 mL glass vial equipped with a stir bar, 4-hydroxy quinazoline **2.01a** (0.146 g, 1 mmol), BOP [(1-Benzotriazol-1-yloxy) tris (dimethylamino) phosphonium hexafluorophosphate] (0.885 g, 2 mmol, 2 equiv), Cs_2CO_3 (0.652 g, 2 mmol, 2 equiv) followed by dry THF (3 mL) was added and the reaction mixture was stirred at rt for 60 min. The resulting mixture was evaporated under reduced pressure, Cs_2CO_3 (0.652 g, 2 mmol, 2 equiv) and allyl alcohol **2.02d** (1.16 g, 20 mmol, 20 equiv) were added followed by stirring at rt until TLC (5 h) indicated complete reaction. The reaction mixture was diluted with water (10 mL) and extracted with EtOAc (3 x 10 mL). The organic layer was dried over anhyd. Na_2SO_4 and concentrated under reduced pressure. The crude products were adsorbed on silica gel and pass through the column (eluent: Hexane/EtOAc) to get analytically pure product 3a$_1$ (0.130 g, 70%) as yellowish liquid; **^{1}H NMR** (400 MHz, $CDCl_3$): δ 8.79 (d, J = 2.9 Hz, 1H), 8.16 (t, J = 2.3 Hz, 1H), 7.92 (t, J = 3.7 Hz, 1H), 7.82-7.79 (m, 1H), 7.55-7.51 (m, 1H), 6.19-6.12 (m, 1H), 5.48 (dd, J = 17.2, 1.5 Hz), 5.34-5.31 (m, 1H), 5.09 (d, J = 0.9 Hz, 1Hz); **^{13}C NMR** (100 MHz, $CDCl_3$): δ 166.3, 154.3, 151.0, 133.5, 132.3, 127.7, 127.0, 123.5, 118.4, 116.6, 67.5.

2.8.2.2. Synthesis of 3-allylquinazolin-4(3H)-one (2.03a$_2$)[38]

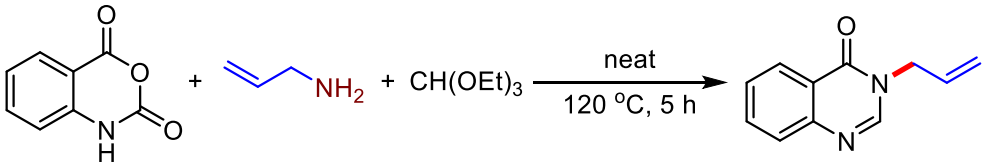

2.01y **2.02j** **2.03a$_2$**

A mixture of isatoic anhydride, **2.01y** (0.163 g, 1 mmol), allylamine, **2.02j** (0.086 g, 1.5 mmol, 1.5 equiv), and triethyl orthoformate (0.41 g, 2.5 mmol) were stirred magnetically at 120 °C (oil bath temp). After completion of the reaction (TLC, 5 h), the crude reaction mixture was recrystallized from EtOH to obtain analytically pure **2.03a$_2$** (0.134 g, 72%) as white solid; **^{1}H NMR** (400 MHz, $CDCl_3$): δ8.34 (d, J = 8.0 Hz, 1H), 8.04 (s, 1H), 7.80-7.72 (m, 2H), 7.55-7.50 (m, 1H), 6.07- 5.97 (m, 1H), 5.31 (t, J =10.1 Hz, 2H), 4.66 (d, J = 5.7 Hz, 2H); **^{13}C NMR** (100.6 MHz, $CDCl_3$): δ160.8, 148.1, 146.2, 134.3, 131.9, 127.5, 127.3, 126.8, 122.1, 118.9, 48.3.

2.8.2.3. Synthesis of 1-allylquinazolin-4(1H)-one (2.03a$_3$)[39]

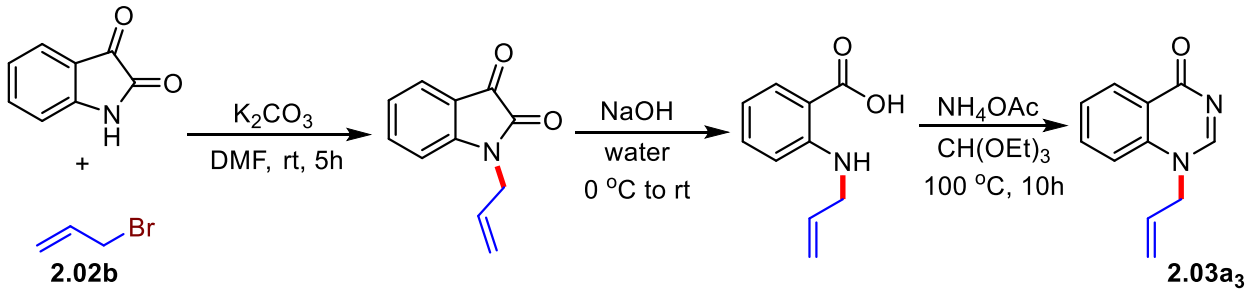

2.02b **2.03a$_3$**

Step 1: To a solution of isatin (1.47 g, 10 mmol) in DMF (10 mL), potassium carbonate (1.65 g, 12 mmol, 1.2 equiv) and allyl bromide (3.62 g, 30 mmol, 3 equiv) were added. After reacting at rt for 5 h (monitored by TLC), the mixture was poured into ice water. The precipitate formed was filtered, dried and used as such without further purification.

Step 2: A solution of sodium hydroxide (0.84 g, 21 mmol) in water (10 mL) was cooled in an ice-water bath. N-allyl isatin (10 mmol) was then added and dissolved. While maintaining the

temperature of below 15 °C, a 30% aqueous solution of hydrogen peroxide (1.8 g, 52.8 mmol) was added dropwise. Stirring was continued at 15–20 °C for 2 h (monitored by TLC). The mixture was cooled in an ice bath and pH was adjusted to 5–6 with glacial acetic acid. After several hours of standing in refrigerator, the precipitate formed was collected by filtration, washed with ice water three times, and dried in air to give the 2-(*N*-allyl amino) benzoic acid.

Step 3: A mixture of 2-(*N*-allyl amino) benzoic acid (0.53 g, 3 mmol), ammonium acetate (0.69 g, 9 mmol) and triethyl orthoformate (2.22 g, 15 mmol) was stirred at 100 °C for 10 h (monitored by TLC). Excess triethyl orthoformate was removed by rotary evaporation, and the residue was applied to a silica-gel column and eluted with DCM: MeOH (95:5) to give analytically pure **2.03a**$_3$ (0.379 g, 68%) as white solid; **^{1}H NMR** (400 MHz, $CDCl_3$): δ 8.24-8.22 (m, 2H), 7.67-7.62 (m, 1H), 7.41-7.37 (m, 1H), 7.29 (d, J = 8.4 Hz 1H), 6.00 - 5.90 (m, 1H), 5.31-5.28 (m, 1H), 5.19-5.15 (m, 1H), 4.74 (d, J = 4.9 Hz 2H); **^{13}C NMR** (100 MHz, $CDCl_3$): δ 169.4, 153.3, 139.2, 133.8,130.6, 128.7, 124.4, 120.4, 119.3, 115.4, 52.2.

2.8.3. Experimental procedure for the investigation of allylic disposition

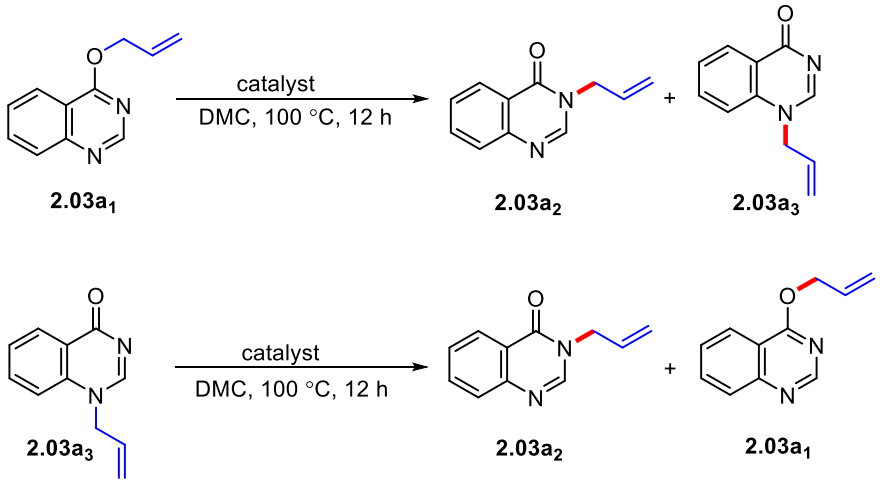

In a glove box, to an oven dried 4 mL glass vial equipped with a stirring bar, **2.03a$_1$** (0.093 g, 0.5 mmol) or **2.03a**$_3$ (0.093 g, 0.5 mmol), $Pd(PPh_3)_4$ (0.578 g, 0.05 mmol, 10 mol%), followed

by DMC (1 mL) was added and the reaction mixture was stirred at 100 °C for 12 h. Then the reaction mixture was cooled to rt, diluted with MeOH (2 x 10 mL) and passed through bed of celite to remove catalyst. An aliquot portion (100 µL) of the organic layer was taken out, diluted with MeOH and subjected to GCMS to observe the selectivity among all the products formed.

In case where **2.03a$_1$** is used as the starting material, it is completely converted to **2.03a$_2$**. The organic layer was dried over anhydrous Na_2SO_4 and concentrated under reduced pressure. The crude products were adsorbed on to silica gel and passed through the column (eluent: Hexane/EtOAc) to get analytically pure product **2.03a$_2$** as white solid (0.086 g, 93%).

2.8.4. Investigation of allylic migration from 2.03a$_1$ in different conditions

Table 2.8: Treatment of **2.03a$_1$** in the presence of different catalysts under reaction conditions.

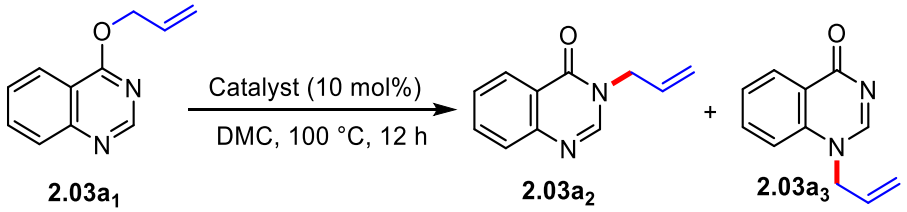

Entry	Catalyst	% Conversion[a]		Selectivity[a]	Yield (%)[b]
		2.03a$_2$	**2.03a$_3$**	**2.03a$_2$: 2.03a$_3$**	**2.03a$_2$**
1	None	0	0	N/A	0
2	K_2CO_3	0	0	N/A	0
3	$In(OTf)_3$	0	0	N/A	0
4	$(PPh_3)_4Pd$	100	0	100 : 00	93

Reaction conditions: 2.03a$_1$ (0.5 mmol) was subjected to under reaction condition in presence of different catalysts/additives in DMC (1 mL) at 100 °C for 12 h. [a] Based on GC-MS. [b] Isolated yield of **2.03a$_2$**

2.8.5. Validation of route B-1 / B-2: investigation of allylic migration from 2.04

2.8.5.1. Synthesis of (E)-4-(but-2-en-1-yloxy)quinazoline (2.04)[38]

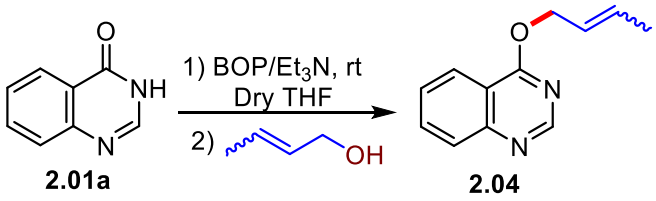

In a glove box, to an oven dried 10 mL glass vial equipped with a stirring bar, 4-hydroxy quinazoline **2.01a** (0.292 g, 2 mmol), BOP reagent (1.77 g, 4 mmol, 2 equiv), Cs_2CO_3 (1.304 g, 2 mmol, 2 equiv) followed by dry THF (6 mL) was added and the reaction mixture was stirred at rt for 60 min. The resulting mixture was evaporated under reduced pressure, Cs_2CO_3 (1.304 g, 4 mmol, 2 equiv) and 2-buten-1-ol (2.88 g, 40 mmol, 20 equiv) were added followed by stirring at the rt until TLC (5 h) indicated reaction completion. The reaction mixture was then diluted with water (15 mL) and extracted with EtOAc (3 x 15 mL). The organic layer was dried over anhydrous Na_2SO_4 and concentrated under reduced pressure. The crude products were adsorbed on to silica gel and passed through the column (eluent: Hexane/EtOAc) to get analytically pure product **2.04** (0.288 g, 72%) as yellowish liquid; **^{1}H NMR** (400 MHz, $CDCl_3$): δ 8.80 (s, 1H), 8.19 (dd, J = 8.2, 0.6 Hz, 1H), 7.95 (d, J = 8.4 Hz, 1H), 7.84-7.80 (m, 1H), 7.57-7.53 (m, 1H), 5.99-7.89 (m, 1H), 5.87-7.83 (m, 1H), 5.03 (dd, J = 6.2, 0.9 Hz, 1H), 1.78 (d, J = 0.8 Hz, 3H); **^{13}C NMR** (100 MHz, $CDCl_3$): δ 166.5, 154.4, 150.9, 133.4, 131.6, 127.6, 126.9, 125.2, 123.6, 116.7, 67.6, 17.8; **HRMS** (ESI-TOF) m/z: [M + H]+ Calcd for $C_{12}H_{13}N_2O$ 201.1028, Found 201.1031.

2.8.5.2. Experimental procedure for the validation of route B-1 / B-2

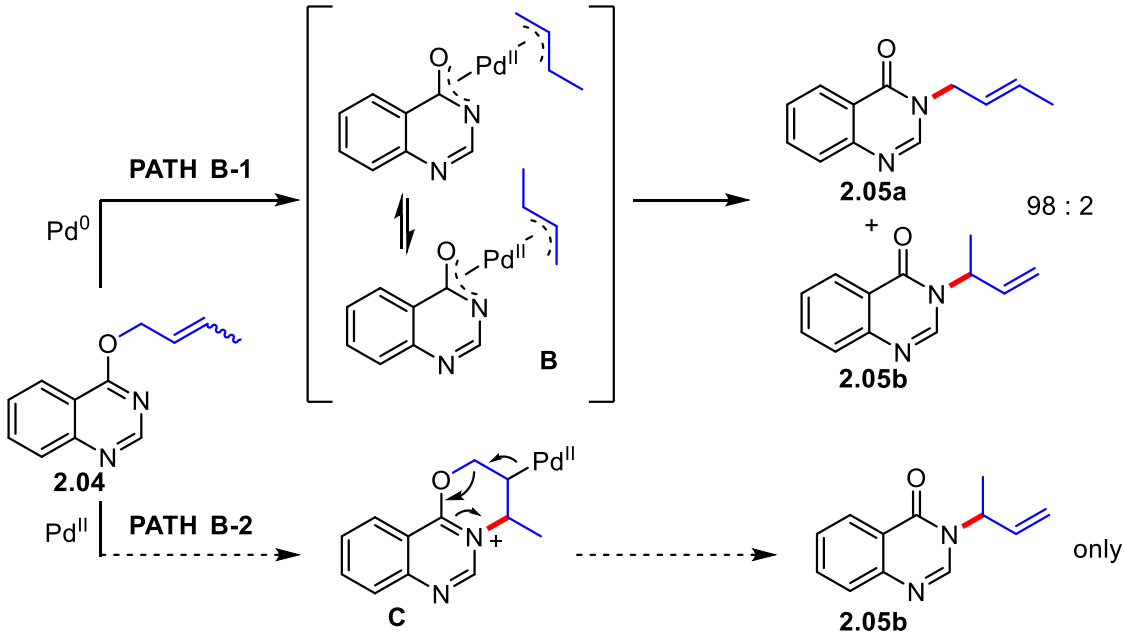

In a glove box, to an oven dried 4 mL glass vial equipped with a stirring bar, **2.04** (0.1 g, 0.5 mmol), $Pd(PPh_3)_4$ (0.578 g, 0.05 mmol, 10 mol%) followed by DMC (1 mL) was added and the reaction mixture was stirred at 100 °C for 12 h. The reaction mixture was cooled to rt, diluted with MeOH (2 x 10 mL) and passed through bed of celite to remove catalyst. An aliquot portion (100 µL) of the organic layer was taken out, diluted with MeOH. and subjected to GCMS to observe the selectivity. The organic layer was dried over anhydrous Na_2SO_4 and concentrated under reduced pressure. The crude products were adsorbed on silica gel and passed through the column (eluent: Hexane/EtOAc) to get analytically pure product **2.05a** as white solid (0.074 g, 74%). **^{1}H NMR** (400 MHz, $CDCl_3$): δ 8.24 (td, J = 8.1, 1.4 Hz, 1H), 7.98 (s, 1H), 7.67-7.62 (m, 2H), 7.44-7.39 (m, 1H), 5.76-5.70 (m, 1H), 5.61-5.57 (m, 1H), 4.50 (td, J = 7.4, 2.3 Hz, 2H), 1.67-1.65 (m, 3H); **^{13}C NMR** (100 MHz, $CDCl_3$): δ 160.9, 160.7, 148.0, 146.2, 146.1, 134.0, 131.0, 130.0, 127.3, 127.12, 127.10, 126.7, 126.6, 124.8, 123.9, 122.1, 47.8, 42.7, 17.6, 13.1; **HRMS** (ESI-TOF) m/z: $[M + H]^+$ Calcd for $C_{12}H_{13}N_2O$ 201.1028, Found 201.1030.

2.8.6. Preparation of starting materials

Compounds **2.01a, 2.01p-2.01w** and allyl alcohols were purchased from commercial sources and used as such. All other starting materials were prepared by a modified procedure from literature.

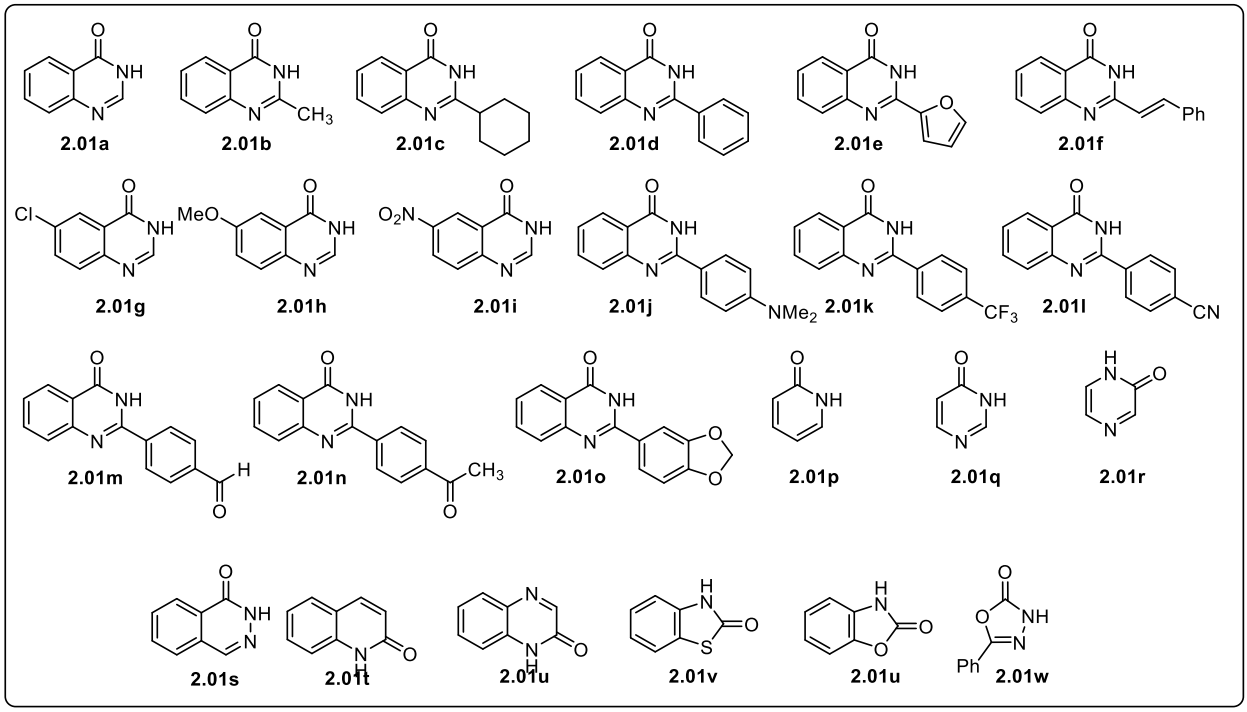

Figure 2.1: *N*-Heterocycles employed for the allylation

2.8.6.1. Experimental procedure for the synthesis of 2.01b

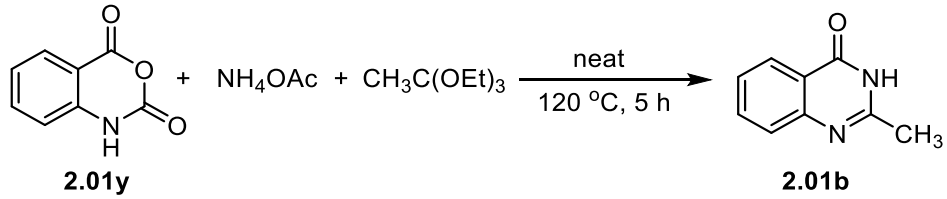

A mixture of isatoic anhydride (0.815 g, 5 mmol), ammonium acetate (0.578 g, 7.5 mmol, 1.5 equiv), and triethyl orthoacetate (1.22 g, 7.5 mmol, 1.5 equiv) were stirred magnetically at 120 °C (oil bath temp). After completion of the reaction (TLC, 5 h), the crude reaction mixture was recrystallized from EtOH to obtain analytically pure **2.01b** (0.640 g, 80%) as white solid.[39] **^{1}H**

NMR (400 MHz, $CDCl_3$): δ 8.27 (dd, *J* = 7.5, 1.2 Hz, 1H), 7.80-7.78 (m, 1H), 7.71 (d, *J* = 7.7 Hz, 1H), 7.52-7.48 (m, 1H), 2.63 (s, 3H); **^{13}C NMR** (100 MHz, $CDCl_3$): δ 164.8, 153.7, 149.8, 135.5, 127.3, 127.0, 126.5, 120.6, 22.6.

2.8.6.2. Experimental procedure for the synthesis of 2.01g

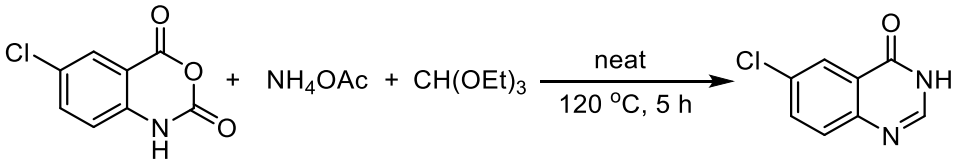

2.01g

A mixture of isatoic anhydride (0.815 g, 5 mmol), ammonium acetate (0.578 g, 7.5 mmol, 1.5 equiv), and triethyl orthoformate (1.22 g, 7.5 mmol, 1.5 equiv) were stirred under heating at 120 °C (oil bath temp). After completion of the reaction (TLC, 5 h), the crude reaction mixture was recrystallized from EtOH to obtain analytically pure compound **2.01g** as an off white solid (0.659 g, 73%). **^{1}H NMR** (400 MHz, DMSO): δ 12.47 (s, br, 1H), 8.12 (s, 1H), 8.03 (d, *J* = 2.4 Hz, 1H), 7.82-7.79 (m, 1H), 7.67 (d, *J* = 8.6 Hz, 1H); **^{13}C NMR** (100 MHz, DMSO): δ 160.2, 147.9, 146.4, 134.8, 131.5, 129.9, 125.3, 124.3.

2.8.6.3. Experimental procedure for the synthesis of 2.01c-2.01f and 2.01j-2.01o

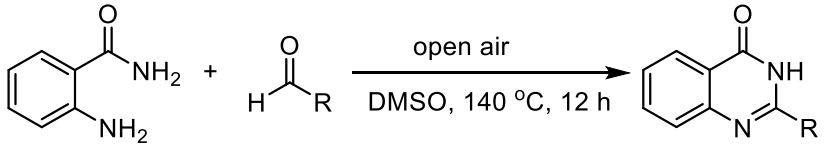

2.01

Anthranilamide (5.0 mmol) and an appropriate aldehyde (6 mmol, 1.2 equiv) were dissolved in DMSO (10 mL). Then, the reaction mixture was stirred at 140 °C in an open flask and monitored by TLC. After complete consumption of the starting materials (12-36 h), the reaction mixture was cooled to rt, the precipitate formed after the addition of water (100 mL) was added to

the reaction mixture and collected via filtration. Recrystallization in ethanol afforded pure 4-hydroxy quinazolines.

2.8.6.4. Experimental procedure for the synthesis of (2.01x)[40]

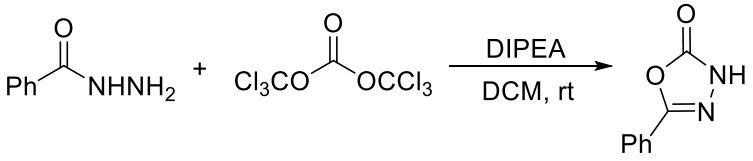

To a round bottom flask containing a magnetic stir bar was added benzhydrazide (2.0 g, 14.7 mmol), CH_2Cl_2 (300 mL) and DIPEA (5.1 mL, 29 mmol, 2 equiv). The flask was fitted with a rubber septum containing two needles: one connected to a positive pressure N_2 line, the other open to air. Triphosgene (1.75 g, 5.9 mmol, 0.4 equiv) and CH_2Cl_2 (10 mL) were added to a 40 mL vial; the vial was sonicated until the triphosgene had dissolved. Using a syringe, the triphosgene/CH_2Cl_2 solution was added drop wise to the stirred solution of benzhydrazide. The solution was stirred at room temperature; by TLC analysis, the reaction was nearly complete within 20 minutes (hexanes/EtOAc). The reaction mixture was concentrated by rotary evaporation; the crude product was purified by chromatography on silica (gradient elution from hexanes to EtOAc) affording **2.01x** (0.689 g, 72%) as a white solid; **^{1}H NMR** (400 MHz, DMSO-d_6): δ 12.51 (br, 1H), 7.85-7.73 (m, 2H), 7.62-7.53 (m, 3H); **^{13}C NMR** (100 MHz, DMSO-d_6): δ 154.7, 154.1, 131.6, 129.5, 125.5, 124.2.

2.9. Analytical data of purified starting materials

2-Cyclohexyl-3*H*-quinazolin-4-one: Prepared from anthranilamide (5.0 mmol) and cyclohexane carboxaldehyde (6 mmol, 1.2 equiv) by the general procedure to give **2.01c** as a white solid (0.913 g, 80%). **^{1}H NMR** (400 MHz, DMSO-d6): δ 12.72 (br, 1H), 8.08 (d, J = 7.5 Hz, 1H), 7.76 (t, J = 7.1 Hz, 1H), 7.59 (d, J = 8.1 Hz, 1H), 7.45 (t, J = 7.4Hz, 1H), 2.61-2.51 (m, 2H), 1.92-1.77 (m, 4H),

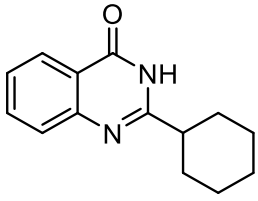

1.69-1.54 (m, 3H), 1.34-1.20 (m, 3H); **^{13}C NMR** (100 MHz, DMSO-d6): δ 162.4; 161.26, 149.29, 134.7, 127.3, 126.4, 126.1, 121.4, 43.3, 30.6, 25.9, 25.8.

2-Phenyl-3*H*-quinazolin-4-one: Prepared from anthranilamide (5.0 mmol) and benzaldehyde (6 mmol, 1.2 equiv) by the general procedure to give **2.01d** as a white solid (0.911 g, 82%). **^{1}H NMR** (400 MHz, DMSO-d6): δ 12.51 (br, 1H), 8.16 (d, J = 7.5 Hz, 3H), 7.85 (t, J = 7.3 Hz, 1H), 7.78 (d, J = 8.4 Hz, 1H), 7.66-7.55 (m, 4H); **^{13}C NMR** (100 MHz, DMSO-d6): δ 162.5, 152.4, 148.6, 134.7, 132.6, 131.4, 128.8, 127.5, 127.4, 126.7, 125.7, 120.7.

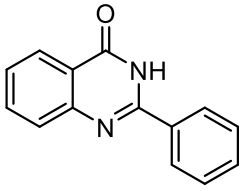

2-Furan-2-yl-3*H*-quinazolin-4-one: Prepared from anthranilamide (5.0 mmol) and furfural (6 mmol, 1.2 equiv) by the general procedure to give **2.01e** as a white solid (0.859 g, 81%); **^{1}H NMR** (400 MHz, DMSO-d_6): δ 12.50 (br, 1H), 8.13 (d, J = 7.4 Hz, 1H), 8.01-7.80 (m, 2H), 7.70-7.64 (m, 2H), 7.50 (t, J = 7.4 Hz, 1H), 6.76 (q, J = 1.5 Hz, 1H); **^{13}C NMR** (100 MHz, DMSO-d_6): δ 162.0, 149.1, 147.1, 146.6, 144.5, 135.1, 127.7, 126.9, 126.4, 121.6, 114.9, 112.9.

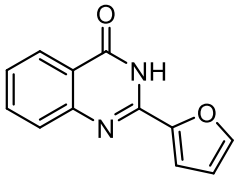

2-Styryl-3*H*-quinazolin-4-one: Prepared from anthranilamide (5.0 mmol) and cinnamaldehyde (6 mmol, 1.2 equiv) by the general procedure to give **2.01f** as a white solid (0.307 g, 62%); **^{1}H NMR** (400 MHz, DMSO-d_6): δ 8.32 (d, J = 7.9 Hz, 1H), 7.99 (d, J = 15.3 Hz, 1H), 7.82 (d, J = 3.5 Hz, 2H) 7.64-7.55 (m, 3H), 7.52-7.49 (m, 1H), 7.35-7.29 (m, 7H), 6.40 (d, J = 15.6 Hz, 1H); **^{13}C NMR** (100 MHz, DMSO): δ 162.7, 152.3, 149.7, 138.9, 135.6, 135.1, 130.4, 129.6, 128.2, 127.7, 126.7, 126.5, 121.8.

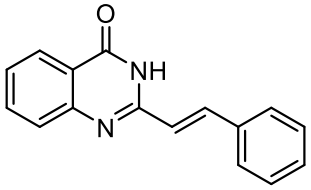

2-(4-Dimethylamino-phenyl)-3*H*-quinazolin-4-one: Prepared from anthranilamide (5.0 mmol) and 4-(dimethylamino)benzaldehyde (6 mmol, 1.2 equiv) by the general procedure to give **2.01j** as a brown solid (0.968 g, 73%); 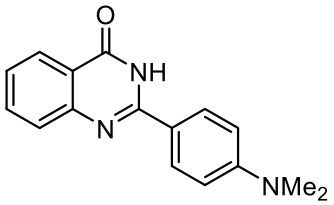

^{1}H NMR (400 MHz, DMSO-d_6): δ 12.18 (br, 1H), 8.09-8.14 (m, 3H), 7.75-7.79 (m, 1H), 7.65 (d, J = 7.6 Hz, 1H), 7.40-7.44 (m, 1H), 6.78 (d, J = 9.1 Hz, 2H), 3.00 (s, 6H); **^{13}C NMR** (100 MHz, DMSO-d_6): δ 162.9, 152.71, 152.70, 149.8, 134.9, 129.3, 127.5, 126.3, 125.8, 120.9, 119.3, 111.7, 66.5, 40.1.

2-(4-Trifluoromethyl-phenyl)-3*H*-quinazolin-4-one: Prepared from anthranilamide (5.0 mmol) and 4-(trifluoromethyl)benzaldehyde (6 mmol, 1.2 equiv) by the general procedure to give **2.01k** as a white solid (1.16 g, 80%); 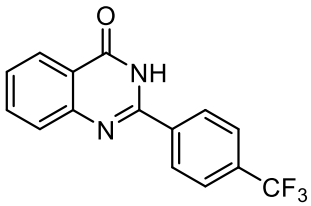

^{1}H NMR (400 MHz, DMSO-d_6): δ 12.75 (br, 1H), 8.38 (d, J = 8.1 Hz, 1H), 8.18 (dd, J = 7.9, 1.2 Hz, 1H), 7.92 (d, J = 8.3 Hz, 2H), 7.85-7.89 (m, 1H), 7.78 (dd, J = 8.1 0.6 Hz, 1H), 7.54-7.59 (m, 1H); **^{13}C NMR** (100 MHz, DMSO-d_6): δ 162.6, 151.6, 148.9, 137.1, 135.2, 131.6 (q, J = 1.33 Hz), 129.2, 128.2, 127.6, 126.4, 125.9 (q, J = 14.8), 123.1, 121.7.

4-(4-Oxo-3,4-dihydro-quinazolin-2-yl)-benzonitrile: Prepared from anthranilamide (5.0 mmol) and 4-cyanobenzaldehyde (6 mmol, 1.2 equiv) by the general procedure to give **2.01l** as a white solid (0.964 g, 78%); 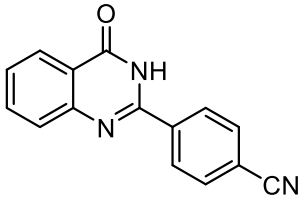

^{1}H NMR (400 MHz, DMSO-d_6): δ 12.7 (br, 1H), 7.35 (d, J = 7.0 Hz, 2H), 8.18 (d, J = 7.7 Hz, 1H), 8.05 (d, J = 6.7 Hz, 2H), 7.86 (t, J = 7.5 Hz, 1H), 7.77 (d, J = 8.4 Hz, 1H), 7.58 (dd, J = 7.5, 7.1 Hz, 1H); **^{13}C NMR** (100 MHz, DMSO-d_6): δ 162.5, 160.2, 148.5, 136.9, 135.2, 132.8, 128.9, 127.7, 127.5, 126.2, 121.5, 118.6, 113.8.

4-(4-Oxo-3,4-dihydro-quinazolin-2-yl)-benzaldehyde: Prepared from anthranilamide (5.0 mmol) and terephthalaldehyde (6 mmol, 1.2 equiv) by the general procedure to give **2.01m** as a white solid (0.950 g, 76%); **^{1}H NMR** (400 MHz, DMSO-d_6): δ 12.72 (br, 1H), 10.12 (s, 1H), 8.38 (d, J = 8.3 Hz, 1H), 8.18 (dd, J = 7.9, 1.0 Hz, 1H), 8.07 (d, J = 8.3 Hz, 2H), 7.89-7.85 (m, 1H), 7.79 (d, J = 8.0 Hz, 2H), 7.58-7.55 (m, 1H); **^{13}C NMR** (100 MHz, DMSO-d_6): δ 193.3, 162.6, 151.9, 148.9, 138.25, 138.19, 135.2, 129.9, 129.0, 129.2, 127.6, 126.4, 121.7.

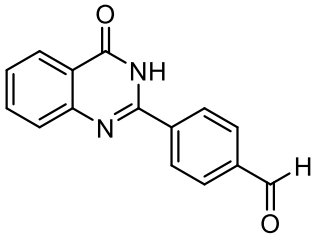

2-(4-Acetyl-phenyl)-3*H*-quinazolin-4-one: Prepared from anthranilamide (5.0 mmol) and 4- acetylbenzaldehyde (6 mmol, 1.2 equiv) by the general procedure to give **2.01n** as a white solid (0.924 g, 70%); **^{1}H NMR** (400 MHz, DMSO-d_6): δ 12.69 (br, 1H), 8.32 (d, J = 8.5 Hz, 2H), 8.18 (dd, J = 7.9, 1.1 Hz, 1H), 8.10 (d, J = 8.4 Hz, 2H), 7.85-7.89 (m, 1H), 7.78 (d, J = 7.8 Hz, 1H), 7.54-7.59 (m, 1H), 2.66 (s, 3H); **^{13}C NMR** (100 MHz, DMSO-d_6): δ 198.1, 162.6, 151.9, 149.0, 139.0, 137.0, 135.2, 128.8, 128.6, 128.2, 127.5, 121.6, 27.4.

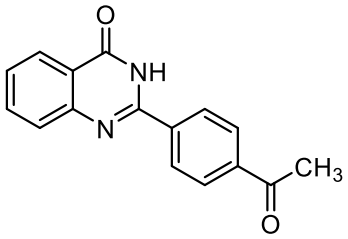

2-Benzo[1,3]dioxol-5-yl-3*H*-quinazolin-4-one: Prepared from anthranilamide (5.0 mmol) and 4- piperonal (1,3-Benzodioxole-5-carboxaldehyde) (6 mmol, 1.2 equiv) by the general procedure to give **2.01n** as a white solid (1.13 g, 85%); **^{1}H NMR** (400 MHz, DMSO-d_6): δ 12.36 (br, 1H), 8.16 (d, J = 7.6 Hz, 1H), 7.85-7.72 (m, 4H), 7.53 (t, J = 7.8 Hz, 1H), 7.12 (d, J = 8.6 Hz, 1H), 6.18 (s, 2H); **^{13}C NMR** (100 MHz, DMSO-d_6): δ 163.7, 147.9, 147.5, 135.8, 134.8, 133.5, 127.6, 125.9, 123.2, 120.5, 177.4, 114.5, 108.2, 107.7, 101.9.

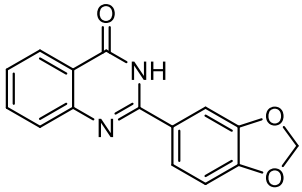

2.10. Experimental procedure for allylation of *N*-heterocycles

In a glove box, to an oven dried 4 mL glass vial equipped with a stirring bar, *N*-heterocycles **2.01** (0.5 mmol), cinnamyl alcohol **2.02da** (0.067 g, 0.5 mmol, 1 equiv), Pd $(PPh_3)_4$ (0.029 g, 0.025 mmol, 5 mol%) followed by DMC (1 mL) were added and the reaction mixture was stirred at 100 °C. The reaction mixture was then cooled to rt, diluted with MeOH (2 x 10 mL) and passed through bed of celite to remove catalyst. The organic layer was dried over anhydrous Na_2SO_4 and concentrated under reduced pressure. The crude products were adsorbed on to silica gel and purified by column chromatography (eluent: Hexane/EtOAc) to get analytically pure product.

2.11. Analytical data of purified cinnamylated products

3-Cinnamyl-3*H*-quinazolin-4-one: Prepared by general procedure to yield **2.03b** as a white solid (0.118 g, 90%); **^{1}H NMR** (400 MHz, $CDCl_3$): δ 8.36 (d, J = 7.9 Hz, 1H), 8.12 (s, 1H), 7.73-7.79 (m, 2H), 7.51-7.55 (m, 2H), 7.26-7.39 (m, 5H), 6.68 (d, J = 15.8 Hz, 1H), 6.32-6.39 (m, 1H), 4.81 (d, J = 2.4 Hz, 2H); **^{13}C NMR** (100 MHz, $CDCl_3$): δ 160.9, 148.2, 146.1, 135.8, 134.5, 134.3, 128.6, 128.3, 127.5, 127.3, 126.8, 126.6, 122.8, 122.2, 48.2; **HRMS** (ESI-TOF) *m/z*: $[M + H]^+$ Calcd for $C_{17}H_{15}N_2O$ 263.1184, Found 263.1178.

3-Cinnamyl-2-methylquinazolin-4(3*H*)-one: Prepared by general procedure to yield **2.03c** as a white solid (0.126 g, 91%); MP 127-128 °C; **^{1}H NMR** (400 MHz, $CDCl_3$): δ 8.33 - 8.28 (m, 1H), 7.74 - 7.62 (m, 2H), 7.47 – 7.45 (m, 1H), 7.43 - 7.21 (m, 5H), 6.55 (dt, J = 16.0, 1.6 Hz, 1H), 6.30 (dt, J = 16.0, 5.8 Hz, 1H), 4.92 (dd, J = 5.9, 1.6 Hz, 2H), 2.69 (s, 3H); **^{13}C NMR** (101 MHz, $CDCl_3$): δ 161.9, 154.3, 147.4, 136.0, 134.3, 132.9, 128.6, 128.1, 126.9, 126.7, 126.49, 126.47,

122.9, 120.5, 45.9, 23.2; **HRMS** (ESI-TOF) m/z: $[M + H]^+$ Calcd for $C_{18}H_{17}N_2O$ 277.1341, Found 277.1339.

3-Cinnamyl-2-cyclohexylquinazolin-4(3*H*)-one: Prepared by general procedure to yield

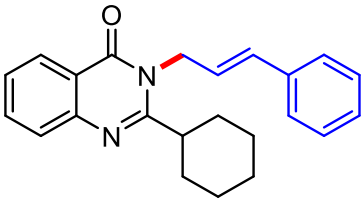

2.03d colorless viscous liquid (0.146 g, 85%); **^{1}H NMR** (400 MHz, $CDCl_3$): δ 8.34 - 8.31 (m, 1H), 7.74 -7.69 (m, 2H), 7.47 - 7.42 (m, 1H), 7.39 - 7.25 (m, 5H), 6.53 (dt, J = 16.0, 1.6 Hz, 1H), 6.35 (dt, J = 16.0, 5.5 Hz, 1H), 5.01 (dd, J = 5.6, 1.7 Hz, 2H), 2.93 – 2.86 (m, 1H), 1.98 - 1.79 (m, 7H), 1.43 - 1.38 (m, 3H); ^{13}C NMR (101 MHz, $CDCl_3$): δ 162.4, 160.6, 147.66, 136.2, 134.1, 132.4, 128.6, 127.9, 127.2, 126.9, 126.5, 126.2, 124.08, 120.4, 44.7, 42.3, 31.7, 26.2, 25.8; **HRMS** (ESI-TOF) m/z: $[M + H]^+$ Calcd for $C_{23}H_{25}N_2O$ 345.1967, Found 345.1962.

3-Cinnamyl-2-phenylquinazolin-4(3*H*)-one: Prepared by general procedure to yield

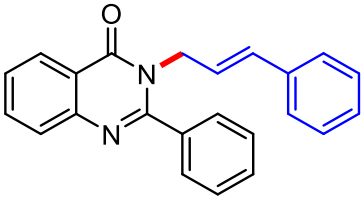

2.03e as a white solid (0.149 g, 88%); MP 105-106 ^{o}C; **^{1}H NMR** (400 MHz, $CDCl_3$): δ 8.44 - 8.36 (m, 1H), 7.85 - 7.75 (m, 2H), 7.63 - 7.49 (m, 6H), 7.37 - 7.19 (m, 5H), 6.30 - 6.14 (m, 2H), 4.79 (d, J = 5.1 Hz, 2H); **^{13}C NMR** (101 MHz, $CDCl_3$): δ 162.1, 156.2, 147.3, 136.2, 135.4, 134.5, 133.6, 130.0, 128.7, 128.5, 128.1, 127.9, 127.6, 127.1, 126.9, 126.5, 123.3, 120.9, 47.9; **HRMS** (ESI-TOF) m/z: $[M + H]^+$ Calcd for $C_{23}H_{19}N_2O$ 339.1497, Found 339.1497.

3-Cinnamyl-2-(furan-2-yl)quinazolin-4(3*H*)-one: Prepared by general procedure to

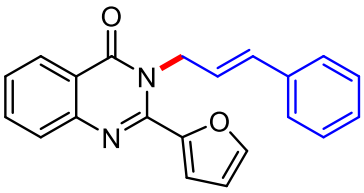

yield **2.03f** as a light yellow solid (0.138 g, 84%); MP 98-100 ^{o}C; **^{1}H NMR** (400 MHz, $CDCl_3$): δ 8.34 (dt, J = 7.9, 1.0 Hz, 1H), 7.83 - 7.73 (m, 2H), 7.67 (dd, J = 1.8, 0.9 Hz, 1H), 7.54 – 7.50 (m, 1H), 7.38 - 7.11 (m, 6H), 6.64 - 6.42 (m, 2H), 6.33 (dt, J = 15.9, 5.9 Hz, 1H), 5.11 (dd, J = 5.9, 1.5 Hz, 2H); **^{13}C NMR** (101 MHz, $CDCl_3$): δ 162.1, 147.5, 147.4, 146.1, 144.5, 136.3, 134.5, 133.1, 128.5,

127.9, 127.6, 127.2, 127.0, 126.5, 123.69, 120.7, 115.5, 112.0, 46.9; **HRMS** (ESI-TOF) m/z: [M + H]$^+$ Calcd for $C_{21}H_{17}N_2O_2$ 329.1290, Found 329.1295.

3-Cinnamyl-2-((*E*)-styryl)quinazolin-4(3*H*)-one: Prepared by general procedure to yield

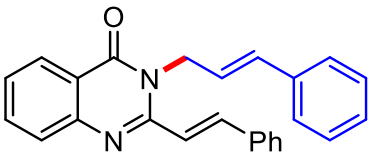

2.03g as a light yellow solid (0.131 g, 72%); MP 180-182 ^{o}C.**^{1}H NMR** (400 MHz, $CDCl_3$) δ 8.35 (dt, J = 8.0, 1.1 Hz, 1H), 8.02 (d, J = 15.4 Hz, 1H), 7.80 - 7.76 (m, 2H), 7.62 - 7.59 (m, 2H), 7.51 - 7.47 (m, 1H), 7.46 - 7.38 (m, 5H), 7.35 – 7.30 (m, 2H), 7.28 - 7.26 (m, 1H), 7.21 (d, J = 15.4 Hz, 1H), 6.65 (dt, J = 16.0, 1.7 Hz, 1H), 6.41 (dt, J = 16.0, 5.6 Hz, 1H), 5.10 (dd, J = 5.5, 1.7 Hz, 2H); **^{13}C NMR** (101 MHz, $CDCl_3$): δ 162.0, 152.4, 147.7, 141.2, 136.1, 135.5, 134.4, 132.9, 129.8, 128.9, 128.6, 128.6, 128.1, 127.8, 127.4, 127.0, 126.5, 126.5, 126.3, 123.4, 120.6, 119.3, 45.5; **HRMS** (ESI-TOF) m/z: [M + H]$^+$ Calcd for $C_{25}H_{20}N_2O$ 365.1654, Found 365.1658.

6-Chloro-3-cinnamylquinazolin-4(3*H*)-one: Prepared by general procedure to yield

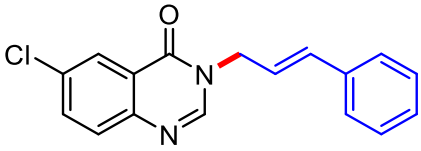

2.03h as an off white solid (0.133 g, 90%); MP 120-121 ^{o}C; **^{1}H NMR** (400 MHz, $CDCl_3$): δ 8.34 - 8.28 (m, 1H), 8.10 (s, 1H), 7.72 - 7.66 (m, 2H), 7.40 - 7.25 (m, 5H), 6.69 (dt, J = 16.0, 1.5 Hz, 1H), 6.34 (dt, J = 15.8, 6.5 Hz, 1H), 4.80 (dd, J = 6.5, 1.4 Hz, 2H); **^{13}C NMR** (101 MHz, $CDCl_3$): δ 159.9, 146.6, 146.3, 135.7, 134.9, 134.7, 133.2, 129.2, 128.7, 128.4, 126.6, 126.2, 123.2, 122.4, 48.3; **HRMS** (ESI-TOF) m/z: [M + H]$^+$ Calcd for $C_{17}H_{14}ClN_2O$ 297.0795, Found 297.0792.

3-Cinnamyl-6-methoxyquinazolin-4(3*H*)-one: Prepared by general procedure to yield

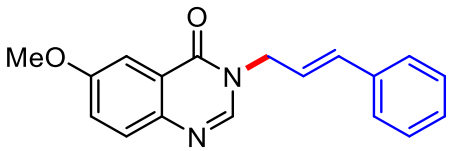

2.03i as a white solid (0.123 g, 84%); MP 172-173 ^{o}C; **^{1}H NMR** (400 MHz, $CDCl_3$): δ 8.02 (s, 1H), 7.71 - 7.63 (m, 2H), 7.39 - 7.33 (m, 3H), 7.31 - 7.26 (m, 3H), 6.67 (dt, J = 15.9, 1.5 Hz, 1H), 6.36 (dt, J = 15.9, 6.4 Hz, 1H), 4.80 (dd, J = 6.5, 1.4 Hz, 2H), 3.94 (s, 3H); **^{13}C NMR** (101 MHz, $CDCl_3$): δ 160.8, 158.8,

144.0, 142.7, 135.8, 134.4 129.1, 128.6, 128.2, 126.6, 124.5, 123.0, 122.9, 106.1, 55.8, 48.2; **HRMS** (ESI-TOF) m/z: $[M + H]^+$ Calcd for $C_{18}H_{17}N_2O_2$ 293.1290, Found 293.1293.

3-Cinnamyl-6-nitroquinazolin-4(3*H*)-one: Prepared by general procedure to yield **2.03e**

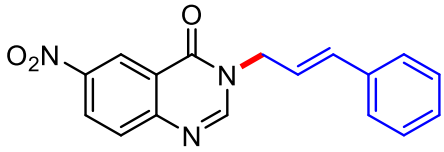

as a yellow solid (0.126 g, 82%); MP 145-146 °C; **^{1}H NMR** (400 MHz, $CDCl_3$): δ 9.22 (d, J = 2.6 Hz, 1H), 8.57 (dd, J = 8.9, 2.6 Hz, 1H), 8.26 (s, 1H), 7.87 (d, J = 8.9 Hz, 1H), 7.42 – 7.29 (m, 5H), 6.71 (d, J = 15.8 Hz, 1H), 6.39 - 6.31 (m, 1H), 4.76 (dd, J = 6.6, 1.2 Hz, 2H); **^{13}C NMR** (101 MHz, $CDCl_3$): δ 159.8, 152.1, 149.0, 146.1, 135.6, 135.4, 129.3, 128.8, 128.6, 128.4, 126.7, 123.5, 122.4, 121.7, 48.7; **HRMS** (ESI-TOF) m/z: $[M + H]^+$ Calcd for $C_{17}H_{14}N_3O_3$ 308.1035, Found 308.1033.

3-Cinnamyl-2-(4-(dimethylamino)phenyl)quinazolin-4(3*H*)-one: Prepared by general procedure to yield **2.03k** as a white semisolid (0.162 g, 85%); **^{1}H NMR** (400 MHz, DMSO-d_6): δ 8.19 - 8.17 (m, 1H), 7.85 - 7.81 (m, 1H), 7.68 - 7.66 (m, 1H), 7.55 - 7.48 (m, 3H), 7.37 - 7.20 (m, 5H), 6.80 - 6.77 (m, 2H), 6.36 - 6.23 (m, 2H), 4.77 - 4.73 (m, 2H), 2.97 (s, 6H); **^{13}C NMR** (101 MHz, DMSO-d_6) δ 162.0, 157.2, 151.5, 147.7, 136.6, 134.9, 131.6, 129.9, 129.0, 128.1, 127.6, 126.9, 126.7, 126.7, 125.3, 122.7, 120.5, 111.5, 48.0, 36.7, 24.8; **HRMS** (ESI-TOF) m/z: $[M + H]^+$ Calcd for $C_{25}H_{24}N_3O$ 382.1919, Found 382.1923.

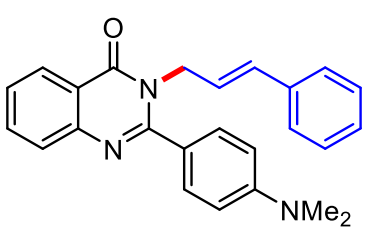

3-Cinnamyl-2-(4-(trifluoromethyl)phenyl)quinazolin-4(3*H*)-one: Prepared by general procedure to yield **2.03l** as a white solid (0.175 g, 86%); MP 138-140 °C; **^{1}H NMR** (400 MHz, $CDCl_3$): δ 8.40 (dd, J = 8.0, 1.4 Hz, 1H), 7.84 - 7.72 (m, 6H), 7.60 – 7.56 (m, 1H), 7.34 - 7.24 (m, 5H), 6.27 - 6.18 (m, 2H), 4.76 (d, J = 5.2 Hz, 2H); **^{13}C NMR** (101 MHz, $CDCl_3$): δ 161.8, 154.8, 147.1, 138.7 (q, JF-CCCC = 1.33 Hz), 135.8, 134.7, 133.7, 132.14 (q, JF-CC = 33.23 Hz) 128.8, 128.6,

128.2, 127.6, 127.5, 127.0, 126.5, 125.7 (q, JF-CCC = 3.73 Hz) 123.7 (q, JF-C = 272.38 Hz), 122.8; 121.0, 47.9; **^{19}F NMR** (376 MHz, DMSO-d_6) δ -61.18; **HRMS** (ESI-TOF) m/z: $[M + H]^+$ Calcd for $C_{24}H_{18}F_3N_2O$ 407.1371, Found 407.1368.

4-(3-Cinnamyl-4-oxo-3,4-dihydroquinazolin-2-yl)benzonitrile : Prepared by general procedure to yield **2.03m** as a white solid (0.154 g, 85%); MP 110-111 ^{o}C; **^{1}H NMR** (400 MHz, $CDCl_3$): δ 8.39 (dd, J = 7.7, 1.5 Hz, 1H), 7.84 - 7.81 (m, 3H), 7.76 - 7.71 (m, 3H), 7.60 - 7.56 (m, 1H), 7.34 - 7.25 (m, 6H), 6.25 - 6.13 (m, 2H), 4.74 (d, J = 5.3 Hz, 2H); **^{13}C NMR** (101 MHz, $CDCl_3$): δ 161.7, 154.3, 146.9, 139.4, 135.8, 134.8, 133.6, 132.5, 129.2, 128.7, 128.3, 127.7, 127.6, 127.0, 126.50, 122.8, 120.9, 118.0, 114.0, 48.0; **HRMS** (ESI-TOF) m/z: $[M + H]^+$ Calcd for $C_{24}H_{18}N_3O$ 364.1450, Found 364.1443.

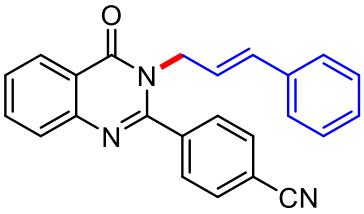

4-(3-Cinnamyl-4-oxo-3,4-dihydroquinazolin-2-yl)benzaldehyde: Prepared by general procedure to yield **2.03n** as a colorless liquid (0.165 g, 90%); **^{1}H NMR** (400 MHz, $CDCl_3$): δ 10.2 (s, 1H), 8.40 (dd, J = 8.1, 1.0 Hz, 1H), 8.06 (dd, J = 6.5, 1.8 Hz, 1H), 7.85 - 7.77 (m, 4H), 7.60 - 7.56 (m, 1H), 7.33 - 7.23 (m, 5H), 6.26 - 7.14 (m, 2H), 4.76 (d, J = 5.0 Hz 2H); **^{13}C NMR** (101 MHz, $CDCl_3$): δ 191.4, 161.9, 154.9, 147.1, 140.7, 137.2, 135.9, 134.7, 133.7, 129.9, 129.1, 128.6, 128.2, 127.63, 127.58, 126.5, 122.9, 120.1, 47.9; **HRMS** (ESI-TOF) m/z: $[M + H]^+$ Calcd for $C_{24}H_{19}N_2O_2$ 367.1447, Found 367.1448.

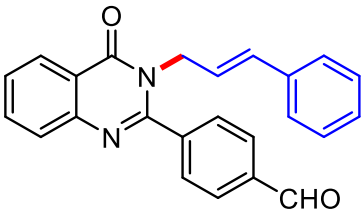

2-(4-Acetylphenyl)-3-cinnamylquinazolin-4(3*H*)-one: Prepared by general procedure to yield **2.03o** as a colorless semisolid (0.162 g, 85%); **^{1}H NMR** (400 MHz, $CDCl_3$): δ 8.39 - 8.37 (m, 1H), 8.12 - 8.10 (m, 2H), 7.86 - 7.74 (m, 2H), 7.71 – 7.69 (m, 2H), 7.57 - 7.53 (m, 1H), 7.32 - 7.21

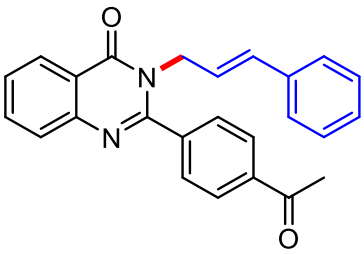

(m, 5H), 6.25 - 6.15 (m, 2H), 4.75 (d, *J* = 4.5 Hz, 2H), 2.68 (s, 3H); **^{13}C NMR** (101 MHz, $CDCl_3$): *δ* 197.2, 161.2, 155.2, 147.1, 139.5, 138.1, 135.9, 134.6, 133.6, 128.6, 128.6, 128.6, 128.1, 127.6, 127.5, 126.9, 126.5, 123.0, 120.9, 47.9, 26.8; **HRMS** (ESI-TOF) m/z: $[M + H]^+$ Calcd for $C_{25}H_{21}N_2O_2$ 381.1603, Found 381.1610.

2-(Benzo[*d*][1,3]dioxol-5-yl)-3-cinnamylquinazolin-4(3*H*)-one: Prepared by general procedure to yield **2.03p** as a white solid (0.159 g, 83%); MP 142-143 °C; **^{1}H NMR** (400 MHz, $CDCl_3$): *δ* 8.38 - 8.36 (m, 1H), 7.81 - 7.70 (m, 2H), 7.55 – 7.51 (m, 1H), 7.40 - 7.22 (m, 6H), 7.10 - 7.06 (m, 2H), 6.95 (d, *J* = 7.8 Hz, 1H), 6.33 – 6.22 (m, 2H), 6.08 (s, 2H), 4.82 (d, *J* = 4.7 Hz, 2H); **^{13}C NMR** (101 MHz, $CDCl_3$): *δ* 162.2, 155.7, 149.1, 147.9, 147.2, 136.2, 134.5, 133.5, 129.0, 128.6, 127.9, 127.5, 127.1, 126.9, 126.5, 123.4, 122.5, 120.9, 108.8, 108.5, 101.7, 48.2; **HRMS** (ESI-TOF) m/z: $[M + H]^+$ Calcd for $C_{24}H_{19}N_2O_3$ 383.1396, Found 383.1401.

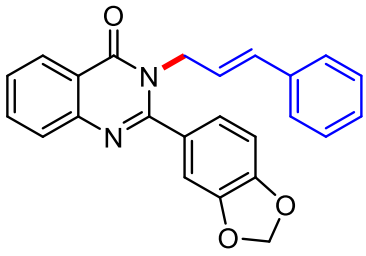

1-Cinnamylpyridin-2(1*H*)-one:[41] Prepared by general procedure to yield **2.03q** as a pale brown liquid (0.085 g, 81%); **^{1}H NMR** (400 MHz, $CDCl_3$): δ 7.39 - 7.24 (m, 7H), 6.63 - 6.57 (m, 2H), 6.33 (dt, *J* = 15.9, 6.5 Hz, 1H), 6.19 (td, *J* = 6.7, 1.4 Hz, 1H), 4.73 (dd, *J* = 6.5, 1.4 Hz, 2H); **^{13}C NMR** (101 MHz, $CDCl_3$): *δ* 162.5, 139.5, 136.9, 136.0, 128.63, 128.5, 128.1, 126.6, 123.6, 121.2, 106.2, 50.7; **HRMS** (ESI-TOF) m/z: $[M + Na]^+$ Calcd for $C_{14}H_{13}NONa$ 234.0895, Found 234.0895.

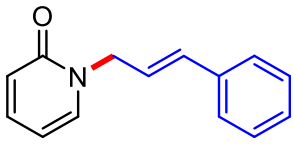

3-Cinnamylpyrimidin-4(3*H*)-one: Prepared by general procedure to yield **2.03r** as a white solid (0.089 g, 84%); MP 138-140 °C; **^{1}H NMR** (400 MHz, $CDCl_3$): *δ* 8.18 (s, 1H), 7.92 (d, *J* = 6.8 Hz, 1H), 7.41 - 7.30 (m, 5H), 6.67 (d, *J* = 16.0 Hz, 1H), 6.51 (dd, *J* = 6.4, 0.4 Hz, 1H), 6.36-6.29 (m, 1H), 4.73 (dd, *J* = 6.8, 1.4 Hz, 1H); **^{13}C NMR** (101 MHz, $CDCl_3$): *δ* 160.7, 153.4, 150.9, 135.6, 135.2, 128.7, 128.4, 126.7, 122.1,

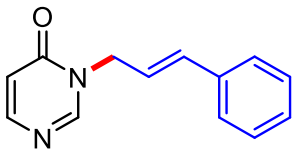

116.1, 48.5; **HRMS** (ESI-TOF) m/z: [M + Na]$^+$ Calcd for $C_{13}H_{12}N_2ONa$ 235.0847, Found 235.0845.

1-Cinnamylpyrazine-2(1*H*)-one: Prepared by general procedure to yield **2.03s** as a white

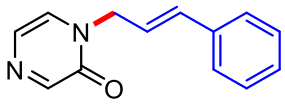

solid (0.089 g, 84%); MP 59-60 ^{o}C; **^{1}H NMR** (400 MHz, CDCl3) δ 8.21 (d, J = 1.2 Hz, 3H), 7.44 – 7.25 (m, 19H), 7.19 (dd, J = 4.4, 1.2 Hz, 3H), 6.68 (dt, J = 15.8, 1.4 Hz, 3H), 6.27 (dt, J = 15.8, 6.7 Hz, 3H), 4.69 (dd, J = 6.7, 1.4 Hz, 6H); **^{13}C NMR** (101 MHz, CDCl3) δ 156.0, 149.7, 135.8, 135.5, 128.7, 128.5, 127.8, 126.7, 124.0, 121.6, 50.3. **HRMS** (ESI-TOF) m/z: [M + Na]+ Calcd for C13H12N2ONa 235.0847, Found 235.0844.

2-Cinnamylphthalazin-1(2*H*)-one: Prepared by general procedure to yield **2.03t** as a

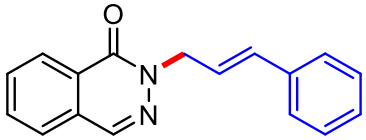

white solid (0.117 g, 89%); MP 64-65 ^{o}C; **^{1}H NMR** (400 MHz, $CDCl_3$): δ 8.46 (dd, J = 7.5, 1.8 Hz, 1H), 8.19 (s, 1H), 7.81 – 7.73 (m, 2H), 7.68 (dd, J = 7.6, 1.6 Hz, 1H), 7.40 - 7.30 (m, 2H), 7.29 - 7.26 (m, 2H), 7.24 - 7.20 (m, 1H), 6.72 (dt, J = 15.8, 1.4 Hz, 1H), 6.47 (dt, J = 15.8, 6.6 Hz, 1H), 5.02 (dd, J = 6.5, 1.3 Hz, 2H); **^{13}C NMR** (101 MHz, $CDCl_3$): δ 159.2, 138.1, 136.5, 133.7, 133.1, 131.7, 129.7, 128.5, 128.0, 127.8, 126.7, 126.6, 126.1, 123.7, 53.2; **HRMS** (ESI-TOF) m/z: [M + H]$^+$ Calcd for $C_{17}H_{15}N_2O$ 263.1184, Found 263.1186.

1-Cinnamylquinolin-2(1*H*)-one: Prepared by general procedure to yield **2.03u** as a white

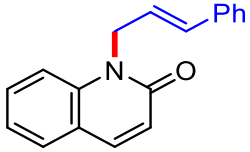

solid (0.112 g, 86%); MP 45-46 ^{o}C; **^{1}H NMR** (400 MHz, $CDCl_3$): δ 7.74 (d, J = 9.5 Hz, 1H), 7.65 - 7.51 (m, 2H), 7.45 (d, J = 8.6 Hz, 1H), 7.35 - 7.20 (m, 6H), 6.78 (d, J = 9.5 Hz, 1H), 6.57 (dt, J = 15.9, 1.8 Hz, 1H), 6.34 (dt, J = 16.0, 5.5 Hz, 1H), 5.14 (dd, J = 5.8, 1.7 Hz, 2H); **^{13}C NMR** (101 MHz, $CDCl_3$): δ 162.1, 139.4, 139.4, 136.3, 132.5, 130.7, 128.94, 128.92, 128.6, 128.5, 127.7, 126.4, 123.5, 122.2, 121.7, 120.9,

114.7, 44.2; **HRMS** (ESI-TOF) m/z: $[M + Na]^+$ Calcd for $C_{18}H_{15}NONa$ 284.1051, Found 284.1047.

1-Cinnamylquinoxalin-2(1*H*)-one: Prepared by general procedure to yield **2.03v** as a

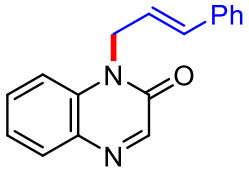

light yellow solid (0.118 g, 90%); MP 91-93 °C; **^{1}H NMR** (400 MHz, $CDCl_3$): δ 8.38 (s, 1H), 7.93 (dd, J = 8.0, 1.5 Hz, 1H), 7.59 (m, 1H), 7.44 (dd, J = 8.5, 1.2 Hz, 1H), 7.41 - 7.22 (m, 7H), 6.63 (dt, J = 16.1, 1.6 Hz, 1H), 6.29 (dt, J = 16.0, 5.8 Hz, 1H), 5.08 (dd, J = 5.8, 1.6 Hz, 2H); **^{13}C NMR** (101 MHz, $CDCl_3$): δ 154.7, 150.3, 135.9, 133.7, 133.6, 132.5, 131.1, 130.7, 128.6, 128.1, 126.5, 123.8, 121.8, 114.3, 43.8; **HRMS** (ESI-TOF) m/z: $[M + H]^+$ Calcd for $C_{17}H_{15}N_2O$ 263.1184, Found 263.1181.

3-Cinnamylbenzo[*d*]thiazol-2(3*H*)-one: Prepared by general procedure to yield **2.03w** as

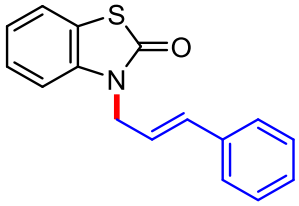

a light yellow solid (0.115 g, 86%); MP 46-47 °C; **^{1}H NMR** (400 MHz, $CDCl_3$): δ 7.46 (dd, J = 7.8, 1.2 Hz, 1H), 7.38 - 7.25 (m, 6H), 7.21 - 7.13 (m, 2H), 6.65 (dt, J = 15.9, 1.6 Hz, 1H), 6.26 (dt, J = 15.9, 6.0 Hz, 1H), 4.76 (dd, J = 6.0, 1.6 Hz, 2H); **^{13}C NMR** (101 MHz, $CDCl_3$): δ 169.8, 137.0, 136.0, 133.5, 128.7, 128.1, 126.6, 126.4, 123.3, 122.7, 122.1, 111.16, 44.6; **HRMS** (ESI-TOF) m/z: $[M + H]^+$ Calcd for $C_{16}H_{14}NOS$ 268.0796, Found 268.0792.

3-Cinnamylbenzo[*d*]oxazol-2(3*H*)-one: Prepared by general procedure to yield **2.03x** as

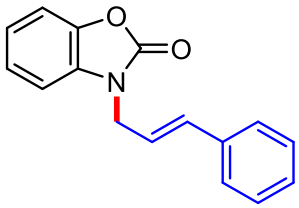

a light brown solid (0.113 g, 90%); MP 100-102 °C; **^{1}H NMR** (400 MHz, $CDCl_3$): δ 7.48 – 7.00 (m, 10H), 6.71 (dt, J = 15.9, 1.6 Hz, 1H), 6.28 (dt, J = 15.9, 6.2 Hz, 1H), 4.64 (dd, J = 6.2, 1.6 Hz, 2H); **^{13}C NMR** (101 MHz, $CDCl_3$): δ 154.4, 142.7, 135.8, 134.2, 131.0, 128.7, 128.3, 126.6, 123.9, 122.5, 121.7, 110.1, 108.9, 44.4; **HRMS** (ESI-TOF) m/z: $[M + H]^+$ Calcd for $C_{16}H_{14}NO_2$ 252.1024, Found 252.1030.

3-Cinnamyl-5-phenyl-1,3,4-oxadiazol-2(3*H*)-one: Prepared by general procedure to

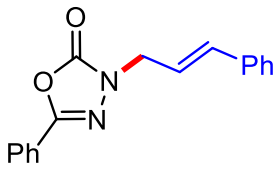

yield **2.03y** as a white solid (0.119 g, 86%); MP 49-50 °C; **^{1}H NMR** (400 MHz, $CDCl_3$): δ 7.90 - 7.64 (m, 2H), 7.54 - 7.42 (m, 5H), 7.37 - 7.27 (m, 3H), 6.74 (dt, *J* = 15.9, 1.4 Hz, 1H), 6.33 (dt, *J* = 15.8, 6.5 Hz, 1H), 4.59 (dd, *J* = 6.6, 1.4 Hz, 2H); **^{13}C NMR** (101 MHz, $CDCl_3$): δ 148.7, 148.6, 131.2, 130.0, 126.8, 124.2, 123.9, 123.5, 121.9, 121.0, 119.1, 117.01, 43.2; **HRMS** (ESI-TOF) m/z: $[M + H]^+$ Calcd for $C_{17}H_{15}N_2O_2$ 279.1133, Found 279.1136.

3-Allyl-quinazolin-4(3*H*)-one: Prepared by general procedure to yield **2.03a$_2$** as a white

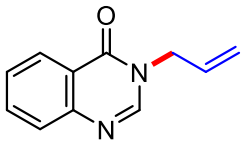

solid (0.084 g, 91%); MP 65-66 °C; **^{1}H NMR** (400 MHz, $CDCl_3$): δ 8.34 (d, *J* = 8.0 Hz, 1H), 8.04 (s, 1H), 7.80-7.72 (m, 2H), 7.55-7.50 (m, 1H), 6.07-5.97 (m, 1H), 5.31 (t, *J* =10.1 Hz, 2H), 4.66 (d, *J* = 5.7 Hz, 2H); **^{13}C NMR** (100.6 MHz, $CDCl_3$): δ 160.8, 148.1, 146.2, 134.3, 131.9, 127.5, 127.3, 126.8, 122.1, 118.9, 48.3; MS (ESI) *m/z*: 186.1.

3-(1-Methylallyl)quinazolin-4(3*H*)-one: Prepared by general procedure to yield **2.05a** as

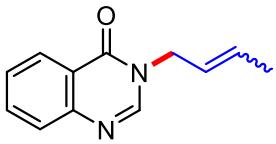

a white semi-solid (0.082 g, 82%); **^{1}H NMR** (400 MHz, $CDCl_3$): δ 8.24 (td, *J* = 8.1, 1.4 Hz, 1H), 7.98 (s, 1H), 7.67-7.62 (m, 2H), 7.44-7.39 (m, 1H), 5.76-5.70 (m, 1H), 5.61-5.57 (m, 1H), 4.50 (td, *J* = 7.4, 2.3 Hz, 2H), 1.67-1.65 (m, 3H); **^{13}C NMR** (100 MHz, $CDCl_3$): δ 160.9, 160.7, 148.0, 146.2, 146.1, 134.0, 131.0, 130.0, 127.3, 127.12, 127.10, 126.7, 126.6, 124.8, 123.9, 122.1, 47.8, 42.7, 17.6, 13.1; **HRMS** (ESI-TOF) m/z: $[M + H]^+$ Calcd for $C_{12}H_{13}N_2O$ 201.1028, Found 201.1030.

3-(2-Methylallyl)quinazolin-4(3*H*)-one: Prepared by general procedure to yield **2.06a** as

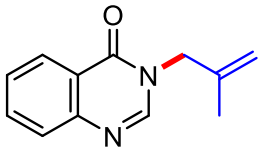

a colorless liquid (0.085 g, 85%); **^{1}H NMR** (400 MHz, $CDCl_3$): δ 8.25-8.28 (m, 1H), 7.96 (s, 1H), 7.65-7.72 (m, 2H), 7.43-7.47 (m, 1H), 4.94 (t, *J* = 1.2 Hz, 1H), 4.94 (d, *J* = 0.7 Hz, 1H), 4.53 (s, 2H), 1.74 (d, *J* = 0.5 Hz, 3H); **^{13}C NMR** (100 MHz,

$CDCl_3$): δ160.8, 148.0, 146.4, 139.8, 134.2, 127.5, 127.2, 126.8, 122.0, 113.5, 50.9, 20.1; **HRMS** (ESI-TOF) m/z: $[M + H]^+$ Calcd for $C_{12}H_{13}N_2O$ 201.1028, Found 201.1031.

3-(Cyclohex-2-en-1-yl)quinazolin-4(3*H*)-one: Prepared by general procedure to yield

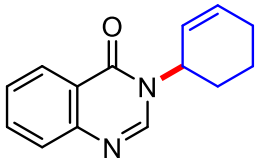

2.06b as a white solid colorless liquid (0.088 g, 78%); **^{1}H NMR** (400 MHz, $CDCl_3$): δ 8.32-8.35 (m, 1H), 8.19 (s, 1H), 7.70-7.76 (m, 2H), 7.49-7.53 (m, 1H), 6.22-6.27 (m, 1H), 5.65-5.69 (m, 1H), 5.55-7.56 (m, 1H), 2.17-2.67 (m, 3H), 1.68-1.82 (m, 3H); **^{13}C NMR** (100 MHz, $CDCl_3$): δ160.9, 144.7, 134.6, 134.1, 127.4, 127.1, 126.9, 125.2, 121.9, 49.9, 29.8, 24.6, 19.6; **HRMS** (ESI-TOF) m/z: $[M + Na]^+$ Calcd for $C_{14}H_{14}N_2ONa$ 249.1004, Found 249.1006.

3-(1,3-Diphenyl-allyl)-3*H*-quinazolin-4-one: Prepared by general procedure to yield

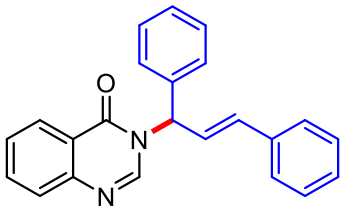

2.06c as a white solid (0.120g, 71%); MP 100-101 ^{o}C; **^{1}H NMR** (400 MHz, $CDCl_3$) δ8.43 – 8.36 (m, 1H), 8.19 (s, 1H), 7.81 – 7.71 (m, 2H), 7.52 (ddd, *J* = 8.2, 5.8, 2.6 Hz, 1H), 7.47 – 7.24 (m, 11H), 6.99 (d, *J* = 5.9 Hz, 1H), 6.76 – 6.58 (m, 2H); **^{13}C NMR** (100 MHz, $CDCl_3$): δ160.7, 147.7, 145.2, 138.2, 135.7, 135.4, 134.4, 129.2, 128.8, 128.5, 128.5, 127.9, 127.6, 127.4, 127.2, 126.8, 125.8, 122.0, 58.5; **HRMS** (ESI-TOF) m/z: $[M + Na]^+$ Calcd for $C_{23}H_{18}N_2ONa$ 361.1317, Found 361.1318.

3-(buta-1,3-dien-1-yl)quinazolin-4(3*H*)-one: Prepared by general procedure to yield

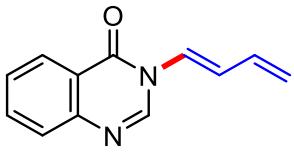

2.06d as a white solid (0.081g, 82%); MP 92-93 ^{o}C; **^{1}H NMR** (400 MHz, $CDCl_3$): δ8.33 (d, *J* = 7.8 Hz, 1H), 8.28 (s, 1H), 7.72-7.80 (m, 2H), 7.53 (t, *J* = 7.5 Hz, 1H), 7.38 (d, *J* = 13.2 Hz, 1H), 6.49-6.57 (m, 2H), 5.45 (d, *J* = 15.9 Hz, 1H), 5.32 (d, *J* = 9.4 Hz, 1H); **^{13}C NMR** (100 MHz, $CDCl_3$); δ159.6, 147.3, 142.5, 134.6, 133.3, 127.76,

127.14, 125.9, 123.1,121.6, 120.1; **HRMS** (ESI-TOF) m/z: $[M + H]^+$ Calcd for $C_{12}H_{11}N_2O$ 199.0871, Found 199.0876.

2.12. References

(1) Roughley, S. D.; Jordan, A. M. The Medicinal Chemist's Toolbox: An Analysis of Reactions Used in the Pursuit of Drug Candidates. *J. Med. Chem.* **2011**, *54* (10), 3451–3479.

(2) Tsuji, J.; Takahashi, H.; Morikawa, M. Organic Syntheses by Means of Noble Metal Compounds XVII. Reaction of π-Allylpalladium Chloride with Nucleophiles. *Tetrahedron Lett.* **1965**, *6* (49), 4387–4388.

(3) Trost, B. M.; Fullerton, T. J. New Synthetic Reactions. Allylic Alkylation. *J. Am. Chem. Soc.* **1973**, *95* (1), 292–294.

(4) Trost, B. M. On Inventing Reactions for Atom Economy. *Acc. Chem. Res.* **2002**, *35* (9), 695–705.

(5) Trost, B. M.; Hung, M. H. On the Regiochemistry of Metal-Catalyzed Allylic Alkylation: A Model. *J. Am. Chem. Soc.* **1984**, *106* (22), 6837–6839.

(6) Patil, M.; Thiel, W. Origin of Selectivity of Tsuji-Trost Allylic Alkylation of Lactones: Highly Ordered Transition States with Lithium-Containing Enolates. *Chem. - A Eur. J.* **2012**, *18* (33), 10408–10418.

(7) Li, C.; Kähny, M.; Breit, B. Rhodium-Catalyzed Chemo-, Regio-, and Enantioselective Addition of 2-Pyridones to Terminal Allenes. *Angew. Chemie Int. Ed.* **2014**, *53* (50), 13780–13784.

(8) Mclaughlin, N. P.; Evans, P.; Pines, M. The Chemistry and Biology of Febrifugine and Halofuginone. *Bioorg. Med. Chem. Lett.* **2014**, *22*, 1993–2004.

(9) Takaya, Y.; Tasaka, H.; Chiba, T.; Uwai, K.; Tanitsu, M. A.; Kim, H. S.; Wataya, Y.; Miura, M.; Takeshita, M.; Oshima, Y. New Type of Febrifugine Analogues, Bearing a Quinolizidine Moiety, Show Potent Antimalarial Activity against Plasmodium Malaria Parasite. *J. Med. Chem.* **1999**, *42* (16), 3163–3166.

(10) Guillon, R.; Pagniez, F.; Picot, C.; Hédou, D.; Tonnerre, A.; Chosson, E.; Duflos, M.; Besson, T.; Logé, C.; Le Pape, P. Discovery of a Novel Broad-Spectrum Antifungal Agent Derived from Albaconazole. *ACS Med. Chem. Lett.* **2013**, *4* (2), 288–292.

(11) Bartroli, J.; Turmo, E.; Algueró, M.; lia Boncompte, E.; Vericat, M. L.; Conte, L.; Ramis, J.; Merlos, M.; García-Rafanell, J.; Forn, J. *New Azole Antifungals. 3. Synthesis and Antifungal Activity of 3-Substituted-4(3H)-Quinazolinones 1,2*; 1998.

(12) Lafrance, M.; Lapointe, D.; Fagnou, K. Mild and Efficient Palladium-Catalyzed Intramolecular Direct Arylation Reactions. *Tetrahedron* **2008**, *64* (26), 6015–6020.

(13) Tundo, P.; Anastas, P.; Black, D. S.; Breen, J.; Collins, T. J.; Memoli, S.; Miyamoto, J.; Polyakoff, M.; Tumas, W. Synthetic Pathways and Processes in Green Chemistry. Introductory Overview. *Pure Appl. Chem.* **2000**, *72* (7), 1207–1228.

(14) Tsuji, J.; Kiji, J.; Imamura, S.; Morikawa, M.; Tsuji, J.; Kiji, J.; Imamura, S.; Morikawa, M. *Organic Syntheses by Means of Noble Metal Compounds. VIII.1 Catalytic Carbonylation of Allylic Compounds with Palladium Chloride*. *J. Am. Chem. Soc.*, **1964**, *86* (20), 4350–4353

(15) Powling, J.; Bernstein, H. J. The Effect of Solvents on Tautomeric Equilibria. *J. Am. Chem. Soc.* **1951**, *73* (9), 4353–4356.

(16) Wah, M. W.; Wiberg, K. B.; Frisch, M. J. Solvent Effects. 3. Tautomeric Equilibria of Formamide and 2-Pyridone in the Gas Phase and Solution. An Ab Initio SCRF Study. *J. Am. Chem. Soc.* **1992**, *114* (5), 1645–1652.

(17) Spencer, J. N.; Holmboe, E.; Kirshenbaum, M.; Firth, D.; Pinto, P. Solvent Effects on the Tautomeric Equilibrium of 2, 4-Pentanedione. *Can. J. Chem.* **1982**, *60*, 1178.

(18) Henderson, R. K.; Jiménez-González, C.; Constable, D. J. C.; Alston, S. R.; Inglis, G. G. A.; Fisher, G.; Sherwood, J.; Binks, S. P.; Curzons, A. D. Expanding GSK's Solvent Selection Guide - Embedding Sustainability into Solvent Selection Starting at Medicinal Chemistry. *Green Chem.* **2011**, *13* (4), 854–862.

(19) Galv??o, T. L. P.; Rocha, I. M.; Ribeiro Da Silva, M. D. M. C.; Ribeiro Da Silva, M. A. V. From 2-Hydroxypyridine to 4(3 H)-Pyrimidinone: Computational Study on the Control of the Tautomeric Equilibrium. *J. Phys. Chem. A* **2013**, *117* (47), 12668–12674.

(20) Gan, L.; Chang, Q.; Zhou, J. Transformations and Tautomeric Equilibrium among Different Intermediates in Proline-Catalyzed Reactions of Aldehydes or Ketones. *Chinese J. Chem. Phys.* **2013**, *26* (1), 54–60.

(21) Ceron-Carrasco, J. P.; Jacquemin, D. Influence of Mg2+on the Guanine-Cytosine Tautomeric Equilibrium: Simulations of the Induced Intermolecular Proton Transfer. *ChemPhysChem* **2011**, *12* (14), 2615–2623.

(22) Balabin, R. M. Tautomeric Equilibrium and Hydrogen Shifts in Tetrazole and Triazoles: Focal-Point Analysis and Ab Initio Limit. *J. Chem. Phys.* **2009**, *131* (15).

(23) Sanchez, R.; Giuliano, B. M.; Melandri, S.; Caminati, W. Tautomeric Equilibrium and Hydroxyl Group Internal Rotation in 4-Hydroxypyridine. *Chem. Phys. Lett.* **2006**, *425* (1–3), 6–9.

(24) Constantino, E.; Solans-Monfort, X.; Sodupe, M.; Bertran, J. Basic and Acidic Bifunctional Catalysis: Application to the Tautomeric Equilibrium of Formamide. *Chem. Phys.* **2003**, *295* (2), 151–158.

(25) Ranganathan, D.; Rathi, R.; Keshavan, K.; Pal Singh, W. The Demonstration of Normal o →N Claisen Rearrangement in Purines. *Tetrahedron*. 1986, pp 4873–4878.

(26) Stewart, H. F.; Seibert, R. P. Catalyzed Rearrangements of 2-Allyloxypyridine and 2-Crotyloxypyridine. *J. Org. Chem.* **1968**, *33* (12), 4560–4561.

(27) Chandra Sheker Reddy, A.; Narsaiah, B.; Venkataratnam, R. V. Palladium (II) Catalysed Claisen Rearrangement: Synthesis of Inaccessible N-Allyl-2(1H)-Pyridones from 2-(Allyloxy)Pyridines. *Tetrahedron Lett.* **1996**, *37* (16), 2829–2832.

(28) Ikariya, T.; Ishikawa, Y.; Hirai, K.; Yoshikawa, S. Rearrangement of Allylic N-Phenylformimidates to N-Allyl-N-Phenylformamides Catalyzed by Palladium Complexes. *Chem. Lett.* **1982**, No. C, 1815–1818.

(29) Lang, S. B.; Locascio, T. M.; Tunge, J. A. Activation of Alcohols with Carbon Dioxide: Intermolecular Allylation of Weakly Acidic Pronucleophiles. *Org. Lett.* **2014**, *16* (16), 4308–4311.

(30) Ozawa, F.; Okamoto, H.; Kawagishi, S.; Yamamoto, S.; Minami, T.; Yoshifuji, M. (π-Allyl)Palladium Complexes Bearing Diphosphinidenecyclobutene Ligands (DPCB): Highly Active Catalysts for Direct Conversion of Allylic Alcohols. *J. Am. Chem. Soc.* **2002**, *124* (37), 10968–10969.

(31) Usui, I.; Schmidt, S.; Keller, M.; Breit, B. Allylation of N-Heterocycles with Allylic Alcohols Employing Self-Assembling Palladium Phosphane Catalysts. *Org. Lett.* **2008**, *10* (6), 1207–1210.

(32) Kinoshita, H.; Shinokubo, H.; Oshima, K. Water Enables Direct Use of Allyl Alcohol for Tsuji-Trost Reaction without Activators. *Org. Lett.* **2004**, *6* (22), 4085–4088.

(33) Utsunomiya, M.; Miyamoto, Y.; Lpposhi, J.; Ohshima, T.; Mashima, K. Direct Use of Allylic Alcohols for Platinum-Catalyzed Monoallylation of Amines. *Org. Lett.* **2007**, *9* (17), 3371–3374.

(34) Takeuchi, R.; Kashio, M. Iridium Complex-Catalyzed Allylic Alkylation of Allylic Esters and Allylic Alcohols: Unique Regio- and Stereoselectivity. *J. Am. Chem. Soc.* **1998**, *120* (34), 8647–8655.

(35) Tao, Z. L.; Zhang, W. Q.; Chen, D. F.; Adele, A.; Gong, L. Z. Pd-Catalyzed Asymmetric Allylic Alkylation of Pyrazol-5-Ones with Allylic Alcohols: The Role of the Chiral Phosphoric Acid in C-O Bond Cleavage and Stereocontrol. *J. Am. Chem. Soc.* **2013**, *135* (25), 9255–9258.

(36) Banerjee, D.; Jagadeesh, R. V.; Junge, K.; Junge, H.; Beller, M. Efficient and Convenient Palladium-Catalyzed Amination of Allylic Alcohols with N-Heterocycles. *Angew. Chemie Int. Ed.* **2012**, *51* (46), 11556–11560.

(37) Kokatla, H. P.; Lakshman, M. K. One-Pot Etherification of Purine Nucleosides and Pyrimidines-Supporting Information. *Org. Lett.* **2010**, *12* (20), 4478–4481.

(38) Kumar, D.; Jadhavar, P. S.; Nautiyal, M.; Sharma, H.; Meena, P. K.; Adane, L.; Pancholia, S.; Chakraborti, A. K. Convenient Synthesis of 2,3-Disubstituted Quinazolin-4(3H)-Ones

and 2-Styryl-3-Substituted Quinazolin-4(3H)-Ones: Applications towards the Synthesis of Drugs. *RSC Adv.* **2015**, *5* (39), 30819–30825.

(39) Wang, Y.; Zhang, M.; Cao, S.; Lin, H.; Gao, M.; Li, Z. Synthesis of 1-Substituted 4(1 *H*)-Quinazolinones Under Solvent-Free Conditions. *Synth. Commun.* **2012**, *42* (18), 2715–2727.

(40) Golfier, M.; Milcent, R. Reaction of Acylhydrazines with Phenyltrichloromethane; A Simple Synthesis of N-Acyl-Phenylmethanehydrazonates and 1,3,4-Oxadiazoles. *Synthesis (Stuttg).* **1979**, *1979* (12), 946–948.

(41) Bowman, W. R.; Bridge, C. F. Regioselective Synthesis of *N* -Alkyl Pyridones. *Synth. Commun.* **1999**, *29* (22), 4051–4059.

CHAPTER 3. PALLADIUM CATALYZED ALLYLIC SP^3 C-H OXIDATIVE AMIDATION OF *N*-HETEROCYCLES

3.1. Introduction

The ubiquitous nature of the C-H bond is a great resource for creating molecules with high complexity but also creates difficulty in designing selective functionalization. Despite intensive efforts to advance new synthetic methods in organic chemistry, the development of effective strategies to convert C–H bonds to other functional groups en route to a wide range of more complicated materials, such as polymers and bioactive molecules, remains a central challenge in catalysis.[1–4] Alkyl C(sp^3)-H bonds, in particular, present both fundamental and practical challenge to functionalize due to their robustness. The poor reactivity of C(sp^3)–H bonds is often attributed to their high bond energies (typically 90–100 kcal/mol), low acidity (estimated pKa = 45 to 60), and unreactive molecular orbital profile.[1–12] On the other hand, allylic sp^3 C-H bonds can be exclusively functionalized taking the advantage of the olefin as a directing group and a lower bond dissociation energy (~70 kcal/mol). This type of modification greatly improves the atom efficiency of the C-C and C-X bond formation avoiding the use of leaving group. However, the methods to catalytically activate/oxidize selected allylic carbon-hydrogen bonds is a fundamental challenge for chemical synthesis as they often result in a complex mixture of oxidized products including linear, branched, and vinyl oxidation or Wacker products. The issues in controlling the selectivity of allylic oxidations have limited their use in chemical synthesis in a broad sense. In general, for constructing allylic substitution motifs via metal catalyzed allylation, two major approaches are commonly employed: (1) Leaving group (LG) approach and (2) C-H activation approach. Leaving group approach under palladium catalysis has inherent advantage of easy ionization to form π-allyl complex, leading to faster reactions and higher selectivity upon nucleophile attack.[13]

3.2. Palladium catalyzed allylic C-H oxidative C-N bond formation

Allylic C-H bond functionalization approach although favorable but is fundamentally challenging, because of combining three dissimilar steps-electrophilic C-H cleavage, nucleophilic attack, and regeneration of Pd(II) by oxidation of Pd(0) generated after the reaction. Development of a Pd(II)/bis-sulfoxide system by White and coworkers[14] have laid a solid ground work for initially palladium catalyzed allylic acetoxylation,[15–18] esterification,[19] and expanded to C-C bond formation[20–23] even with high stereoselectivity.[24–26]

3.2.1. Intramolecular allylic C-H amination

Palladium(II)-promoted addition of nitrogen nucleophiles to olefins (amino palladation) is a well-established process leading to many interesting reactions such as oxidative amination,[27–30] aminoacetoxylation,[31,32] aminohalogination,[33] and deamination.[34–36] Allylic C-H amination, on the other hand, requires a weak Lewis basic nucleophile preventing its interference with the electrophilic C-H cleavage step and acidic enough to be deprotonated by counter ion of the Pd(II) catalyst. In the case of intermolecular allylic C-H amination, in addition to reactivity, also face regioselectivity and chemoselectivity issue of competing reactivity of olefin moiety.[37] Keeping in to account all these difficulties, White and coworkers first reported an intramolecular allylic C-H amination to generate *anti*-oxazolidinone products (Scheme 3.1).[38] Tethering a nitrogen nucleophile (*N*-tosyl carbamate) was essential for the transformation as independent intermolecular study did not yield any product. Mechanistic studies indicated an allylic C-H cleavage by electrophilic Pd(II) catalyst forming π-allylpalladium intermediate. Palladium catalyst counterion, acts as an exogenous base then deprotonates tethered nucleophile paving way for nucleophilic substitution on to π–allyl intermediate forming a stable five membered ring. The

catalytic source of weak base then regenerated during the reoxidation of Pd(0) with quinone oxidant.

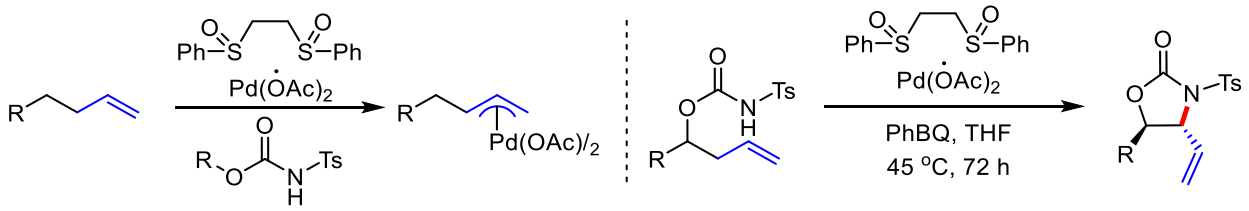

Scheme 3.1: Oxazolidinone synthesis via intramolecular allylic C-H amination

3.2.2. Intermolecular allylic C-H amination

Compared to intramolecular, intermolecular allylic C-H amination is even more challenging because of the olefin isomerization and meeting the electronic demands on the palladium metal center for each individual step of the catalytic cycle. In general, early studies on allylic C-H amination for the formation of linear allylic amines selectively relied on utilizing solvent quantities of substrate to give the best yields (based on oxidant) limiting their use.[39,40] A clear development in intermolecular allylic C-H amination was reported by White and coworkers by realizing the importance of Lewis acid additives to accelerate the nucleophile functionalization from a palladium π-allyl dimer (Scheme 3.2).[41,42] Catalytic amounts of Cr(salen)Cl was found to be most effective Lewis acid promoter for intermolecular allylic C-H amination generating the product with excellent E/Z and linear/branched ratio.

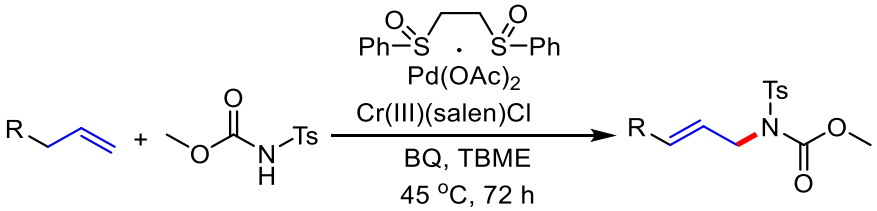

Scheme 3.2: Intermolecular allylic C-H amination promoted by Lewis acid

It was suggested that Lewis acid increases the electrophilic nature of the BQ bound palladium π-allyl complex, facilitating easy nucleophilic attack.[43] On the other hand, reactivity of

non-basic nucleophiles (pKa < 25) can be increased by deprotonation using an exogenous base via a "nucleophile" activation approach.[44] White and coworkers, taking advantage of the "nucleophile" activation approach developed a Bronsted base, *N*,*N*-diisopropylethylamine enhanced allylic C-H amination improving the substrate scope and selectivity (Scheme 3.3).[45]

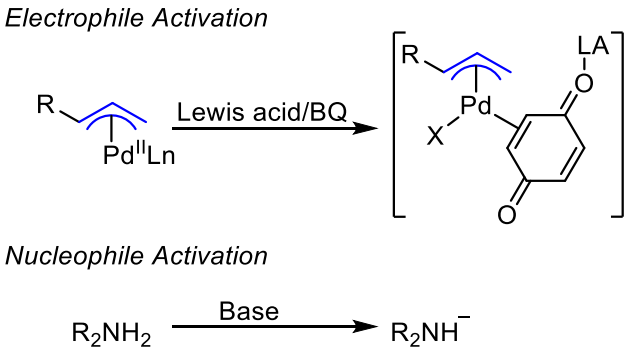

Scheme 3.3: Modes of activation for the functionalization of Pd π-allyl intermediates with nitrogen nucleophiles

Since this initial report there has been a tremendous interest in the development of catalytic systems for allylic C-H amination of variety of amine nucleophiles.[46–48] The main caveat among the methods reported in the literature for allylic amination is that none of these methods utilized cyclic aminating nucleophiles. Even among the acyclic amine nucleophiles, most reported methods are focused on the use of different catalysts, and or oxidants restricting amine partner to mostly *N*-tosyl or nosyl carbamates.[46–48] Cyclic aminating partners, on the other hand poses significant challenges both in terms of reactivity and sterics. As part of our continuous efforts on the functionalization of heterocycles, we sought to explore the possibility of allylic C-H oxidative amidation of electron deficient cyclic *N*-heterocycles.

3.3. Results and discussion

With the success of the palladium catalyzed Tsuji-Trost allylation of *N*-heterocycles established, we sought to explore allylic C-H amination methodology for functionalizing *N*-heterocycles to increase the atom efficiency and negate the necessity of leaving group from

classical reaction methodology (Scheme 3.4). During the past decade, variety of Pd(II) catalysts enabled allylic C-H functionalization reactions such as oxygenation, amination, alkylation, carbonylation, silylation, fluorination, and borylation. The direct allylation of electron-deficient *N*-heterocycles remained challenge until our finding. This is in part due to their tautomerizable nature, presenting challenges not only with less reactivity but also with regio and chemoselectivity.

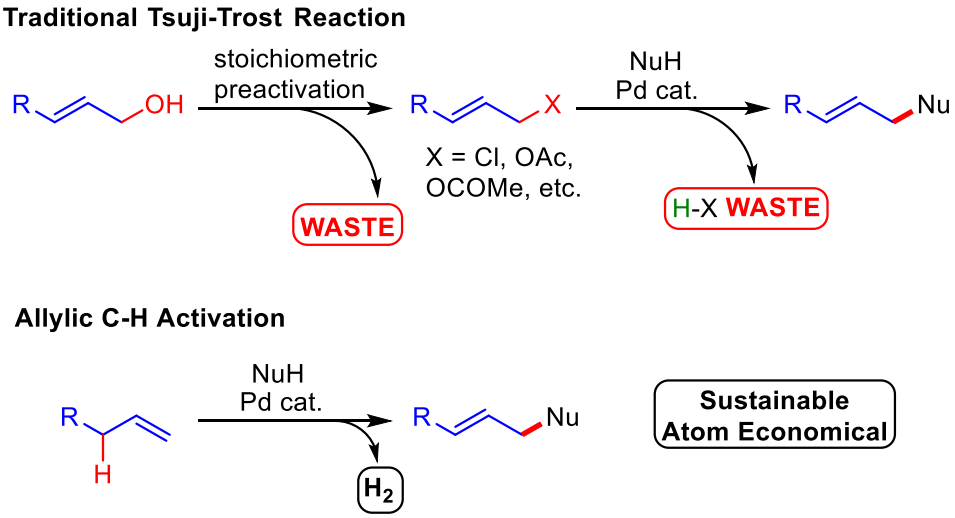

Scheme 3.4: Classical Tsuji-Trost reaction vs Allylic C-H activation

3.4. Preliminary investigation

3.4.1. Allylic C-H amidation: investigation of literature protocol

Our preliminary studies were primarily focused on functionalizing tautomeric *N*-heterocycles using established protocols of allylic C-H amination rather than developing new methodology. We started our investigation, initially examining the utility of the amination protocol reported by White[7d,7e] for the reaction of (4*H*)-quinazolone **3.01a** with allylbenzene **3.02a** (Table 3.1). However, no allylic amidation to form **3.03a**/**3.03b** was observed under these conditions. Addition of known activators such as Bronsted base (DIPEA) or Lewis acid [(salen)Cr(III)Cl] also did not afford any product formation.

Table 3.1: Allylic amidation of **3.01a** using **3.02a** under White amination protocol

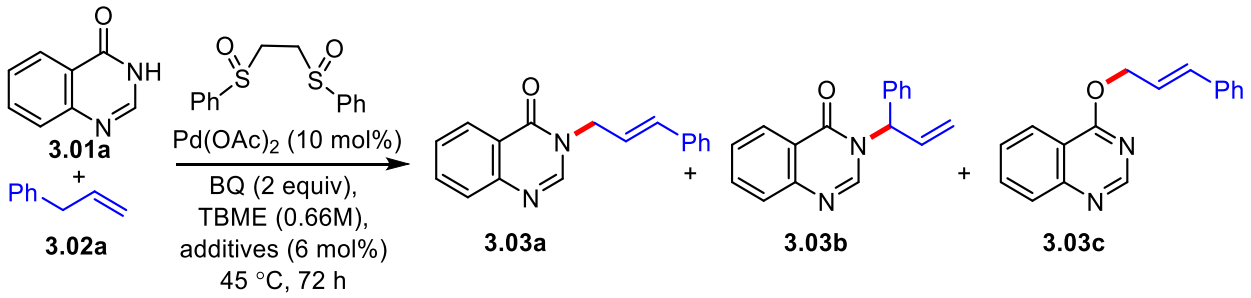

Entry	Additives	Conversion[a,b]	**3.03a : 3.03b : 3.03c**	Yield (**3.03a**)[c]
1	None	0	N/A	N/A
2	DIPEA	0	N/A	N/A
3	(salen)Cr(III)Cl	0	N/A	N/A

Reaction conditions: 3.01a (0.2 mmol) was treated with **3.02a** (0.3 mmol, 1.5 equiv) under white amination protocol. [a]Based on ^{1}H NMR of the crude reaction mixture (with respect to **3.01a**) using CH_2I_2 as internal standard. [b]Starting **3.01a** was found intact. [c]Isolated yield.

3.4.2. Screening of modified reaction conditions

Since, allylic C-H oxidative reactions tend to be highly selective to reaction conditions, and it has been previously shown that change in solvents or temperature could accelerate the rate of nucleophilic attack from a palladium π-allyl dimer, prompting an examination of these conditions. To our disappointment, change in any of these parameters both under Lewis acidic (Table 3.2) or Bronsted basic (Table 3.3) conditions did not yield any *N*-allylated or *O*-allylated product. This led us to believe that the reaction conditions generally employed for allylic C-H amination are not efficient for the allylation of electron deficient tautomerizable *N*-heterocycles prompting us to carefully investigate and develop a reaction methodology.

Table 3.2: Allylic amidation of **3.01a** using **3.02a** under modified White amination protocol with Lewis acid additive

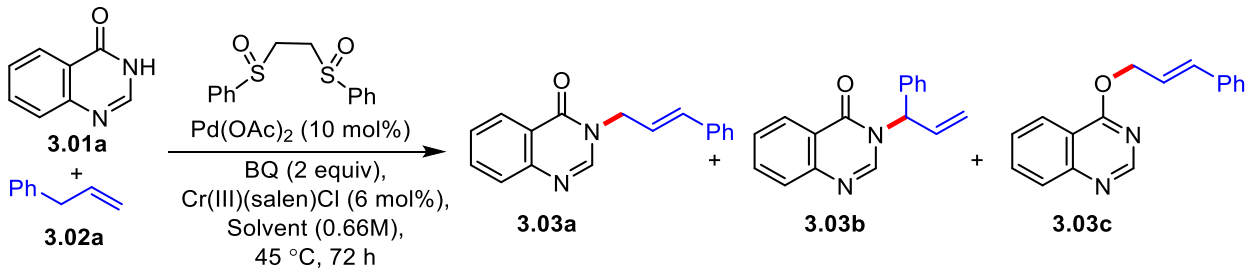

Entry	Solvent	Temp	Conversion [a,b]	**3.03a : 3.03b : 3.03c** [c]	Yield **3.03a**[d]
1	1,4-Dioxane	45	0	N/A	N/A
2	THF	45	0	N/A	N/A
3	DMF	45	0	N/A	N/A
4	DMSO	45	0	N/A	N/A
5	TBME	100	0	N/A	N/A
6	1,4-Dioxane	100	0	N/A	N/A
7	THF	100	0	N/A	N/A
8	DMF	100	0	N/A	N/A
9	DMSO	100	<10	100: 0 : 0	N/A

Reaction conditions: 3.01a (0.2 mmol) was treated with **3.02a** (0.3 mmol, 1.5 equiv) under white amination protocol with change in conditions. [a]Based on ^{1}H NMR of the crude reaction mixture (with respect to **3.01a**) using CH_2I_2 as internal standard. [b]Starting **1a** was found intact. [c]^{1}H NMR (using CH_2I_2 as internal standard) and GC-MS analysis of the crude reaction mixture determined the ratio of L/B and N/O selectivity respectively. [d]Isolated yield.

Table 3.3: Allylic amidation of **3.01a** using **3.02a** under modified White amination protocol with Bronsted base additive

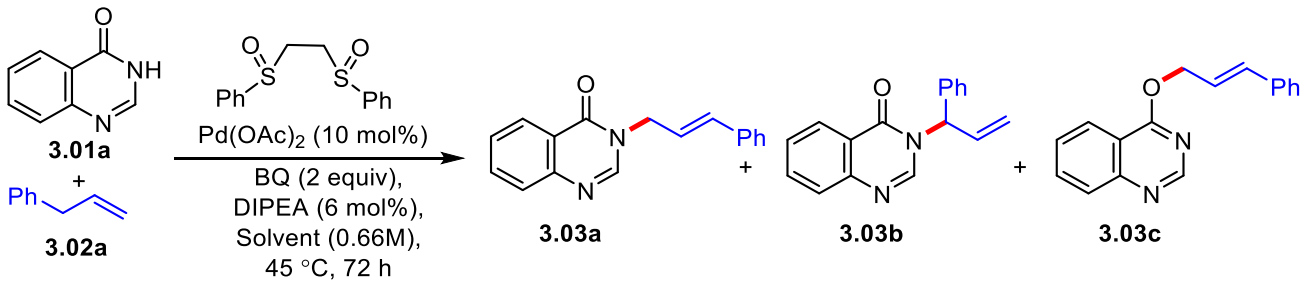

Entry	Solvent	Temp	Conversion [a,b]	**3.03a : 3.03b : 3.03c** [c]	Yield **3.03a**[d]
1	1,4-Dioxane	45	0	N/A	N/A
2	THF	45	0	N/A	N/A
3	DMF	45	0	N/A	N/A
4	DMSO	45	0	N/A	N/A
5	TBME	100	0	N/A	N/A
6	1,4-Dioxane	100	0	N/A	N/A
7	THF	100	0	N/A	N/A
8	DMF	100	0	N/A	N/A
9	DMSO	100	<10	100: 0 : 0	N/A

Reaction conditions: 3.01a (0.2 mmol) was treated with **3.02a** (0.3 mmol, 1.5 equiv) under white amination protocol with change in conditions. [a]Based on ^{1}H NMR of the crude reaction mixture (with respect to **3.01a**) using CH_2I_2 as internal standard. [b]Starting **1a** was found intact. [c]^{1}H NMR (using CH_2I_2 as internal standard) and GC-MS analysis of the crude reaction mixture determined the ratio of L/B and N/O selectivity respectively. [d]Isolated yield.

3.4.3. Reaction optimization: screening of palladium catalysts

Investigation of different palladium catalysts gave us more insights in to the allylic C-H amination of *N*-heterocycles. A clear effect of palladium catalyst counterion and ligand were found. More basic counter ions such as acetate (Table 3.4, entry 1 and 9) (pKa = 4.8) or trifluoroacetate (Table 3.4, entry 2) (pKa = -0.25), which are generally considered as very efficient for allylic C-H oxidations, were found to be detrimental in case of *N*-heterocycles. On the other hand, chloride counter ions (pKa = -8.0) were very effective for forming product in good yields (Table 3.4, entry 3, 5, and 6). Not surprisingly, phosphine ligated palladium complexes, which

were found to be ineffective in allylic C-H oxidation reactions,[49] were also found detrimental (Table 3.4, entry 4 and 7). Among all the tested Pd-catalysts, $PdCl_2$ was found to be optimal for the formation of product in good yields.

Table 3.4: Investigation of Pd-catalysts for the allylic amidation of **3.01a** with **3.02a**

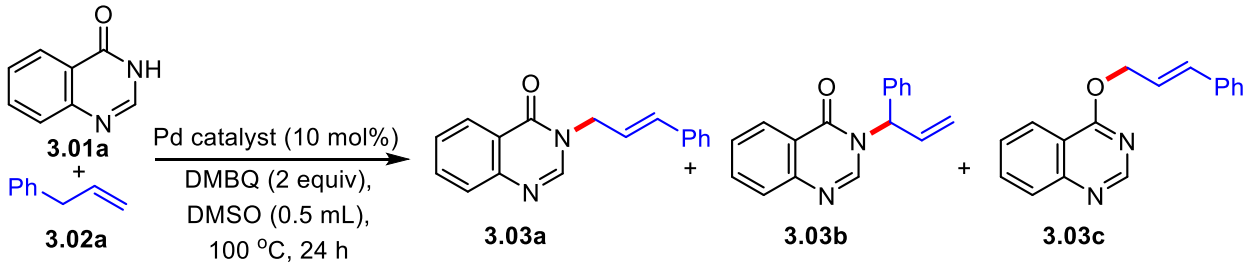

Entry	Pd-catalyst	Conversion[a]	**3.03a : 3.03b : 3.03c**[c,d]	Yield (**3.03a**)[e]
1	$Pd(OAc)_2$	<5[b]	100 : 0: 0	N/A
2	$Pd(TFA)_2$	27	100 : 0: 0	13
3	$PdCl_2$	91	100 : 0: 0	85
4	$(PPh_3)_2PdCl_2$	<5[b]	100 : 0: 0	N/A
5	$(PhCN)_2PdCl_2$	62	100 : 0: 0	55
6	$[PdCl(allyl)]_2$	69	100 : 0: 0	57
7	$Pd(dppf)Cl_2$	0[b]	N/A	N/A
8	IPrPd(allyl) Cl	21	100 : 0: 0	13
9	White Catalyst	<10[b]	100 : 0: 0	N/A
7	None	0[b]	N/A	N/A

Reaction conditions: 3.01a (0.2 mmol) was treated with **3.02a** (0.3 mmol, 1.5 equiv) in presence of different Pd-catalyst (10 mol %) and DMBQ (2 equiv) in DMSO (0.5 mL) at 100 °C for 24 h. [a]Based on ^{1}H NMR of the crude reaction mixture (with respect to **3.01a**) using CH_2I_2 as internal standard. [b]Starting **3.01a** was found intact. [c]^{1}H NMR (using CH_2I_2 as internal standard) analysis of the crude reaction mixture determined the ratio of E/Z and L/B selectivity. [d]GC-MS analysis of the crude reaction mixture determined the ratio of N/O selectivity. [e]Isolated yield.

3.4.4. Reaction optimization: solvent screen

With optimized $PdCl_2$ as the catalyst, we performed a solvent screen and found that DMSO is essential for the formation of product (Table 3.5, entry 10, 12 and 13). We hypothesize that in our reaction conditions DMSO can perform multiple functions. 1) It can act as a ligand/ coordinating group to palladium forming an active $Pd(DMSO)_2Cl_2$ catalyst for a facile C-H bond

cleavage. 2) DMSO increases the solubility of 4-Hydroxy quinazolinone (**3.01a**) 3) DMSO in combination with BQ can act as an oxidizing agent for the regeneration of Pd(II).

Table 3.5: Effect of solvents on the $PdCl_2$-catalylyzed the allylic amidation of **3.01a** with **3.02a**

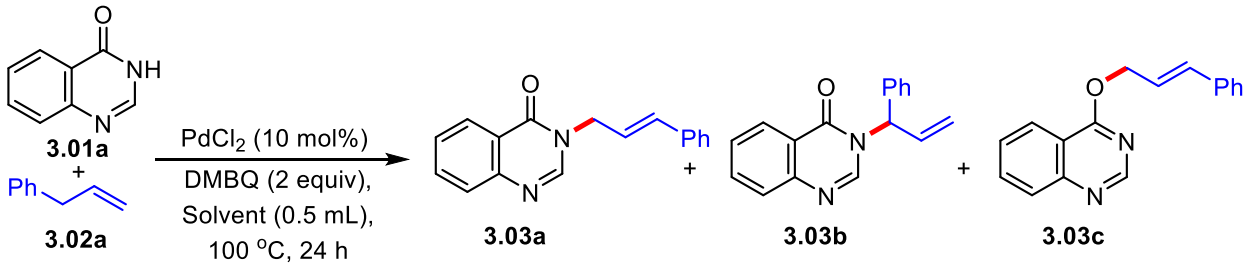

Entry	Solvent	Conversion[a]	**3.03a: 3.03b: 3.03c**[c,d]	Yield (**3.03a**)[e]
1	DMF	0[b]	N/A	N/A
2	MTBE	0[b]	N/A	N/A
3	THF	0[b]	N/A	N/A
4	DCE	0[b]	N/A	N/A
5	1,4-Dioxane	0[b]	N/A	N/A
6	Toluene	0[b]	N/A	N/A
7	DMC	0[b]	N/A	N/A
8	DME	0[b]	N/A	N/A
9	THF: DMSO (4:1)	0[b]	N/A	N/A
10	THF: DMSO (1:4)	81	100: 0: 0	63
11	1,4-Dioxane: DMSO (4:1)	0[b]	N/A	N/A
12	1,4-Dioxane: DMSO (1:4)	72	100: 0: 0	58
13	DMSO	93	100: 0: 0	86

Reaction conditions: 3.01a (0.2 mmol) was treated with **3.02a** (0.3 mmol, 1.5 equiv) in presence of $PdCl_2$ (10 mol %) and DMBQ (2 equiv) in different solvents (0.5 mL) at 100 °C for 24 h. [a]Based on ^{1}H NMR of the crude reaction mixture (with respect to **3.01a**) using CH_2I_2 as internal standard. [b]Starting **3.01a** was found intact. [c]^{1}H NMR (using CH_2I_2 as internal standard) analysis of the crude reaction mixture determined the ratio of E/Z and L/B selectivity. [d]GC-MS analysis of the crude reaction mixture determined the ratio N/O selectivity. [e]Isolated yield.

3.4.5. Reaction optimization: effect of acids or bases

Addition of acids or bases were known to increase the overall efficiency of allylic C-H amination.[42,45] In hope of developing mild conditions, we screened different acids and bases (Table 3.6). While tertiary amine bases yielded appreciable quantities of the product (Table 3.6, entries 1

and 4), addition carboxylate bases completely hindered the reaction (Table 3.6, entries 5-7). Addition of acids (Table 3.6, entries 8 and 9) also completely shut down the reaction consistent with the Pd-catalyst screening, where $Pd(OAc)_2$ or $Pd(TFA)_2$ did not yield any product highlighting the importance of counterion for the smooth formation of the product.

Table 3.6: Effect of acids/bases on the $PdCl_2$-catalyzed allylic amidation of **3.01a** with **3.02a**

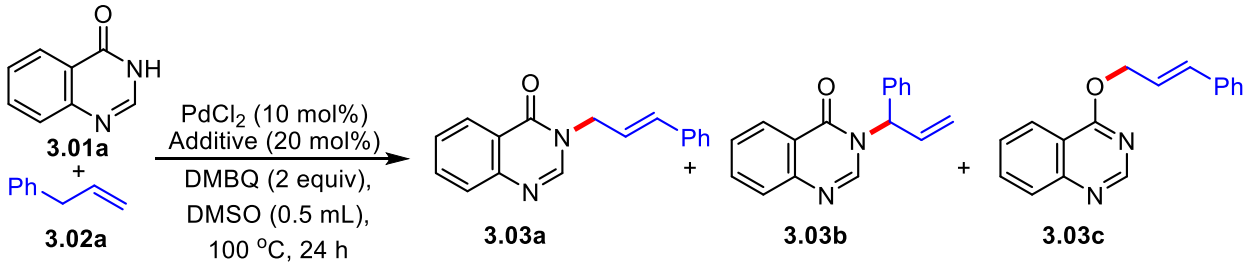

Entry	Acid/Base	Conversion[a]	**3.03a: 3.03b: 3.03c**[d,e]	Yield (**3.03a**)[f]
1	DIPEA	25[b]	100: 0: 0	13
2	DIPA	0[c]	N/A	N/A
3	DBU	0[c]	N/A	N/A
4	TEA	28[b]	100: 0: 0	15
5	NaOAc	0[c]	N/A	N/A
6	K_2CO_3	0[c]	N/A	N/A
7	Cs_2CO_3	0[c]	N/A	N/A
8	AcOH	0[c]	N/A	N/A
9	TFA	0[c]	N/A	N/A

Reaction conditions: 3.01a (0.2 mmol) was treated with **3.02a** (0.3 mmol, 1.5 equiv) in presence of $PdCl_2$ (10 mol %) and DMBQ (2 equiv) in DMSO (0.5 mL) in presence of acids/bases (20 mol%) at 100 °C for 24 h. [a]Based on ^{1}H NMR of the crude reaction mixture (with respect to **3.01a**) using CH_2I_2 as internal standard. [b]Unreacted **3.01a** was recovered intact. [c]Starting **3.01a** was found intact. [d]^{1}H NMR (using CH_2I_2 as internal standard) analysis of the crude reaction mixture determined the ratio of E/Z and L/B selectivity. [e]GC-MS analysis of the crude reaction mixture determined the ratio N/O selectivity. [f]Isolated yield.

3.4.6. Optimization of reaction conditions

An overall extensive screening of the reaction parameters provided us with the utilization of 10 mol % $PdCl_2$, 1.5 equivalents of 2,6-dimethylbenzoquinone as oxidant in 1M solution of DMSO at 100 °C for 24h as optimal conditions to yield **3.03a** as the sole product in 92% yield.

These conditions are operationally simple and do not require any additional additives, which are found to be essential in all the reported literature.

Table 3.7: Investigation of optimal reaction parameters for the $PdCl_2$-catalyzed allylic amidation of **3.01a** with **3.02a**

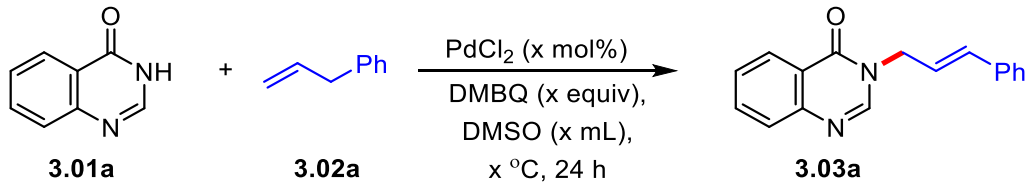

3.01a **3.02a** **3.03a**

Entry	Temperature (x °C)	Catalyst (x mol%)	Solvent (x mL)	DMBQ (x equiv)	Yield (**3.03a**) (%)[a]
1	120	10	0.5	2	93
2	100	10	0.5	2	92
3	80	10	0.5	2	75
4	50	10	0.5	2	0
5	rt	10	0.5	2	0
6	100	15	0.5	2	92
7	100	5	0.5	2	79
8	100	2	0.5	2	41
9	100	10	0.3	2	92
10	100	10	0.2	2	92
11	100	10	neat	2	35
12	100	10	0.2	2	92
13	**100**	**10**	**0.2**	**1.5**	**92**
14	100	10	0.2	1.2	78
15	100	10	0.2	1	51

Reaction conditions: 3.01a (0.2 mmol) was treated with **3.02a** (0.3 mmol, 1.5 equiv) in presence of different variations of $PdCl_2$, DMBQ in DMSO for 24 h. [a]Isolated yield

3.5. Olefin substrate scope for allylic amidation reaction of 4-hydroxy quinazolinone

Inspired by optimized results using allyl benzene **3.02a,** substrate scope with respect to olefins were investigated to demonstrate the generality of intermolecular allylic C-H amidation. Table 3.8 summarizes the results of the products obtained via allylic amidation of 4-hydroxyquinazoline **3.01a** and terminal olefins. In general, a wide range of either commercially

available or readily accessible terminal olefins smoothly underwent allylic C−H amidation reaction with **3.01a** in high yield and excellent chemo- (N vs O), regio- (linear vs branched), and stereoselectivity (*E* vs *Z*). It is significant to note that the reaction was seemingly insensitive to the electronic feature of the aryl moiety of the olefin substrates as both electron-donating (**3.04b** and **3.04c**) and electron-withdrawing (**3.04d,** and **3.04e**) substituted allyl benzenes reacted smoothly with high yields. Highly substituted and electron withdrawing pentafluorinated olefin (**3.04f)** also reacted well under optimized conditions forming the product in good yield. Olefins attached to heteroaryl compounds (**3.04h** and **3.04i**) or sterically demanding naphthyl compounds (**3.04j**) also formed product in excellent yields explaining the versatility of the optimized conditions. Aliphatic terminal olefins, which are generally less reactive, also reacted with **3.01a** affording products **3.04k-3.04m,** albeit in slightly lower yields.

Table 3.8: Intermolecular allylic C-H amidation of **3.01a** with terminal olefins

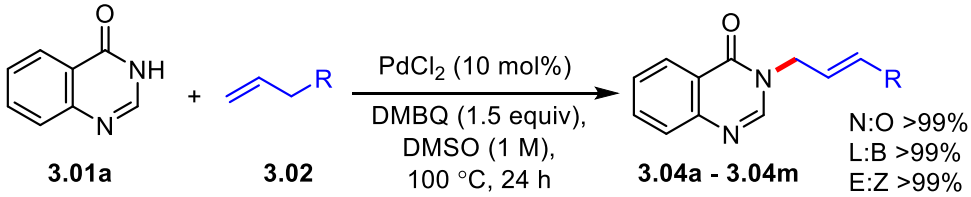

3.01a + **3.02** → **3.04a - 3.04m**

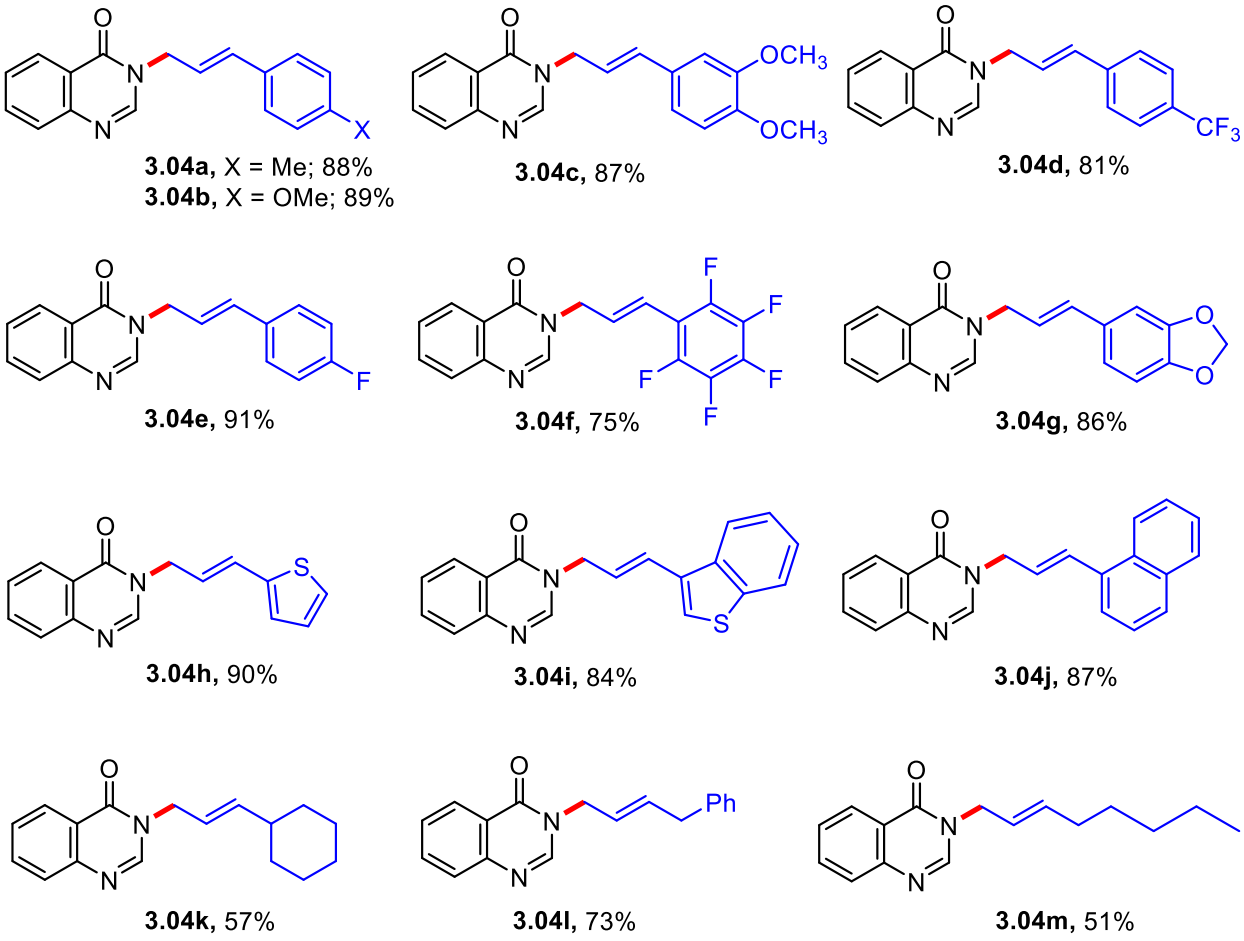

Reaction conditions: Reactions were conducted on 0.2 mmol scale, **3.01a** (0.2 mmol), **3.02** (1.5 equiv, 0.3 mmol), $PdCl_2$ (10 mol%), DMBQ (1.5 equiv, 0.3 mmol), DMSO (0.2 mL, 1M), 100 °C, 24 h. [b1]H NMR analysis of crude reaction determined the ratio of *E/Z* and L/B ratio. [c]GC-MS analysis of crude reaction mixture determined N/O ratio of products.

3.6. N-Heterocycle substrate scope for allylic C-H amidation of allylbenzene

We next examined the scope of *N*-heterocycles as nucleophile in the direct allylic C-H amidation of allylbenzene (Table 3.9). Differently substituted quinazolinones reacted well to produce high yields with excellent chemo- and regioselectivity towards linear isomer. Both electron-withdrawing (**3.05a**) and electron-donating (**3.05b**) quinazolinones reacted smoothly providing products in good yields. Additionally, more hindered 2-substituted quinazolinones with both electron withdrawing and donating substituents at para position also allylated with high efficiency (**3.05c**−**3.05f**). We envisioned that such an amidation strategy could be extended beyond the quinazolinone nucleus to other biologically relevant heterocycles with varying nucleophilicity. As shown in Table 3.9, we were delighted to discover that N-heterocycles such as phthalazine (**3.05g**), pyrimidine (**3.05h**), pyrazine (**3.05i**), and pyridines (**3.05j**−**3.05m**) all reacted well with excellent yields and high chemo-, regio-, and stereoselectivities towards *N*-allylation under optimized conditions. This demonstrates the versatility of our methodology to afford a range of allylated heterocycles. It is noteworthy to mention the excellent N vs O selectivity for the pyridinone and pyrazinone nucleophiles (**3.05i-3.05m)** as high linear selectivity towards *N*-allylation is oftentimes very difficult to achieve due to the labile nature of oxo-hydroxy tautomeric equilibria. In these cases of labile equilibrium, we also observed trace amounts of byproducts resulting from O-allylation and regioisomeric allylation (linear and branched products). These products, albeit in less yields shed light on the possibility of reaction optimization to produce exclusively O-allylated products. However, even after extensive optimization we could not form O-allylated products in appreciated yields.

Table 3.9: Intermolecular allylic C-H amidation with different *N*-heterocycles

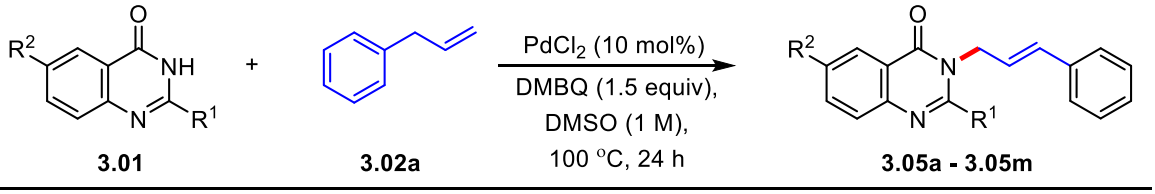

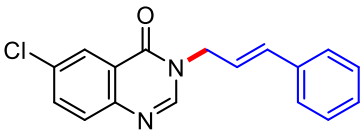

3.05a, 88%

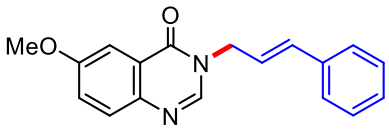

3.05b, 86%

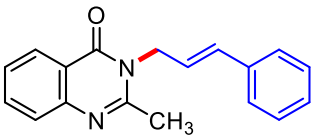

3.05c, 89%

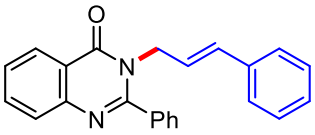

3.05d, 82%

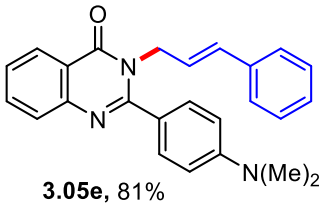

3.05e, 81%

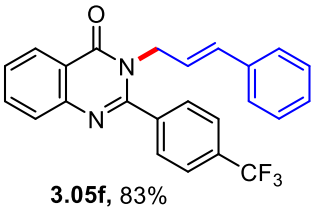

3.05f, 83%

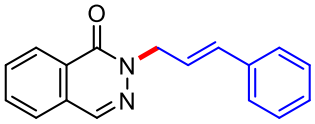

3.05g, 76%

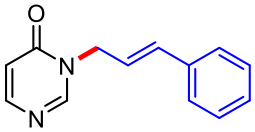

3.05h, 74%
N : O = 92 : 8
L : B = 95 : 5
E : Z = >99

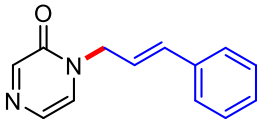

3.05i, 71%
N : O = 98 : 1
L : B = 96 : 4
E : Z = >99

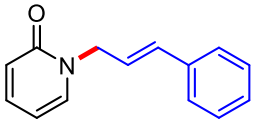

3.05j, 71%
N : O = 93 : 7
L : B = 97 : 3
E : Z = >99

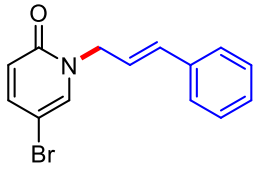

3.05k, 70%
N : O = 94 : 6
L : B = 95 : 5
E : Z = >99

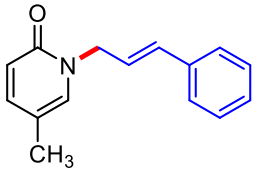

3.05l, 72%
N : O = 91 : 9
L : B = >99
E : Z = >99

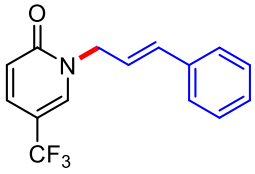

3.05m, 74%
N : O = 97 : 3
L : B = 92 : 8
E : Z = >99

Reaction conditions: Reactions were conducted on 0.2 mmol scale, **3.01** (0.2 mmol), **3.02a** (1.5 equiv, 0.3 mmol), $PdCl_2$ (10 mol%), DMBQ (1.5 equiv, 0.3 mmol), DMSO (0.2 mL, 1M), 100 °C, 24 h. [b1]H NMR analysis of crude reaction determined the ratio of *E/Z* and L/B ratio. [c]GC-MS analysis of crude reaction mixture determined N/O ratio of products.

3.7. Elucidating the mechanism: possible pathways

Exclusive or high selectivity towards linear N-allylation prompted us to investigate the mechanism of the reaction. To gain insight in to the mechanism of operation in our reaction condition, we proposed four different mechanistic pathways that govern the outcome of the allylic C-H oxidative amidation (Scheme 3.5).

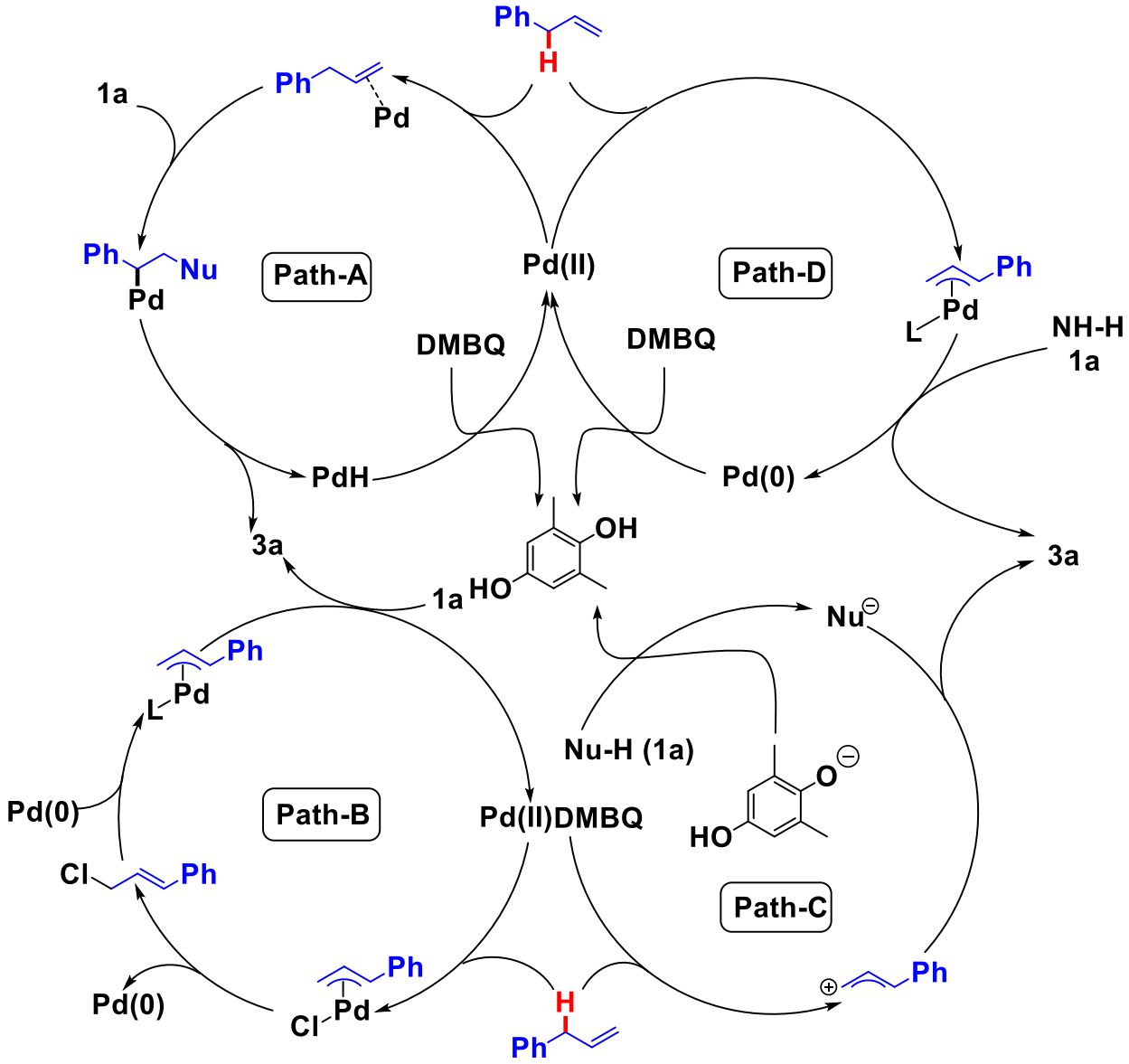

Scheme 3.5: Possible catalytic cycles for allylic C-H amidation

Path-A includes the Wacker-type aminopalladation/β-hydride elimination as the key step.[50–52] However the mechanism does not correspond to the fact that internal olefins when employed under reaction conditions did not yield any product. Further, a Wacker oxidation usually results in attack of the nucleophile at the secondary carbon over a primary carbon. As a control experiment, allylbenzene, in the absence of **3.01a**, underwent isomerization to **3.08** under the reaction conditions (~12%, GC-MS), suggesting that allylbenzene is capable of undergoing C−H activation through a Pd-allyl intermediate. Further, no isomerization of **3.08** to **3.02a** was observed. Thus, it is unlikely that the oxidative amidation process proceeds through an aminopalladation pathway (Scheme 3.6).

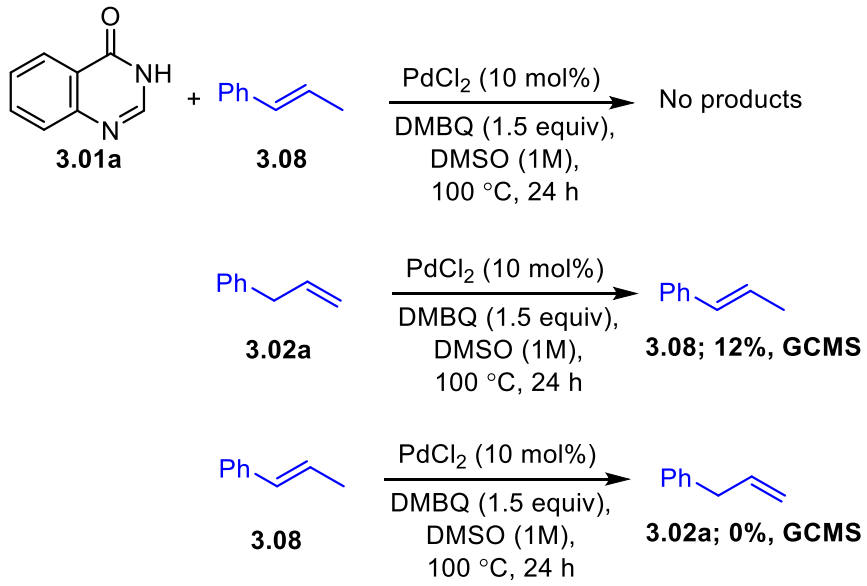

Scheme 3.6: Control studies for validating Wacker type process

Path-B includes the formation of cinnamyl chloride by C-H activation followed by chloride attack on the Pd-allyl intermediate, and cinnamyl chloride then undergo Tsuji-Trost reaction to give product.[53–55] In an independent study, treatment of **3.09** with **3.01a** under the reaction conditions produced **3.03a** only as a trace product (Scheme 3.7).

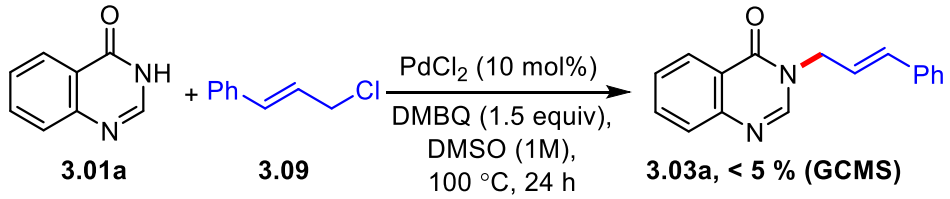

Scheme 3.7: Control study to validate Tsuji-Trost reaction

Path-C was based on work by Cheng and Bao on DDQ mediated oxidative coupling of diarylallylic C-H bond with methylenic C-H bond. They proposed a mechanism involves the formation of allyl cation by quinone mediated oxidation of olefin. However, DMBQ did not afford any product in the absence of $PdCl_2$ (Scheme 3.8).[56]

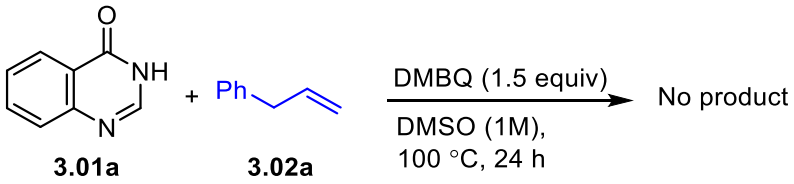

Scheme 3.8: Control study to validate DMBQ mediated allylic C-H amidation

Path-D involves formation of π-allylpalladium complex as the key intermediate, which is formed by the electrophilic allylic C-H bond cleavage by a sulfoxide-assisted palladium catalyst. Nucleophilic attack of the nitrogen of N-heteroarenes would form the allylated product **3.03a** followed by subsequent reoxidation of Pd(0) to Pd(II) by DMBQ to complete the catalytic cycle. To validate the pathway, a stoichiometric reaction, excluding nucleophile **3.01a**, in DMSO was performed and monitored by ^{1}H NMR. A dimeric π-allylpalladium chloride complex-B was observed, confirming the allylic C−H bond cleavage. When **3.01a** was then added, formation of **3.03a** was observed with similar yield and regioselectivity. In the absence of DMSO (using dioxane as solvent), the formation of dimeric π-allylpalladium chloride complex-B was not observed, suggesting the sulfoxide ligation to $PdCl_2$ was essential to effect Pd-mediated allylic C−H cleavage to form a monomeric π-allylpalladium intermediate that is detected in the form of

dimeric complex-B. Single-crystal X-ray structures of the sulfoxide ligated $PdCl_2$ (complex-A) and dimeric π-allylpalladium chloride complex-B were obtained to confirm their formation (Scheme 3.9).

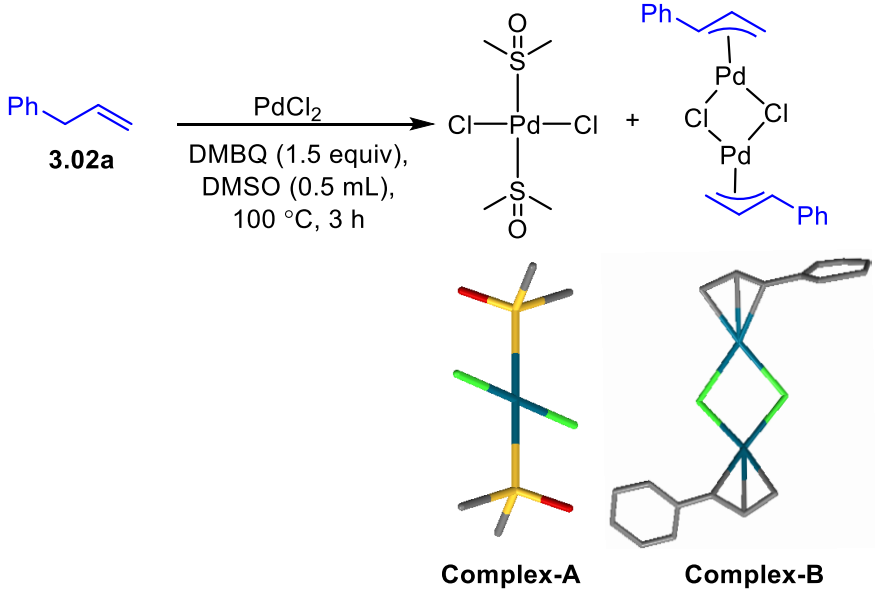

Scheme 3.9: Control study to validate allylic C-H oxidation/formation of π-allylpalladium complex

3.8. Intermolecular competitive studies of terminal olefins

To gain insight into the effect of electronics on the relative reactivity of allyl arenes in the allylation reaction, independent set of competitive reactions were carried between an equimolar mixture of allyl benzene **3.02a**, with electron donating 4-allylanisole **3.02b**, and allyl benzene **3.02a** with1-allyl-4-(trifluoromethyl) benzene **3.02c**, and allyl benzene **3.02a** with 2-allylthiophene **3.02d**, and allyl benzene **3.02a** with allyl cyclohexane **3.02e** were treated with 4-hydroxy quinazoline **3.01a** (Scheme 3.10). Selective amidation with allyl benzene **3.02a** took place in preference to electron donating (**3.02b**), heteroaryl (**3.02d**), and aliphatic olefins (**3.02e**), however, in the case of competition between allyl benzene **3.02a** and electron withdrawing (**3.02c**), selectivity favored toward **3.02c.** The observed selectivity indicates the differential susceptibility

of allylic C−H bond cleavage to form "π-allylpalladium" and or the relative electrophilicity allyl complex toward nucleophilic addition. In general, electron withdrawing groups on the aryl group of terminal olefins increases the reactivity of allylic C-H bond forming π-allylpalladium, in preference from electron donating substituents.

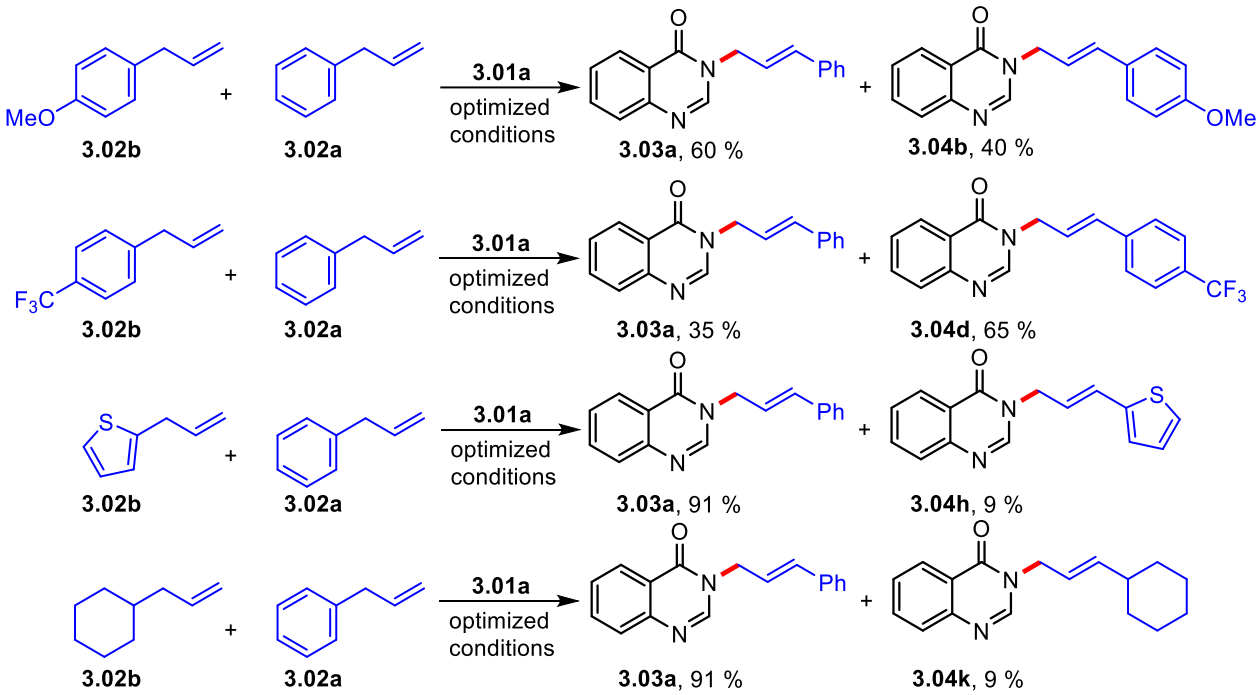

Scheme 3.10: Intermolecular competitive studies between terminal olefins

3.9. Summary and conclusion

In summary, we have developed a general Pd(II)/sulfoxide catalyzed allylic C−H activation method for the direct intermolecular amidation of terminal olefins with tautomerizable heterocycles (quinazoline, phthalazine, pyrimidine, pyrazine, and pyridine) with excellent chemo, regio-, and stereoselectivity. This operationally simple method proceeded with high substrate generality under uniform conditions (catalyst, solvent, temperature) offering a valuable tool to obtain structurally diverse N-heterocycles amenable for medicinal chemistry applications.

3.10. Outlook and future work

Isolation of palladium complexes **A** and **B** directly from $PdCl_2$, DMSO or olefin is an important advancement in π-allylpalladium chloride catalyst synthesis. This methodology provides an easy access to substituted π-cinnamylpalladium chloride dimer synthesis that are otherwise requires multiple steps and harmful reagents. We envisioned that these readily generated complexes could be utilized as precatalysts for a variety of important synthetic transformations. Scheme 3.11 highlights one of the challenging reaction of alkyne C-H activation/ *N*-amination reaction catalyzed by insitu formed electron deficient π-allylpalladium chloride dimer.

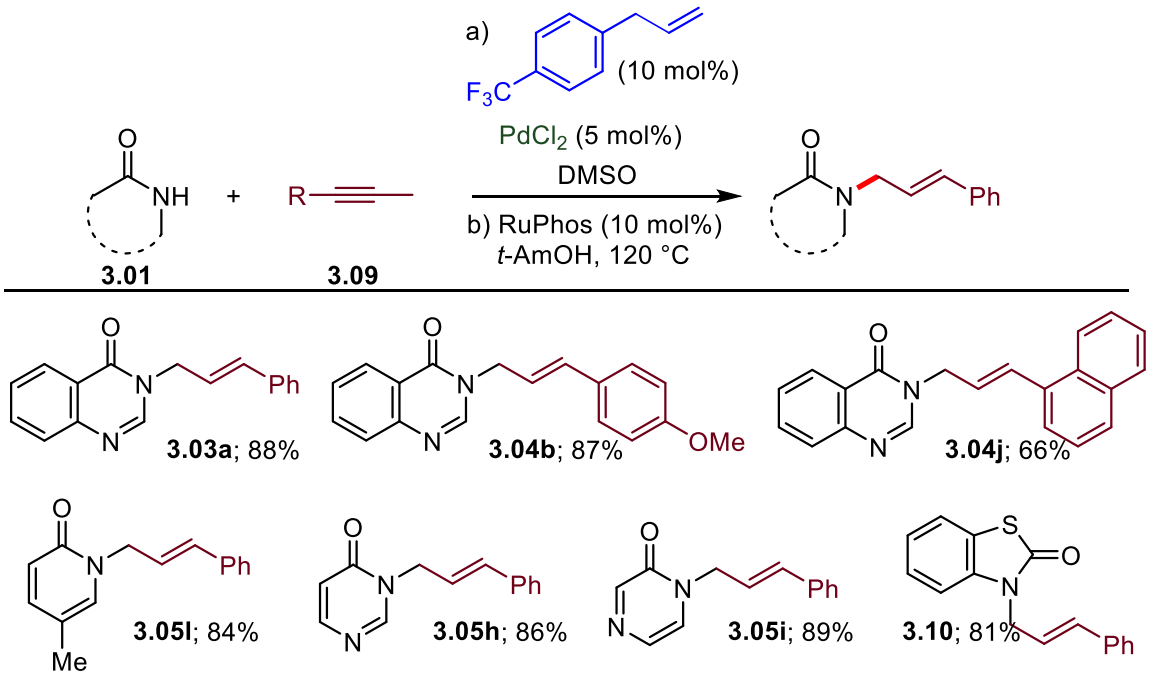

Scheme 3.11: Electron deficient π-allylpalladium chloride dimer for alkyne C-H activation/amination

The electron deficient π-allylpalladium chloride dimers were also found to be superior catalysts in other cross-coupling reactions (Scheme 3.12) compared to unsubstituted and parent cinnamyl derived π-allylpalladium chloride catalysts. The future studies in the group are focused on isolating the catalysts with varied electronics, to carry out mechanistic studies for the formation

of Pd(I) dimers, and to develop an efficient catalyst system for unreactive electrophiles such as amides and esters.

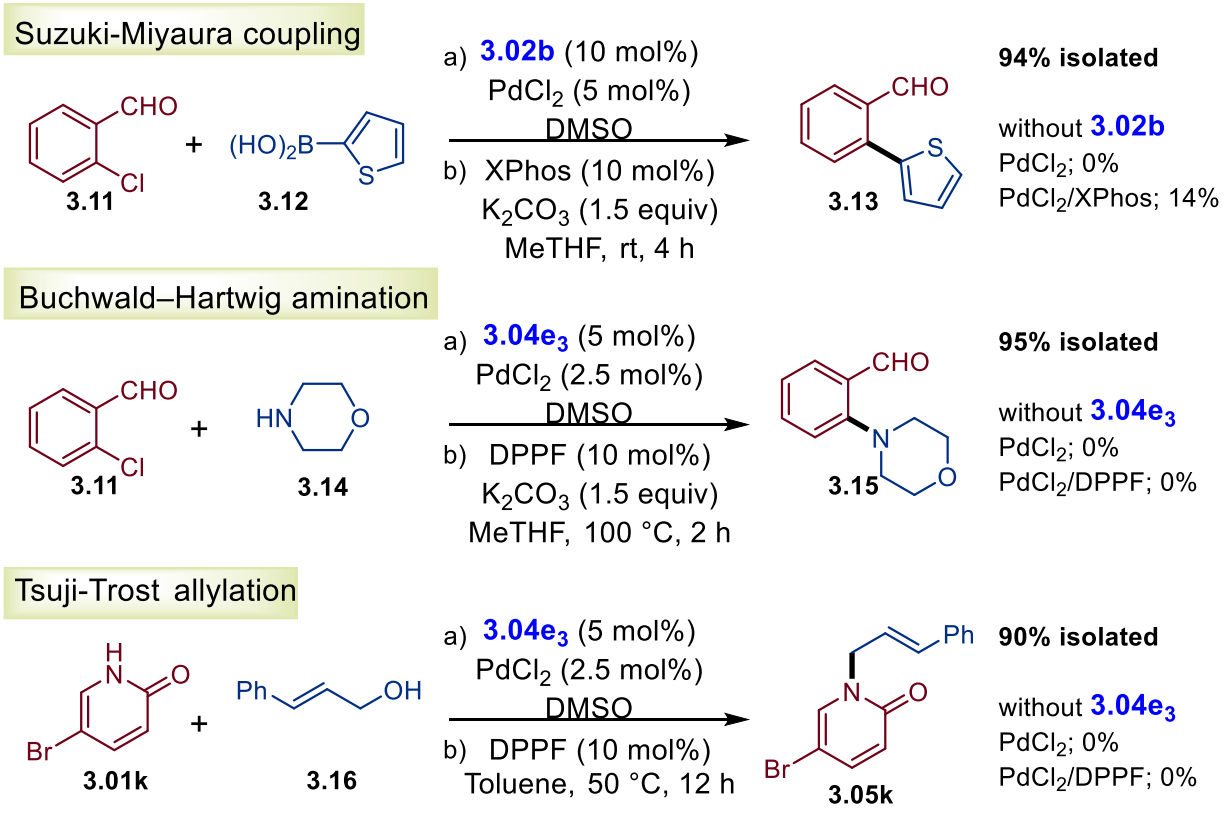

Scheme 3.12: Optimized precatalysts for coupling reactions.

3.11. Experimental section

3.11.1. General information

Unless otherwise noted, all manipulations were carried out under a nitrogen atmosphere using standard Schlenk-line or glovebox techniques. All glassware was oven-dried for at least 1h prior to use. THF, toluene, ether, and hexane were degassed by purging with nitrogen for 45 min and dried with a solvent purification system (MBraun MB-SPS). DMF, dioxane, dimethoxyethane, dichloroethane, methanol, and ethanol were dried over activated 3 Å molecular sieves and degassed by purging with nitrogen. All commercially obtained reagents/solvents were purchased from Alfa Aesar®, Sigma-Aldrich®, Acros®, TCI America®, Mallinckrodt®, and

Oakwood® Products, and used as received without further purification. TLC plates were visualized by exposure to ultraviolet light. Organic solutions were concentrated by rotary evaporation at ~10 torr. Flash column chromatography was performed with 32–63 microns silica gel. ^{1}H NMR spectra were obtained on a 400 MHz spectrometer, and chemical shifts were recorded relative to residual protiated solvent. ^{13}C NMR spectra were obtained at 100 MHz, and chemical shifts were recorded to the solvent resonance. Both ^{1}H and ^{13}C NMR chemical shifts were reported in parts per million downfield from tetramethylsilane (δ = 0 ppm). 19F NMR spectra were obtained at 282.4 MHz, and all chemical shifts were reported in parts per million upfield of CF3COOH (δ = -78.5 ppm). Coupling constants (*J*) are reported in hertz (Hz). Standard abbreviations indicating multiplicity were used as follows: s (singlet), br (broad), d (doublet), t (triplet), q (quartet) and m (multiplet). Data for ^{13}C NMR spectra are reported in terms of chemical shift (δ ppm). High-resolution mass spectra were obtained from a Bruker Daltronics BioTOF HRMS spectrometer.

3.11.2. Preparation of starting materials

3.11.2.1. Experimental procedure for the synthesis 2-methyl quinazolones

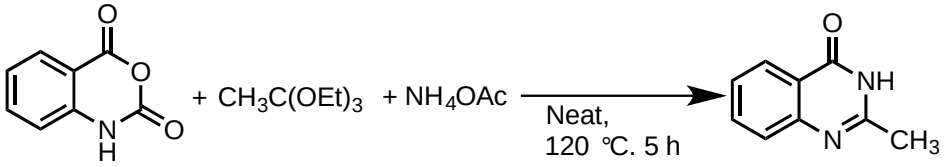

A mixture of isatoic anhydride (0.815 g, 5 mmol), ammonium acetate (0.578 g, 7.5 mmol, 1.5 equiv), and triethyl orthoacetate (1.22 g, 7.5 mmol, 1.5 equiv) were stirred magnetically at 120 °C (oil bath temp). After completion of the reaction (TLC, 5 h), the crude reaction mixture was recrystallized from EtOH to obtain analytically pure 2-methyl quinazolone (0.640 g, 80%) as white solid; **^{1}H NMR** (400 MHz, $CDCl_3$): δ8.27 (dd, *J* = 7.5, 1.2 Hz, 1H), 7.80-7.78 (m, 1H), 7.71 (d, *J*

= 7.7 Hz, 1H), 7.52-7.48 (m, 1H), 2.63 (s, 3H); **^{13}C NMR** (100 MHz, $CDCl_3$): δ 164.8, 153.7, 149.8, 135.5, 127.3, 127.0, 126.5, 120.6, 22.6.

3.11.2.2. Representative experimental procedure for the synthesis of 2-aryl quinazolones

R = Aryl, heteroaryl, cycloalkyl, styryl

Anthranilamide (5.0 mmol) and an aldehyde (6 mmol, 1.2 equiv) were dissolved in DMSO (10 mL). Then, the reaction mixture was stirred at 100 ^{o}C in an open flask and monitored by TLC. After complete consumption of the starting materials (12-36 h), the reaction mixture was cooled to rt. When water (100 mL) was added to the reaction mixture, the precipitate was formed and collected by filtration. Recrystallization in ethanol afforded substituted quinazolones.

3.11.2.3. Experimental procedure for the synthesis terminal alkene

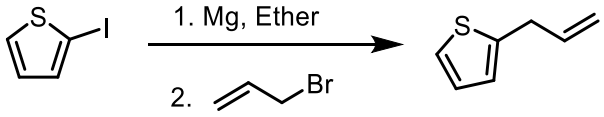

2-Iodothiophene (210 mg, 1mmol) was reacted with Mg turnings (36 mg, 1.5 mmol) in diethyl ether to form Grignard reagent. This solution was added dropwise to the reaction mixture containing allyl bromide (144 mg, 1.2 mmol) in diethyl ether at 0^0 C. the reaction mixture was then stirred at rt for 4h. Saturated ammonium chloride was then added to the reaction mixture and extracted with ethyl acetate (3 x 50 mL). Combined organics were then washed with brine solution, dried with sodium sulfate and evaporated under reduced pressure. The crude product was then column purified to yield 2-allyl thiophene as colorless liquid (94 mg, 76% yield). **^{1}H NMR** (400 MHz, DMSO-d_6) δ 7.33 (dd, *J* = 5.1, 1.3 Hz, 1H), 6.96 (dd, *J* = 5.2, 3.4 Hz, 1H), 6.86 (dq, *J* = 3.4,

1.1 Hz, 1H), 5.98 (ddt, *J* = 16.7, 10.0, 6.7 Hz, 1H), 5.23 – 5.04 (m, 2H), 3.57 (dq, *J* = 6.8, 1.3 Hz, 2H).

3.11.3. Experimental procedure for stochiometric study for palladium complexes

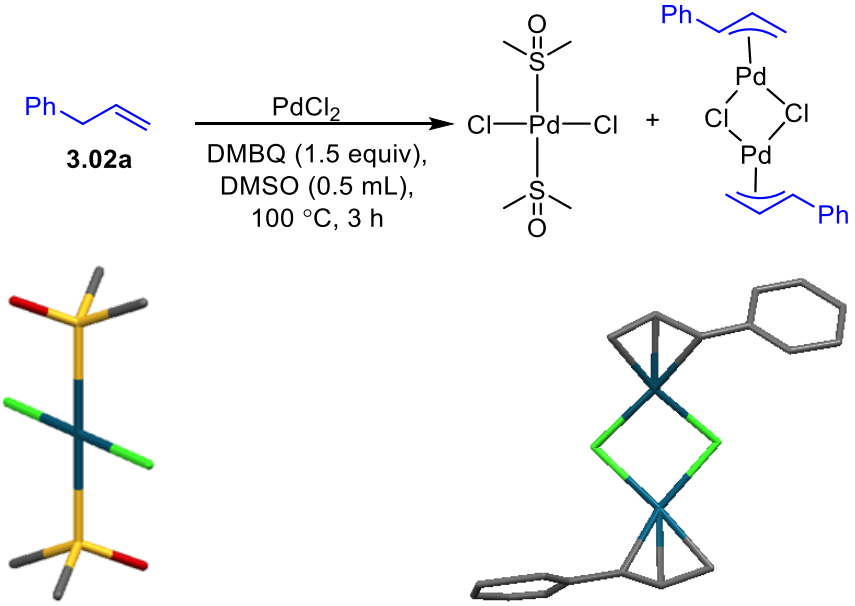

Figure 2.2: ORTEP diagrams of palladium complexes showing 40% probability ellipsoids

Experimental procedure: To a 1-dram vial fitted with a teflon cap, on a 0.5 mmol scale, palladium chloride (1 equiv), dimethyl benzoquinone (1.5 equiv, 0.75 mmol), **2a** (2 equiv, 1 mmol), DMSO (0.5 mL) and magnetic stir bar were added simultaneously under nitrogen atmosphere. Then the vial was transferred to a preheated magnetic stir plate at 100 ^{o}C and the progress of reaction was monitored by ^{1}H NMR. After 3 h, the reaction mixture was cooled to rt, layered with MeOH and allowed the crystals to grow.

3.11.4. General procedure for inter-molecular competition study involving two different terminal olefins

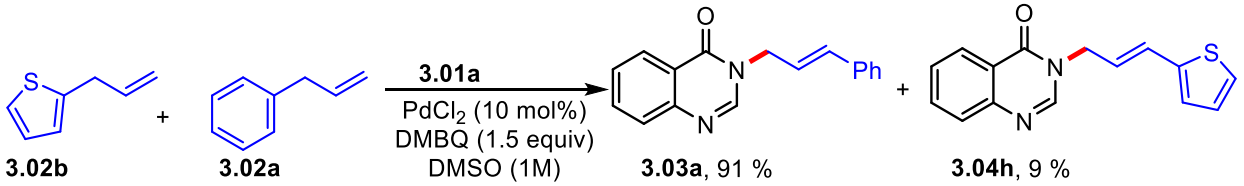

To a 4-dram vial fitted with a teflon cap, on a 0.2 mmol scale, palladium chloride (0.1 equiv, 0.02 mmol), dimethyl benzoquinone (1.5 equiv, 0.3 mmol), **3.02a** (0.2 equiv, 0.2 mmol), **3.02d** (0.2 equiv, 0.2 mmol), **3.01a** (0.2 equiv, 0.2 mmol), DMSO (0.2 mL) and magnetic stir bar were added simultaneously under nitrogen atmosphere. Then the vial was transferred to a preheated magnetic stir plate at 100 ^{o}C. After 24 h, the reaction mixture was then cooled to rt, diluted with MeOH (2 x 5 mL) and passed through bed of celite to remove catalyst. An aliquot portion (100 µL) of the organic layer was taken out, diluted with MeOH and subjected to GCMS to observe the selectivity, which reflected 91:09 selectivity in favor of **3.02a**

3.11.5. General experimental procedure for allylic C-H amidation of *N*-heterocycles

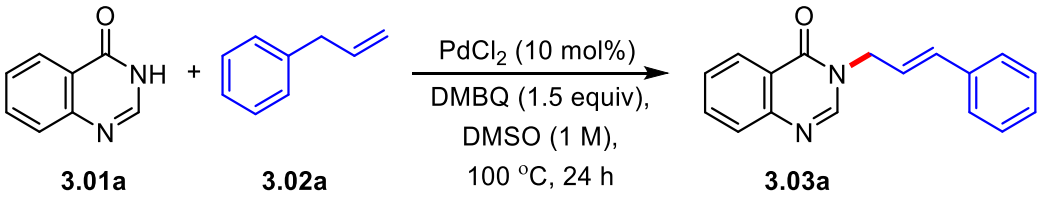

To a 1-dram vial fitted with a teflon cap, on a 0.2 mmol scale, palladium chloride (0.1 equiv, 0.02 mmol), dimethyl benzoquinone (1.5 equiv, 0.3 mmol), **3.02a** (1.5 equiv, 0.3 mmol), **3.01a** (1 equiv), DMSO (0.2 mL) and magnetic stir bar were added simultaneously under nitrogen atmosphere. Then the vial was transferred to a preheated magnetic stir plate at 100 ^{o}C. After 24 h, the reaction mixture was cooled to rt, adsorbed on to silica gel and purified by column

chromatography using hexane and ethyl acetate (10%-25%) as mobile phase to get analytically pure 3-(3-Phenyl-allyl)-3*H*-quinazolin-4-one **3.03a** as a pale yellow solid (92%).

3.11.6. Scale up study

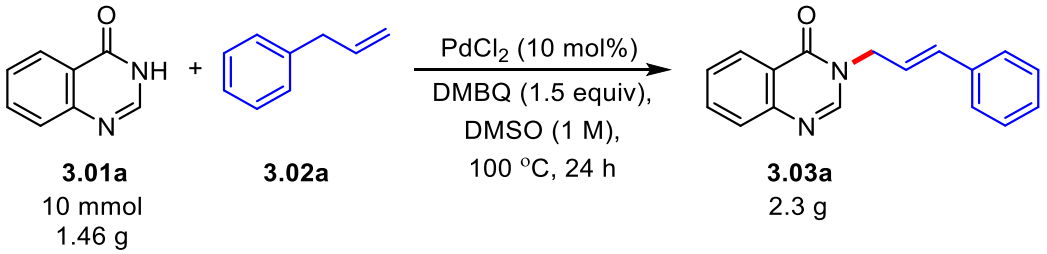

3.01a
10 mmol
1.46 g

3.02a

3.03a
2.3 g

To a 6-dram vial fitted with a teflon cap, palladium chloride (177.3 mg, 0.1 equiv, 1 mmol), dimethyl benzoquinone (2.0 g, 1.5 equiv, 15 mmol), **3.02a** (1.8 g, 1.5 equiv, 15 mmol), **3.01a** (1.46 g, 1 equiv, 10 mmol), DMSO (10 mL) and magnetic stir bar were added simultaneously. Then the vial was transferred to a preheated magnetic stir plate at 100 °C. After 48 h, the reaction mixture was cooled to rt and diluted with ethyl acetate (20 mL). The organic layer was washed with saturated cold brine solution (2*20 mL each) to remove the DMSO and water-soluble contents. The aqueous layer was further extracted with ethyl acetate (2*10 mL). To the combined organic layer, anhydrous sodium sulfate was added to remove the traces of moisture. The collected organic layer was evaporated under reduced pressure. The crude reaction mixture was then adsorbed on to silica gel and purified by column chromatography using hexane and ethyl acetate (10%-25%) as mobile phase to get analytically pure 3-(3-Phenyl-allyl)-3*H*-quinazolin-4-one **3.03a** (2.3 g, 88%).

3.12. Analytical data of reported compounds

3-(3-Phenyl-allyl)-3H-quinazolin-4-one: Prepared by general procedure to yield **3.03a** as

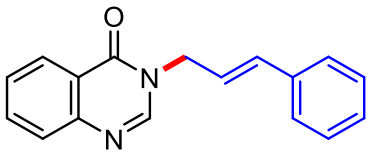

a white solid (48.2 mg, 93%). **^{1}H NMR** (400 MHz, $CDCl_3$) δ 8.40 – 8.32 (m, 1H), 8.12 (s, 1H), 7.83 – 7.70 (m, 2H), 7.56 – 7.50 (m, 1H), 7.42 – 7.22 (m, 5H), 6.73 – 6.63 (m, 1H), 6.40 – 6.32 (m, 1H), 4.85 – 4.77 (m, 2H); **^{13}C NMR** (100 MHz, $CDCl_3$) δ 160.9, 148.2, 146.1, 135.8, 134.5, 134.3, 128.7, 128.3, 127.5, 127.3, 126.8,

126.6, 122.8, 122.2, 48.2; HRMS (ESI-TOF) *m/z*: $[M + H]^+$ Calcd for $C_{17}H_{15}N_2O$ 263.1184, Found 263.1178.

3-(3-p-Tolyl-allyl)-3H-quinazolin-4-one: Prepared by general procedure to yield **3.04a** as

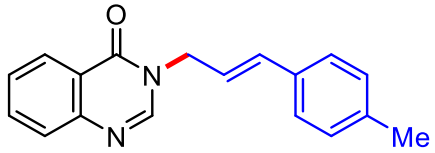

a pale yellow solid (48.6 mg, 88%). **^{1}H NMR** (400 MHz, $CDCl_3$) δ 8.36 (ddd, *J* = 8.1, 1.5, 0.7 Hz, 1H), 8.12 (s, 1H), 7.82 – 7.72 (m, 2H), 7.54 (ddd, *J* = 8.2, 6.8, 1.5 Hz, 1H), 7.32 – 7.25 (m, 2H), 7.14 (d, *J* = 8.0 Hz, 2H), 6.66 (dt, *J* = 15.8, 1.3 Hz, 1H), 6.31 (dt, *J* = 15.8, 6.5 Hz, 1H), 4.80 (dd, *J* = 6.5, 1.4 Hz, 2H), 2.35 (s, 3H); **^{13}C NMR** (100 MHz, $CDCl_3$) δ 160.9, 148.1, 146.2, 138.2, 134.5, 134.3, 133.0, 129.4, 127.5, 127.3, 126.8, 126.5, 122.2, 121.7, 48.2, 21.2; **HRMS** (ESI-TOF) *m/z*: $[M + H]^+$ Calcd for $C_{18}H_{16}N_2O$ 277.1341, Found 277.1332.

3-[3-(4-Methoxy-phenyl)-allyl]-3H-quinazolin-4-one: Prepared by general procedure to

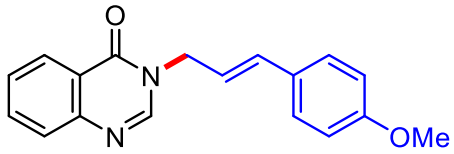

yield **3.04b** as a pale yellow solid (52 mg, 89%). **^{1}H NMR** (400 MHz, $CDCl_3$) δ 8.36 (ddd, *J* = 8.0, 1.5, 0.6 Hz, 1H), 8.13 (s, 1H), 7.84 – 7.71 (m, 2H), 7.54 (ddd, *J* = 8.2, 6.9, 1.5 Hz, 1H), 7.38 – 7.30 (m, 2H), 6.90 – 6.83 (m, 2H), 6.64 (dt, *J* = 15.8, 1.4 Hz, 1H), 6.22 (dt, *J* = 15.8, 6.6 Hz, 1H), 4.79 (dd, *J* = 6.6, 1.4 Hz, 2H), 3.82 (s, 3H); **^{13}C NMR** (100 MHz, $CDCl_3$) δ 161.0, 159.7, 148.2, 146.2, 134.3, 134.1, 128.5, 127.9, 127.5, 127.3, 126.8, 122.2, 120.4, 114.1, 55.3, 48.3; **HRMS** (ESI-TOF) *m/z*: $[M + H]^+$ Calcd for $C_{18}H_{16}N_2O_2$ 293.1290, Found 293.1281.

3-[3-(3,4-Dimethoxy-phenyl)-allyl]-3H-quinazolin-4-one: Prepared by general

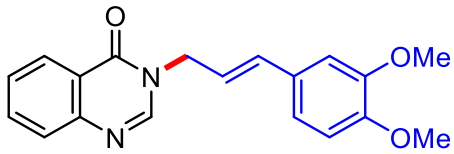

procedure to yield **3.04c** as a pale yellow solid (56 mg, 87%). **^{1}H NMR** (400 MHz, $CDCl_3$) δ 8.34 (ddd, *J* = 8.0, 1.5, 0.7 Hz, 1H), 8.12 (s, 1H), 7.81 – 7.70 (m, 2H), 7.52 (ddd, *J* = 8.2, 6.8, 1.5 Hz, 1H), 6.95 – 6.88 (m, 2H), 6.84 – 6.77 (m, 1H), 6.62 (dt, *J* = 15.7, 1.3 Hz, 1H), 6.22 (dt, *J* = 15.8, 6.5 Hz, 1H), 4.78

(dd, *J* = 6.5, 1.4 Hz, 2H), 3.87 (s, 6H); **^{13}C NMR** (100 MHz, $CDCl_3$) δ 160.9, 149.3, 149.1, 148.1, 146.2, 134.3, 134.3, 128.8, 127.5, 127.3, 126.8, 122.2, 120.7, 120.1, 111.0, 108.8, 55.9, 55.8, 48.3; **HRMS** (ESI-TOF) *m/z*: $[M + H]^+$ Calcd for $C_{18}H_{16}N_2O_2$ 293.1290, Found 293.1281.

3-[3-(4-Trifluoromethyl-phenyl)-allyl]-3H-quinazolin-4-one: Prepared by general procedure to yield **3.04d** as a pale yellow solid (53 mg, 81%). **^{1}H NMR** (400 MHz, $CDCl_3$) δ 8.36 (dd, *J* = 8.0, 1.4 Hz, 1H), 8.11 (s, 1H), 7.84 – 7.72 (m, 2H), 7.56 (dt, *J* = 8.1, 7.1 Hz, 3H), 7.47 (d, *J* = 8.2 Hz, 2H), 6.69 (d, *J* = 15.9 Hz, 1H), 6.46 (dt, *J* = 15.9, 6.2 Hz, 1H), 4.83 (dd, *J* = 6.2, 1.4 Hz, 2H); **^{13}C NMR** (100 MHz, $CDCl_3$) δ 160.9, 148.12, 146.02, 139.21, 134.43, 132.76, 130.0 (q, *J* = 32.6 Hz), 127.60, 127.50, 126.80, 126.79, 125.6 (q, *J* = 3.6 Hz), 126.7 (q, *J* = 272.6 Hz), 122.12, 48.05; **^{19}F NMR** (376 MHz, DMSO-d_6) *δ* -61.17; **HRMS** (ESI-TOF) *m/z*: $[M + H]^+$ Calcd for $C_{18}H_{13}F_3N_2O$ 331.1058, Found 331.1057.

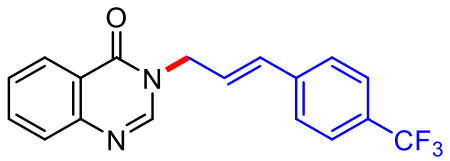

3-[3-(4-Fluoro-phenyl)-allyl]-3H-quinazolin-4-one: Prepared by general procedure to yield **3.04e** as a pale yellow solid (51 mg, 91%). **^{1}H NMR** (400 MHz, $CDCl_3$) δ 8.35 (dd, *J* = 8.0, 1.5 Hz, 1H), 8.11 (s, 1H), 7.83 – 7.71 (m, 2H), 7.54 (ddd, *J* = 8.1, 6.9, 1.5 Hz, 1H), 7.40 – 7.31 (m, 2H), 7.05 – 6.96 (m, 2H), 6.64 (dt, *J* = 15.8, 1.4 Hz, 1H), 6.28 (dt, *J* = 15.8, 6.4 Hz, 1H), 4.79 (dd, *J* = 6.3, 1.4 Hz, 2H); **^{13}C NMR** (100 MHz, $CDCl_3$) δ 162.7 (d, *J* = 248.9 Hz), 160.91, 148.13, 146.10, 134.33, 133.24, 132.0 (d, *J* = 3.4 Hz), 128.2 (d, *J* = 8.7 Hz) 127.5 (d, *J* = 15.6 Hz), 126.80, 122.57 (d, *J* = 2.4 Hz), 122.16, 115.6 (d, *J* = 22.6 Hz), 99.99, 48.16; **^{19}F NMR** (376 MHz, $CDCl_3$) δ -113.27; **HRMS** (ESI-TOF) *m/z*: $[M + H]^+$ Calcd for $C_{17}H_{13}FN_2O$ 281.1090, Found 281.1082.

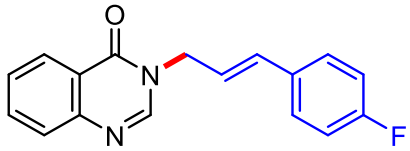

3-(3-Pentafluorophenyl-allyl)-3H-quinazolin-4-one: Prepared by general procedure to yield **3.04f** as a pale brown solid (53 mg, 75%). 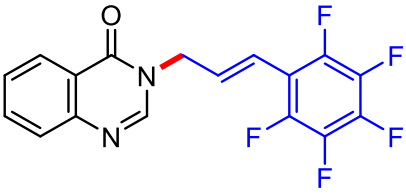 **^{1}H NMR** (400 MHz, $CDCl_3$) δ 8.35 (ddd, *J* = 8.0, 1.5, 0.6 Hz, 1H), 8.10 (s, 1H), 7.86 – 7.72 (m, 2H), 7.55 (ddd, *J* = 8.2, 6.9, 1.4 Hz, 1H), 6.71 (dt, *J* = 16.3, 6.0 Hz, 1H), 6.59 (dt, *J* = 16.4, 1.4 Hz, 1H), 4.86 (dd, *J* = 6.0, 1.3 Hz, 2H); **^{13}C NMR** (100 MHz, $CDCl_3$) δ 160.8, 148.1, 145.8, 144.6 (dm, *J* = 251.2 Hz), 140.7 (dm, 262.6 Hz), 136.4 (m), 134.5, 132.3 (ddd, 2.5 Hz), 127.6, 127.6, 126.8, 122.1, 118.5, 110.7 (ddd, 4.4 Hz), 48.7; **^{19}F NMR** (376 MHz, $CDCl_3$) δ -142.16, -142.28 (m), -154.70 (tt, *J* = 21.0, 1.7 Hz), -162.23, -162.59 (m); **HRMS** (ESI-TOF) *m/z*: $[M + H]^+$ Calcd for $C_{17}H_9F_5N_2O$ 353.0713, Found 353.0709.

3-(3-Benzo[1,3]dioxol-5-yl-allyl)-3H-quinazolin-4-one: Prepared by general procedure to yield **3.04g** as a brown solid (53 mg, 86%). 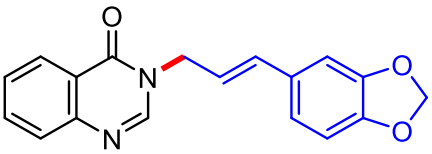 **^{1}H NMR** (400 MHz, $CDCl_3$) δ 8.34 (ddd, *J* = 8.1, 1.4, 0.7 Hz, 1H), 8.10 (s, 1H), 7.82 – 7.70 (m, 2H), 7.52 (ddd, *J* = 8.2, 6.8, 1.5 Hz, 1H), 6.91 (d, *J* = 1.7 Hz, 1H), 6.81 (dd, *J* = 8.0, 1.7 Hz, 1H), 6.75 (d, *J* = 8.0 Hz, 1H), 6.59 (dt, *J* = 15.8, 1.4 Hz, 1H), 6.17 (dt, *J* = 15.7, 6.5 Hz, 1H), 5.95 (s, 2H), 4.77 (dd, *J* = 6.4, 1.4 Hz, 2H); **^{13}C NMR** (100 MHz, $CDCl_3$) δ 160.9, 148.1, 148.1, 147.8, 146.2, 134.3, 134.2, 130.2, 127.5, 127.3, 126.8, 122.2, 121.6, 120.9, 108.3, 105.8, 101.2, 48.2; **HRMS** (ESI-TOF) *m/z*: $[M + H]^+$ Calcd for $C_{18}H_{14}N_2O_3$ 307.1083, Found 307.1076.

3-(3-Thiophen-2-yl-allyl)-3H-quinazolin-4-one: Prepared by general procedure to yield **3.04h** as a dark brown solid (48 mg, 90%). 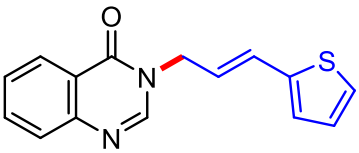 **^{1}H NMR** (400 MHz, $CDCl_3$) δ 8.35 (ddd, *J* = 8.0, 1.5, 0.6 Hz, 1H), 8.10 (s, 1H), 7.82 – 7.70 (m, 2H), 7.53 (ddd, *J* = 8.2, 6.8, 1.5 Hz, 1H), 7.19 (dt, *J* = 4.9, 0.9 Hz, 1H), 7.03 – 6.93 (m, 2H), 6.83 – 6.78 (m, 1H), 6.17 (dt, *J* = 15.6, 6.5 Hz, 1H), 4.76 (dd, *J* = 6.6, 1.4 Hz, 2H); **^{13}C NMR**

(100 MHz, $CDCl_3$) δ 160.9, 148.1, 146.1, 140.7, 134.3, 127.7, 127.5, 127.5, 127.4, 126.8, 126.8, 125.2, 122.2, 122.1, 47.9; **HRMS** (ESI-TOF) *m/z*: $[M + H]^+$ Calcd for $C_{15}H_{12}N_2OS$ 269.0749, Found 269.0742.

3-(3-Benzo[b]thiophen-3-yl-allyl)-3H-quinazolin-4-one: Prepared by general procedure

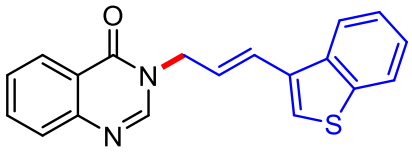

to yield **3.04i** as a pale yellow solid (53 mg, 84%). **^{1}H NMR** (400 MHz, $CDCl_3$) δ 8.39 – 8.36 (m, 1H), 8.17 (s, 1H), 7.93 – 7.83 (m, 2H), 7.84 – 7.74 (m, 2H), 7.55 (ddd, J = 8.2, 6.7, 1.6 Hz, 1H), 7.48 (s, 1H), 7.46 – 7.35 (m, 2H), 7.00 – 6.95 (m, 1H), 6.48 – 6.41 (m, 1H), 4.87 (dd, J = 6.5, 1.5 Hz, 2H); **^{13}C NMR** (100 MHz, $CDCl_3$) δ 160.9, 148.1, 146.1, 140.4, 137.3, 134.4, 132.5, 127.6, 127.4, 126.9, 126.8, 124.7, 124.5, 124.3, 123.5, 122.9, 122.2, 121.8, 48.5; **HRMS** (ESI-TOF) *m/z*: $[M + H]^+$ Calcd for $C_{19}H_{14}N_2OS$ 319.0905, Found 319.0907.

3-(3-Naphthalen-1-yl-allyl)-3H-quinazolin-4-one: Prepared by general procedure to

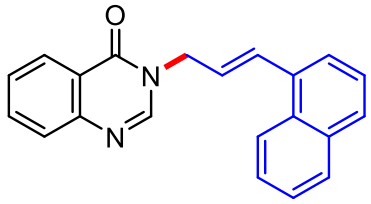

yield **3.04j** as a pale brown solid (54 mg, 87%). **^{1}H NMR** (400 MHz, $CDCl_3$) δ 8.42 – 8.36 (m, 1H), 8.22 (s, 1H), 8.08 (dt, *J* = 8.2, 1.2 Hz, 1H), 7.89 – 7.84 (m, 1H), 7.84 – 7.74 (m, 3H), 7.60 (dt, *J* = 7.3, 1.0 Hz, 1H), 7.58 – 7.51 (m, 3H), 7.51 – 7.41 (m, 2H), 6.40 (dt, *J* = 15.5, 6.4 Hz, 1H), 4.93 (dd, *J* = 6.5, 1.5 Hz, 2H); **^{13}C NMR** (100 MHz, $CDCl_3$) δ 160.9, 148.1, 146.1, 134.3, 133.6, 133.5, 132.0, 131.0, 128.6, 128.6, 127.6, 127.4, 126.9, 126.3, 126.0, 125.9, 125.5, 124.3, 123.5, 122.2, 48.4; **HRMS** (ESI-TOF) *m/z*: $[M + H]^+$ Calcd for $C_{22}H_{18}N_2O$ 327.1497, Found 327.1485.

3-(3-Cyclohexyl-allyl)-3H-quinazolin-4-one: Prepared by general procedure to yield

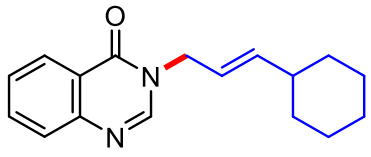

3.04k as a colorless liquid (31 mg, 57%). **^{1}H NMR** (400 MHz, $CDCl_3$) δ 8.34 (dd, *J* = 8.0, 1.4 Hz, 1H), 8.06 (s, 1H), 7.77 (ddd, *J* = 8.3, 6.9, 1.5 Hz, 1H), 7.72 (dd, *J* = 8.2, 1.4 Hz, 1H), 7.52 (ddd, *J* = 8.2, 6.9, 1.5 Hz, 1H), 5.76

(ddt, *J* = 15.4, 6.4, 1.3 Hz, 1H), 5.62 – 5.54 (m, 1H), 4.60 (dt, *J* = 6.3, 1.1 Hz, 2H), 2.07 – 1.94 (m, 1H), 1.80 – 1.68 (m, 4H), 1.27 – 1.01 (m, 5H), 0.96 – 0.77 (m, 1H); **^{13}C NMR** (100 MHz, $CDCl_3$) δ 160.9, 148.1, 146.2, 142.4, 134.2, 127.4, 127.2, 126.8, 122.2, 121.0, 48.0, 40.3, 32.5, 26.1, 25.9; **HRMS** (ESI-TOF) *m/z*: $[M + H]^+$ Calcd for $C_{17}H_{20}N_2O$ 269.1654, Found 269.1643.

3-(4-Phenyl-but-2-enyl)-3H-quinazolin-4-one: Prepared by general procedure to yield

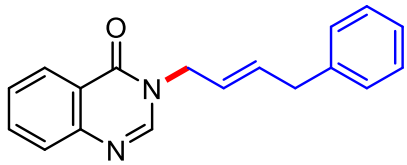

3.04l as a pale yellow solid (40 mg, 73%). **^{1}H NMR** (400 MHz, $CDCl_3$) δ 8.36 (dd, *J* = 7.9, 1.5 Hz, 1H), 8.05 (s, 1H), 7.82 – 7.68 (m, 2H), 7.53 (ddd, *J* = 8.1, 7.0, 1.4 Hz, 1H), 7.36 – 7.27 (m, 4H), 7.28 – 7.20 (m, 1H), 6.48 (dt, *J* = 15.7, 1.3 Hz, 1H), 6.20 (dt, *J* = 15.6, 7.1 Hz, 1H), 4.16 (t, *J* = 7.0 Hz, 2H), 2.75 (qd, *J* = 7.1, 1.4 Hz, 2H); **^{13}C NMR** (100 MHz, $CDCl_3$) δ 161.1, 148.2, 146.5, 136.9, 134.2, 133.7, 128.6, 127.5, 127.5, 127.3, 126.7, 126.2, 124.9, 122.2, 46.9, 32.7; **HRMS** (ESI-TOF) *m/z*: $[M + H]^+$ Calcd for $C_{18}H_{16}N_2O$ 277.1341, Found 277.1352.

3-Oct-2-enyl-3H-quinazolin-4-one: Prepared by general procedure to yield **3.04m** as a

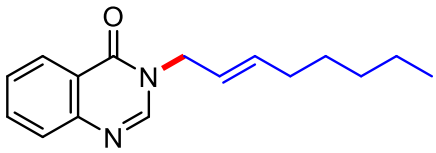

colorless oil (26 mg, 51%). **^{1}H NMR** (400 MHz, $CDCl_3$) δ 8.30 – 8.25 (m, 1H), 8.01 (s, 1H), 7.72 – 7.68 (m, 1H), 7.67 – 7.64 (m, 1H), 7.47 – 7.43 (m, 1H), 5.81 – 5.70 (m, 1H), 5.62 – 5.54 (m, 1H), 4.56 – 4.53 (m, 3H), 2.04 – 1.98 (m, 3H), 1.36 – 1.31 (m, 2H), 1.27 – 1.19 (m, 4H), 0.85 – 0.81 (m, 3H); **^{13}C NMR** (100 MHz, $CDCl_3$) δ 160.8, 148.1, 146.2, 136.6, 134.1, 127.4, 127.1, 126.7, 123.4, 122.1, 47.9, 32.1, 31.3, 28.5, 22.4, 14.0; **HRMS** (ESI-TOF) *m/z*: $[M + H]^+$ Calcd for $C_{16}H_{20}N_2O$ 257.1654, Found 257.1660.

6-Chloro-3-(3-phenyl-allyl)-3H-quinazolin-4-one: Prepared by general procedure to

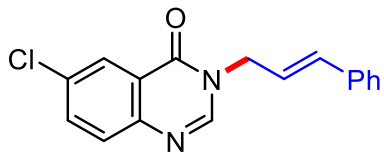

yield **3.05a** as an off white solid (52 mg, 88%) **^{1}H NMR** (400 MHz, $CDCl_3$) δ 8.34 – 8.28 (m, 1H), 8.10 (s, 1H), 7.74 – 7.65 (m,

2H), 7.39 (dt, *J* = 6.1, 1.6 Hz, 2H), 7.33 (ddd, *J* = 7.5, 6.7, 1.5 Hz, 2H), 7.30 – 7.25 (m, 1H), 6.69 (dt, *J* = 15.9, 1.4 Hz, 1H), 6.34 (dt, *J* = 15.8, 6.5 Hz, 1H), 4.80 (dd, *J* = 6.6, 1.5 Hz, 2H); **^{13}C NMR** (101 MHz, $CDCl_3$) δ 159.9, 146.6, 146.3, 135.7, 134.9, 134.7, 133.2, 129.2, 128.7, 128.4, 126.6, 126.2, 123.2, 122.4, 48.3; **HRMS** (ESI-TOF) m/z: $[M + H]^+$ Calcd for $C_{17}H_{14}ClN_2O$ 297.0795, Found 297.0792.

6-Methoxy-3-(3-phenyl-allyl)-3H-quinazolin-4-one: Prepared by general procedure to

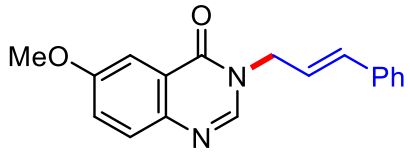

yield **3.05b** as a white solid (52 mg, 89%) **^{1}H NMR** (400 MHz, $CDCl_3$) δ 8.02 (s, 1H), 7.71 (d, *J* = 3.0 Hz, 1H), 7.66 (d, *J* = 8.9 Hz, 1H), 7.40 – 7.35 (m, 3H), 7.35 – 7.29 (m, 2H), 7.29 – 7.23 (m, 1H), 6.67 (dt, *J* = 15.8, 1.3 Hz, 1H), 6.36 (dt, *J* = 15.9, 6.4 Hz, 1H), 4.80 (dd, *J* = 6.4, 1.4 Hz, 2H), 3.94 (s, 3H); **^{13}C NMR** (100 MHz, $CDCl_3$) δ 160.8, 158.8, 144.0, 142.7, 135.8, 134.4, 129.1, 128.6, 128.2, 126.6, 124.5, 123.0, 122.9, 106.1, 55.9, 48.2; **HRMS** (ESI-TOF) m/z: $[M + H]^+$ Calcd for $C_{18}H_{17}N_2O_2$ 293.1290, Found 293.1293.

2-Methyl-3-(3-phenyl-allyl)-3H-quinazolin-4-one: Prepared by general procedure to

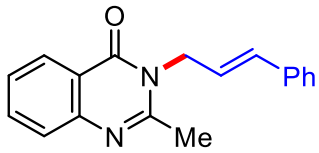

yield **3.05c** as a white solid (49 mg, 89%). **^{1}H NMR** (400 MHz, $CDCl_3$) δ 8.29 (ddd, *J* = 8.0, 1.6, 0.6 Hz, 1H), 7.74 (ddd, *J* = 8.5, 7.1, 1.6 Hz, 1H), 7.66 – 7.62 (m, 1H), 7.45 (ddd, *J* = 8.2, 7.1, 1.2 Hz, 1H), 7.38 – 7.33 (m, 2H), 7.32 – 7.27 (m, 2H), 7.26 – 7.21 (m, 1H), 6.55 (dt, *J* = 16.0, 1.6 Hz, 1H), 6.30 (dt, *J* = 16.0, 5.8 Hz, 1H), 4.92 (dd, *J* = 5.9, 1.6 Hz, 2H), 2.69 (s, 3H); **^{13}C NMR** (100 MHz, $CDCl_3$) δ 161.9, 154.3, 147.4, 136.0, 134.3, 133.0, 128.6, 128.1, 126.9, 126.7, 126.5, 126.5, 122.9, 120.5, 46.0, 23.2; **HRMS** (ESI-TOF) m/z: $[M + H]^+$ Calcd for $C_{18}H_{17}N_2O$ 277.1341, Found 277.1339.

2-Phenyl-3-(3-phenyl-allyl)-3H-quinazolin-4-one: Prepared by general procedure to yield **3.05d** as a white solid (55 mg, 82%). **^{1}H NMR** (400 MHz, $CDCl_3$) δ 8.43 – 8.36 (m, 1H), 7.81 – 7.78 (m, 2H), 7.61 – 7.51 (m, 6H), 7.30 (d, *J* = 4.2 Hz, 4H), 7.27 – 7.21 (m, 1H), 6.29 – 6.16 (m, 2H), 4.79 (d, *J* = 5.1 Hz, 2H); **^{13}C NMR** (100 MHz, $CDCl_3$) δ 162.1, 156.2, 147.3, 136.2, 135.4, 134.5, 133.6, 130.0, 128.7, 128.6, 128.1, 127.9, 127.6, 127.1, 126.9, 126.5, 123.3, 121.0, 47.9; **HRMS** (ESI-TOF) m/z: $[M + H]^+$ Calcd for $C_{23}H_{19}N_2O$ 339.1497, Found 339.1497.

2-(4-Dimethylamino-phenyl)-3-(3-phenyl-allyl)-3H-quinazolin-4-one: Prepared by general procedure to yield **3.05e** as a white semisolid (62 mg, 81%). **^{1}H NMR** (400 MHz, DMSO-d_6) δ 8.21 – 8.15 (m, 1H), 7.83 (ddd, *J* = 8.4, 7.1, 1.6 Hz, 1H), 7.67 (dt, *J* = 8.1, 0.9 Hz, 1H), 7.56 – 7.47 (m, 3H), 7.38 – 7.34 (m, 2H), 7.32 – 7.26 (m, 2H), 7.25 – 7.19 (m, 1H), 6.82 – 6.75 (m, 2H), 6.37 – 6.19 (m, 2H), 2.97 (s, 6H); **^{13}C NMR** (100 MHz, DMSO) δ 162.0, 157.2, 151.5, 147.7, 136.6, 134.9, 131.6, 129.9, 129.0, 128.1, 127.6, 126.9, 126.7, 126.7, 125.3, 122.7, 120.5, 111.5, 48.0, 40.2; **HRMS** (ESI-TOF) m/z: $[M + H]^+$ Calcd for $C_{25}H_{24}N_3O$ 382.1919, Found 382.1923.

3-(3-Phenyl-allyl)-2-(4-trifluoromethyl-phenyl)-3H-quinazolin-4-one: Prepared by general procedure to yield **3.05f** as a white solid (67 mg, 83%). **^{1}H NMR** (400 MHz, $CDCl_3$) δ 8.40 (dd, *J* = 7.9, 1.4 Hz, 1H), 7.84 – 7.79 (m, 3H), 7.77 (dd, *J* = 8.1, 1.3 Hz, 1H), 7.75 – 7.71 (m, 2H), 7.58 (ddd, *J* = 8.2, 7.0, 1.4 Hz, 1H), 7.35 – 7.23 (m, 5H), 6.28 – 6.11 (m, 2H), 4.77 (dd, *J* = 5.6, 0.9 Hz, 2H); **^{13}C NMR** (100 MHz, $CDCl_3$) δ 161.8, 154.8, 147.1, 138.7, 135.9, 134.7, 133.7, 132.1 (q, *J* = 33.0 Hz), 128.8, 128.6, 128.2, 127.6, 127.5, 127.0, 126.5, 125.7 (q, *J* = 3.8 Hz), 123.7 (q, *J*

= 273.3 Hz), 122.9, 121.0, 47.9; **^{19}F NMR** (376 MHz, DMSO-d_6) δ -61.18; **HRMS** (ESI-TOF) m/z: $[M + H]^+$ Calcd for $C_{24}H_{18}F_3N_2O$ 407.1371, Found 407.1368.

2-(3-Phenyl-allyl)-2H-phthalazin-1-one: Prepared by general procedure to yield **3.05g** as

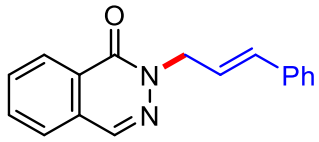

a white solid (40 mg, 76%). **^{1}H NMR** (400 MHz, $CDCl_3$) δ 8.46 (dd, J = 7.5, 1.8 Hz, 1H), 8.19 (s, 1H), 7.81 – 7.71 (m, 2H), 7.69 – 7.67 (m, 1H), 7.40 – 7.37 (m, 2H), 7.34 – 7.25 (m, 2H), 7.25 – 7.18 (m, 1H), 6.74 – 6.70 (m, 1H), 6.51 – 6.43 (m, 1H), 5.02 (dd, J = 6.4, 1.3 Hz, 2H); **^{13}C NMR** (100 MHz, $CDCl_3$) δ 159.2, 138.1, 136.5, 133.8, 133.1, 131.7, 129.7, 128.5, 128.0, 127.8, 126.7, 126.6, 126.1, 123.7, 53.3; **HRMS** (ESI-TOF) m/z: $[M + H]^+$ Calcd for $C_{17}H_{15}N_2O$ 263.1184, Found 263.1186.

3-(3-Phenyl-allyl)-3H-pyrimidin-4-one: Prepared by general procedure to yield **3.05h** as

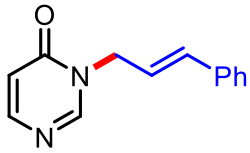

a white solid (31 mg, 74%). **^{1}H NMR** (400 MHz, $CDCl_3$) δ 8.19 (s, 1H), 7.92 (d, *J* = 6.6 Hz, 1H), 7.42 – 7.38 (m, 2H), 7.37 – 7.32 (m, 2H), 7.32 – 7.29 (m, 1H), 6.68 (dt, *J* = 16.0, 1.4 Hz, 1H), 6.51 (dd, *J* = 6.6, 1.0 Hz, 1H), 6.32 (dt, *J* = 15.9, 6.6 Hz, 1H), 4.73 (dd, *J* = 6.6, 1.4 Hz, 2H); **^{13}C NMR** (100 MHz, $CDCl_3$) δ 160.7, 153.4, 150.9, 135.6, 135.2, 128.7, 128.4, 126.7, 122.1, 116.1, 48.5; **HRMS** (ESI-TOF) m/z: $[M + Na]^+$ Calcd for $C_{13}H_{12}N_2ONa$ 235.0847, Found 235.0845.

1-(3-Phenyl-allyl)-1H-pyrazin-2-one: Prepared by general procedure to yield **3.05i** as a

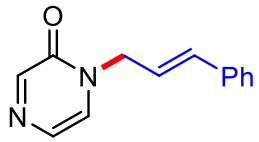

white solid (30 mg, 71%). **^{1}H NMR** (400 MHz, $CDCl_3$) δ 8.23 – 8.18 (m, 1H), 7.42 – 7.38 (m, 2H), 7.38 – 7.36 (m, 1H), 7.36 – 7.32 (m, 2H), 7.32 – 7.29 (m, 1H), 7.19 (dd, *J* = 4.4, 1.2 Hz, 1H), 6.68 (dt, *J* = 15.8, 1.4 Hz, 1H), 6.27 (dt, *J* = 15.8, 6.7 Hz, 1H), 4.69 (dd, *J* = 6.7, 1.4 Hz, 2H); **^{13}C NMR** (100 MHz, $CDCl_3$) δ 156.0, 149.7, 135.8, 135.5, 128.7, 128.5, 127.8, 126.7, 124.0, 121.6, 50.3; **HRMS** (ESI-TOF) m/z: [M + Na]+ Calcd for $C_{13}H_{12}N_2ONa$ 235.0847, Found 235.0844.

1-(3-Phenyl-allyl)-1H-pyridin-2-one: Prepared by general procedure to yield **3.05j** as a

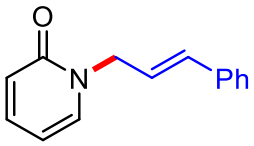

pale brown liquid (30 mg, 71%). **^{1}H NMR** (400 MHz, $CDCl_3$) δ 7.40 – 7.36 (m, 2H), 7.36 – 7.33 (m, 2H), 7.33 – 7.28 (m, 2H), 7.28 – 7.23 (m, 1H), 6.64 – 6.56 (m, 2H), 6.33 (dt, *J* = 15.9, 6.5 Hz, 1H), 6.19 (td, *J* = 6.7, 1.4 Hz, 1H), 4.73 (dd, *J* = 6.5, 1.4 Hz, 2H); **^{13}C NMR** (100 MHz, $CDCl_3$) δ 162.5, 139.5, 136.9, 136.0, 134.1, 128.6, 128.1, 126.6, 123.6, 121.2, 106.2, 50.7; **HRMS** (ESI-TOF) m/z: $[M + Na]^+$ Calcd for $C_{14}H_{13}NONa$ 234.0895, Found 234.0895.

5-Bromo-1-(3-phenyl-allyl)-1H-pyridin-2-one: Prepared by general procedure to yield

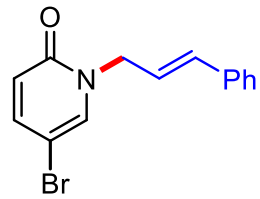

3.05k as a brown liquid (41 mg, 70%). **^{1}H NMR** (400 MHz, $CDCl_3$) δ 7.42 (d, J = 2.6 Hz, 1H), 7.32 (d, J = 6.9 Hz, 2H), 7.30 – 7.24 (m, 3H), 7.24 – 7.18 (m, 1H), 6.56 (d, J = 15.8 Hz, 1H), 6.46 (d, J = 9.7 Hz, 1H), 6.22 (dt, J = 15.8, 6.5 Hz, 1H), 4.61 (d, J = 6.5 Hz, 2H); **^{13}C NMR** (100 MHz, $CDCl_3$) δ 160.8, 142.5, 137.0, 135.8, 134.8, 128.7, 128.4, 128.3, 126.6, 122.9, 122.1, 98.0, 50.9; **HRMS** (ESI-TOF) m/z: $[M + Na]^+$ Calcd for $C_{14}H_{12}BrNONa$ 311.9994, Found 311.9997.

5-Methyl-1-(3-phenyl-allyl)-1H-pyridin-2-one: Prepared by general procedure to yield

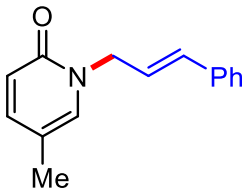

3.05l as a brown liquid (32 mg, 72%). **^{1}H NMR** (400 MHz, $CDCl_3$) δ 7.40 – 7.35 (m, 2H), 7.33 – 7.21 (m, 3H), 7.18 (dd, J = 9.2, 2.6 Hz, 1H), 7.10 – 7.06 (m, 1H), 6.61 – 6.52 (m, 2H), 6.31 (dt, J = 15.8, 6.4 Hz, 1H), 4.69 (dd, J = 6.5, 1.4 Hz, 2H), 2.06 (s, 3H); **^{13}C NMR** (100 MHz, CDCl3) δ 161.7, 142.1, 136.1, 134.4, 133.8, 128.6, 128.0, 126.6, 123.9, 120.6, 115.2, 50.6, 17.1; **HRMS** (ESI-TOF) m/z: $[M + Na]^+$ Calcd for $C_{15}H_{15}NONa$ 248.1046, Found 248.1049.

1-(3-Phenyl-allyl)-5-trifluoromethyl-1H-pyridin-2-one: Prepared by general procedure

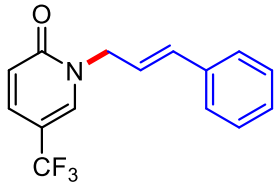

to yield **3.05m** as a **c**olorless liquid (41 mg, 74%). **^{1}H NMR** (400 MHz, $CDCl_3$) δ 7.75 (dt, *J* = 3.0, 1.4 Hz, 1H), 7.47 (dd, *J* = 9.6, 2.7 Hz, 1H), 7.44 – 7.38 (m, 2H), 7.38 – 7.32 (m, 2H), 7.32 – 7.27 (m, 1H), 6.73 – 6.63 (m, 2H), 6.31 (dt, *J* = 15.9, 6.7 Hz, 1H), 4.75 (dd, *J* = 6.7, 1.4 Hz, 2H); **^{13}C NMR** (100 MHz, CDCl3) δ 161.72, 136.5 (q, 5.4 Hz), 135.62, 135.36, 135.1 (q, 2.4 Hz), 128.71, 128.45, 126.69, 123.3 (q, *J* = 268.8 Hz), 122.24, 121.6, 109.7 (q, *J* = 35.1 Hz), 51.4; **^{19}F NMR** (376 MHz, CDCl3) δ -62.32; **HRMS** (ESI-TOF) *m/z*: $[M + H]^+$ Calcd for $C_{15}H_{12}F_3NO$ 280.0949, Found 280.0945.

3.13. References

(1) Ryabov, A. D. Mechanisms of Intramolecular Activation of Carbon-Hydrogen Bonds in Transition-Metal Complexes. *Chem. Rev.* **1990**, *90* (2), 403–424.

(2) Arndtsen, B. A.; Bergman, R. G.; Mobley, T. A.; Peterson, T. H. Selective Intermolecular Carbon-Hydrogen Bond Activation by Synthetic Metal Complexes in Homogeneous Solution. *Acc. Chem. Res.* **1995**, *28* (3), 154–162.

(3) Shilov, A. E.; Shul'pin, G. B. Activation of C−H Bonds by Metal Complexes. *Chem. Rev.* **1997**, *97* (8), 2879–2932.

(4) Kakiuchi, F.; Murai, S. Catalytic C−H/Olefin Coupling. *Acc. Chem. Res.* **2002**, *35* (10), 826–834.

(5) Balcells, D.; Clot, E.; Eisenstein, O. C—H Bond Activation in Transition Metal Species from a Computational Perspective. *Chem. Rev.* **2010**, *110* (2), 749–823.

(6) Hashiguchi, B. G.; Bischof, S. M.; Konnick, M. M.; Periana, R. A. Designing Catalysts for Functionalization of Unactivated C–H Bonds Based on the CH Activation Reaction. *Acc. Chem. Res.* **2012**, *45* (6), 885–898.

(7) Labinger, J. A.; Bercaw, J. E. Understanding and Exploiting C–H Bond Activation. *Nature* **2002**, *417* (6888), 507–514.

(8) Dupont, J.; Consorti, C. S.; Spencer, J. The Potential of Palladacycles: More Than Just Precatalysts. *Chem. Rev.* **2005**, *105* (6), 2527–2572.

(9) Alberico, D.; Scott, M. E.; Lautens, M. Aryl−Aryl Bond Formation by Transition-Metal-Catalyzed Direct Arylation. *Chem. Rev.* **2007**, *107* (1), 174–238.

(10) Jazzar, R.; Hitce, J.; Renaudat, A.; Sofack-Kreutzer, J.; Baudoin, O. Functionalization of Organic Molecules by Transition-Metal-Catalyzed C(Sp3)□H Activation. *Chem. - A Eur. J.* **2010**, *16* (9), 2654–2672.

(11) Baudoin, O. Transition Metal-Catalyzed Arylation of Unactivated C(Sp3)–H Bonds. *Chem. Soc. Rev.* **2011**, *40* (10), 4902.

(12) Periana, R. A.; Bhalla, G.; Tenn, W. J.; Young, K. J. H.; Liu, Y.; Mironov, O.; Jones, C. J.; Ziatdinov, V. R. Perspectives on Some Challenges and Approaches for Developing the next Generation of Selective, Low Temperature, Oxidation Catalysts for Alkane Hydroxylation Based on the CH Activation Reaction. *J. Mol. Catal. A Chem.* **2004**, *220*, 7–25.

(13) Patil, M.; Thiel, W. Origin of Selectivity of Tsuji-Trost Allylic Alkylation of Lactones: Highly Ordered Transition States with Lithium-Containing Enolates. *Chem. - A Eur. J.* **2012**, *18* (33), 10408–10418.

(14) Chen, M. S.; White, M. C. A Sulfoxide-Promoted, Catalytic Method for the Regioselective Synthesis of Allylic Acetates from Monosubstituted Olefins via C-H Oxidation. *J. Am. Chem. Soc.* **2004**, *126* (5), 1346–1347.

(15) Chen, M. S.; Prabagaran, N.; Labenz, N. A.; White, M. C. Serial Ligand Catalysis: A Highly Selective Allylic C-H Oxidation. *J. Am. Chem. Soc.* **2005**, *127* (19), 6970–6971.

(16) Delcamp, J. H.; White, M. C. Sequential Hydrocarbon Functionalization: Allylic C-H Oxidation/Vinylic C-H Arylation. *J. Am. Chem. Soc*. **2006**, *128*(47), 15076–15077.

(17) Campbell, A. N.; White, P. B.; Guzei, I. A.; Stahl, S. S. Allylic C-H Acetoxylation with a 4,5-Diazafluorenone-Ligated Palladium Catalyst: A Ligand-Based Strategy to Achieve Aerobic Catalytic Turnover. *J. Am. Chem. Soc*. **2010**, *132*(43), 15116–15119.

(18) Henderson, W. H.; Check, C. T.; Proust, N.; Stambuli, J. P. Allylic Oxidations of Terminal Olefins Using a Palladium Thioether Catalyst. *Org. Lett*. **2010**, *12*(4), 824–827.

(19) Qi, X.; Chen, P.; Liu, G. Advances and Challenges in Palladium-Catalyzed Intermolecular Selective Allylic C-H Functionalization of Alkenes. *Science China Chemistry*. **2015**, 1249–1251.

(20) Young, A. J.; White, M. C. Catalytic Intermolecular Allylic C-H Alkylation. *J. Am. Chem. Soc*. **2008**, *130*(43), 14090–14091.

(21) Lin, S.; Song, C. X.; Cai, G. X.; Wang, W. H.; Shi, Z. J. Intra/Intermolecular Direct Allylic Alkylation via Pd(II)-Catalyzed Allylic C-H Activation. *J. Am. Chem. Soc*. **2008**, *130*(39) 12901–12903.

(22) Engelin, C.; Jensen, T.; Rodriguez-Rodriguez, S.; Fristrup, P. Mechanistic Investigation of Palladium-Catalyzed Allylic C-H Activation. *ACS Catal.* **2013**, *3* (3), 294–302.

(23) Trost, B. M.; Mahapatra, S.; Hansen, M. Palladium-Catalyzed C-H Activation of N-Allyl Imines: Regioselective Allylic Alkylations to Deliver Substituted Aza-1,3-Dienes. *Angew. Chemie Int. Ed.* **2015**, *54* (20), 6032–6036.

(24) Trost, B. M.; Li, X. Pd-Catalyzed Asymmetric Allylic Alkylations via C–H Activation of N-Allyl Imines with Glycinates. *Chem. Sci.* **2017**, *8* (10), 6815–6821.

(25) Wang, P.-S.; Liu, P.; Zhai, Y.-J.; Lin, H.-C.; Han, Z.-Y.; Gong, L.-Z. Asymmetric Allylic C−H Oxidation for the Synthesis of Chromans Scheme 1. Asymmetric Allylic C−H Oxidation Reactions. *J. Am. Chem. Soc* **2015**, *137*.

(26) Trost, B. M.; Thaisrivongs, D. A.; Donckele, E. J. Palladium-Catalyzed Enantioselective Allylic Alkylations through C-H Activation. *Angew. Chemie Int. Ed.* **2013**, *52* (5), 1523–1526.

(27) Hegedus, L. S.; Allen, G. F.; Waterman, E. L. Palladium Assisted Intramolecular Amination of Olefins. A New Synthesis of Indoles. *J. Am. Chem. Soc.* **1976**, *98* (9), 2674–2676.

(28) Rönn, M.; Bäckvall, J.-E.; Andersson, P. G. Palladium(II)-Catalyzed Cyclization Using Molecular Oxygen as Reoxidant. *Tetrahedron Lett.* **1995**, *36* (42), 7749–7752.

(29) Overman, L. E.; Remarchuk, T. P. Catalytic Asymmetric Intramolecular Aminopalladation: Enantioselective Synthesis of Vinyl-Substituted 2-Oxazolidinones, 2-Imidazolidinones, and 2-Pyrrolidinones. *J. Am. Chem. Soc.* **2002**, *124* (1), 12–13.

(30) Brice, J. L.; Harang, J. E.; Timokhin, V. I.; Anastasi, N. R.; Stahl, S. S. Aerobic Oxidative Amination of Unactivated Alkenes Catalyzed by Palladium. *J. Am. Chem. Soc.* **2005**, *127* (9), 2868–2869.

(31) Alexanian, E. J.; Lee, C.; Sorensen, E. J. Palladium-Catalyzed Ring-Forming Aminoacetoxylation of Alkenes. *J. Am. Chem. Soc.* **2005**, *127* (21), 7690–7691.

(32) Liu, G.; Stahl, S. S. Highly Regioselective Pd-Catalyzed Intermolecular Aminoacetoxylation of Alkenes and Evidence for Cis -Aminopalladation and S N 2 C−O Bond Formation. *J. Am. Chem. Soc.* **2006**, *128* (22), 7179–7181.

(33) Manzoni, M. R.; Zabawa, T. P.; Kasi, D.; Chemler, S. R. Palladium(II)-Catalyzed Intramolecular Aminobromination and Aminochlorination of Olefins. *Organometallics* **2004**, *23* (23), 5618–5621.

(34) Bäckvall, J.-E. Stereospecific Palladium-Promoted Vicinal Diamination of Olefins. *Tetrahedron Lett.* **1978**, *19* (2), 163–166.

(35) Streuff, J.; Hövelmann, C. H.; Nieger, M.; Muñiz, K. Palladium(II)-Catalyzed Intramolecular Diamination of Unfunctionalized Alkenes. *J. Am. Chem. Soc.* **2005**, *127* (42), 14586–14587.

(36) Zabawa, T. P.; Kasi, D.; Chemler, S. R. Copper(II) Acetate Promoted Intramolecular Diamination of Unactivated Olefins. *J. Am. Chem. Soc.* **2005**, *127* (32), 11250–11251.

(37) Yu, X.-Q.; Huang, J.-S.; Zhou, X.-G.; Che, C.-M. Amidation of Saturated C−H Bonds Catalyzed by Electron-Deficient Ruthenium and Manganese Porphyrins. A Highly Catalytic Nitrogen Atom Transfer Process. *Org. Lett.* **2000**, *2* (15), 2233–2236.

(38) Fraunhoffer, K. J.; White, M. C. Syn-1,2-Amino Alcohols via Diastereoselective Allylic C-H Amination. *J. Am. Chem. Soc.* **2007**, *129*(23), 7274–7276.

(39) Liu, G.; Yin, G.; Wu, L. Palladium-Catalyzed Intermolecular Aerobic Oxidative Amination of Terminal Alkenes: Efficient Synthesis of Linear Allylamine Derivatives. *Angew. Chemie Int. Ed.* **2008**, *47* (25), 4733–4736.

(40) Leblanc, Y.; Zamboni, R.; Bernstein, M. A. Amination of Olefinic Compounds with Bis(2,2,2-Trichloroethyl) Azodicarboxylate. *J. Org. Chem.* **1991**, *56* (5), 1971–1972.

(41) Covell, D. J.; White, M. C. A Chiral Lewis Acid Strategy for Enantioselective Allylic C-H Oxidation. *Angew. Chemie Int. Ed.* **2008**, *47* (34), 6448–6451.

(42) Reed, S. A.; White, M. C. Catalytic Intermolecular Linear Allylic C−H Amination via Heterobimetallic Catalysis. *J. Am. Chem. Soc.* **2008**, *130* (11), 3316–3318.

(43) Albéniz, A. C.; Espinet, P.; Martín-Ruiz, B. The Pd-Catalyzed Coupling of Allyl Halides and Tin Aryls: Why the Catalytic Reaction Works and the Stoichiometric Reaction Does Not. *Chem. Eur. J.* **2001**, *7* (11), 2481–2489.

(44) Lafrance, M.; Lapointe, D.; Fagnou, K. Mild and Efficient Palladium-Catalyzed Intramolecular Direct Arylation Reactions. *Tetrahedron* **2008**, *64* (26), 6015–6020.

(45) Reed, S. A.; Mazzotti, A. R.; White, M. C. A Catalytic, Brønsted Base Strategy for Intermolecular Allylic C-H Amination. *J. Am. Chem. Soc.* **2009**, *131* (33), 11701–11706.

(46) Nishikawa, Y.; Kimura, S.; Kato, Y.; Yamazaki, N.; Hara, O. Pd(II)-Catalyzed Allylic C-H Amination for the Preparation of 1,2- and 1,3-Cyclic Ureas. *Org. Lett*. **2015**, *17*(4), 888–891.

(47) Park, Y.; Kim, Y.; Chang, S. Transition Metal-Catalyzed C–H Amination: Scope, Mechanism, and Applications. *Chem. Rev.* **2017**, *117* (13), 9247–9301.

(48) Duarte, F. J. S.; Poli, G.; Calhorda, M. J. Mechanistic Study of the Direct Intramolecular Allylic Amination Reaction Catalyzed by Palladium(II). *ACS Catal.* **2016**, *6* (3), 1772–1784.

(49) Osberger, T. J.; White, M. C. N -Boc Amines to Oxazolidinones via Pd(II)/Bis-Sulfoxide/Brønsted Acid Co-Catalyzed Allylic C-H Oxidation. *J. Am. Chem. Soc.* **2014**, *136* (31), 11176–11181.

(50) Larock, R. C.; Hightower, T. R.; Hasvold, L. A.; Peterson, K. P. Palladium(II)-Catalyzed Cyclization of Olefinic Tosylamides. *J. Org. Chem.* **1996**, *61* (11), 3584–3585.

(51) Pei, T.; Wang, X.; Widenhoefer, R. A. Palladium-Catalyzed Intramolecular Oxidative Alkylation of Unactivated Olefins. *J. Am. Chem. Soc.* **2003**, *125* (3), 648–649.

(52) Smidt, J.; Hafner, W.; Jira, R.; Sieber, R.; Sedlmeier, J.; Sabel, A. The Oxidation of Olefins with Palladium Chloride Catalysts. *Angew. Chemie Int. Ed.* **1962**, *1* (2), 80–88.

(53) Trost, B. M.; Van Vranken, D. L. Asymmetric Transition Metal-Catalyzed Allylic Alkylations. *Chem. Rev.* **1996**, *96* (1), 395–422.

(54) Trost, B. M.; Crawley, M. L. Asymmetric Transition-Metal-Catalyzed Allylic Alkylations: Applications in Total Synthesis. *Chem. Rev.* **2003**, *103* (8), 2921–2944.

(55) Trost, B. M.; Machacek, M. R.; Aponick, A. Predicting the Stereochemistry of Diphenylphosphino Benzoic Acid (DPPBA)-Based Palladium-Catalyzed Asymmetric Allylic Alkylation Reactions: A Working Model. *Acc. Chem. Res.* **2006**, *39* (10), 747–760.

(56) Cheng, D.; Bao, W. Highly Efficient Metal-Free Cross-Coupling by C-H Activation between Allylic and Active Methylenic Compounds Promoted by DDQ. *Adv. Synth. Catal.* **2008**, *350* (9), 1263–1266.

CHAPTER 4. π-BOND DIRECTED C-2 AMINATION OF INDOLES: CATALYTIC DEVELOPMENT AND MECHANISTIC INVESTIGATION

4.1. Introduction

Indole, a nitrogen-containing heterocycle with a central position in organic chemistry is a "privileged" structure in medicinal chemistry. The indole framework is also ubiquitously present in natural products (Figure 1), that possess impressive biological activities and therefore constitute major targets in organic synthetic chemistry. Indole alkaloids, one of the largest classes of nitrogen-containing secondary metabolites, contain one or more indole/indoline moieties. They are widely found in plants, bacteria, fungi and animals.[1–3] Direct C-H functionalization of indoles has been the hot area of research over the years as it represents a step- and atom-economical approach over classical protocols.[3] However, one of the main challenges associated with this approach is the inherent low reactivity of C-H bonds, entailing that harsh reaction conditions are often required to provide the target products.

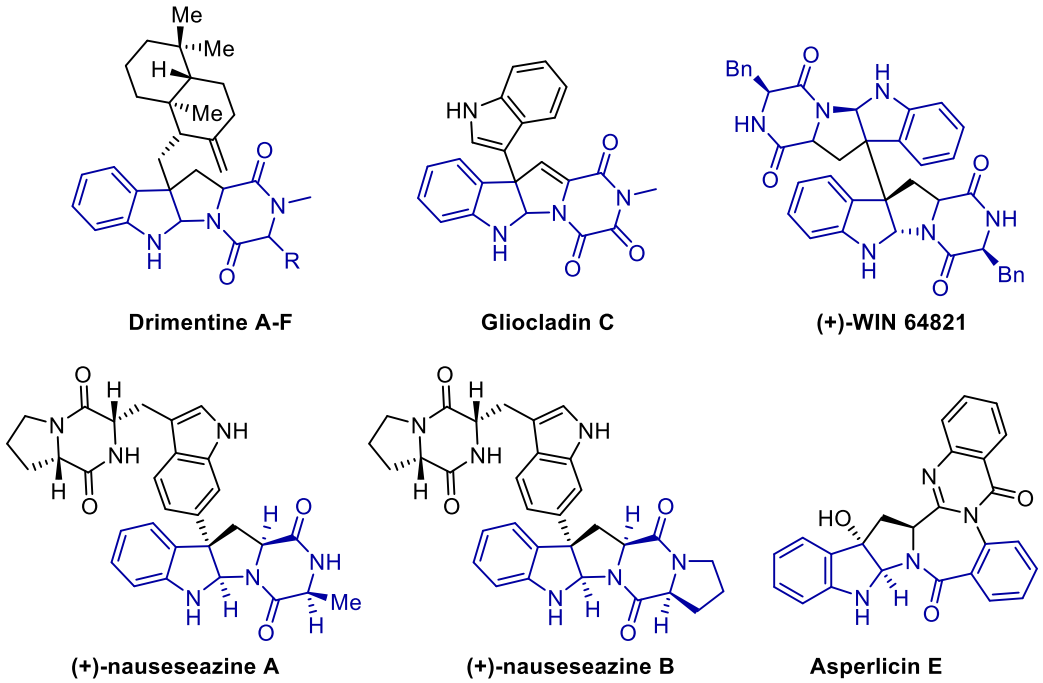

Figure 4.1: Natural products with pyrrolidine-indole core

Pioneering examples on indole C-H activation have been reported as early as in the 1980s, but it was not until the 2000s that the indole C-H functionalization advance. Although noticeable progress has been made in transition metal catalyzed directed C-H functionalization of indoles, the direct functionalization of indoles with bioactive N-heteroarenes is still infancy.

4.2. Transition metal catalyzed directed dehydrogentative cross-coupling for C-N bond formation at indole C-2 position

4.2.1. Directing group at *N*-1 of indole

A complementary methodology of Buchwald-Hartwig amination, catalytic direct C-N bond formation *via* C-H activation without the need for pre-functionalized substrates, has been extensively reported in the literature. Although directed C-H arylation and alkylation of indoles has been well explored, the corresponding C-N bond forming reactions remains very rare.[3,4] Li and coworkers reported a Rh(III) catalyzed approach for directed C-H amidation of indoles using sulfonyl azides as an aminating source (Scheme 4.1).[5] They utilized pyrimidine, a well explored directing group in indole C-2 functionalization for the selective amination at C-2 carbon forming 2-aminated indoles in excellent yields. Yi and coworkers also utilized the same directing group for the preparation of 2-amidoindoles employing benzoyloxy acetamide as the amidation reagent.[6]

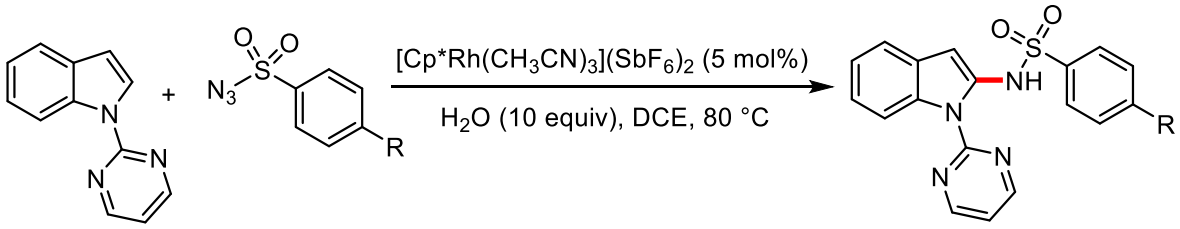

Scheme 4.1: Rh-catalyzed regioselective indole C-2 amidation

In 2014, Kanai and coworkers have improved upon the methodology demonstrating the first-time utilization of cobalt-catalyst for C-2 selective amidation of indole with the chelation assistance from *N*-pyrimidyl directing group. A readily available [Cp*Co(CO)I_2] complex was

employed as a precatalysts, to form active Cp*Co^{III} insitu via base activation. In addition to sulfonyl azides, they also employed phosphoryl azides for C-H phosphoamidation of indoles (Scheme 4.2).[7,8] The process although very effective and one of the rare example of indole C-2 phosphoamidation, it presents several drawbacks such as long reaction times, sensitivity to steric hindrance at the C-3 position, and limited substrate scope.

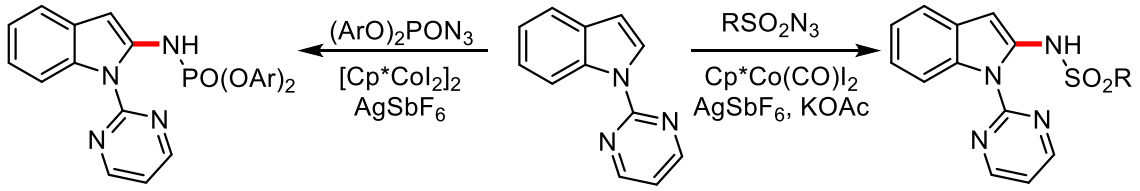

Scheme 4.2: Co-catalyzed directed C-2 amidation of indoles

Very recently, Ackerman and coworkers reported a pyridine directed amidation of indoles using dioxazolones. A similar co-catalyst system reported by Kanai was employed as the catalyst for the C-2 selective amidation (Scheme 4.3).[9]

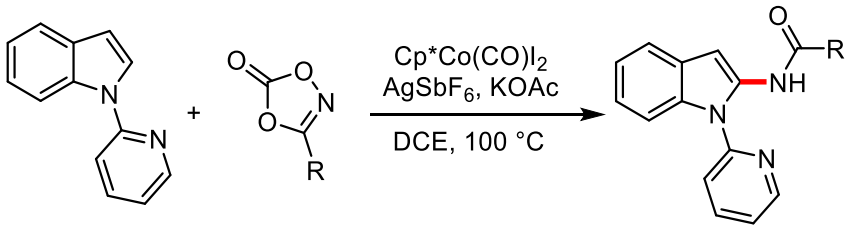

Scheme 4.3: Cobalt (III)-catalyzed amidation of indoles with dioxazolones

4.2.2. Directing group at C-3 of indole

Nagarajan and coworkers employed a carbonyl group at the C-3 position of the indole as the directing group for palladium catalyzed selective C-2 amidation. However, their catalysis required prefunctionalized indoles as the substrates (Scheme 4.4).[10,11]

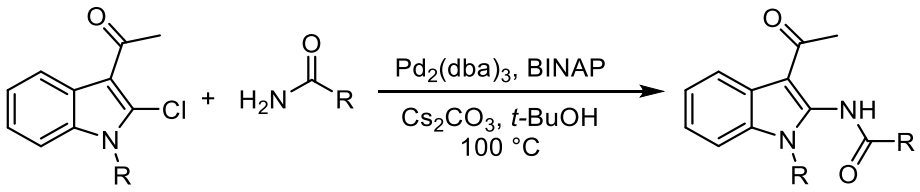

Scheme 4.4: Pd-catalyzed directed C-2 amidation

Other than these reports for amidation there is not much progress in selective C-2 amidation reactions. Therefore, the development of new and efficient methods for the direct construction of 2-amido indoles is highly desirable.

4.3. Initial discovery/origin of work

During our investigation on the development of Pd-catalyzed allylic C-H oxidative amidation reaction using terminal olefins with quinazolone **4.01a**, we found an unusual C-2 amidation of indole with heterocycles (**4.03b**, 21%, structure confirmed by X-ray crystal) in case of 3-allyl indole **4.02a**, instead of expected **4.03a**. (Scheme 4.5). This was further corroborated by the reaction of **4.02a** with other *N*-heteroarene, 2-pyridone **4.04a,** to form corresponding indole C-2 amination product **4.05a**.

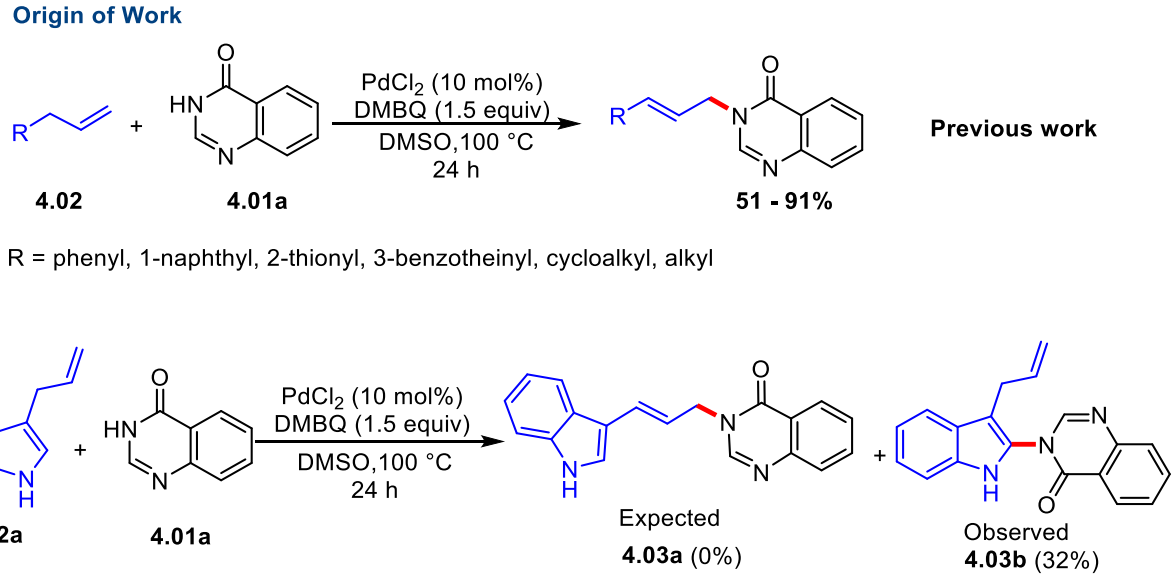

Scheme 4.5: Selectivity switch during the reaction of **4.01a** with 3-allyl indole **4.02a** under Pd (II)-catalysis

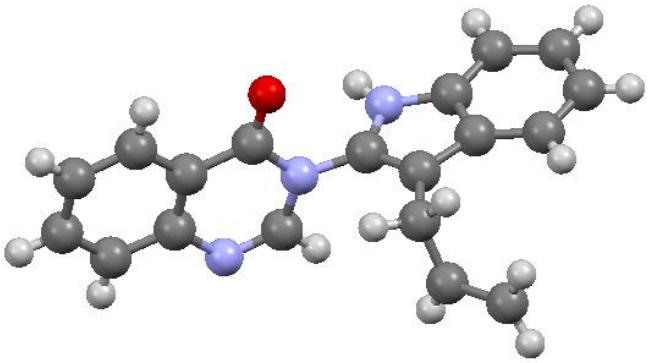

Figure 4.2: ORTEP diagrams of **4.03b** showing 40% probability ellipsoids

Surprisingly, such transformations were not observed in other well studied allylic C-H activation/amination protocol (White protocol). Indole C-2 substitution was also not observed using simple indole **4.02b** suggesting the criticality of allyl functionality. Consequently, a detailed study was conducted to elucidate this unprecedented reaction and subsequently to find out robust catalytic system for a versatile indole C_2-H amination using biorelevant tautomerizable *N*-heteroarenes (Scheme 4.6).

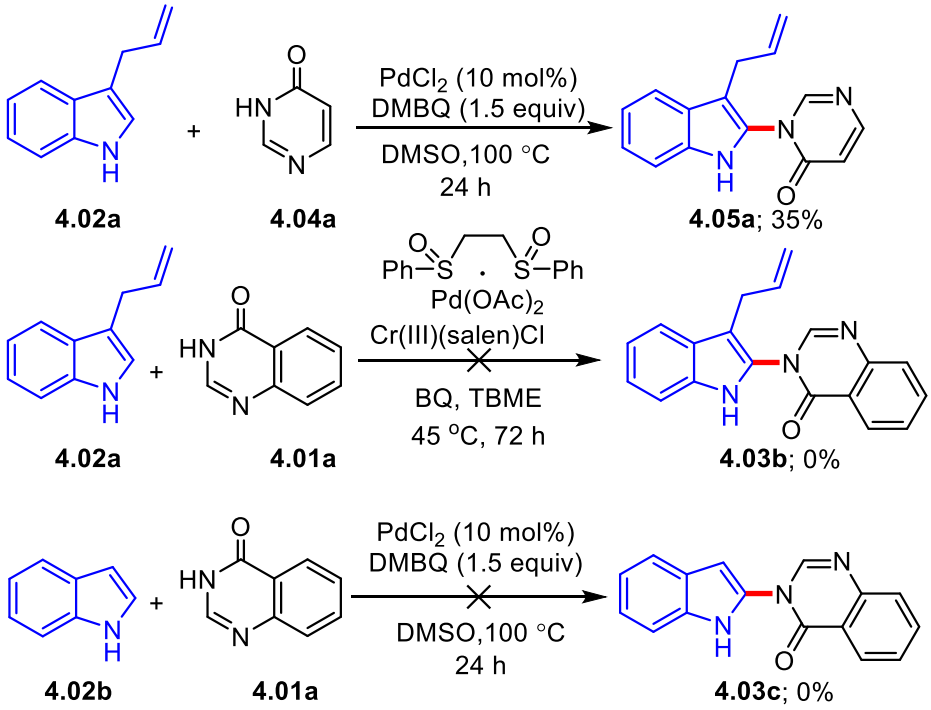

Scheme 4.6: Control study for indole C-2 amidation under different conditions

4.4. Reaction optimization

4.4.1. Catalyst screening

With the initial observation of the product **4.03b**, and control studies indicating the importance of allyl group and catalyst conditions, we started our investigation with the screening of different palladium catalysts (Table 4.1). As can be evident, only Pd salts with chloride counter ions were effective in the transformation (entry 3 and 5). Most importantly, phosphine or NHC ligated complexes also shown to have a negative impact, shutting down the reaction completely. In all the cases of optimization, we observed an appreciable quantity of oxindole formation as the side product.

Table 4.1: Investigation of effect of Pd-catalysts on the indole C2-Amination of **4.01a** with **4.02a**

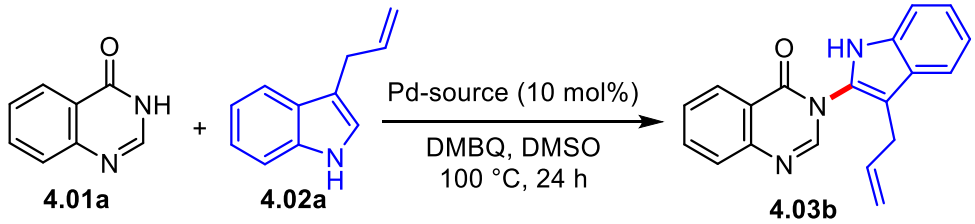

Entry	Pd-catalyst	Yield (%)/**4.03b**[a]
1	$Pd(OAc)_2$	0[b]
2	$Pd(TFA)_2$	0[b]
3	$PdCl_2$	32
4	$(PPh_3)_2PdCl_2$	0[b]
5	$(PhCN)_2PdCl_2$	28
6	$[PdCl(allyl)]_2$	0[b]
7	$Pd(dppf)Cl_2$	0[b]
8	IPrPd(allyl) Cl	0[b]
9	White Catalyst	0[b]
10	None	0[b]

Reaction conditions: 4.01a (0.2 mmol) was treated with **4.02a** (0.4 mmol, 2.0 equiv) in presence of different Pd-catalyst (10 mol %), DMBQ (1.5 equiv) in DMSO (0.5 mL) at 100 °C for 24 h. [a]Isolated yield. [b]3-allyl oxindole was formed as the product

4.4.2. Solvent screening

With establishing simple $PdCl_2$ as the efficient catalyst, we screened different solvents in hope of increasing the reactivity and product formation. The reaction of **4.01a** with allyl indole **4.02a** was performed in different solvents. As is the case of allylation C-H activation of *N*-heterocycles,[12] DMSO was found essential in the product formation. Infact, a 1:1 mixture of DCE and DMSO was found to be even more effective forming the product in 40% yield. Furthermore, the reaction produced improved yields in the absence of oxidant (entry 13, Table 4.2).

Table 4.2: Investigation of solvent effect on the indole C_2-Amination of **4.01a** with **4.02a** in presence of $PdCl_2$

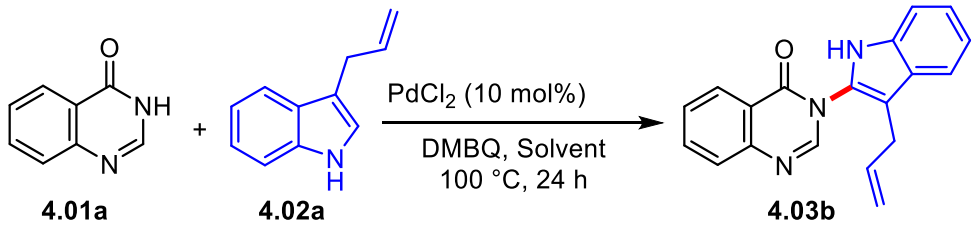

4.01a **4.02a** **4.03b**

Entry	Solvent	Yield (%)/**4.03b**[a]
1	DMF	0[b]
2	MTBE	0[b]
3	THF	0[b]
4	DCE	0[b]
5	1,4-Dioxane	0[b]
6	Toluene	0[b]
7	TFE	0[b]
8	THF: DMSO (1:1)	15[c]
9	1,4-Dioxane: DMSO (1:1)	19[c]
10	DCE: DMSO (1:1)	40[c]
11	Toluene: DMSO (1:1)	20[c]
12	DMSO	32[c]
13	DCE:DMSO (1:1)	48[c,d]

Reaction conditions: 4.01a (0.2 mmol) was treated with **4.02a** (0.4 mmol, 2.0 equiv) in presence of $PdCl_2$ (10 mol%), DMBQ (1.5 equiv) in different solvents (0.5 mL) at 100 °C for 24 h. [a]Isolated yield [b]SM remained as such. [c]3-allyl oxindole was formed as a side product. [d]No DMBQ

4.5. Development of efficient catalytic system

4.5.1. Transition metal catalyst screening

With results suggesting the π-bond directed C-H activation/amination as key mechanistic pathway, next, we considered the opportunity to discover high yielding and cost-effective alternative of Pd-catalysis. A reaction of **4.01a** with **4.02a** was carried out using other transition metal catalyst system to form **4.03b.** Alternative to palladium, variety of Ru-, Ni-, and Co- based catalysts were investigated (Table 4.3). While Co- catalysts were found be ineffective, superior yields of **4.03b** were observed using $RuCl_3.xH_2O$ (55%), $NiCl_2$ (52%) and $NiCl_2$.glyme (57%) as the catalysts. We further optimized reaction conditions with both Ru and Ni catalyst systems. But only Ni-catalyst system development will be discussed in this chapter.

Table 4.3: Investigation of different metal catalyst on the indole C_2-Amination of **4.01a** with **4.02a**

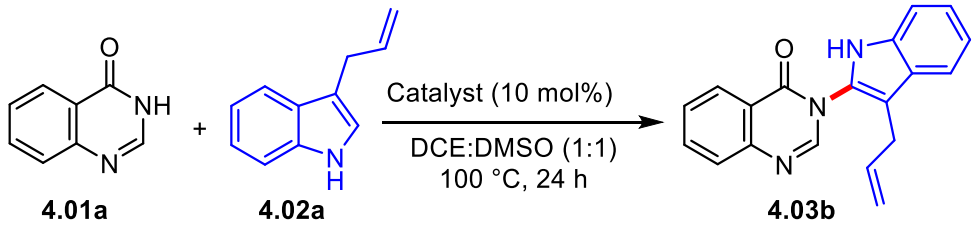

4.01a **4.02a** **4.03b**

Entry	Solvent	Yield (%)/**4.03b**[a]
1	$RuCl_3$. xH_2O	55 (52)
2	$RuBr_3$. xH_2O	30
3	$RuCl_3$	50 (49)
4	$[Ru(COD)Cl_2]_n$	38
5	$[Ru(p\text{-}cymene)Cl_2]_2$	42
6	$Ru[PPh_3]_3(CO)(Cl)H$	0[b]
7	$Ru(PPh_3)_2(cp)Cl$	50
8	$Ru_3(CO)_{12}$	0[b]
9	Tris(1,10-Phen) $RuCl_2$. xH_2O	57
10	$Ni(cod)_2$	35
11	$Ni(OAc)_2$	0[b]
12	$NiCl_2$	52
13	$NiCl_2$ glyme	57
14	$NiBr_2$	traces
15	$Ni(acac)_2$	15
16	$NiCl_2(PPh_3)_2$	37
17	$CoCl_2$	0[b]
18	$CoBr_2$	0[b]

Reaction conditions: 4.01a (0.2 mmol) was treated with **4.02a** (0.4 mmol, 2.0 equiv) in presence of different metal catalysts (10 mol%), in DCE:DMSO (1:1, 0.5 mL) at 100 °C for 24 h. [a]yields were determined by ^{1}H NMR of the crude reaction mixture with Nitromethane as the internal standard. [b]SM remained as such. [c]3-allyl oxindole was formed as a side product.

4.5.2. Solvent screening

To explore the catalytic activity of $NiCl_2$, we started optimization reaction with screening the effect of solvents. A reaction of **4.01a** with **4.02a** was carried out using $NiCl_2$, in different solvents. Surprisingly, the Ni-catalyzed reaction is found to be highly sensitive to the solvents and a mixture of DCE and DMSO is essential for the formation of **4.03b** (Table 4.4). There was no reaction when DCE was used in the absence of DMSO (entry 2), but traces of product were formed in DMSO alone (entry 5). The ratio of both the solvents and concentration of the reaction mixture also shown to have effect on the overall yield of the product (entries 12-18). A 0.2M solution of DCE and DMSO in a 4:1 ratio was found to be optimal yielding the product in 89% yield (entry 17). Decreasing the concentration had a negative impact on the reaction, decreasing the yield of the product (entry 18).

Table 4.4: Investigation of concentration and solvent effect on the indole C_2-Amination of **4.01a** with **4.02a**

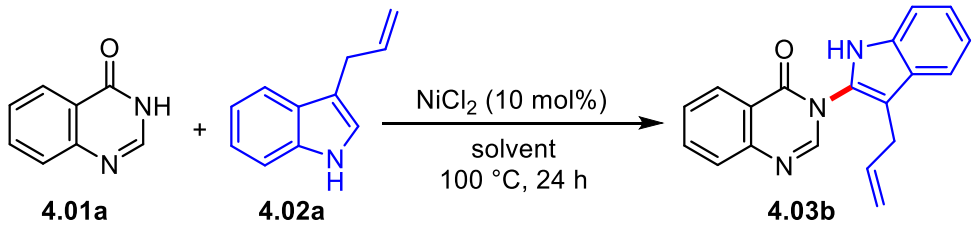

4.01a **4.02a** **4.03b**

Entry	Solvent	Yield (%)/**4.03b**[a]
1	THF	0[b]
2	DCE	0[b]
3	1,4-Dioxane	0[b]
4	Toluene	0[b]
5	DMSO	traces
6	ACN	0[b]
7	DME	0[b]
8	THF: DMSO (1:1)	0[b]
9	1,4-Dioxane: DMSO (1:1)	0[b]
10	DME: DMSO (1:1)	0[b]
11	ACN: DMSO (1:1)	0[b]
12	DCE: DMSO (1:1)	51
13	DCE: DMSO (2:1)	63
14	DCE: DMSO (4:1)	75
15	DCE: DMSO (1:2)	42
16	DCE: DMSO (1:4)	28
17	DCE: DMSO (4:1)	89[c]
18	DCE: DMSO (4:1)	70[d]

Reaction conditions: 4.01a (0.2 mmol) was treated with **4.02a** (0.4 mmol, 2.0 equiv) in presence of $NiCl_2$ (10 mol%), in different solvents (0.5 mL) at 100 °C for 24 h. [a]isolated yield. [b]SM remained as such.[c]1mL of solvent was used. [d]2mL of solvent was used

4.5.3. Effect of catalyst loading and temperature

We then turned our attention to the catalyst loading and temperature required for the reaction (Table 4.5). Decreasing the temperature even to 80 °C has a profound effect with a sharp decline in the yields. On the contrary, increasing the temperature to 120 °C doesn't have much effect. Decreasing the catalytic loadings to 5 mol%, decreased yields, while increasing to 15 mol% doesn't have much effect.

Table 4.5: Investigation of effect of catalyst loading and temperature on the indole C_2-Amination of **4.01a** with **4.02a**

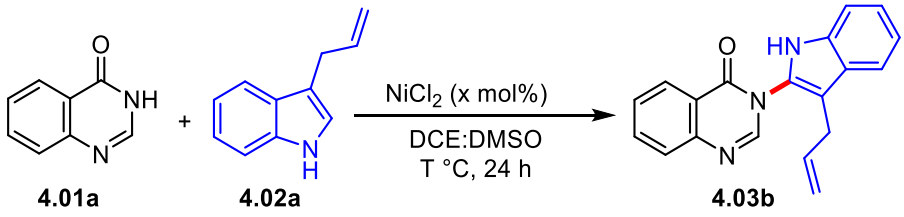

4.01a **4.02a** **4.03b**

Entry	Temp (X °C)	Catalyst (mol%)	Yield (%)/**4.03b**[a]
1	60	10	0[c]
2	80	10	25
3	100	10	90
4	120	10	92
5	100	5	70
6	100	15	88

Reaction conditions: 4.01a (0.2 mmol) was treated with **4.02a** (0.4 mmol, 2.0 equiv) in presence of $NiCl_2$, in DCE:DMSO (4:1, 1.0 mL) at 100 °C for 24 h. [a]isolated yield. [b]SM remained as such.

4.6. Mechanistic consideration

Our initial optimization study led us to believe the operation of multiple mechanistic pathways leading to product formation. Based on literature studies and our own understanding we conducted a careful study to validate each possible pathway listed below under both palladium and nickel catalytic conditions.

1. Allylic C-H activation/ π-allyl continuum pathway

2. Oxidative dearomatization-nucleophilic addition pathway

3. Catellani type C-H activation/amination pathway

4. π-bond directed Friedel–Crafts-type amination pathway

4.6.1. Allylic C-H activation/ π-allyl continuum pathway

Requirement of allyl group for the selective C-2 functionalization led us to investigate the involvement of continuum of π-allyl palladium intermediate. In 2015, Trost and coworkers reported an unprecedented alternative modes of Pd-catalyzed C(sp^3)-H activation of N-allyl imines. Initial allylic C-H oxidation formed a π-allylpalladium intermediate, which exists in equilibrium because of the presence of attached allylic chain. Depending upon the sterics of incoming nucleophile, they were able to isolate the product arising from both all-carbon π-allyl complex **A** and the product arising from 2-aza π-allyl complex **B** (Scheme 4.7).[13]

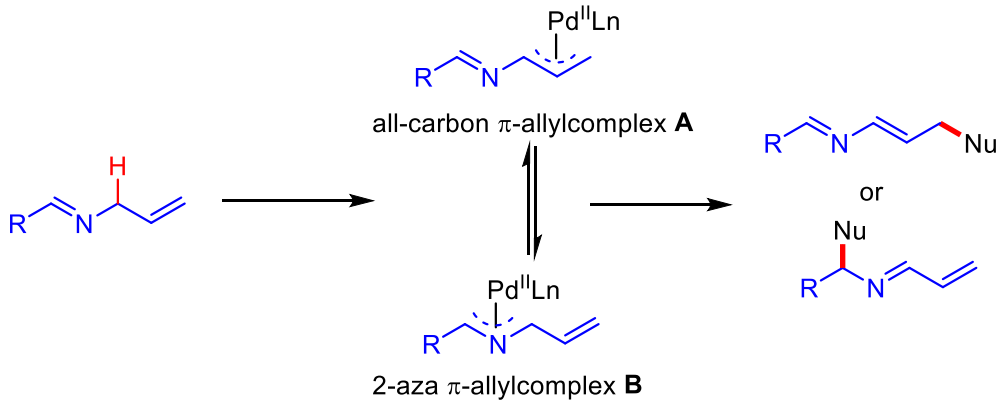

Scheme 4.7: Possible outcomes from nucleophilic attack on π-allyl complexes

We envisioned that even in the case of 3-allyl indole **4.02a,** a similar all carbon π-allyl continuum can occur generating an equilibrium mixture of π-allylmetal complexes (**C** and **D**). Depending upon the conditions employed, these complexes potentially can lead to both the products **4.03a** and **4.03b** (Scheme 4.8).

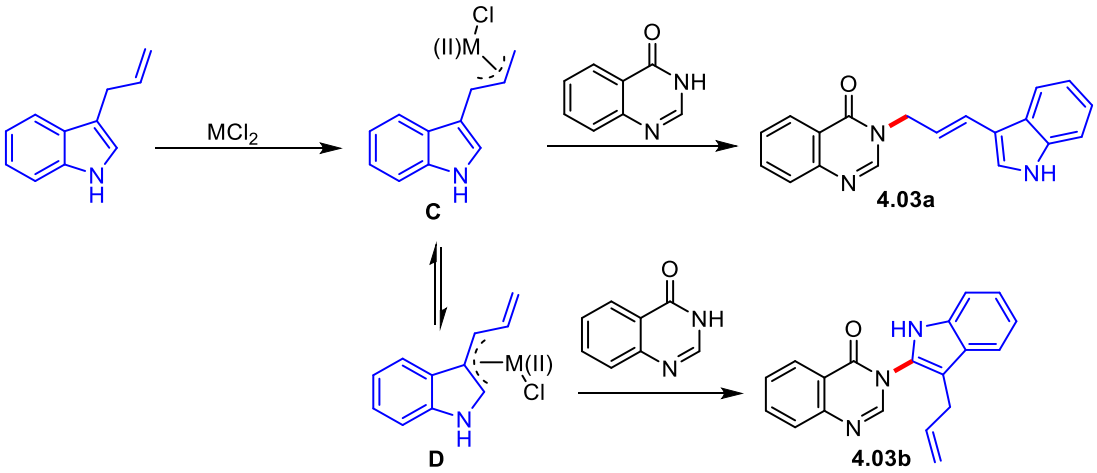

Scheme 4.8: π-Allyl continuum for product formation in the case of 3-allylindole

However, when a substrate with no allylic hydrogens **4.02d** was subjected to reaction conditions, corresponding C-2 substituted product was formed in good yield, contradicting the allylic C-H activation pathway. This was further supported when 3-butenyl indole **4.02i** also gave the corresponding C-2 substituted product under reaction conditions (Scheme 4.9).

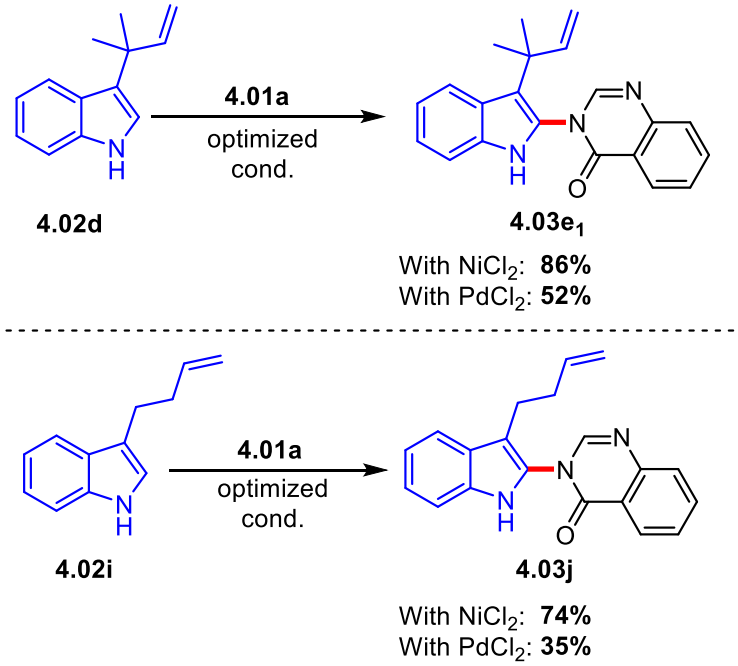

Scheme 4.9: Control experiments to validate π-allyl continuum pathway

4.6.2. Oxidative dearomatization-nucleophilic addition pathway

During the optimization of reaction conditions, in some cases where the product formation was low, we isolated 3-allyl-1,3-dihydro-indol-2-one (**4.06a**) as the side product. This gave us an insight for a Kornblum type DMSO assisted oxidative dearomatization – amination pathway (Scheme 4.10).[14] Electrophilic metal catalysts under reaction conditions can attack on the more reactive C-3 position of indole forming an intermediate iminium ion, followed by a Kornblum type oxidation with DMSO yielding **4.06a.**

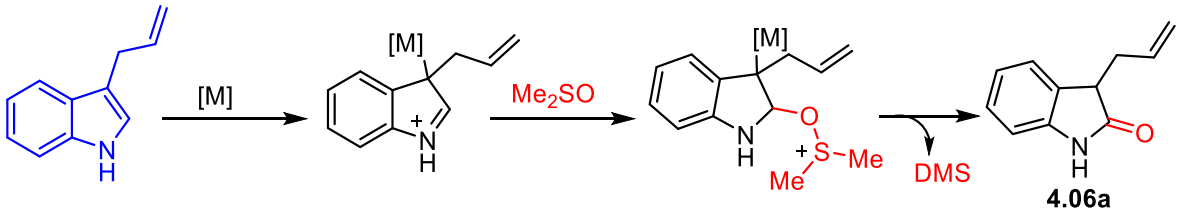

Scheme 4.10: DMSO assisted oxindole synthesis/amination pathway

N-heterocycles can then attack on oxindole **4.06a** undergoing a nucleophilic amination/ rearomatization to form the product **4.03b**. In a control study, preformed **4.06a** was subjected to reaction conditions. Both the starting materials were recovered as such in quantitative yields and no product formation indicated that the oxidized product **4.06a** was in fact a deleterious side product rather than an intermediate for the indole C-2 substitution (Scheme 4.11).

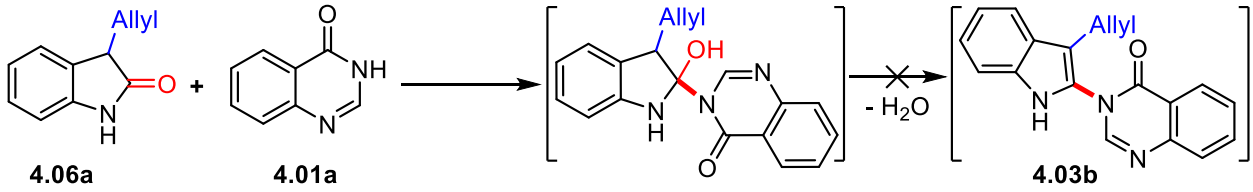

Scheme 4.11: Validation of oxidative dearomatization pathway by preformed **4.06a**

4.6.3. Catellani type C-H activation/amination pathway

A Catellani reaction or cooperative catalytic action of palladium/norbornene system for selective C-H bond functionalization was also considered to be a possible mechanistic pathway

for indole C-2 substitution. In 2011, Bach and coworkers reported a Pd(II) catalyzed norbornene mediated Catellani type C-H activation for the selective formation of C-2 substituted indoles. They also carried out a detailed mechanistic investigation to find out mode of activation and the attack of palladium on to indole. Catalytic cycle as shown in Scheme 4.12 was proposed involving *N*-palladation of indole via N-H activation followed by *syn*-aminopalladation of norbornene forms **IN8**. *ortho*-C-H palladation generates **IN4**, upon oxidative addition, reductive elimination, and norbornene expulsion forms the product and regenerates the catalyst.[15,16]

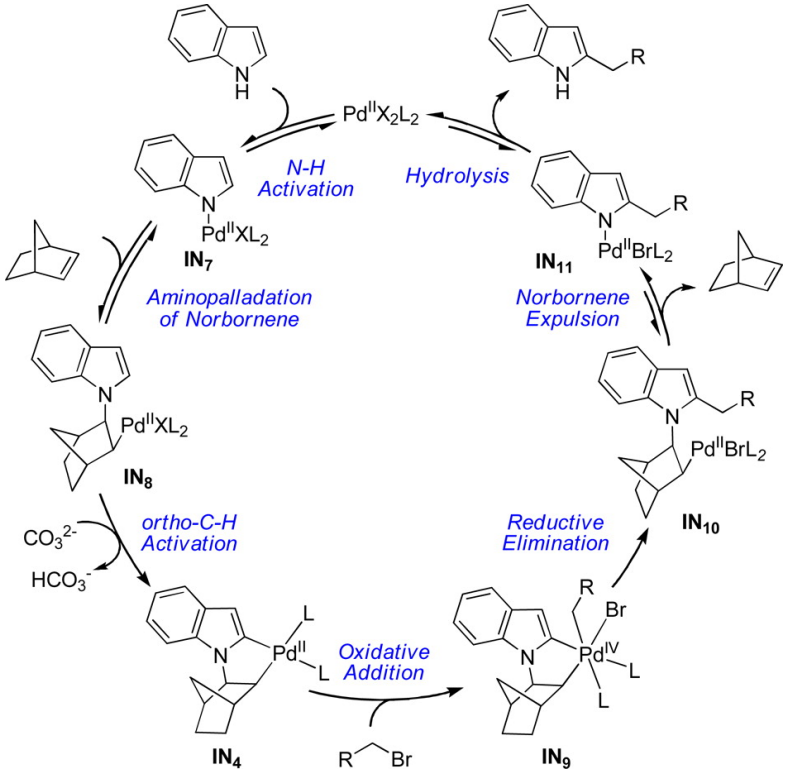

Scheme 4.12: Catellani type reaction for selective indole C-2 functionalization

We envisioned that even in the case of allyl indole functionalization, intermediates like **IN8** and **IN4** can form, where in olefinic bond of allyl group serves the purpose of norbornene. Oxidative addition of *N*-heterocycles followed by reductive elimination forms the C-2 selective product (Scheme 4.13)

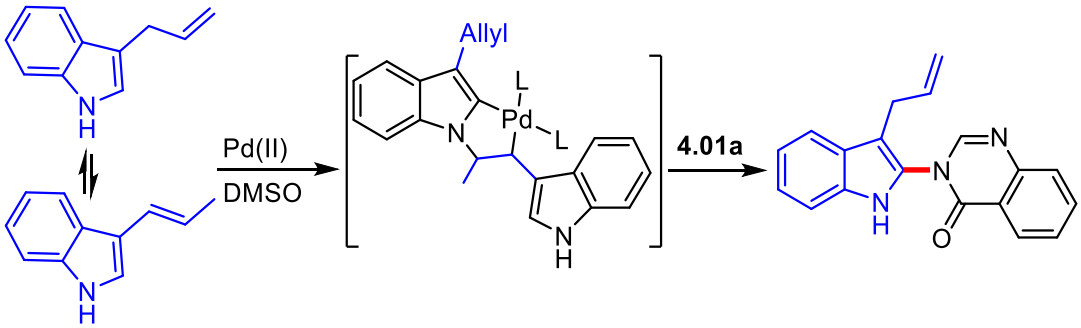

Scheme 4.13: Catellani type pathway for C-2 functionalization of indoles.

If the reaction was to proceed by this pathway, a free N-H bond is needed for the formation of intermediate palladacycle. To validate the pathway, we prepared *N*-methyl-3-allylindole 4.02c and subjected to reaction conditions, to find out the formation of corresponding C-2 amidation product 4.03d in respectable yields (Scheme 4.14). Formation of product even with N-substituted indole ruled out the possibility of this pathway. To further confirm, we also performed the reaction of indole in presence of Pd(II)/norbornene catalytic system under both neutral or basic conditions with no formation of product.

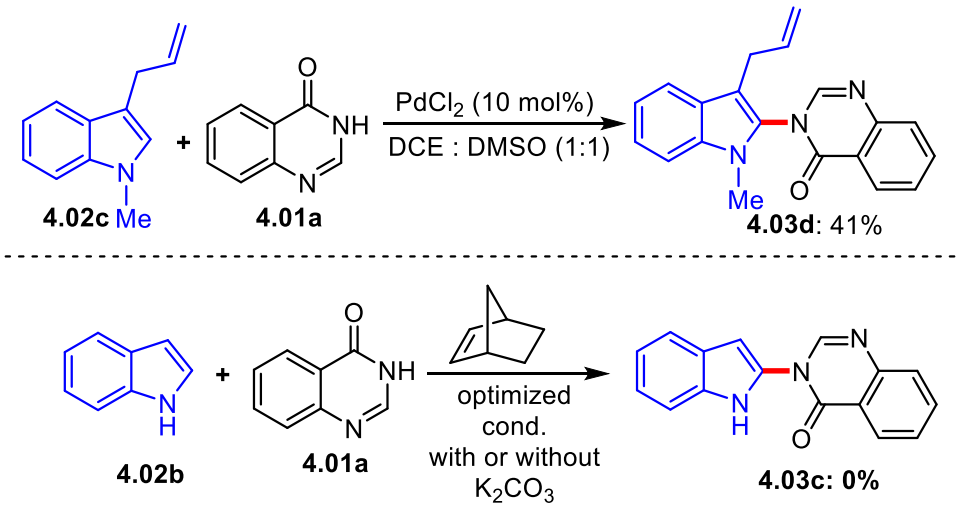

Scheme 4.14: Control studies to validate Catellani type pathway for indole C-2 amidation

4.6.4. π-bond directed Friedel–Crafts-type amination pathway

Ruling out all the other possible pathways, lastly, we envisioned the π-bond directed Friedel–Crafts-type amination pathway.[17–23] Use of directing groups for selective C-H functionalization is very well known and various heteroatom directing groups have been reported in the literature.[24] The use of carbon-carbon double bond as directing group is relatively under explored, and one of the first report for the utilization of olefinic bond as directing group was reported by Chang and coworkers.[23] In 2012, they reported the utilization of allylic double bond as the directing group for Fujiwara-Moritani reaction (Scheme 4.15).

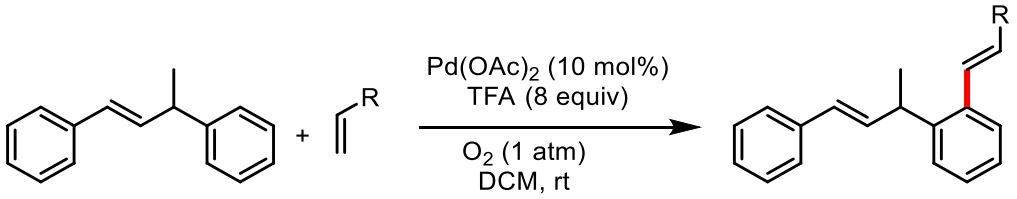

Scheme 4.15: Olefin directed Fujiwara-Moritani reaction

To get more insight and to validate the olefin assisted indole C-2 functionalization few control experiments were performed (Scheme 4.16)

(i) Reaction of 3-phenyl indole **4.02e** with **4.01a** did not yield any product, with both the starting materials intact

(ii) Use of other hetero-atom based π-assistance (3-formyl **4.02f** & 2-cyano **4.02g**) were ineffective to facilitate indole C2-H amination

(iii) Reaction of 3-vinyl indole **4.02h** with **4.01a** also did not yield any product

Interestingly, in all the above cases, the π-bond is located one carbon less than the allyl group, and yielded no product, on the contrary when 3-butenyl indole **4.02i** was subjected to standard conditions desired product **4.03j** was formed. These results are of significant value, indicating the appropriately substituted π-bond assistance is critical for the progress of reactions.

This was further confirmed by the progress of reaction with indole-3-acetonitrile **4.02j**, a higher chain analog of **4.02g**, to form the respective amination product **4.03k**.

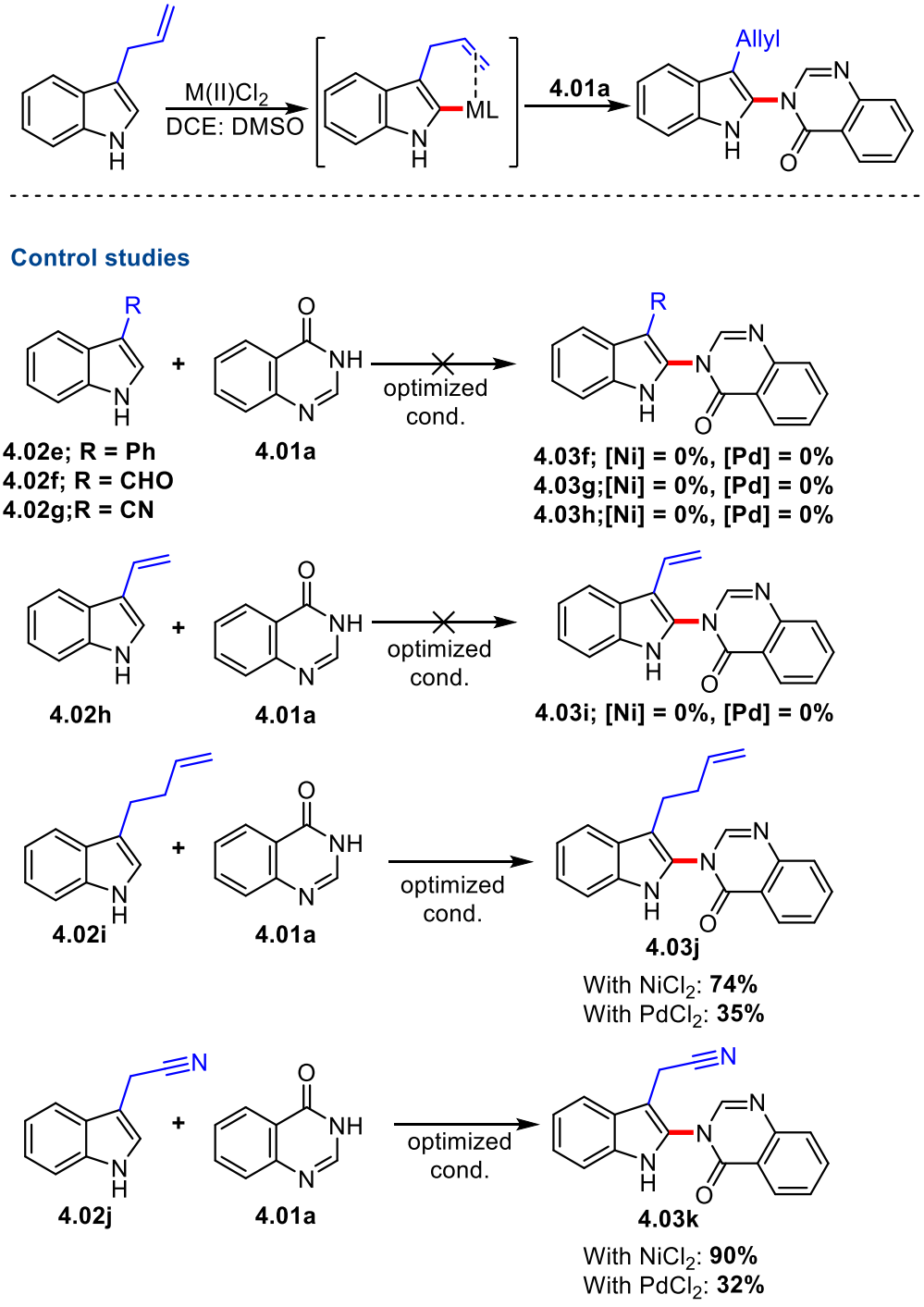

Scheme 4.16: Control studies validating π-bond assisted indole C-2 functionalization

To gain mechanistic insight, deuterium incorporation studies were undertaken (Scheme 4.17). Treatment of **4.02a** in the absence of **4.01a** but with MeOD present resulted in 72% and 40% C-2 deuteration under Pd and Ni catalysis respectively,[25] indicating a reversible C−H metallation/protonation. We believe that deuteration proceed by π-bond-assisted C−H activation by metal complexes to generate a metallocycles, followed by its deuteration to give the deuterated allyl indole product. In the presence of **4.01a**, amination proceeded with no incorporation of deuterium.

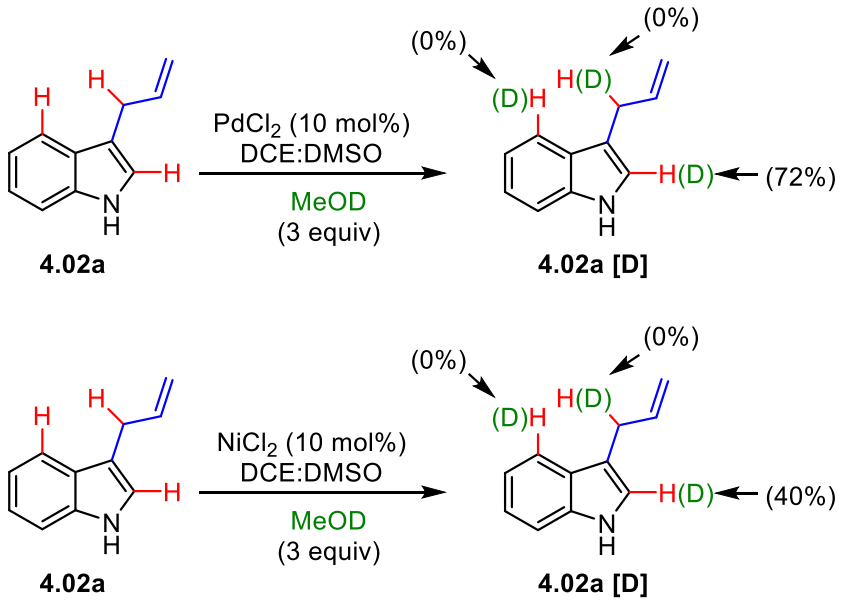

Scheme 4.17: Deuterium scrambling experiments of **4.02a**

To further validate the π-bond assisted Friedel-Crafts-type pathway, kinetic isotope effect (KIE) studies were conducted under both palladium and nickel catalysis. Independent but parallel reactions of **4.02a** and **4.02a [D]** indicated a KIE value of 1.0 and 0.72 under Pd and Ni catalysis respectively (Figure 4.3). Although KIE data of Pd-catalyzed reaction did not give much details about the mechanism of the reaction, inverse KIE in case of Ni-catalysis provided key details about the mechanism. Inverse KIE, a characteristic of the sp^2 to sp^3 hybridization change indicated the possibility of Friedel-Crafts type metal insertion at the indole C-2 position, generating a positive

charge at C-3 position, followed by a deprotonation to form intermediate indole C-2 metalated species.

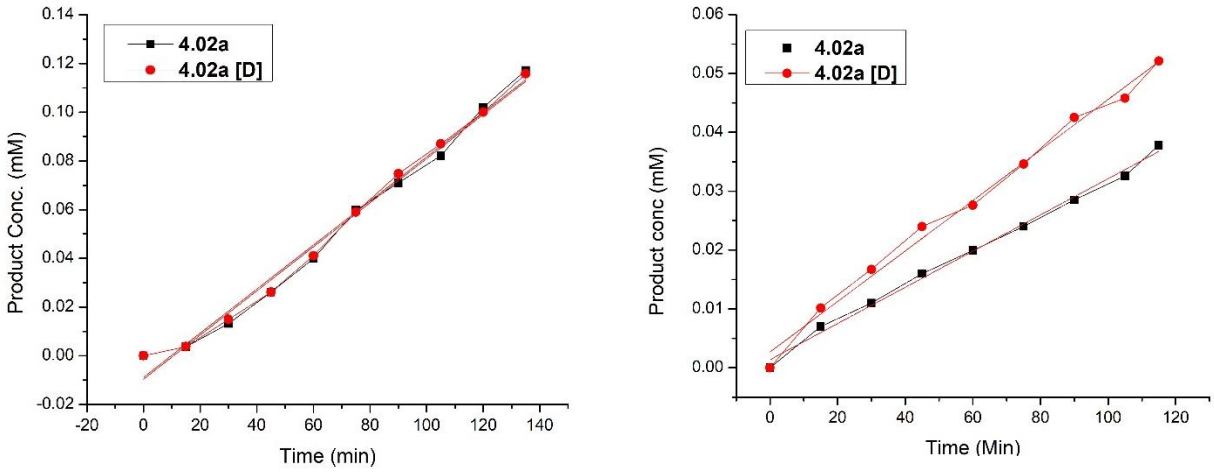

Figure 4.3: KIE studies of 4.02a and 4.02a [D] under (i) Pd catalysis (ii) Ni catalysis

This was further validated by the effect of substituent electronics on the overall reactivity of indole C-2 amidation, with electron donating groups giving higher yields as compared to electron withdrawing groups. Hammett plots with 5-substituted indoles revealed a ρ value of -0.71, indicating an increase in the positive charge in the rate determining step.

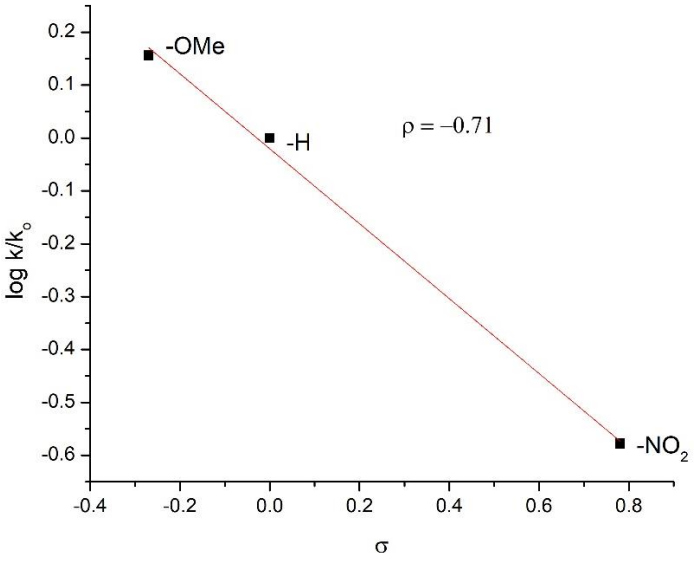

Figure 4.4: Hammett plot for the electronic effects on indole C-2 amidation

Considering all the mechanistic rationale, and control studies we propose a Friedel-Crafts type directed metal insertion at indole C-2 position, followed by amidation with heterocycles to form indole C-2 aminated product. A plausible catalytic cycle was shown in scheme 4.18. Metal catalyst first coordinates to the π-bond of the C-3 substituent, followed by a Friedel-Crafts type metal insertion at C-2 position forms the intermediate **Int-A**, leading to an accumulation of positive charge at C-3 position (a negative ρ value in Hammett plots). The inverse secondary KIE (0.72) in the case of $NiCl_2$, further validates the hybridization change in rate determining step rather than C-H bond cleavage. A reversible deprotonation of the **Int-A** leads to a stable, and aromatic intermediate **Int-B**. *N*-heterocycles then attack the metal center forming **Int-C,** which can then undergo a reductive elimination to form the product **4.03b**, releasing Ni(0). Dichloromethane mediated reoxidation od Ni(0) to Ni(II) regenerated the active catalyst for the next catalytic cycle.

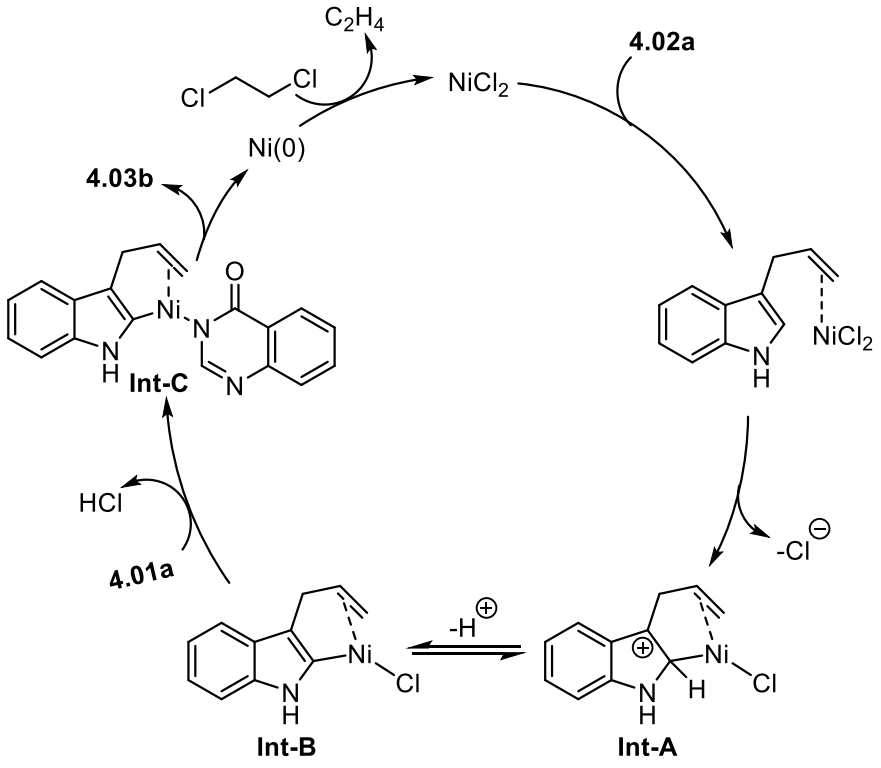

Scheme 4.18: Plausible catalytic cycle for the indole C-2 amidation with *N*-heterocycles

4.7. Substrate scope

With the optimized conditions in hand, and establishing mechanistic details suggesting a π-bond directed indole C-2 functionalization, we then examined the scope of the reaction methodology (Scheme 4.19). For each substrate, the reactions were performed under optimized Pd- and Ni-catalysis. Differently substituted allyl indoles [26] reacted well to produce respective products in good to excellent yields. Both EDG (**4.03l**), EWG (**4.03m**, **4.03p**-**4.03r**) bearing indoles reacted well, however yields were inferior in case of indole with electron withdrawing substituent. Halogen functionality also tolerated well with good to excellent yields (**4.03n**, **4.03o**). It is noteworthy to mention that reactions were also compatible with sensitive functionalities such as –CO_2Me (**4.03p**), -CHO (**4.03q**), and –CN (**4.03r**). With respect to quinazolines, reactions were compatible with variously C-6/7 substituted quinazolones (6-NO_2, **4.03s**; 6-OMe, **4.03t**; 6-Br, **4.03u**; 6-F, **4.03v;** 7-F, **4.03w**) to produce the desired product in excellent yields under Ru-/Ni-catalysis. We envisioned that such an amination strategy could be extended beyond the quinazolone nucleus to other biologically relevant *N*-heteroarenes. As shown below, we were delighted to discover that *N*-heteroarenes such as pyrimidine **4.05a** and pyridines (**4.05b**-**4.05c**) were reacted well with excellent yields and chemoselectivity under Pd-/Ni-catalysis. This demonstrates the versatility of developed methodology to afford a range of functionalized-bis-heterocycles. Although, reaction did not precede with 3-vinyl indole **4.02h** in any case, it is remarkable to note the excellent yields of products in case differently substituted 3-allyl indoles (**4.03x**, and **4.03j**).

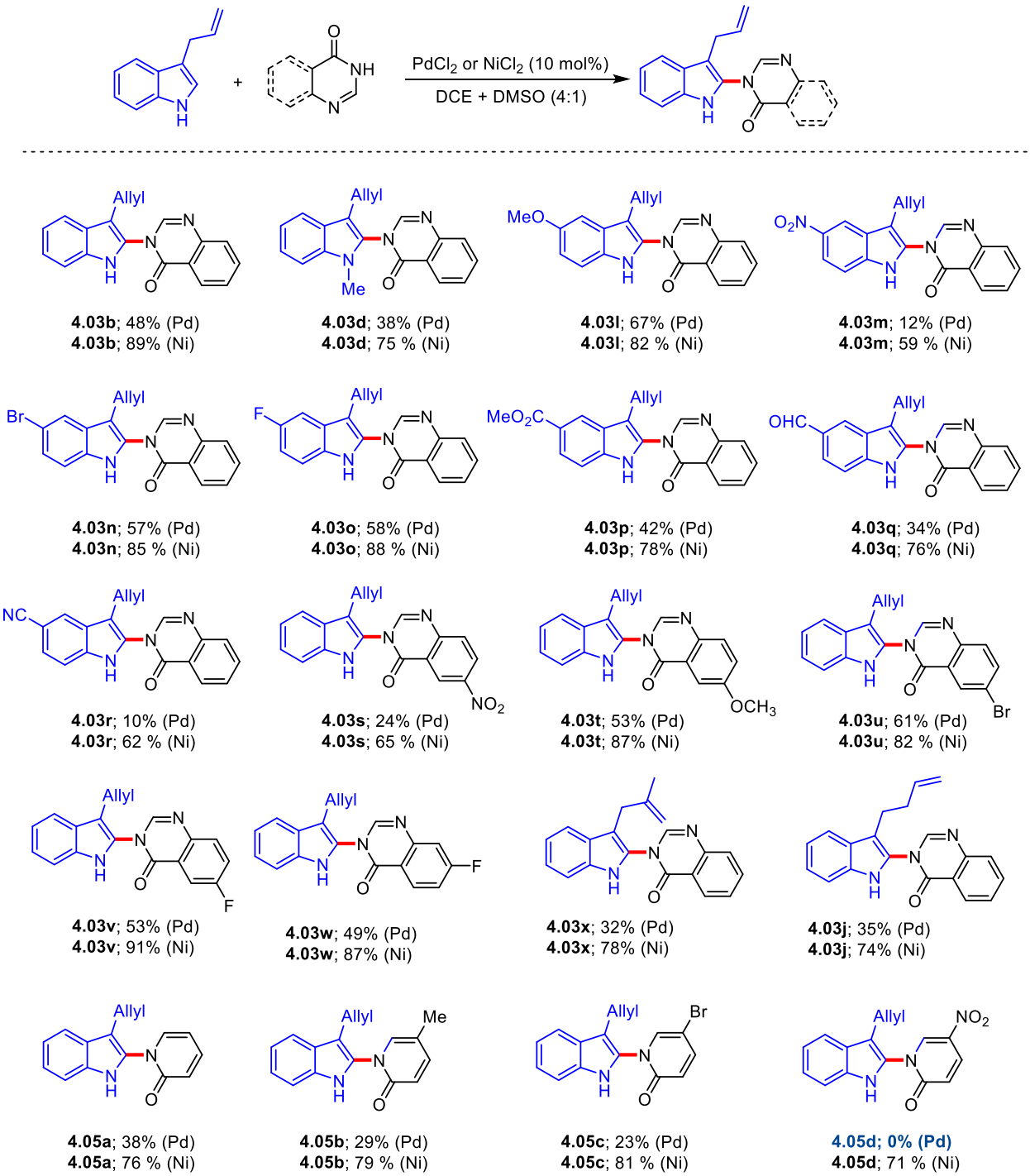

Scheme 4.19: Substrate scope: C-2 amination of various indoles (**4.02**) with *N*-heteroarenes (**4.01**) under optimized conditions for Pd-/Ni-catalysis

Scope of other π-bonded-directing groups was also examined. Under each optimized metal conditions,2-(1H-indol-3-yl) acetaldehyde **4.02k**, ethyl 2-(1H-indol-3-yl) acetate **4.02l**, 2-(1H-indol-3-yl)acetonitrile **4.02j** reacted elegantly to produce respective indole-2-amination products with variable yields, the highest being with nickel (Scheme 4.20). Point to be noted that 2-formyl indole, 2-ethoxycarbonyl indole, and 2-cyano indole were failed to deliver the desired product under optimized conditions, suggesting the appropriate spacing of directing π-bond is critical.

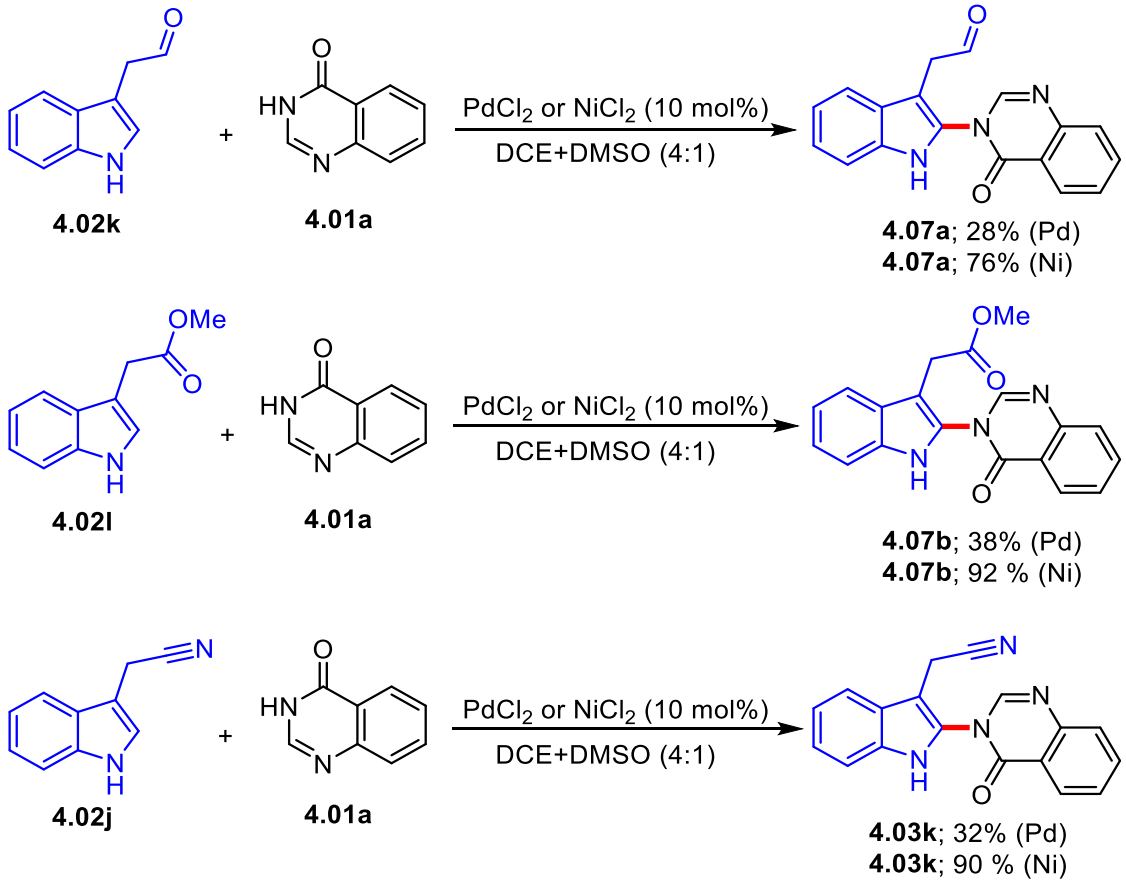

Scheme 4.20: C-2 Amination of indoles - exploitation of other π-bonds for directed C-H activation

4.8. Summary and conclusion

Overall, these highly chemo- and regioselective indole C2-amination reactions are powerful tools for the construction of indole based bis-heterocycles using cost-effective metal-based catalysts such as nickel and ruthenium via π-bond directed C-H bond activation pathway

with step economy and in an environmentally friendly fashion. The developed protocol is scalable, high yielding and offers broad scopes with high functional group tolerance. The products formed are amenable to downstream modification to various synthetically useful compounds of high biological and material importance.

4.9. Experimental procedures

4.9.1. General information

Unless otherwise noted, all manipulations were carried out under a nitrogen atmosphere using standard Schlenk-line or glovebox techniques. All glassware was oven-dried for at least 1h prior to use. THF, toluene, ether, and hexane were degassed by purging with nitrogen for 45 min and dried with a solvent purification system (MBraun MB-SPS). DMF, dioxane, dimethoxyethane, dichloroethane, methanol, and ethanol were dried over activated 3 Å molecular sieves and degassed by purging with nitrogen. All commercially obtained reagents/solvents were purchased from Alfa Aesar®, Sigma-Aldrich®, Acros®, TCI America®, Mallinckrodt®, and Oakwood® Products, and used as received without further purification. TLC plates were visualized by exposure to ultraviolet light. Organic solutions were concentrated by rotary evaporation at ~10 torr. Flash column chromatography was performed with 32–63 microns silica gel. ^{1}H NMR spectra were obtained on a 400 MHz spectrometer, and chemical shifts were recorded relative to residual protiated solvent. ^{13}C NMR spectra were obtained at 100 MHz, and chemical shifts were recorded to the solvent resonance. Both ^{1}H and ^{13}C NMR chemical shifts were reported in parts per million downfield from tetramethylsilane (δ = 0 ppm). ^{19}F NMR spectra were obtained at 282.4 MHz, and all chemical shifts were reported in parts per million upfield of CF3COOH (δ = -78.5 ppm). Coupling constants (*J*) are reported in hertz (Hz). Standard abbreviations indicating multiplicity were used as follows: s (singlet), br (broad), d (doublet), t (triplet), q (quartet) and m (multiplet).

Data for ^{13}C NMR spectra are reported in terms of chemical shift (δ ppm). High-resolution mass spectra were obtained from a Bruker Daltronics BioTOF HRMS spectrometer.

4.9.2. Initial observation of indole C2-Amination

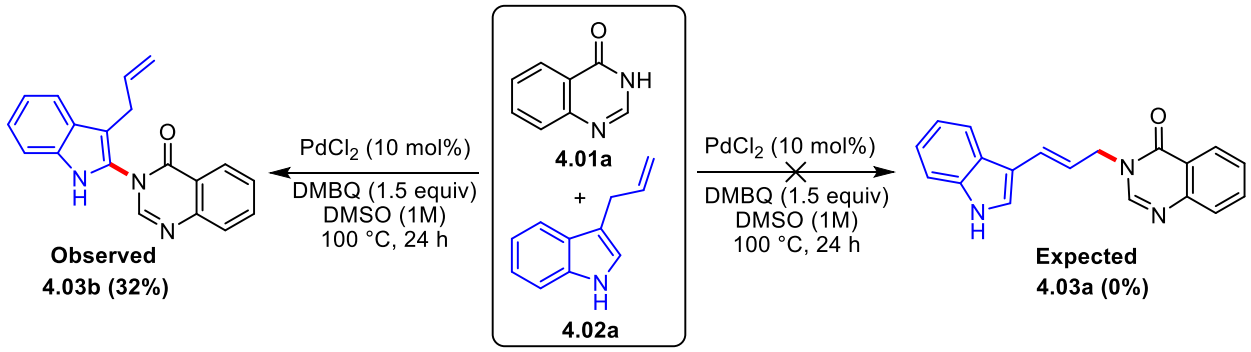

In a glove box, a 1-dram vial was charged with palladium chloride (0.1 equiv, 0.02 mmol), dimethyl benzoquinone (1.5 equiv, 0.3 mmol), **4.02a** (2.0 equiv, 0.3 mmol), **4.01a** (1 equiv), DMSO (0.2 mL) and magnetic stir bar simultaneously. Then the vial was transferred to a preheated magnetic stir plate at 100 °C. After 24 h, the reaction mixture was cooled to rt, adsorbed on to silica gel and purified by column chromatography (TLC: 40% ethyl acetate in hexane R*f* = 0.4) to get analytically pure 3-(3-Allyl-1H-indol-2-yl)-3H-quinazolin-4-one, **4.03a** (32%). **^{1}H NMR** (400 MHz, $CDCl_3$) δ 9.40 (s, 1H), 8.10 (s, 1H), 8.08 – 8.04 (m, 1H), 7.76 – 7.71 (m, 1H), 7.70 – 7.68 (m, 1H), 7.67 – 7.63 (m, 1H), 7.39 – 7.35 (m, 1H), 7.19 – 7.12 (m, 2H), 7.06 – 6.99 (m, 1H), 6.01 (ddt, *J* = 17.1, 10.0, 6.0 Hz, 1H), 5.13 – 4.99 (m, 2H), 3.48 (dt, *J* = 6.0, 1.7 Hz, 2H); **^{13}C NMR** (101 MHz, $CDCl_3$) δ 161.5, 147.5, 146.4, 135.8, 135.0, 134.4, 127.8, 127.7, 127.4, 126.7, 126.6, 123.5, 121.6, 120.0, 119.5, 116.0, 111.7, 109.1, 27.9.

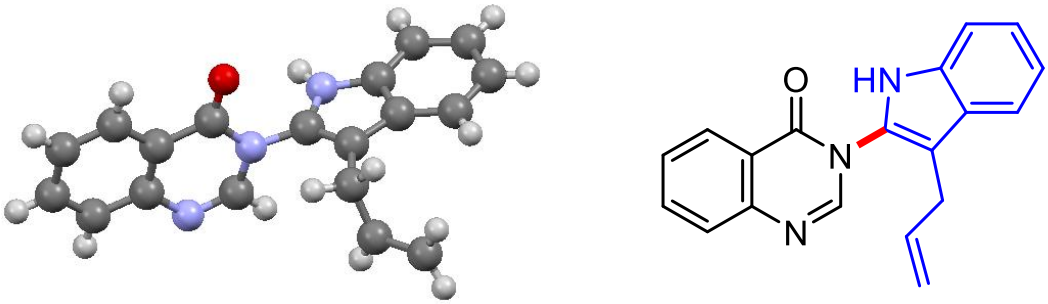

Figure 4.5: ORTEP diagrams of **4.03a** showing 40% probability ellipsoids

4.9.3. Mechanistic investigation

4.9.3.1. Oxidative dearomatization - nucleophilic addition pathway (3A)

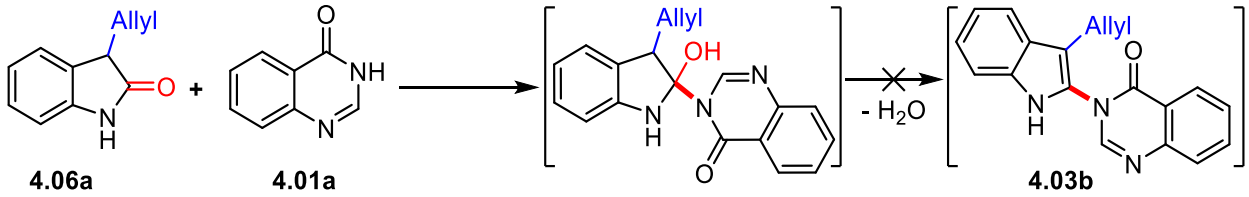

Control study: In a glove box, a 1-dram vial was charged with palladium chloride (0.1 equiv, 0.02 mmol), **4.06a** (2.0 equiv, 0.3 mmol), **4.01a** (1 equiv), DMSO (0.5 mL), DCE (0.5 mL) and magnetic stir bar simultaneously. Then the vial was transferred to a preheated magnetic stir plate at 100 ^{o}C. After 24 h, the reaction mixture was cooled to rt. NMR analysis of the crude mixture shown no product formation with both the starting materials intact, ruling out the possibility of oxidative dearomatization-nucleophilic addition pathway.

4.9.3.2. Norbornene type C–H functionalization/amination pathway (3B)

Control study-1: Reaction of 3-allyl-1-methyl indole

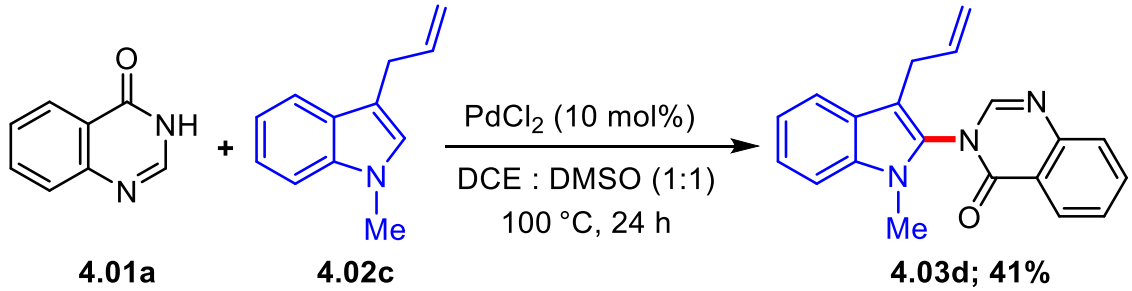

In a glove box, a 1-dram vial was charged with palladium chloride (0.1 equiv, 0.02 mmol), **4.02c** (2.0 equiv, 0.3 mmol), **4.01a** (1 equiv), DMSO (0.5 mL), DCE (0.5 mL) and magnetic stir bar simultaneously. Then the vial was transferred to a preheated magnetic stir plate at 100 °C. After 24 h, the reaction mixture was cooled to rt. The crude mixture was adsorbed on to silica gel and column purified to isolate **4.03d** (41% yield). **^{1}H NMR** (400 MHz, $CDCl_3$) δ 8.42 (ddd, *J* = 8.0, 1.5, 0.6 Hz, 1H), 8.03 (s, 1H), 7.89 (ddd, *J* = 8.4, 7.0, 1.5 Hz, 1H), 7.84 (ddd, *J* = 8.2, 1.4, 0.6 Hz, 1H), 7.69 (dt, *J* = 8.0, 1.0 Hz, 1H), 7.62 (ddd, *J* = 8.2, 7.0, 1.5 Hz, 1H), 7.42 – 7.34 (m, 2H), 7.22 (ddd, *J* = 8.0, 6.5, 1.6 Hz, 1H), 6.01 – 5.91 (m, 1H), 5.04 (dq, *J* = 17.0, 1.7 Hz, 1H), 4.98 (dq, *J* = 10.0, 1.5 Hz, 1H), 3.61 (s, 3H), 3.54 – 3.47 (m, 1H), 3.45 – 3.37 (m, 1H); **^{13}C NMR** (101 MHz, $CDCl_3$) δ 161.1, 147.9, 146.6, 135.9, 135.4, 135.1, 129.0, 128.0, 127.9, 127.4, 126.0, 123.3, 122.1, 120.0, 119.9, 115.7, 109.7, 109.5, 77.3, 77.0, 76.7, 29.4, 28.1.

Control study-2: Catellani-type C–H activation/amination

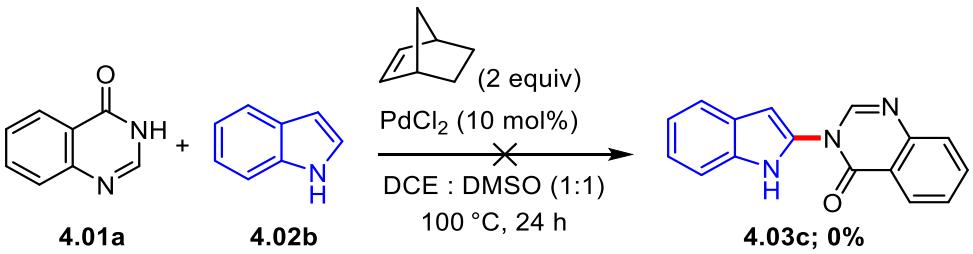

4.01a **4.02b** **4.03c; 0%**

In a glove box, a 1-dram vial was charged with palladium chloride (0.1 equiv, 0.02 mmol), **4.02b** (2.0 equiv, 0.3 mmol), **4.01a** (1 equiv), norbornene (2 equiv), K_2CO_3 (1.5 equiv), DMSO (0.5 mL), DCE (0.5 mL) and magnetic stir bar simultaneously. Then the vial was transferred to a preheated magnetic stir plate at 100 °C. After 24 h, the reaction mixture was cooled to rt. The crude mixture shown no product formation and the SM remained as such in both cases with and without the addition of base.

4.9.3.3. Allylic C–H activation pathway (3C)

Control study-1: Reaction of 3-(1,1-Dimethyl-allyl)-1H-indole

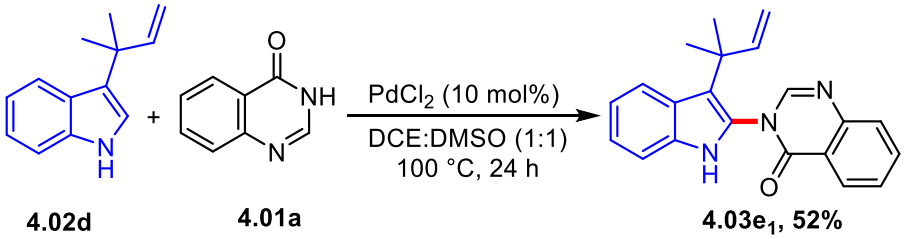

4.02d **4.01a** **4.03e$_1$, 52%**

In a glove box, a 1-dram vial was charged with palladium chloride (0.1 equiv, 0.02 mmol), **4.02d** (2.0 equiv, 0.3 mmol), **4.01a** (1 equiv), DMSO (0.5 mL), DCE (0.5 mL) and magnetic stir bar simultaneously. Then the vial was transferred to a preheated magnetic stir plate at 100 °C. After 24 h, the reaction mixture was cooled to rt. The crude mixture was adsorbed on to silica gel and column purified to isolate **4.03e$_1$** (52% yield). **^{1}H NMR** (400 MHz, $CDCl_3$) δ 9.51 (s, 1H), 8.04 (s, 1H), 7.85 – 7.76 (m, 2H), 7.67 – 7.62 (m, 2H), 7.20 (ddd, J = 8.2, 5.1, 3.3 Hz, 1H), 7.04 (ddd, J = 8.2, 7.1, 1.1 Hz, 1H), 6.90 (ddd, J = 8.3, 7.0, 1.1 Hz, 1H), 6.59 (d, J = 8.2 Hz, 1H), 6.09 (dd, J = 17.4, 10.6 Hz, 1H), 5.04 (dd, J = 17.5, 1.2 Hz, 1H), 4.80 (dd, J = 10.6, 1.1 Hz, 1H), 1.51 (s, 6H); **^{13}C NMR** (101 MHz, $CDCl_3$) δ 162.3, 147.6, 147.1, 146.8, 134.9, 134.6, 127.7, 127.5, 126.4, 125.4, 124.9, 123.1, 121.9, 121.2, 119.3, 118.3, 111.5, 110.9, 38.5, 28.1.

Control study-2: Reaction of 3-butenylindole

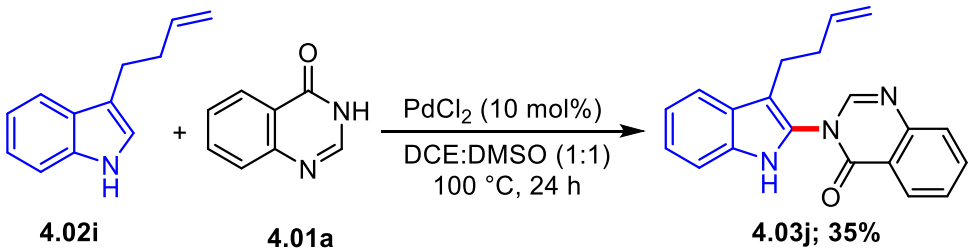

4.02i **4.01a** **4.03j; 35%**

In a glove box, a 1-dram vial was charged with palladium chloride (0.1 equiv, 0.02 mmol), **4.02i** (2.0 equiv, 0.3 mmol), **4.01a** (1 equiv), DMSO (0.5 mL), DCE (0.5 mL) and magnetic stir bar simultaneously. Then the vial was transferred to a preheated magnetic stir plate at 100 °C.

After 24 h, the reaction mixture was cooled to rt. The crude mixture was adsorbed on to silica gel and column purified to isolate **4.03j** (35% yield). **^{1}H NMR** (400 MHz, $CDCl_3$) δ 9.01 (s, 1H), 8.15 (ddd, *J* = 8.0, 1.5, 0.6 Hz, 1H), 8.12 (s, 1H), 7.78 (ddd, *J* = 8.4, 6.9, 1.5 Hz, 1H), 7.75 – 7.71 (m, 1H), 7.68 (ddt, *J* = 5.9, 3.1, 0.8 Hz, 1H), 7.44 (ddd, *J* = 8.2, 6.9, 1.5 Hz, 1H), 7.21 – 7.15 (m, 2H), 7.13 – 7.08 (m, 1H), 5.83 (ddt, *J* = 16.9, 10.2, 6.7 Hz, 1H), 5.05 – 4.92 (m, 2H), 2.86 – 2.75 (m, 2H), 2.45 (tdt, *J* = 7.9, 6.6, 1.4 Hz, 2H); **^{13}C NMR** (101 MHz, $CDCl_3$) δ 161.5, 147.6, 146.4, 137.7, 135.1, 135.0, 134.5, 127.9, 127.7, 127.0, 126.8, 126.6, 123.5, 121.7, 120.0, 119.5, 115.5, 111.6, 34.1, 23.3.

4.9.3.4. Olefin (π-bond) assisted C–H activation/amination pathway (3D)

Control study-1: Reaction of 3-butenylindole

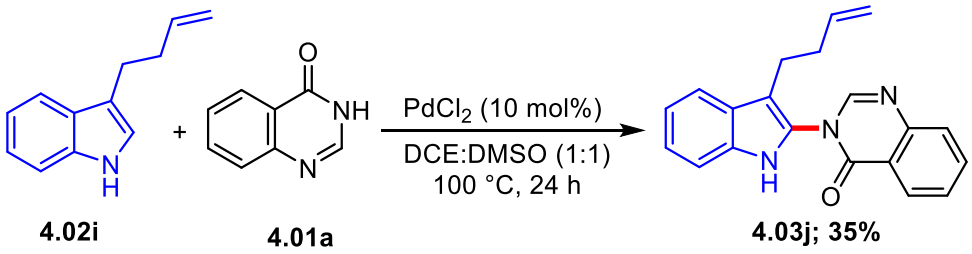

4.02i **4.01a** **4.03j; 35%**

In a glove box, a 1-dram vial was charged with palladium chloride (0.1 equiv, 0.02 mmol), **4.02i** (2.0 equiv, 0.3 mmol), **4.01a** (1 equiv), DMSO (0.5 mL), DCE (0.5 mL) and magnetic stir bar simultaneously. Then the vial was transferred to a preheated magnetic stir plate at 100 °C. After 24 h, the reaction mixture was cooled to rt. The crude mixture was adsorbed on to silica gel and column purified to isolate **4.03j** (35% yield). **^{1}H NMR** (400 MHz, $CDCl_3$) δ 9.01 (s, 1H), 8.15 (ddd, *J* = 8.0, 1.5, 0.6 Hz, 1H), 8.12 (s, 1H), 7.78 (ddd, *J* = 8.4, 6.9, 1.5 Hz, 1H), 7.75 – 7.71 (m, 1H), 7.68 (ddt, *J* = 5.9, 3.1, 0.8 Hz, 1H), 7.44 (ddd, *J* = 8.2, 6.9, 1.5 Hz, 1H), 7.21 – 7.15 (m, 2H), 7.13 – 7.08 (m, 1H), 5.83 (ddt, *J* = 16.9, 10.2, 6.7 Hz, 1H), 5.05 – 4.92 (m, 2H), 2.86 – 2.75 (m, 2H), 2.45 (tdt, *J* = 7.9, 6.6, 1.4 Hz, 2H); **^{13}C NMR** (101 MHz, $CDCl_3$) δ 161.5, 147.6, 146.4, 137.7,

135.1, 135.0, 134.5, 127.9, 127.7, 127.0, 126.8, 126.6, 123.5, 121.7, 120.0, 119.5, 115.5, 111.6, 34.1, 23.3.

Control study-2: Reaction of indole-3-acetonitrile

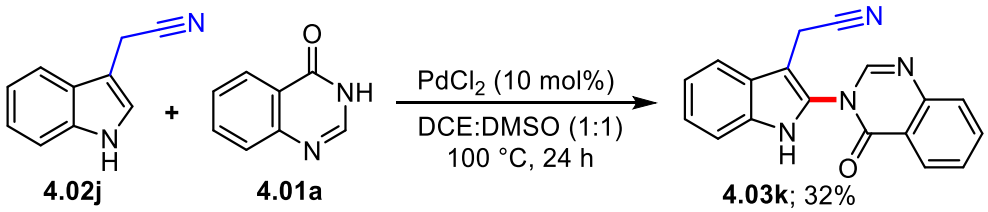

In a glove box, a 1-dram vial was charged with palladium chloride (0.1 equiv, 0.02 mmol), **4.02j** (2.0 equiv, 0.3 mmol), **4.01a** (1 equiv), DMSO (0.5 mL), DCE (0.5 mL) and magnetic stir bar simultaneously. Then the vial was transferred to a preheated magnetic stir plate at 100 °C. After 24 h, the reaction mixture was cooled to rt. The crude mixture was adsorbed on to silica gel and column purified to isolate **4.03k** (32% yield). **^{1}H NMR** (400 MHz, DMSO-d_6) δ 11.93 (s, 1H), 8.43 (s, 1H), 8.27 (dd, *J* = 7.9, 1.5 Hz, 1H), 7.95 (ddd, *J* = 8.7, 7.2, 1.6 Hz, 1H), 7.85 – 7.79 (m, 1H), 7.74 (d, *J* = 7.9 Hz, 1H), 7.70 – 7.64 (m, 1H), 7.48 (d, *J* = 8.1 Hz, 1H), 7.30 (ddd, *J* = 8.2, 7.1, 1.2 Hz, 1H), 7.20 (ddd, *J* = 8.3, 7.1, 1.1 Hz, 1H), 4.07 (s, 2H); **^{13}C NMR** (101 MHz, DMSO) δ 160.5, 147.9, 147.4, 135.6, 134.1, 128.9, 128.3, 128.0, 127.1, 125.9, 123.6, 122.2, 120.4, 119.2, 118.8, 112.3, 100.6, 12.3.

4.9.3.5. H/D exchange study

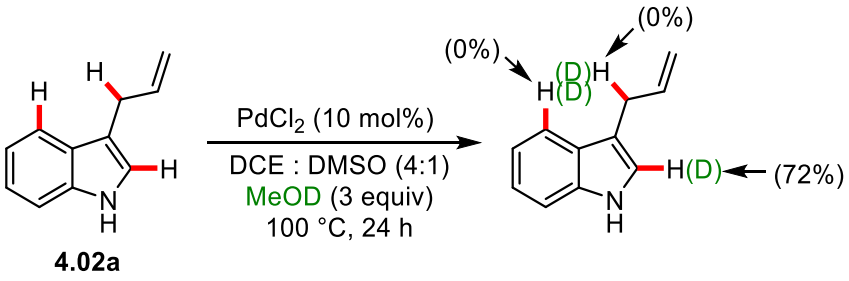

Procedure for deuteration reaction: To a 1-dram vial fitted with a teflon cap, and a magnetic stir bar on a 0.2 mmol scale, $PdCl_2$ (0.1 equiv, 0.02 mmol), **4.02a** (1 equiv), DMSO (0.2

mL), DCE (0.8 mL) and MeOD (3 equiv) were added simultaneously under nitrogen atmosphere. Then the vial was transferred to a preheated magnetic stir plate at 100 ^{o}C. After 24 h, the reaction mixture was cooled to rt. The reaction mixture was passed through celite bed washing with dichloromethane. The combined organics were concentrated. ^{1}H NMR spectroscopic analysis of the crude reaction mixture indicated 72 % deuteration at indole C-2 position.

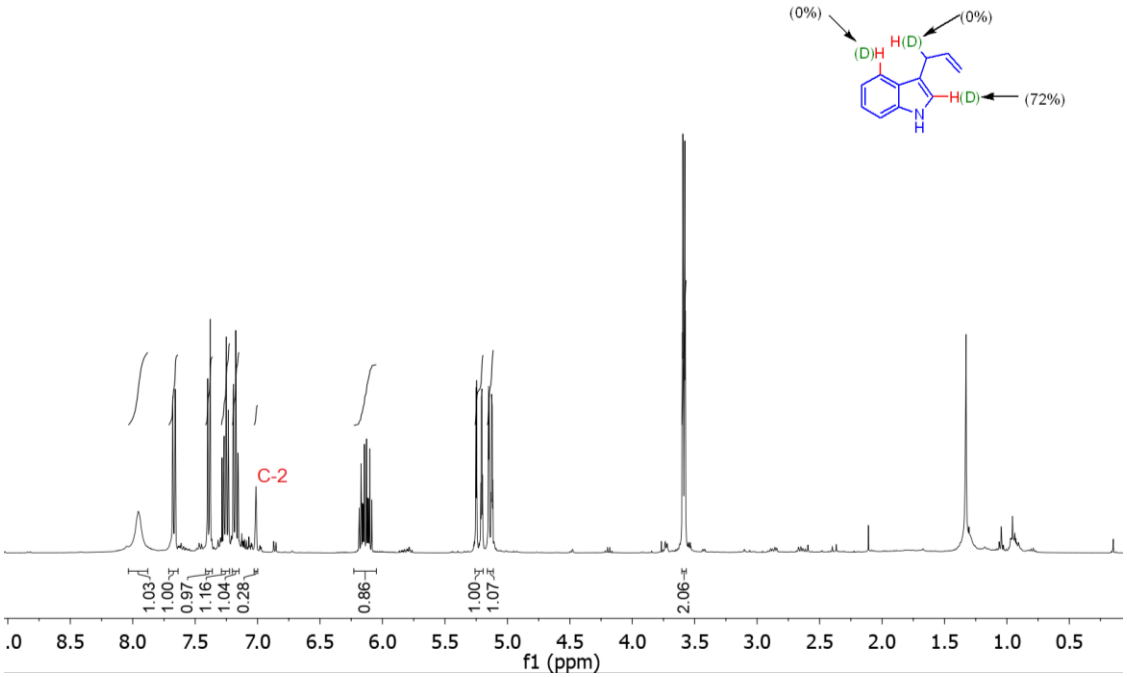

Figure 4.6: Pd-catalyzed deuterium incorporation of allyl indole under reaction conditions

4.9.4. Preparation of starting materials

4.9.4.1. Experimental procedure for the synthesis 3-Allyl-1H-indole [27]

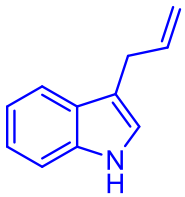

Following a slightly modified reported procedure, oven dried round bottom flask was charged with indole (4.5 g, 38.4 mmol), $Pd(PPh_3)_4$ (2.217 g, 1.92 mmol, 0.05 equiv.), allyl alcohol (2.60 mL, 38.4 mmol, 1 equiv.), 1M triethylborane in THF (11.52 mL, 11.52 mmol, 0.3 equiv.) in THF (90 mL). The solution was heated to 70 °C over 12 h. EtOAc (50 mL) and a saturated aqueous solution of sodium bicarbonate (150 mL) were added to the solution. The aqueous layer was extracted with EtOAc (4 x 50 mL),

anhydrous sodium sulfate was used to dry the organic layer. The organic layer was concentrated under reduced pressure and the crude product was purified by column chromatography [hexanes/EtOAc] to give 3-Allyl-1H-indole (5.6 g, 93%) as a yellow oil. **^{1}H NMR** (400 MHz, CDCl3) δ 7.91 (s, 1H), 7.69 – 7.66 (m, 1H), 7.41 – 7.38 (m, 1H), 7.26 (ddd, J = 8.1, 7.0, 1.2 Hz, 1H), 7.18 (ddd, J = 8.0, 7.0, 1.1 Hz, 1H), 7.02 – 7.01 (m, 1H), 6.19 – 6.09 (m,f 1H), 5.23 (dq, J = 17.0, 1.8 Hz, 1H), 5.14 (dq, J = 10.0, 1.5 Hz, 1H), 3.59 (dq, J = 6.5, 1.3 Hz, 2H). **^{13}C NMR** (101 MHz, CDCl3) δ 137.3, 136.4, 127.5, 122.0, 121.7, 119.3, 119.1, 115.2, 114.5, 111.1, 29.9.

4.9.4.2. Experimental procedure for the synthesis of 3-(but-3-en-1-yl) N-H indoles [28]

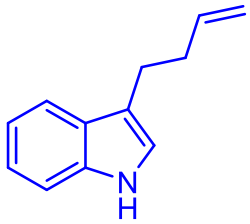

Following a slightly modified reported procedure, to a solution of the indole (0.58 g, 4.9 mmol) in benzene was added a solution of MeMgCl (1.6 mL, 3.0 M solution in THF) at rt. After 10 min, 4-bromobutene (0.5 mL, 4.2 mmol) was added and the reaction mixture was heated to reflux. After 27 h, the reaction mixture was cooled and quenched with sat. NH_4Cl. The organic phase was separated, and the aqueous phase was extracted twice with EtOAc. The organic layer was washed with water and brine, dried over $NaSO_4$, and concentrated in vacuo. The residue was purified by column chromatography on silica gel to afford 3-(but-3-en-1-yl) N-H indoles as yellow oil (0.3 mL, 35%). **^{1}H NMR** (400 MHz, $CDCl_3$) δ 7.87 (m, 1H), 7.73 – 7.67 (m, 1H), 7.39 (dt, *J* = 8.2, 0.9 Hz, 1H), 7.30 – 7.24 (m, 1H), 7.22 – 7.18 (m, 1H), 7.03 – 7.02 (m, 1H), 6.07 – 5.97 (m, 1H), 5.23 – 5.13 (m, 1H), 5.10 – 5.06 (m, 1H), 2.97 – 2.92 (m, 2H), 2.59 – 2.53 (m, 2H); **^{13}C NMR** (101 MHz, $CDCl_3$) δ 138.8, 136.3, 127.6, 122.0, 121.2, 119.2, 119.0, 116.3, 114.7, 111.1, 34.3, 24.8.

4.9.4.3. Experimental procedure for the synthesis of 3-Allyl-1-methylindole

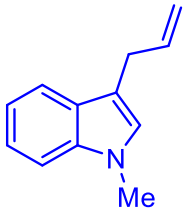

A solution of 3-Allyl-1*H*-indole (0.5 g, 3.2 mmol), in DMF (6 mL) was cooled to 0 °C, NaH (0.09 g, 3.8 mmol) was added in portion and stirred at rt for 1h. After 1h, the solution was again cooled to 0 °C, and iodomethane (2.4 mL, 3.8 mmol) was added dropwise and stirred at rt. After 3h, the solution was poured on to ice and extracted twice with EtOAc. The organic layer was washed with water and brine, dried over $NaSO_4$, and concentrated in vacuo. The residue was purified by column chromatography on silica gel to afford 3-Allyl-1-methylindole as yellow oil (0.46 g, 85%). **^{1}H NMR** (400 MHz, $CDCl_3$) δ 7.81 – 7.73 (m, 1H), 7.47 – 7.35 (m, 2H), 7.30 – 7.25 (m,1H), 6.99 – 6.94 (m, 1H), 6.29 – 6.19 (m, 1H), 5.34 (dq, *J* = 17.1, 1.8 Hz, 1H), 5.26 – 5.22 (m, 1H), 3.84 (s, 3H), 3.70 – 3.67 (m, 2H).

4.9.5. General experimental procedure for indole C_2-Amination with N-heterocycles

4.9.5.1. Pd-catalyzed indole C-2 amidation

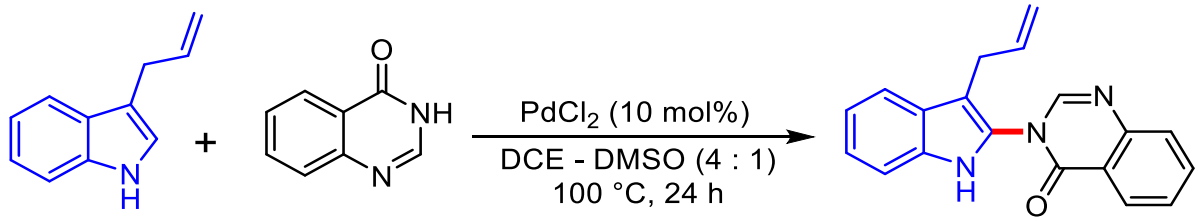

4.02a **4.01a** **4.03b; 48%**

To a 1-dram vial fitted with a teflon cap, and a magnetic stir bar on a 0.2 mmol scale, $PdCl_2$ (0.1 equiv, 0.02 mmol), **4.01a** (29.2 mg, 1 equiv), DMSO (0.2 mL), DCE (0.8 mL) and **4.02a** (2.0 equiv, 0.4 mmol) were added simultaneously under nitrogen atmosphere. Then the vial was transferred to a preheated magnetic stir plate at 100 °C. After 24 h, the reaction mixture was cooled to rt, adsorbed on to silica gel and purified by column chromatography using hexane and ethyl acetate (10%-25%) as mobile phase to get analytically pure compound as a yellow solid (51 mg, 85%). **^{1}H NMR** (400 MHz, $CDCl_3$) δ 9.40 (s, 1H), 8.10 (s, 1H), 8.08 – 8.04 (m, 1H), 7.76 – 7.71

(m, 1H), 7.70 – 7.68 (m, 1H), 7.67 – 7.63 (m, 1H), 7.39 – 7.35 (m, 1H), 7.19 – 7.12 (m, 2H), 7.06 – 6.99 (m, 1H), 6.01 (ddt, *J* = 17.1, 10.0, 6.0 Hz, 1H), 5.13 – 4.99 (m, 2H), 3.48 (dt, *J* = 6.0, 1.7 Hz, 2H); **^{13}C NMR** (101 MHz, $CDCl_3$) δ 161.5, 147.5, 146.4, 135.8, 135.0, 134.4, 127.8, 127.7, 127.4, 126.7, 126.6, 123.5, 121.6, 120.0, 119.5, 116.0, 111.7, 109.1, 27.9.

4.9.5.2. Ni- catalyzed indole C-2 amidation

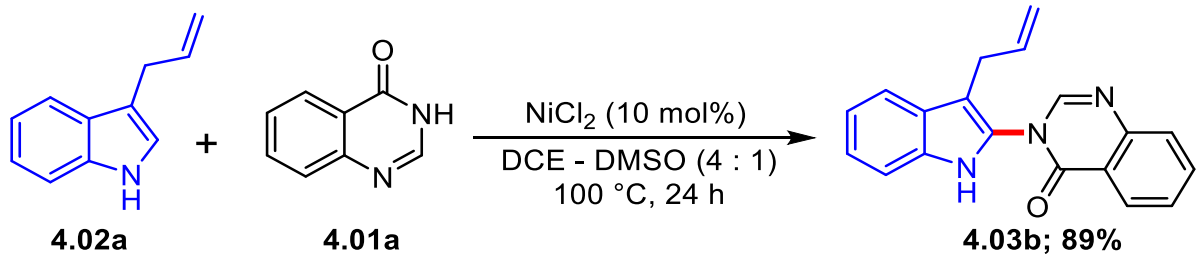

To a 1-dram vial fitted with a teflon cap, and a magnetic stir bar on a 0.2 mmol scale, $NiCl_2$ (0.1 equiv, 0.02 mmol), **4.01a** (29.2 mg, 1 equiv), DMSO (0.2 mL), DCE (0.8 mL) and **4.02a** (2.0 equiv, 0.4 mmol) were added simultaneously under nitrogen atmosphere. Then the vial was transferred to a preheated magnetic stir plate at 100 ^{o}C. After 24 h, the reaction mixture was cooled to rt, adsorbed on to silica gel and purified by column chromatography using hexane and ethyl acetate (10%-25%) as mobile phase to get analytically pure compound as a yellow solid (51 mg, 85%). **^{1}H NMR** (400 MHz, $CDCl_3$) δ 9.40 (s, 1H), 8.10 (s, 1H), 8.08 – 8.04 (m, 1H), 7.76 – 7.71 (m, 1H), 7.70 – 7.68 (m, 1H), 7.67 – 7.63 (m, 1H), 7.39 – 7.35 (m, 1H), 7.19 – 7.12 (m, 2H), 7.06 – 6.99 (m, 1H), 6.01 (ddt, *J* = 17.1, 10.0, 6.0 Hz, 1H), 5.13 – 4.99 (m, 2H), 3.48 (dt, *J* = 6.0, 1.7 Hz, 2H); **^{13}C NMR** (101 MHz, $CDCl_3$) δ 161.5, 147.5, 146.4, 135.8, 135.0, 134.4, 127.8, 127.7, 127.4, 126.7, 126.6, 123.5, 121.6, 120.0, 119.5, 116.0, 111.7, 109.1, 27.9.

4.9.6. Analytical characterization of purified compounds

3-(3-Allyl-1H-indol-2-yl)-3H-quinazolin-4-one: Prepared by general procedure to yield

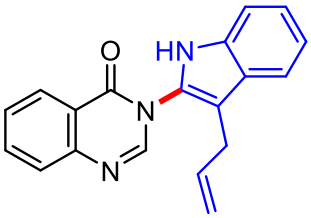

4.03b as a yellow solid. **^{1}H NMR** (400 MHz, $CDCl_3$) δ 9.40 (s, 1H), 8.10 (s, 1H), 8.08 – 8.04 (m, 1H), 7.76 – 7.71 (m, 1H), 7.70 – 7.68 (m, 1H), 7.67 – 7.63 (m, 1H), 7.39 – 7.35 (m, 1H), 7.19 – 7.12 (m, 2H), 7.06 – 6.99 (m, 1H), 6.01 (ddt, *J* = 17.1, 10.0, 6.0 Hz, 1H), 5.13 – 4.99 (m, 2H), 3.48 (dt, *J* = 6.0, 1.7 Hz, 2H); **^{13}C NMR** (101 MHz, $CDCl_3$) δ 161.5, 147.5, 146.4, 135.8, 135.0, 134.4, 127.8, 127.7, 127.4, 126.7, 126.6, 123.5, 121.6, 120.0, 119.5, 116.0, 111.7, 109.1, 27.9.

3-(3-Allyl-1-methyl-1H-indol-2-yl)-3H-quinazolin-4-one: Prepared by general

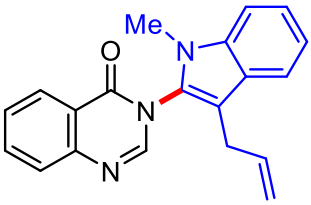

procedure to yield **4.03d** as a colorless viscous liquid. **^{1}H NMR** (400 MHz, $CDCl_3$) δ 8.42 (ddd, *J* = 8.0, 1.5, 0.6 Hz, 1H), 8.03 (s, 1H), 7.89 (ddd, *J* = 8.4, 7.0, 1.5 Hz, 1H), 7.84 (ddd, *J* = 8.2, 1.4, 0.6 Hz, 1H), 7.69 (dt, *J* = 8.0, 1.0 Hz, 1H), 7.62 (ddd, *J* = 8.2, 7.0, 1.5 Hz, 1H), 7.42 – 7.34 (m, 2H), 7.22 (ddd, *J* = 8.0, 6.5, 1.6 Hz, 1H), 6.01 – 5.91 (m, 1H), 5.04 (dq, *J* = 17.0, 1.7 Hz, 1H), 4.98 (dq, *J* = 10.0, 1.5 Hz, 1H), 3.61 (s, 3H), 3.54 – 3.47 (m, 1H), 3.45 – 3.37 (m, 1H); **^{13}C NMR** (101 MHz, $CDCl_3$) δ 161.1, 147.9, 146.6, 135.9, 135.4, 135.1, 129.0, 128.0, 127.9, 127.4, 126.0, 123.3, 122.1, 120.0, 119.9, 115.7, 109.7, 109.5, 77.3, 77.0, 76.7, 29.4, 28.1.

3-(3-Allyl-5-methoxy-1H-indol-2-yl)-3H-quinazolin-4-one: Prepared by general

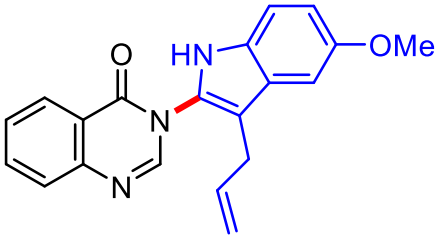

procedure to yield **4.03l** as a yellow solid. **^{1}H NMR** (400 MHz, $CDCl_3$) δ 9.30 (s, 1H), 8.09 (s, 1H), 8.06 (ddd, *J* = 8.0, 1.5, 0.7 Hz, 1H), 7.73 (ddd, *J* = 8.3, 6.9, 1.5 Hz, 1H), 7.68 (ddd, *J* = 8.2, 1.5, 0.6 Hz, 1H), 7.37 (ddd, *J* = 8.2, 6.9, 1.5 Hz, 1H), 7.05 (d, *J* = 2.4 Hz, 1H), 6.93 (dd, *J* = 8.8, 0.6 Hz, 1H), 6.81 (dd, *J* = 8.8, 2.4 Hz, 1H), 6.00 (ddt, *J* = 17.1, 10.1, 5.9 Hz, 1H),

5.10 – 5.01 (m, 2H), 3.89 (s, 3H), 3.44 (dt, *J* = 6.0, 1.7 Hz, 2H); **^{13}C NMR** (101 MHz, CDCl3) δ 161.5, 154.3, 147.5, 146.3, 135.7, 134.9, 129.5, 127.9, 127.8, 127.6, 127.1, 126.7, 121.6, 115.9, 113.7, 112.5, 108.8, 101.4, 55.9, 27.9.

3-(3-Allyl-5-nitro-1H-indol-2-yl)-3H-quinazolin-4-one: Prepared by general procedure

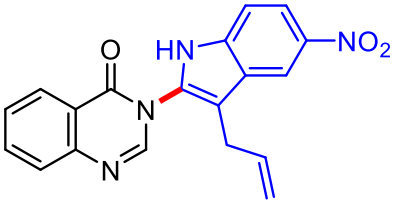

to yield **4.03m** as a yellow solid. **^{1}H NMR** (400 MHz, $CDCl_3$) δ 10.05 (s, 1H), 8.57 (d, *J* = 2.2 Hz, 1H), 8.13 (s, 1H), 8.06 (dd, *J* = 7.9, 1.4 Hz, 1H), 7.97 (dd, *J* = 9.0, 2.2 Hz, 1H), 7.79 (ddd, *J* = 8.5, 6.8, 1.5 Hz, 1H), 7.73 (dd, *J* = 8.2, 1.4 Hz, 1H), 7.43 (ddd, *J* = 8.1, 7.0, 1.4 Hz, 1H), 7.05 (d, *J* = 9.0 Hz, 1H), 6.02 (ddt, *J* = 16.3, 10.1, 5.9 Hz, 1H), 5.16 – 5.05 (m, 2H), 3.54 (dt, *J* = 6.2, 1.7 Hz, 2H); **^{13}C NMR** (101 MHz, $CDCl_3$) δ 161.5, 147.2, 145.4, 142.0, 137.1, 135.5, 134.8, 130.0, 128.3, 127.8, 126.7, 125.9, 125.5, 121.2, 118.9, 117.0, 116.9, 111.5, 27.7.

3-(3-Allyl-5-bromo-1H-indol-2-yl)-3H-quinazolin-4-one: Prepared by general

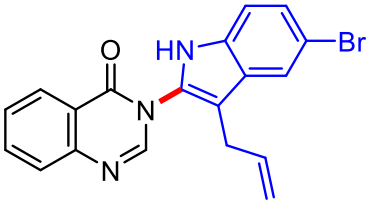

procedure to yield **4.03n** as a light yellow solid. **^{1}H NMR** (400 MHz, $CDCl_3$) δ 9.44 (s, 1H), 8.09 (s, 1H), 8.05 – 7.99 (m, 1H), 7.79 – 7.68 (m, 3H), 7.37 (ddd, *J* = 8.2, 6.8, 1.5 Hz, 1H), 7.20 (dd, *J* = 8.6, 1.9 Hz, 1H), 6.82 (d, *J* = 8.6 Hz, 1H), 5.99 (ddt, *J* = 17.6, 9.6, 5.9 Hz, 1H), 5.11 – 5.03 (m, 2H), 3.43 (dt, *J* = 6.1, 1.7 Hz, 2H); **^{13}C NMR** (101 MHz, $CDCl_3$) δ 161.6, 147.5, 145.9, 135.3, 135.2, 132.9, 128.3, 128.2, 127.9, 127.8, 126.6, 126.5, 122.1, 121.5, 116.4, 113.4, 113.0, 108.8, 27.7.

3-(3-Allyl-5-fluoro-1H-indol-2-yl)-3H-quinazolin-4-one: Prepared by general procedure

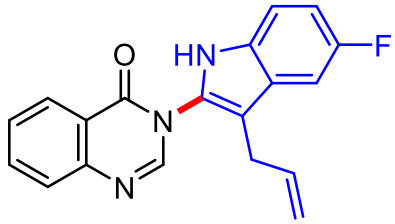

to yield **4.03o** as a light yellow solid. **^{1}H NMR** (400 MHz, $CDCl_3$) δ 9.54 (s, 1H), 8.10 (s, 1H), 8.03 – 7.94 (m, 1H), 7.76 – 7.68 (m, 2H), 7.53 (dd, *J* = 8.8, 5.2 Hz, 1H), 7.34 (ddd, *J* = 8.2,

6.7, 1.8 Hz, 1H), 6.89 (td, *J* = 9.2, 2.2 Hz, 1H), 6.56 (dd, *J* = 9.5, 2.3 Hz, 1H), 5.99 (ddt, *J* = 16.3, 10.0, 6.0 Hz, 1H), 5.12 – 5.02 (m, 2H), 3.45 (dt, *J* = 6.1, 1.7 Hz, 2H); **^{13}C NMR** (101 MHz, $CDCl_3$) δ 161.71, 161.67, 159.3, 147.4, 146.3, 135.3 (*J* = 44.7 Hz), 134.3 (*J* = 12.9 Hz), 127.8 (*J* = 28.4 Hz), 127.3 (*J* = 4.4 Hz), 126.6, 122.2 (*J* = 164.5 Hz), 120.5 (*J* = 10.4 Hz), 116.2, 109.4, 109.2, 109.0, 97.9, 97.6, 27.9; **^{19}F NMR** (376 MHz, $CDCl_3$) δ -118.6.

3-Allyl-2-(4-oxo-4H-quinazolin-3-yl)-1H-indole-5-carboxylic acid methyl ester:

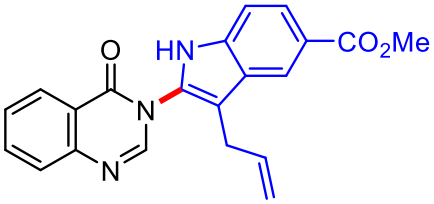

Prepared by general procedure to yield **4.03p** as a light yellow solid. **^{1}H NMR** (400 MHz, DMSO-d_6) δ 12.06 (s, 1H), 8.40 (s, 1H), 8.32 (d, *J* = 1.6 Hz, 1H), 8.26 (dd, *J* = 7.9, 1.5 Hz, 1H), 7.95 (ddd, *J* = 8.5, 7.2, 1.6 Hz, 1H), 7.86 (dd, *J* = 8.6, 1.7 Hz, 1H), 7.80 (dd, *J* = 8.2, 1.2 Hz, 1H), 7.69 – 7.63 (m, 1H), 7.53 (dd, *J* = 8.6, 0.7 Hz, 1H), 5.92 (ddt, *J* = 17.0, 10.0, 6.1 Hz, 1H), 5.03 (dq, *J* = 16.9, 1.6 Hz, 1H), 4.94 (dq, *J* = 10.1, 1.5 Hz, 1H), 3.88 (s, 3H), 3.46 (dt, *J* = 6.3, 1.6 Hz, 2H). **^{13}C NMR** (101 MHz, DMSO-d_6) δ 167.5, 160.5, 147.9, 147.6, 137.0, 136.6, 135.7, 130.0, 128.4, 128.1, 127.0, 126.4, 123.9, 122.3, 122.0, 121.2, 116.0, 112.1, 110.0, 52.3, 27.6.

3-Allyl-2-(4-oxo-4H-quinazolin-3-yl)-1H-indole-5-carbaldehyde: Prepared by general

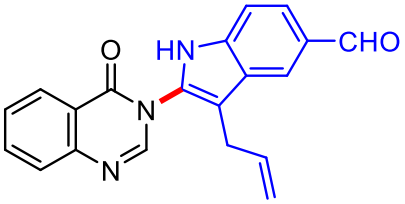

procedure to yield **4.03q** as an off light yellow solid. **^{1}H NMR** (400 MHz, DMSO-d_6) δ 12.19 (s, 1H), 10.03 (s, 1H), 8.42 (s, 1H), 8.35 – 8.23 (m, 2H), 8.00 – 7.91 (m, 1H), 7.85 – 7.75 (m, 2H), 7.67 (t, *J* = 7.6 Hz, 1H), 7.60 (d, *J* = 8.5 Hz, 1H), 5.94 (ddt, *J* = 16.5, 10.0, 6.2 Hz, 1H), 5.10 – 5.03 (m, 1H), 4.94 (dd, *J* = 10.0, 2.1 Hz, 1H), 3.50 (dt, *J* = 6.6, 1.6 Hz, 2H); **^{13}C NMR** (101 MHz, DMSO) δ 192.9, 160.5, 147.9, 147.5, 137.8, 136.5, 135.7, 130.2, 129.4, 128.4, 128.1, 127.0, 126.7, 125.1, 122.9, 122.0, 116.1, 112.8, 110.7, 27.7.

3-Allyl-2-(4-oxo-4H-quinazolin-3-yl)-1H-indole-5-carbonitrile: Prepared by general procedure to yield **4.03r** as a light yellow solid. **^{1}H NMR** (400 MHz, DMSO-d_6) δ 12.25 (s, 1H), 8.40 (s, 1H), 8.25 (ddd, *J* = 8.0, 1.5, 0.6 Hz, 1H), 8.20 (dd, *J* = 1.6, 0.8 Hz, 1H), 7.95 (ddd, *J* = 8.2, 7.2, 1.6 Hz, 1H), 7.83 – 7.78 (m, 1H), 7.66 (ddd, *J* = 8.2, 7.3, 1.2 Hz, 1H), 7.63 – 7.57 (m, 2H), 5.88 (ddt, *J* = 16.9, 10.0, 6.3 Hz, 1H), 5.04 (dd, *J* = 17.1, 1.8 Hz, 1H), 4.91 (dd, *J* = 10.0, 1.7 Hz, 1H), 3.46 (dt, *J* = 6.5, 1.5 Hz, 2H).**^{13}C NMR** (101 MHz, DMSO) δ 160.5, 147.9, 147.4, 136.4, 136.1, 135.8, 130.7, 128.4, 128.1, 127.0, 126.7, 125.6, 125.6, 122.0, 121.0, 116.1, 113.4, 109.8, 101.8, 27.5.

3-(3-Allyl-1H-indol-2-yl)-6-nitro-3H-quinazolin-4-one: Prepared by general procedure to yield **4.03s** as a yellow solid. **^{1}H NMR** (400 MHz, $CDCl_3$) δ 8.98 (d, *J* = 2.7 Hz, 2H), 8.54 (dd, *J* = 9.0, 2.7 Hz, 1H), 8.29 (s, 1H), 7.90 (d, *J* = 8.9 Hz, 1H), 7.64 (dd, *J* = 6.5, 2.4 Hz, 1H), 7.26 – 7.12 (m, 3H), 6.01 (ddt, *J* = 16.3, 10.1, 5.9 Hz, 1H), 5.11 – 5.03 (m, 2H), 3.50 (dt, *J* = 6.1, 1.7 Hz, 2H); **^{13}C NMR** (101 MHz, $CDCl_3$) δ 160.2, 151.5, 149.3, 146.3, 135.4, 134.5, 129.5, 128.9, 126.6, 126.4, 124.1, 123.3, 122.1, 120.5, 119.7, 116.3, 111.6, 109.6, 27.9.

3-(3-Allyl-1H-indol-2-yl)-6-methoxy-3H-quinazolin-4-one: Prepared by general procedure to yield **4.03t** as a light yellow solid. **^{1}H NMR** (400 MHz, DMSO-d_6) δ 11.61 (s, 1H), 8.26 (s, 1H), 7.75 (d, *J* = 8.8 Hz, 1H), 7.62 (d, *J* = 8.0 Hz, 2H), 7.53 (dd, *J* = 8.9, 3.0 Hz, 1H), 7.42 (d, *J* = 8.1 Hz, 1H), 7.22 (t, *J* = 7.6 Hz, 1H), 7.10 (t, *J* = 7.5 Hz, 1H), 5.89 (ddt, *J* = 16.6, 9.6, 6.3 Hz, 1H), 5.02 (dd, *J* = 17.3, 2.1 Hz, 1H), 4.93 – 4.87 (m, 1H), 3.92 (s, 3H), 3.38 (d, *J* = 6.5 Hz,

2H); **^{13}C NMR** (101 MHz, DMSO) δ 160.4, 159.0, 145.6, 142.4, 136.8, 134.3, 129.8, 128.5, 126.9, 124.8, 123.0, 122.9, 119.7, 119.6, 115.7, 112.0, 108.4, 107.1, 56.3, 27.9.

3-(3-Allyl-1H-indol-2-yl)-6-bromo-3H-quinazolin-4-one: Prepared by general procedure to yield **4.03u** as a light yellow solid. **^{1}H NMR** (400 MHz, DMSO-d_6) δ 11.62 (s, 1H), 8.45 (s, 1H), 8.36 (d, *J* = 2.3 Hz, 1H), 8.06 (dd, *J* = 8.7, 2.4 Hz, 1H), 7.76 (d, *J* = 8.7 Hz, 1H), 7.63 (dd, *J* = 7.9, 1.1 Hz, 1H), 7.45 (dt, *J* = 8.2, 0.9 Hz, 1H), 7.24 (ddd, *J* = 8.2, 7.1, 1.2 Hz, 1H), 7.11 (ddd, *J* = 8.0, 7.1, 1.0 Hz, 1H), 5.91 (ddt, *J* = 17.1, 9.9, 6.3 Hz, 1H), 5.04 (dq, *J* = 17.1, 1.7 Hz, 1H), 4.91 (dq, *J* = 10.0, 1.5 Hz, 1H), 3.42 (dt, *J* = 6.4, 1.6 Hz, 2H); **^{13}C NMR** (101 MHz, DMSO) δ 159.5, 148.4, 147.0, 138.4, 136.8, 134.4, 130.4, 129.1, 128.0, 126.9, 123.7, 123.1, 120.8, 119.8, 119.7, 115.7, 112.1, 108.6, 27.9.

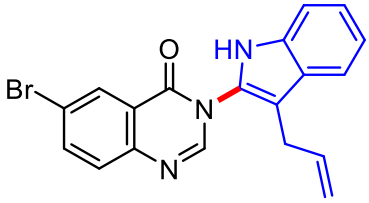

3-(3-Allyl-1H-indol-2-yl)-6-fluoro-3H-quinazolin-4-one: Prepared by general procedure to yield **4.03v** as a light yellow solid. **^{1}H NMR** (400 MHz, DMSO-d_6) δ 11.60 (s, 1H), 8.38 (s, 1H), 7.95 (dd, *J* = 8.6, 2.9 Hz, 1H), 7.89 (dd, *J* = 9.0, 5.0 Hz, 1H), 7.83 (td, *J* = 8.6, 2.9 Hz, 1H), 7.62 (dd, *J* = 7.9, 1.1 Hz, 1H), 7.42 (dt, *J* = 8.2, 1.0 Hz, 1H), 7.22 (ddd, *J* = 8.2, 7.1, 1.2 Hz, 1H), 7.10 (ddd, *J* = 8.1, 7.1, 1.0 Hz, 1H), 5.89 (ddt, *J* = 17.1, 10.0, 6.3 Hz, 1H), 5.02 (dq, *J* = 17.1, 1.8 Hz, 1H), 4.90 (dq, *J* = 10.0, 1.5 Hz, 1H), 3.40 (dt, *J* = 6.3, 1.6 Hz, 2H); **^{13}C NMR** (101 MHz, DMSO) δ 162.4, 160.0, 159.9, 159.9, 147.4 (d, *J* = 2.16 Hz), 144.9 (d, *J* = 2.16 Hz), 136.8, 134.4, 131.0 (d, *J* = 9.0 Hz), 127.5 (d, *J* = 122.81 Hz), 124.0 (d, *J* = 23.83 Hz), 123.5 (d, *J* = 8.53 Hz), 123.0, 119.8, 119.7, 115.7, 112.0, 111.8 (d, *J* = 111.83 Hz), 108.5, 27.9; **^{19}F NMR** (376 MHz, $CDCl_3$) δ -112.0.

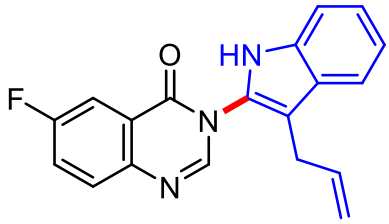

3-(3-Allyl-1H-indol-2-yl)-7-fluoro-3H-quinazolin-4-one: Prepared by general procedure

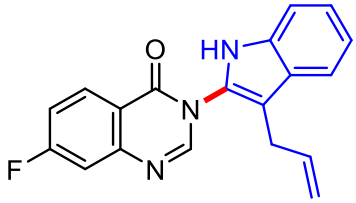

to yield **4.03w** as a light yellow solid. **^{1}H NMR** (400 MHz, $CDCl_3$) δ 8.90 (s, 1H), 8.24 (dd, *J* = 8.9, 6.0 Hz, 1H), 8.14 (s, 1H), 7.69 – 7.61 (m, 1H), 7.41 (dd, *J* = 9.3, 2.5 Hz, 1H), 7.27 – 7.14 (m, 4H), 6.02 (ddt, *J* = 17.1, 10.1, 5.9 Hz, 1H), 5.14 – 5.02 (m, 2H), 3.50 (dt, *J* = 6.0, 1.7 Hz, 2H); **^{13}C NMR** (101 MHz, $CDCl_3$) δ 166.8 (d, *J* = 256.5 Hz), 160.6, 149.8 (d, *J* = 12.8 Hz), 147.5, 135.6, 134.4, 129.7 (d, *J* = 10.5 Hz), 127.0 (d, *J* = 56.3 Hz), 123.8, 120.3, 119.7, 118.5, 118.5, 116.6 (d, *J* = 24.0 Hz), 116.1, 113.4 (d, *J* = 22.4 Hz), 111.5, 109.2, 27.9. **^{19}F NMR** (376 MHz, $CDCl_3$) δ -112.0

3-(3-Allyl-1H-indol-2-yl)-3H-pyrimidin-4-one: Prepared by general procedure to yield

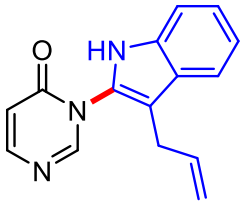

4.05a as a light brown solid. **^{1}H NMR** (400 MHz, DMSO-d_6) δ 11.61 (s, 1H), 8.48 (s, 1H), 8.04 (d, *J* = 6.8 Hz, 1H), 7.61 (d, *J* = 7.9 Hz, 1H), 7.40 (d, *J* = 8.1 Hz, 1H), 7.21 (t, *J* = 7.5 Hz, 1H), 7.09 (t, *J* = 7.5 Hz, 1H), 6.62 – 6.55 (m, 1H), 5.02 (dq, *J* = 17.0, 1.8 Hz, 1H), 4.93 (dq, *J* = 10.0, 1.6 Hz, 1H), 3.36 – 3.34 (m, 2H); **^{13}C NMR** (101 MHz, DMSO) δ 160.4, 154.3, 153.2, 136.6, 134.3, 127.9, 126.8, 123.1, 119.7, 119.7, 116.2, 115.7, 112.0, 108.2, 27.8.

1-(3-Allyl-1H-indol-2-yl)-5-methyl-1H-pyridin-2-one: Prepared by general procedure to

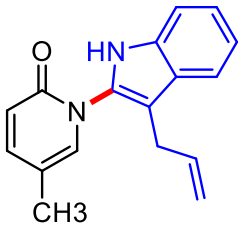

yield **4.05b** as a light yellow solid. **^{1}H NMR** (400 MHz, $CDCl_3$) δ 10.07 (s, 1H), 7.59 – 7.53 (m, 1H), 7.26 (dd, *J* = 9.4, 2.5 Hz, 1H), 7.16 (dt, *J* = 2.1, 1.3 Hz, 1H), 7.09 – 6.99 (m, 3H), 6.52 (d, *J* = 9.3 Hz, 1H), 6.03 (ddt, *J* = 17.1, 10.0, 6.0 Hz, 1H), 5.11 – 5.04 (m, 2H), 3.44 (dt, *J* = 6.0, 1.7 Hz, 2H), 2.10 (s, 3H); **^{13}C NMR** (101 MHz, $CDCl_3$) δ 162.4, 143.6, 136.4, 136.3, 134.2, 131.3, 126.7, 122.7, 120.9, 119.5, 119.1, 115.5, 115.4, 111.7, 106.8, 28.1, 16.9.

1-(3-Allyl-1H-indol-2-yl)-5-bromo-1H-pyridin-2-one: Prepared by general procedure to

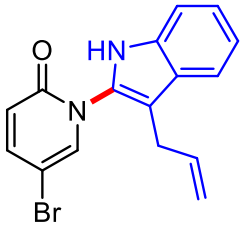

yield **4.05c** as a light brown solid. **^{1}H NMR** (400 MHz, DMSO-d_6) δ 11.56 (s, 1H), 7.97 (d, *J* = 2.7 Hz, 1H), 7.68 (dd, *J* = 9.8, 2.8 Hz, 1H), 7.57 (d, *J* = 7.9 Hz, 1H), 7.37 (d, *J* = 8.1 Hz, 1H), 7.19 (ddd, *J* = 8.2, 7.0, 1.2 Hz, 1H), 7.07 (ddd, *J* = 8.0, 7.0, 1.0 Hz, 1H), 6.54 (d, *J* = 9.8 Hz, 1H), 5.88 (ddt, *J* = 16.5, 10.0, 6.3 Hz, 1H), 5.04 (dq, *J* = 17.1, 1.8 Hz, 1H), 4.95 (dq, *J* = 10.0, 1.6 Hz, 1H), 3.32 (dt, *J* = 6.4, 1.6 Hz, 2H); **^{13}C NMR** (101 MHz, DMSO) δ 160.6, 144.3, 139.7, 136.8, 134.1, 130.7, 126.8, 122.8, 122.4, 119.6, 119.5, 115.6, 111.9, 107.1, 97.4, 28.0.

1-(3-Allyl-1H-indol-2-yl)-5-nitro-1H-pyridin-2-one: Prepared by general procedure to

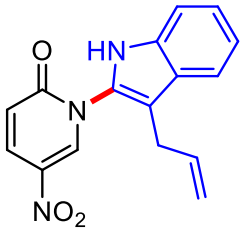

yield **4.05d** as a light yellow solid. **^{1}H NMR** (400 MHz, $CDCl_3$) δ 9.15 (s, 1H), 8.69 (d, *J* = 3.1 Hz, 1H), 8.17 (dd, *J* = 10.1, 3.1 Hz, 1H), 7.63 (d, *J* = 7.7 Hz, 1H), 7.20 (dddd, *J* = 15.9, 8.0, 6.3, 1.7 Hz, 3H), 6.64 (d, *J* = 10.1 Hz, 1H), 6.03 (ddt, *J* = 17.1, 10.1, 5.9 Hz, 1H), 5.15 – 5.05 (m, 2H), 3.50 (dt, *J* = 6.0, 1.7 Hz, 2H); **^{13}C NMR** (101 MHz, $CDCl_3$) δ 161.6, 140.4, 135.2, 134.2, 134.0, 131.2, 129.2, 126.5, 124.2, 120.5, 120.2, 119.8, 116.6, 111.6, 108. 6, 28.0.

3-[3-(2-Methyl-allyl)-1H-indol-2-yl]-3H-quinazolin-4-one: Prepared by general

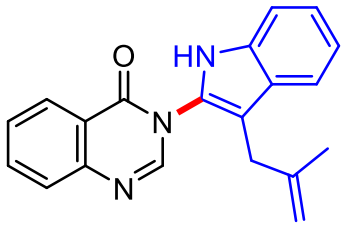

procedure to yield **4.03x** as a white solid. **^{1}H NMR** (400 MHz, $CDCl_3$) δ 9.16 (s, 1H), 8.22 – 8.10 (m, 2H), 7.83 – 7.70 (m, 2H), 7.64 (dd, *J* = 6.9, 2.1 Hz, 1H), 7.50 – 7.41 (m, 1H), 7.25 – 7.09 (m, 3H), 4.80 (s, 1H), 4.69 (s, 1H), 3.43 (s, 2H), 1.77 (s, 3H); **^{13}C NMR** (101 MHz, $CDCl_3$) δ 161.3, 147.5, 146.2, 143.5, 135.0, 134.4, 128.0, 127.8, 127.7, 127.0, 126.8, 123.5, 121.7, 120.1, 119.9, 111.9, 111.5, 109.0, 32.0, 22.6.

3-(3-But-3-enyl-1H-indol-2-yl)-3H-quinazolin-4-one: Prepared by general procedure to yield **4.03j** as a light yellow solid. 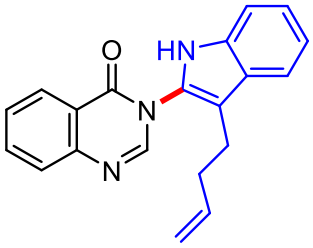 **^{1}H NMR** (400 MHz, $CDCl_3$) δ 9.01 (s, 1H), 8.15 (ddd, *J* = 8.0, 1.5, 0.6 Hz, 1H), 8.12 (s, 1H), 7.78 (ddd, *J* = 8.4, 6.9, 1.5 Hz, 1H), 7.75 – 7.71 (m, 1H), 7.68 (ddt, *J* = 5.9, 3.1, 0.8 Hz, 1H), 7.44 (ddd, *J* = 8.2, 6.9, 1.5 Hz, 1H), 7.21 – 7.15 (m, 2H), 7.13 – 7.08 (m, 1H), 5.83 (ddt, *J* = 16.9, 10.2, 6.7 Hz, 1H), 5.05 – 4.92 (m, 2H), 2.86 – 2.75 (m, 2H), 2.45 (tdt, *J* = 7.9, 6.6, 1.4 Hz, 2H); **^{13}C NMR** (101 MHz, $CDCl_3$) δ 161.5, 147.6, 146.4, 137.7, 135.1, 135.0, 134.5, 127.9, 127.7, 127.0, 126.8, 126.6, 123.5, 121.7, 120.0, 119.5, 115.5, 111.6, 34.1, 23.3.

[2-(4-Oxo-4H-quinazolin-3-yl)-1H-indol-3-yl]-acetonitrile: Prepared by general procedure to yield **4.03k** as a white solid. 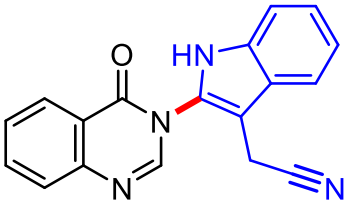 **^{1}H NMR** (400 MHz, DMSO-d_6) δ 11.93 (s, 1H), 8.43 (s, 1H), 8.27 (dd, *J* = 7.9, 1.5 Hz, 1H), 7.95 (ddd, *J* = 8.7, 7.2, 1.6 Hz, 1H), 7.85 – 7.79 (m, 1H), 7.74 (d, *J* = 7.9 Hz, 1H), 7.70 – 7.64 (m, 1H), 7.48 (d, *J* = 8.1 Hz, 1H), 7.30 (ddd, *J* = 8.2, 7.1, 1.2 Hz, 1H), 7.20 (ddd, *J* = 8.3, 7.1, 1.1 Hz, 1H), 4.07 (s, 2H); **^{13}C NMR** (101 MHz, DMSO) δ 160.5, 147.9, 147.4, 135.6, 134.1, 128.9, 128.3, 128.0, 127.1, 125.9, 123.6, 122.2, 120.4, 119.2, 118.8, 112.3, 100.6, 12.3.

[2-(4-Oxo-4H-quinazolin-3-yl)-1H-indol-3-yl]-acetic acid methyl ester: Prepared by general procedure to yield **4.07b** as a white solid. 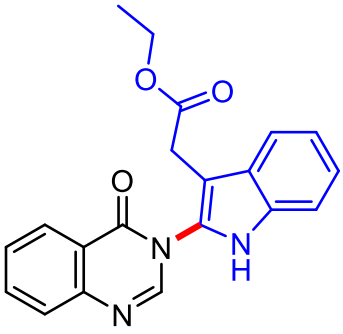 **^{1}H NMR** (400 MHz, Chloroform-*d*) δ 9.50 (s, 1H), 8.32 (s, 1H), 8.08 – 8.04 (m, 1H), 7.74 (ddd, *J* = 8.3, 6.9, 1.5 Hz, 1H), 7.70 (ddd, *J* = 8.1, 1.5, 0.7 Hz, 1H), 7.67 – 7.62 (m, 1H), 7.39 (ddd, *J* = 8.2, 6.9, 1.5 Hz, 1H), 7.21 – 7.12 (m, 2H), 7.07 – 7.03 (m, 1H), 3.71 (s, 2H), 3.66 (s, 3H); **^{13}C**

NMR (101 MHz, $CDCl_3$) δ 171.3, 161.3, 147.2, 146.5, 135.1, 134.2, 128.2, 127.9, 127.6, 126.7, 126.4, 123.8, 121.5, 120.5, 119.2, 111.7, 104.6, 77.4, 77.0, 76.7, 52.3, 29.6.

4.10. References

(1) Mhaske, S. B.; Argade, N. P. The Chemistry of Recently Isolated Naturally Occurring Quinazolinone Alkaloids. *Tetrahedron* **2006**, *62* (42), 9787–9826.

(2) Skaanderup, P. R.; Madsen, R. A Short Synthetic Route to the Calystegine Alkaloids. *J. Org. Chem.* **2003**, *68* (6), 2115–2122.

(3) Sandtorv, A. H. Transition Metal-Catalyzed C-H Activation of Indoles. *Adv. Synth. Catal.* **2015**, *357* (11), 2403–2435.

(4) Quintela, J. M.; Peinador, C.; Veiga, M. C.; Botana, L. M.; Alfonso, A.; Riguera, R. Synthesis, Antihistaminic and Cytotoxic Activity of Pyridothieno- and Pyridodithienotriazines. *Eur. J. Med. Chem.* **1998**, *33* (11), 887–897.

(5) Shi, J.; Zhou, B.; Yang, Y.; Li, Y. Rhodium-Catalyzed Regioselective Amidation of Indoles with Sulfonyl Azides via C–H Bond Activation. *Org. Biomol. Chem.* **2012**, *10* (45), 8953.

(6) Shi, J.; Zhao, G.; Wang, X.; Xu, H. E.; Yi, W. Rhodium(<scp>iii</Scp>)-Catalyzed Regioselective C2-Amidation of Indoles with N-(2,4,6-Trichlorobenzoyloxy)Amides and Its Synthetic Application to the Development of a Novel Potential PPARγ Modulator. *Org. Biomol. Chem.* **2014**, *12* (35), 6831–6836.

(7) Sun, B.; Yoshino, T.; Matsunaga, S.; Kanai, M. Air-Stable Carbonyl(Pentamethyl-cyclopentadienyl)Cobalt Diiodide Complex as a Precursor for Cationic (Pentamethyl-cyclopentadienyl)Cobalt(Iii) Catalysis: Application for Directed C-2 Selective C-H Amidation of Indoles. *Adv. Synth. Catal.* **2014**, *356* (7), 1491–1495.

(8) Sun, B.; Yoshino, T.; Matsunaga, S.; Kanai, M. A Cp*CoI 2 -Dimer as a Precursor for Cationic Co(Iii)-Catalysis: Application to C–H Phosphoramidation of Indoles. *Chem. Commun.* **2015**, *51* (22), 4659–4661.

(9) Mei, R.; Loup, J.; Ackermann, L. Oxazolinyl-Assisted C–H Amidation by Cobalt(III) Catalysis. *ACS Catal.* **2016**, *6* (2), 793–797.

(10) Kumar, A. S.; Amulya Rao, P. V.; Nagarajan, R. Synthesis of Pyrido[2,3-b]Indoles and Pyrimidoindoles via Pd-Catalyzed Amidation and Cyclization. *Org. Biomol. Chem.* **2012**, *10* (26), 5084.

(11) Kumar, A. S.; Nagarajan, R. Synthesis of α-Carbolines via Pd-Catalyzed Amidation and Vilsmeier−Haack Reaction of 3-Acetyl-2-Chloroindoles. *Org. Lett.* **2011**, *13* (6), 1398–1401.

(12) Vemula, S. R.; Kumar, D.; Cook, G. R. Palladium-Catalyzed Allylic Amidation with N-Heterocycles via Sp^3 C-H Oxidation. *ACS Catal.* **2016**, *6* (8).

(13) Trost, B. M.; Mahapatra, S.; Hansen, M. Palladium-Catalyzed C-H Activation of N-Allyl Imines: Regioselective Allylic Alkylations to Deliver Substituted Aza-1,3-Dienes. *Angew. Chemie Int. Ed.* **2015**, *54* (20), 6032–6036.

(14) Xue, N.; Guo, R.; Tu, X.; Luo, W.; Deng, W.; Xiang, J. Efficient Synthesis of Vinyl Sulfones by Manganese-Catalyzed Decarboxylative Coupling of Cinnamic Acids with Aromatic Sulfinic Acid Sodium Salts. *Synlett* **2016**, *27* (19), 2695–2698.

(15) Jiao, L.; Bach, T. Palladium-Catalyzed Direct 2-Alkylation of Indoles by Norbornene-Mediated Regioselective Cascade C–H Activation. *J. Am. Chem. Soc.* **2011**, *133* (33), 12990–12993.

(16) Jiao, L.; Herdtweck, E.; Bach, T. Pd(II)-Catalyzed Regioselective 2-Alkylation of Indoles via a Norbornene-Mediated C–H Activation: Mechanism and Applications. *J. Am. Chem. Soc.* **2012**, *134* (35), 14563–14572.

(17) Gandeepan, P.; Cheng, C. H. Pd-Catalyzed π-Chelation Assisted Ortho-C-H Activation and Annulation of Allylarenes with Internal Alkynes. *Org. Lett.* **2013**, *15* (9), 2084–2087.

(18) Minami, Y.; Yamada, K.; Hiyama, T. Palladium-Catalyzed Hydrobenzylation of Ortho -Tolyl Alkynyl Ethers by Benzylic C□H Activation: Remarkable Alkynoxy-Directing Effect. *Angew. Chemie Int. Ed.* **2013**, *52* (40), 10611–10615.

(19) Iitsuka, T.; Hirano, K.; Satoh, T.; Miura, M. Rhodium-Catalyzed Annulative Coupling of 3-Phenylthiophenes with Alkynes Involving Double C-H Bond Cleavages. *Chem. - A Eur. J.* **2014**, *20* (2), 385–389.

(20) Du, B.; Jiang, X.; Sun, P. Palladium-Catalyzed Highly Selective Ortho -Halogenation (I, Br, Cl) of Arylnitriles via Sp 2 C–H Bond Activation Using Cyano as Directing Group. *J. Org. Chem.* **2013**, *78* (6), 2786–2791.

(21) Gandeepan, P.; Cheng, C.-H. Transition-Metal-Catalyzed π-Bond-Assisted C□H Bond Functionalization: An Emerging Trend in Organic Synthesis. *Chem. - An Asian J.* **2015**, *10* (4), 824–838.

(22) Li, Q.; Yu, Z.-X. Conjugated Diene-Assisted Allylic C−H Bond Activation: Cationic Rh(I)-Catalyzed Syntheses of Polysubstituted Tetrahydropyrroles, Tetrahydrofurans, and Cyclopentanes from Ene-2-Dienes. *J. Am. Chem. Soc.* **2010**, *132* (13), 4542–4543.

(23) Gandeepan, P.; Cheng, C.-H. Allylic Carbon–Carbon Double Bond Directed Pd-Catalyzed Oxidative Ortho -Olefination of Arenes. *J. Am. Chem. Soc.* **2012**, *134* (13), 5738–5741.

(24) Sambiagio, C.; Schönbauer, D.; Blieck, R.; Dao-Huy, T.; Pototschnig, G.; Schaaf, P.; Wiesinger, T.; Zia, M. F.; Wencel-Delord, J.; Besset, T.; et al. A Comprehensive Overview of Directing Groups Applied in Metal-Catalysed C–H Functionalisation Chemistry. *Chem. Soc. Rev.* **2018**, *47* (17), 6603–6743.

(25) Gómez-Gallego, M.; Sierra, M. A. Kinetic Isotope Effects in the Study of Organometallic Reaction Mechanisms. *Chem. Rev.* **2011**, *111* (8), 4857–4963.

(26) Kimura, M.; Tomizawa, T.; Horino, Y.; Tanaka, S.; Tamaru, Y. Et3B–Pd-Promoted Allylation of Benzaldehyde with Allylic Alcohols. *Tetrahedron Lett.* **2000**, *41* (19), 3627–3629.

(27) Kimura, M.; Futamata, M.; Mukai, R.; Tamaru, Y. Pd-Catalyzed C3-Selective Allylation of Indoles with Allyl Alcohols Promoted by Triethylborane. *J. Am. Chem. Soc.* **2005**, *127* (13), 4592–4593.

(28) Daniels, B. E.; Ni, J.; Reisman, S. E. Synthesis of Enantioenriched Indolines by a Conjugate Addition/Asymmetric Protonation/Aza-Prins Cascade Reaction. *Angew. Chemie Int. Ed.* **2016**, *55* (10), 3398–3402.

CHAPTER 5. CHEMO- AND REGIO-SELECTIVE C-H/N-H BOND FUNCTIONALIZATION OF 2-STYRYL QUINAZOLIN-4(3H)-ONES: EN ROUTE TO 2-AMINO PYRIDINES

Carbocyclic/heterocyclic fused 3*H*-quinazolin-4-one ring is regarded as a "privileged structure" owing to its diverse biological activities of naturally occurring alkaloids (Figure 5.1). [1,2] With a wide spectrum of biological properties like antibacterial, antifungal, anticonvulsant, anti-inflammatory and anti-HIV to name a few,[3–10] development of convenient methods for their synthetic analogue rapid syntheses is highly desirable. The general and well explored method for the synthesis of tricyclic pyrido-fused quinazolinones involves the lactamization of 2-(pyridin-2-ylamino)benzoic acid.[11,12] However, the traditional synthetic route required multiple steps, transition metal catalyzed C-H bond functionalizations become an alternative and have partially circumvented the existing shortcomings. Especially directed C-H/N-H bond functionalizations followed by alkyne annulation is a more direct way for the synthesis of fused quinazolinones.

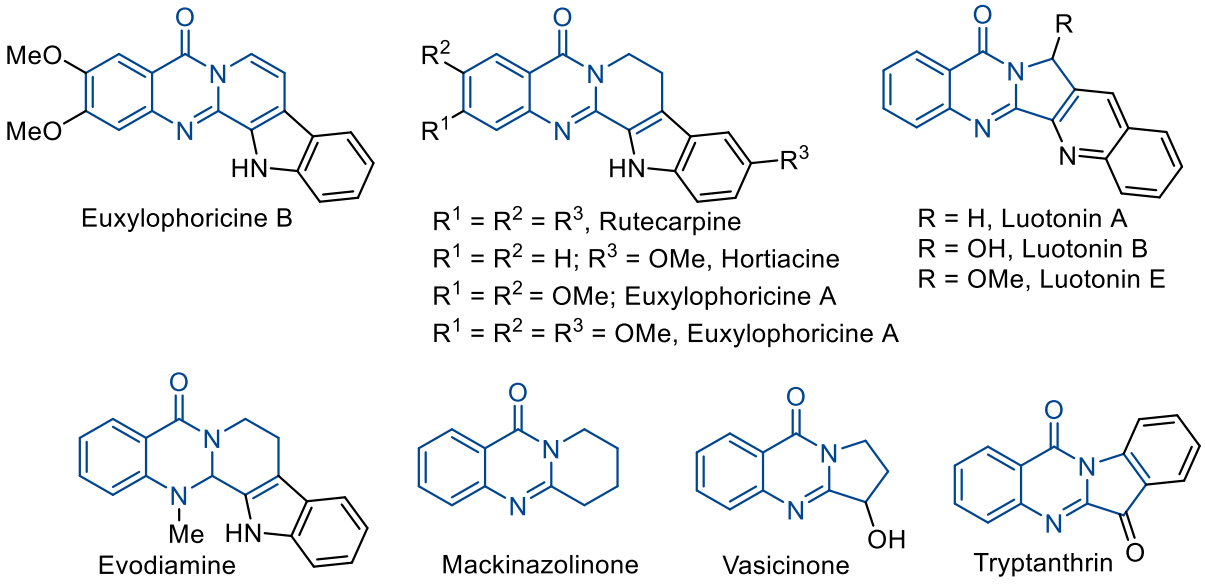

Figure 5.1: Representative examples of naturally occurring biologically active fused quinazolin-4(3H)-ones

5.1. Transition metal catalyzed C-H/N-H functionalization/oxidative annulation

Transition metal catalysts derived from Rh, Ru, Ni, and Pd etc. have been reported for functionalization/annulation of aromatic sp^2 C−H bonds with alkynes, alkenes, and other unsaturated molecules in the presence of an oxidant for generation of carbocycles/heterocycles. [13–16] Pioneering work in this area revealed that rhodium complexes enabled effective annulation reactions of alkynes through chelation assisted chemo- and regioselective functionalization of both C-H and N-H bonds. A variety of directing groups have been successfully employed for various Rh mediated annulation processes which included, but were not limited to, carboxylic acid, phenolic hydroxyl, imine, oxime, benzamide, hydroxamic acid, amide, acetanilide, enamine, azide and heterocycles such as imidazole, indole, pyridine etc.[15] The high cost of the required rhodium (III) catalyst was identified as one of the major limitations of this approach. In contrast, significantly less expensive ruthenium (II) complexes were shown as viable catalysts for oxidative alkyne annulations. The success of ruthenium (II) catalysis was attributed to their facile transformation into cyclometallated species via C−H bond cleavage, their compatibility with currently used oxidants, and stability to both air and water.[17–19]

After the pioneering work from Ackerman and coworkers on the utilization of low cost Ru-catalysts for the synthesis of fused indole derivatives.[20] There has been immense interest in the utilization of Ru-catalysts for effective C-H/N-H functionalization/annulation reactions. Li and coworkers utilized the similar protocol for the synthesis of fused quinazolinones *via* an oxidative annulation aromatic C-H bond/quinoline amide C-H bond functionalization (Scheme 5.1).[21]

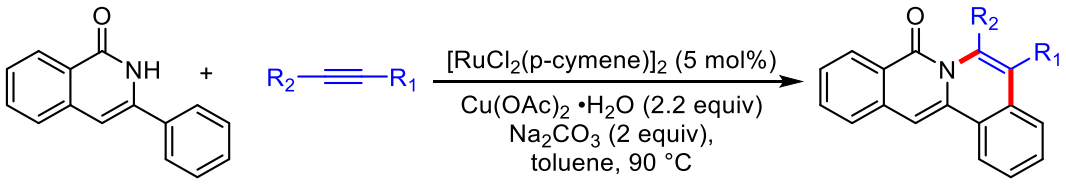

Scheme 5.1: Fused quinolizinone synthesis *via* Ru-catalyzed oxidative annulation

5.2. Oxidative annulation of 2-styrylquinazolinones

While great advances in C-H functionalization/annulation, have been made, the ability to selectively functionalized olefinic C-H bonds in presence of others competitive sp^2 C-H (olefinic/arene) bonds without specific directing groups remains a challenge.[22–30] With our interest in functionalizing quinazoline core for the synthesis of biologically active compounds, we sought to explore oxidative annulation of 2-styryl quinazolinones.[31–34] This is particularly challenging because of multiple competitive sp^2 C-H bonds and tautomerizable X-H (X = N/O) bonds (Figure 5.2).

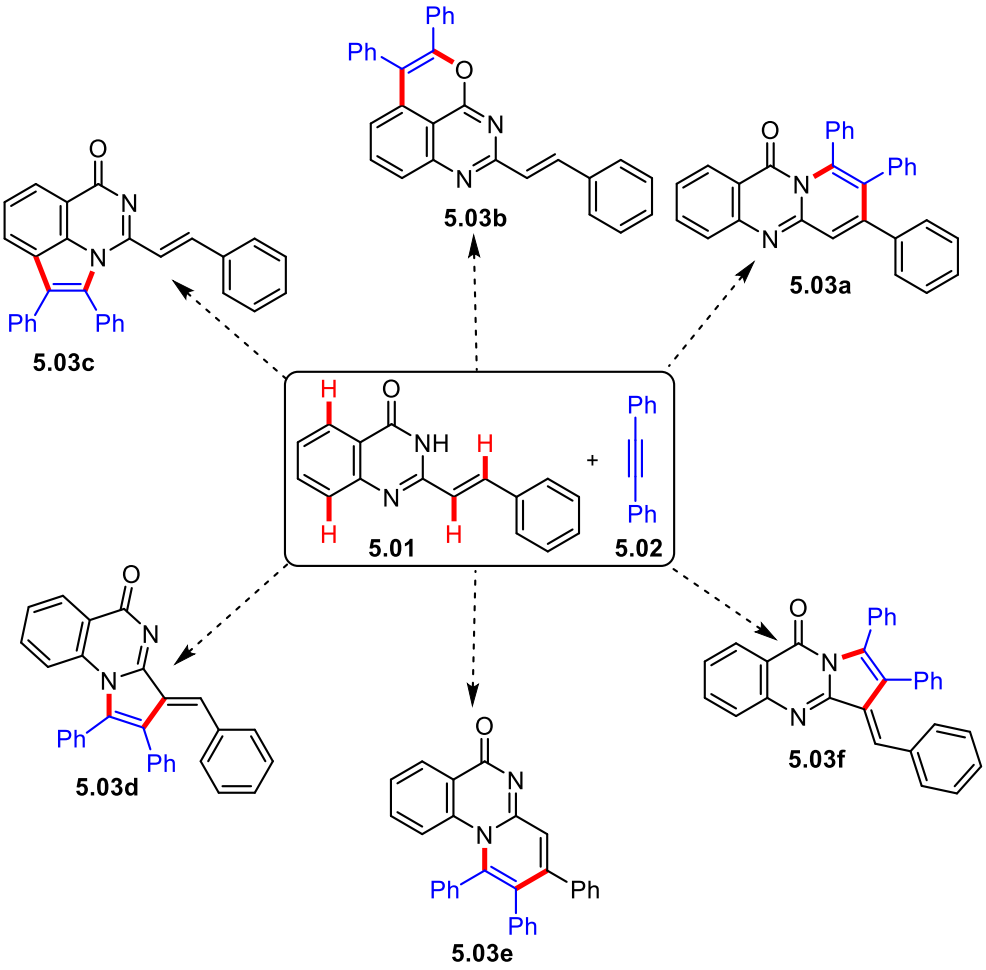

Figure 5.2: Possible products formed by oxidative annulation of 2-styryl quinazolinones.

5.3. Initial observation of fused quinazolinone *via* C-H/N-H functionalization

To investigate the oxidative annulation reaction of 2-styryl quinazolinones with alkynes, a reaction of **5.01a** with diphenyl acetylene **5.02** with different Ru catalysts in DMF was performed using silver acetate as an oxidant. To our delight, $[RuCl_2(p\text{-cymene})]_2$ and $[Ru(COD)Cl_2]_n$ was found effective yielding only cyclized product **5.03a** from vinylic C-H bond and amide N-H functionalization (Entry 3 and 4, Table 5.1).

Table 5.1: Investigation of ruthenium catalysts for the oxidative annulation of 2-styryl quinazolinone

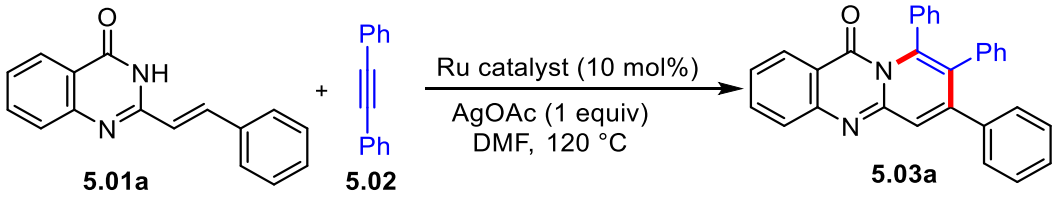

Entry	Catalyst	Yield (%)[a]
1	$[Rh(C_2H_4)_2Cl]_2$	0[b]
2	$RuCl_3 \cdot xH_2O$	0[b]
3	$[Ru(COD)Cl_2]_n$	21
4	$[Ru(p\text{-cymene})Cl_2]_2$	35
5	$Ru(Me\text{-}allyl)_2(cod)$	traces
6	$Ru_3(CO)_{12}$	traces
7	$RuH_2(CO)(PPh_3)_3$	0[b]
8	$Tris(1,10\text{-}Phen)RuCl_2.xH_2O$	0[b]

Reaction conditions: 5.01a (0.12 mmol) was treated with **5.02** (0.18 mmol, 1.5 equiv) in presence of Ru catalysts (10 mol%) and AgOAc (1 equiv) in DMF (1 mL). [a]Isolated yield of **5.03a**.[b]Starting **5.01a** was found intact. [e]Isolated yield of **3e** in parentheses when reactions were conducted in the presence of 1 equiv AgOAc.

5.4. Investigation of solvent effects on the oxidative annulation

Delighted by the effectiveness of the [Ru(*p*-cymene)Cl_2]$_2$ for the selective formation of annulated product **5.03a** in appreciable yields led us to further investigate the optimized conditions. An elaborative screening of solvents indicated the effectiveness of ethereal solvents, with 1,4-dioxane being the best yielding the product in 46% yield (Entry 6, Table 5.2)

Table 5.2: Effect of solvents on the selective C-H bond functionalization/annulation of **5.01a** with **5.02** in presence of [Ru(*p*-cymene)Cl_2]$_2$

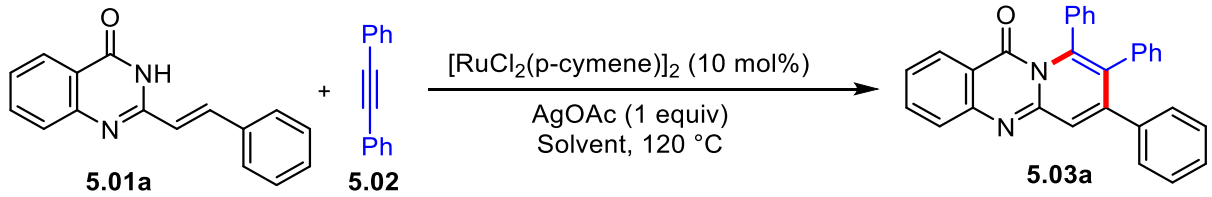

Entry	Solvent	Yield (%)[a]
1	EtOH	26
2	^{i}-PrOH	20
3	^{t}-BuOH	15
4	^{t}-Amyl-OH	10
5	PhMe	26
6	1,4-Dioxane	46
7	THF	24
8	DCE	28
9	MeCN	25
10	DME	26
11	DMF	32
12	DMSO	10
13	DMC	21
14	$MeNO_2$	22

Reaction conditions: 5.01a (0.12 mmol) was treated with **5.02** (0.18 mmol, 1.5 equiv) in presence of [Ru(*p*-cymene)Cl_2]$_2$ (10 mol%) and AgOAc (1 equiv) in different solvents (1 mL) at 120 °C for 24 h. [a]Isolated yield of **5.03a**.

5.5. Investigation of oxidant effects on the oxidative annulation

Given the fact that the reactions were oxidative in nature, we also examined various oxidants for the cyclization of 2-styryl quinazolinones with alkynes. Most of the inorganic oxidants screened were found to be effective yielding the product in respectable yield. Organic oxidants, on the other hand were found inferior in the oxidative annulation (Entry 9-12, Table 5.03). When a combination of two different metal oxidants (AgOAc and $Cu(OAc)_2 \cdot xH_2O$) were used in the reaction mixture, the yields of the cyclized product improved (Entry 13 and 14, Table 5.3)

Table 5.3: Effect of oxidants on the selective C-H bond functionalization/annulation of **5.01a** with **5.02** in the presence of $[Ru(p\text{-cymene})Cl_2]_2$ in dioxane

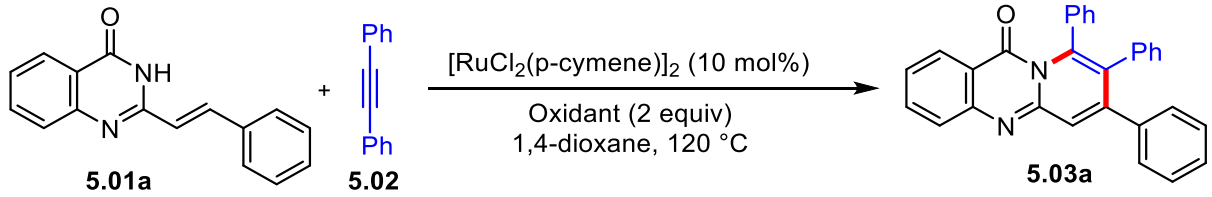

Entry	Oxidant	Yield (%)[a]
1	$AgBF_4$	30
2	$AgClO_4$	32
3	AgOTf	35
4	$AgCO_3$	38
5	$AgSbF_6$	40
6	AgOAc	42
7	$Cu(OAc)_2.xH_2O$	30
8	$CuSO_4.5H_2O$	31
9	Methyl-*p*-benzoquinone	15
10	2,6-Dimethylbenzoquinone	28
11	2,6-tert-Butyl-1,4-benzoquinone	22
12	Duroquinone	26
13	AgOAc : $Cu(OAc)_2.xH_2O$ (1:1)[b]	58
14	AgOAc : $CuSO_4.5H_2O$ (1:1)[b]	45

Reaction conditions: 5.01a (0.12 mmol) was treated with **5.02** (0.18 mmol, 1.5 equiv) in presence of $[Ru(p\text{-cymene})Cl_2]_2$ (10 mol%) and different oxidants (2 equiv) in dioxane (1 mL) at 120 °C for 24 h. [a]Isolated yield of **3e**. [b]Combination of oxidants as 1 :1 (1 equiv each).

5.6. Investigation of effects of acids/bases on the oxidative annulation

Addition of acid or base additives were found to be effective in activating transition metal catalyst for the deprotonation of C-H bond.[35] So, we screened different bases and acids for the cyclization reaction. From our previous studies, we found that addition of bases to the quinazolinone core inhibits the reactivity, not surprisingly addition of bases inhibited the oxidative annulation reaction of 2-styryl quinazolinones with alkynes (Entry 1-7, Table 5.4). On the contrary, addition of acids enhanced the reactivity forming product in increased yields (Entry 8 and 9, Table 5.4), with trifluoroacetic acid being the best.

Table 5.4: Effect of acids and bases on oxidative annulation of **5.01a** with **5.02** in presence of $[Ru(p\text{-cymene})Cl_2]_2$ in 1,4-dioxane

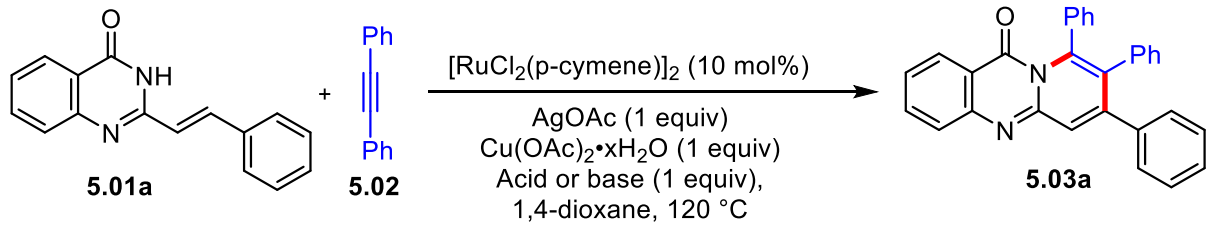

Entry	Base/Acid	Yield (%)[a]
1	K_2CO_3	12
2	Na_2CO_3	14
3	K^{t}-OBu	15
4	$LiNH_2$	10
5	DBU	13
6	DMAP	10
7	TEA	11
8	AcOH	65
9	TFA	76

Reaction conditions: 5.01a (0.12 mmol) was treated with **5.02** (0.18 mmol, 1.5 equiv) in presence of $[Ru(p\text{-cymene})Cl_2]_2$ (10 mol%) and AgOAc (1 equiv) in DMF (1 mL) in presence of different bases and acids (1 equiv) at 120 °C for 24 h. [a]Isolated yield of **3a**.

Further screening of the reaction conditions with respect to the amounts of alkyne, oxidants and catalyst loading gave the optimized condition to be the use of 5 mol% [Ru(*p*-cymene)Cl_2]$_2$, 20 mol% of AgOAc, 1 equiv each of Cu(OAc)$_2$·xH_2O and TFA in dioxane at 100 °C gave the product in 76% yield (Scheme 5.2).

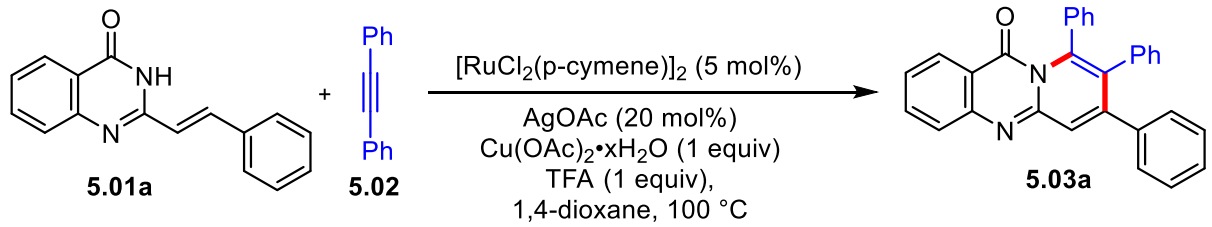

Scheme 5.2: Optimized reaction conditions for oxidative annulation of 2-styryl quinazolinones

5.7. Optimization and importance of each of reaction components

A series of control experiments was performed. In the absence of any one of the reaction components, either reduced yields or no conversion was observed (Table 5.5). These results show that the Ru-catalyst ([Ru(*p*-cymene)Cl_2]$_2$), AgOAc, Cu(OAc)$_2$.xH_2O, and TFA are all essential for the optimal reaction conditions.

Table 5.5: Control experiments

Entry	Ru-catalyst (5 mol%)	AgOAc (20 mol%)	Cu(OAc)$_2$.xH_2O (1 equiv)	TFA (1 equiv)	Yield (%)[a]
1	+	+	+	+	63
2	+	+	+	-	46
3	+	+	-	-	11
5	+	-	-	-	traces
9	-	-	-	-	0
6	-	+	+	+	0

Reaction conditions: 5.01a (35 mg, 0.12 mmol) was treated with **5.02** (32 mg, 0.18 mmol, 1.5 equiv) under different reaction conditions in 1,4-dioxane (1 mL, 1 : 0.4) at 100 °C for 24 h. [a]Isolated yield of **5.03a**

5.8. Mechanistic investigation of Ru-catalyzed oxidative annulation

Assuming a heteroatom directed C-H activation, four different sp^2 C-H bonds would be accessible for insertion by the catalyst and because of the tautomeric equilibrium at least six different annulated products could result (Figure 5.2). Exclusive formation of **5.03a,** considering the number of possible reaction pathways the was unexpected but gratifying.

5.8.1. Deuterium incorporation and KIE studies under reaction conditions

5.8.1.1. Deuterium incorporation

To gain mechanistic insight, the incorporation of deuterium into the substrate and product was examined. When the quinazolinone **5.01b** was subjected to the reaction conditions in the absence of alkyne but with D_2O present, deuterium was found largely at the observed site of reactivity H_d (70%) with a trace of incorporation at H_c (10%). No deuterium was observed at H_a or H_b, indicating the possibility of a reversible C-H activation/metal insertion. We believe that deuteration proceeds by an acetate-assisted C-H activation by Ru(II)-complexes to generate a ruthenacycle intermediate followed by its deuteriolysis to give the deuteration product. When alkyne **5.02** was added to the reaction mixture containing D_2O, annulation proceeded with essentially no incorporation of deuterium, suggesting a 5-membered ruthenacycle intermediate resulting from N-H and C-H bond insertion was likely (Scheme 5.3). It should also be noted that, with two exceptions, all ruthenium-catalyzed alkyne oxidative annulations reported to date involve initial cyclometallation to form five-membered ruthenacycles.[36,37]

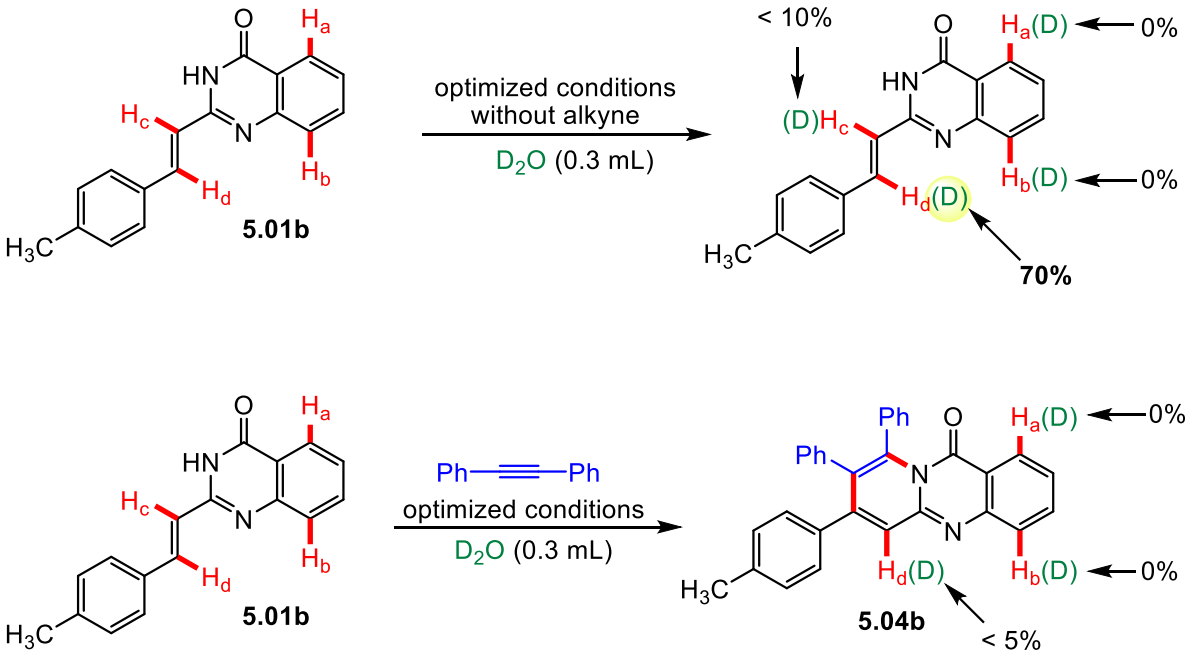

Scheme 5.3: Incorporation of deuterium in the presence or absence of alkyne

5.8.1.2. KIE studies for Ru-catalyzed oxidative annulation

Parallel but independent reactions using **5.01a** and **[D$_6$]- 5.01a** revealed a significant kinetic isotope effect ($k_H/k_D \approx 3$) suggesting C-H insertion as the rate determining step. To further validate the rate determining step, an intermolecular kinetic isotope effect experiment was investigated between **5.01a** + **[D$_6$]- 5.01a** (1:1) and **5.02**, the obtained KIE value ($P_H/P_D \approx 3.2$) concluded the C-H insertion as the rate determining step (Scheme 5.4). A KIE of this magnitude is in good agreement with a concerted acetate-assisted metalation transition state.[38,39]

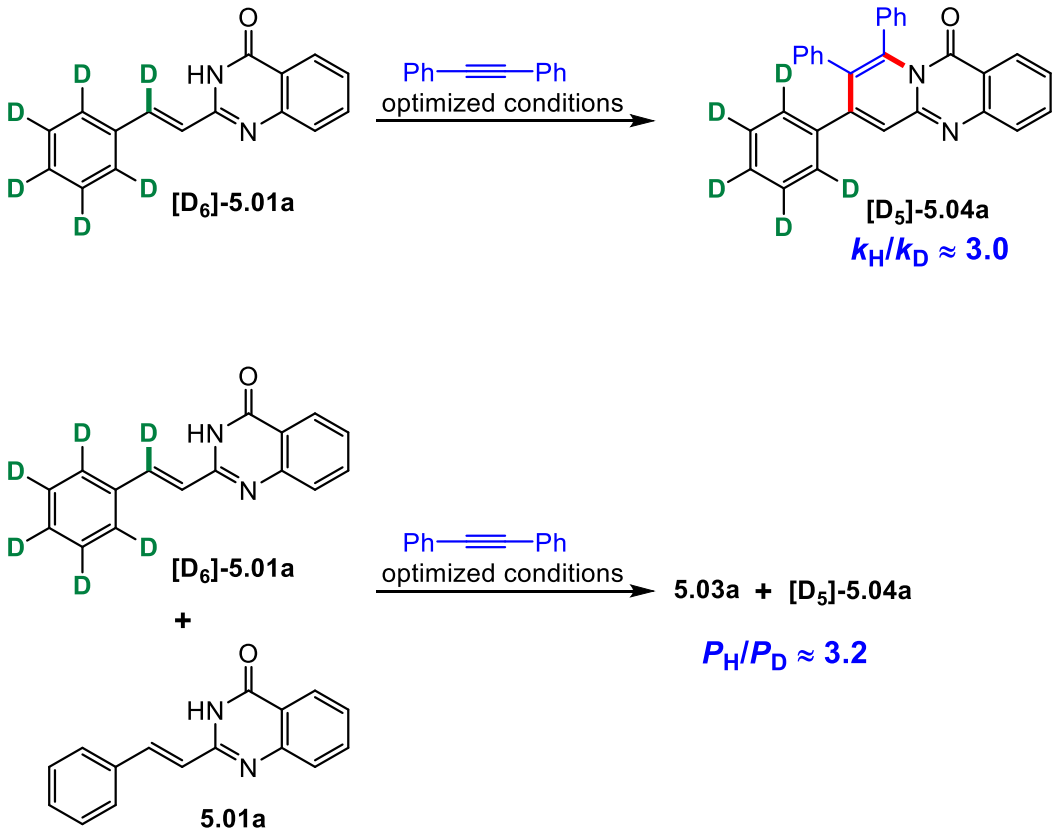

Scheme 5.4: Kinetic isotopic effect studies of the oxidative annulation reactions

5.8.2. Catalytic cycle and control studies

To investigate the effect or importance of extended π-conjugation, and whether larger ruthenacycle could be formed, quinazolinone **5.05** bearing an extended diene was subjected to the optimized reaction conditions in presence of alkyne **5.02** to produce only **5.06** (Scheme 5.5). In addition, when aliphatic olefin **5.07** was reacted under optimized conditions also produced cyclized product **5.08** in good yield, suggesting that the lability of the C-H due to extended conjugation was not critical.[40,41]

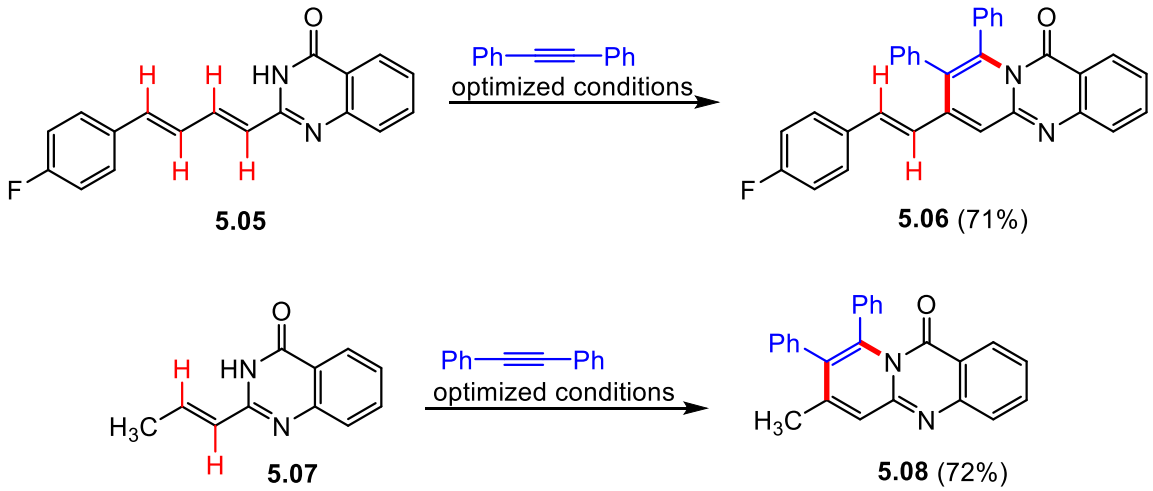

Scheme 5.5: Effect of extended conjugation on oxidative annulation

To further probe the mechanism, we focused our studies on whether the initial attack of alkyne occurs at carbon center or nitrogen center prior to cyclization. Independently we prepared a potential intermediate **5.09** formed by the initial attack of alkyne on amide nitrogen. Under reaction condition, it did not yield any product. This result strongly supports the intermediacy of a 5-membered ruthenacycle complex with initial bond formation at the carbon rather than at nitrogen. We also investigated the importance of the presence of both N-H and C-H bonds for the reaction to proceed. When N-blocked **5.10** (N-Me) or C-blocked **5.11** (C-Me) substrates were subjected to reaction conditions, no reaction occurred indicating the importance of both C-H and N-H bonds (Scheme 5.6).

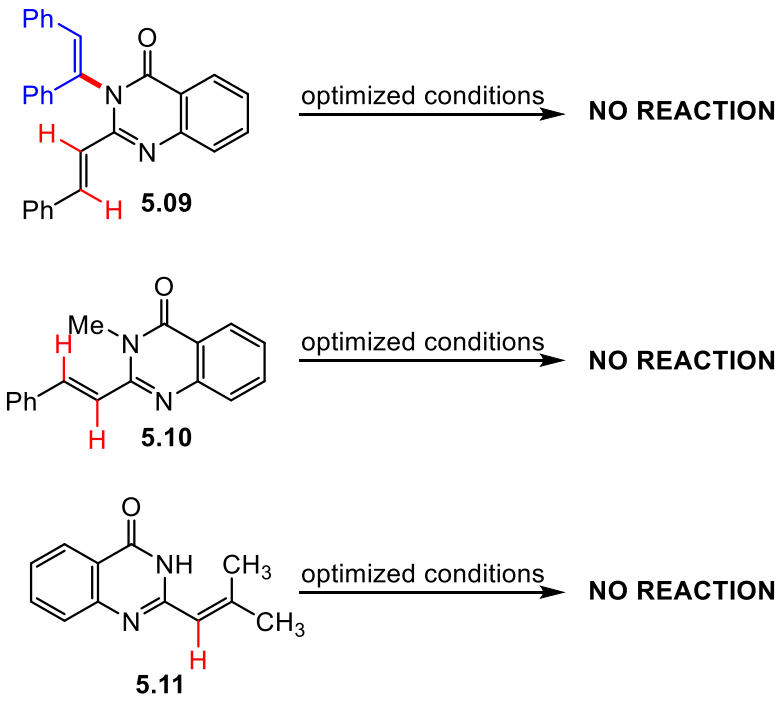

Scheme 5.6: Effect of C-H or N-H blocking on the oxidative annulation

Based on our mechanistic studies and previous literature reports on ruthenium catalyzed C−H activation and functionalization reactions, a catalytic cycle was proposed that accounts for the product formation is shown in Scheme 5.7.[42,43] Initial step of the catalytic cycle being the counter ion exchange between AgOAc and Ru-complex affording the cationic ruthenium acetate species [I]. Subsequent concerted acetate-assisted reversible cycloruthenation via rate determining C-H insertion would lead to the 5-membered ruthenacycle [II] (step A). Alkyne coordination (step B) to the ruthenacycle forms the intermediate [III], which is followed by a migratory insertion (step C) to generate a 7-membered ruthenacycle [IV]. Reductive elimination (step D) with concomitant Cu^{II}-promoted oxidation of Ru(0) back to the Ru^{II} species [I], releases the fused pyrido[2,1-b]quinazolin-11-ones.

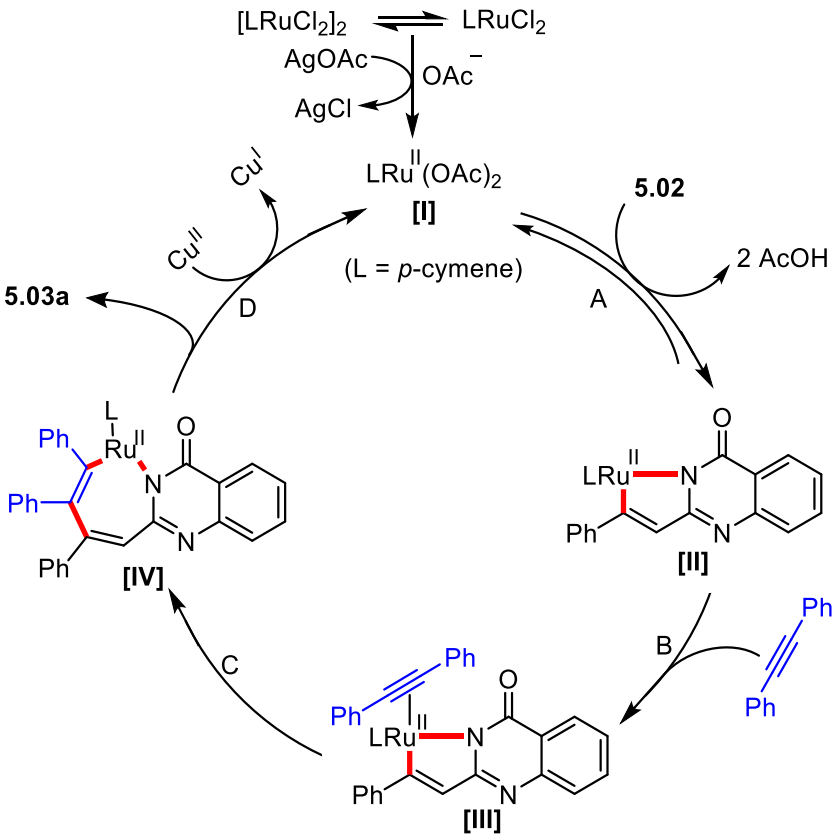

Scheme 5.7: Proposed catalytic cycle

5.9. Substrate scope: synthesis of fused quinazolinones

With the optimized conditions in hand and understanding the mechanism of the reaction, the substrate scope of oxidative annulation was investigated. As depicted in Scheme 5.8, a series of 2-styryl quinazolin-4(3*H*)-ones reacted well with **5.02** to form the analogous products in good yields. A wide range of functional groups (**5.04a** – **5.04k**) were tolerated well validating the robustness of this protocol. Further, vinyl quinazolines bearing heteroaromatic groups (pyridyl **5.04n**, thiophenyl **5.04o**, furyl **5.04p**, and indolyl **5.04q**) and extended alkenes **5.06** reacted smoothly with alkynes demonstrating the utility of the protocol to generate diverse products. A variety of internal alkynes with varied electronics were also compatible with the reaction (–Br **5.04i**, -CF_3 **5.04j**, -OMe **5.04k**, bisthiophene **5.04t**, and dialkyl **5.04u**). Using an unsymmetrical

alkyl-aryl acetylene, product **5.04v** was formed with excellent regioselectivity (89:11) supporting the mechanistic hypothesis that C-C bond formation occurred prior to C-N bond formation (Scheme **5.7**, steps C). In contrast, terminal alkynes were unreactive. Gratifyingly, thio-analogs of alkynes smoothly reacted to from **5.04w** and **5.04x**.

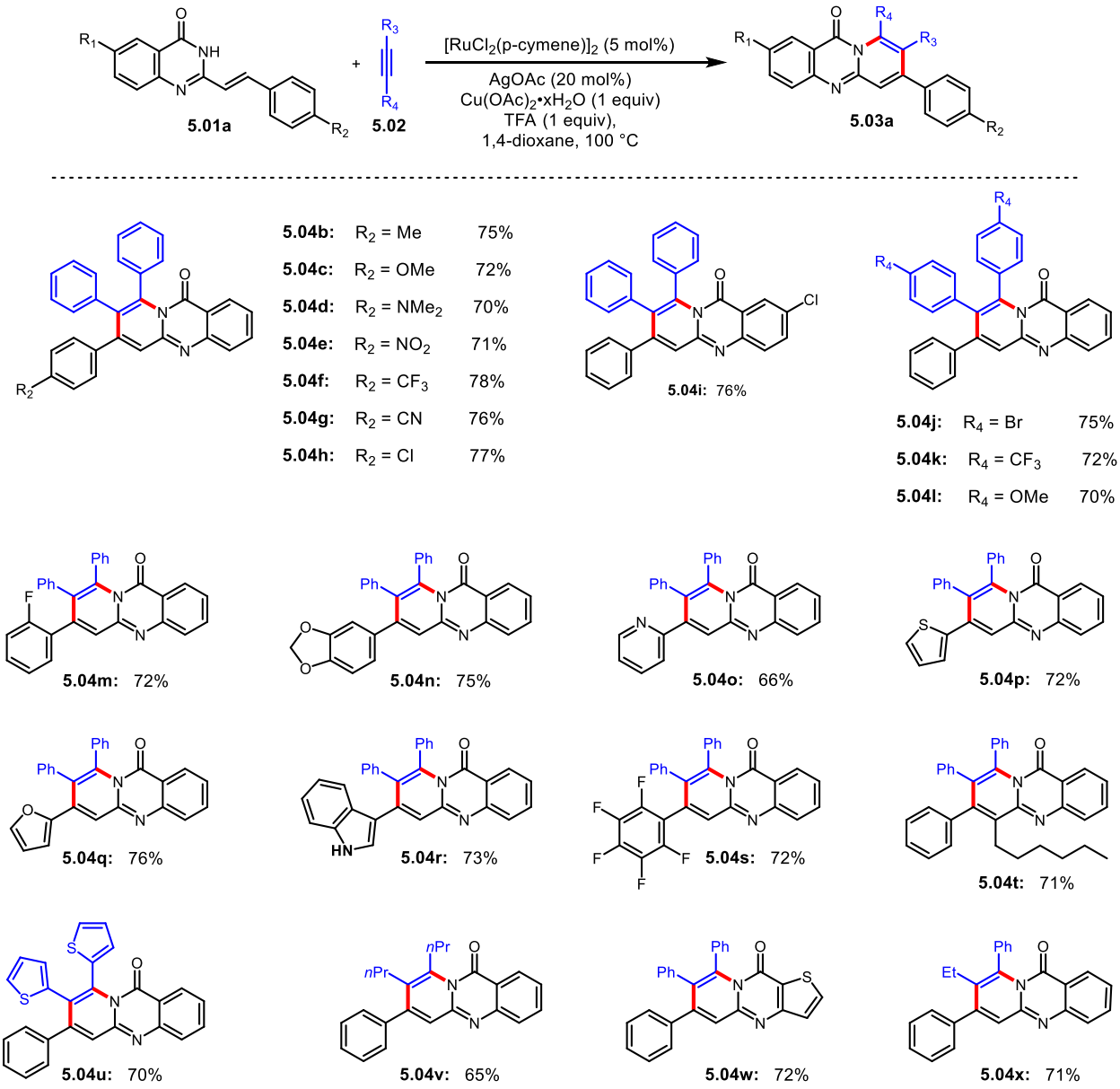

Scheme 5.8: Substrate scope of Ru-catalyzed oxidative annulation of 2-styryl quinazolinones

5.10. Amide alcoholysis/2-amino pyridine synthesis

The cooperative merging of synthetic tools in tandem to achieve more efficient syntheses of high value products is a valuable strategy. We envisioned quinazolinone heterocycles could serve as a template for C-H bond functionalization affording annulated products as a latent pyridine. Upon *in situ* amide alcoholysis, the fused quinazolinone would open to reveal highly substituted 2-aminopyridines (Scheme 5.9)

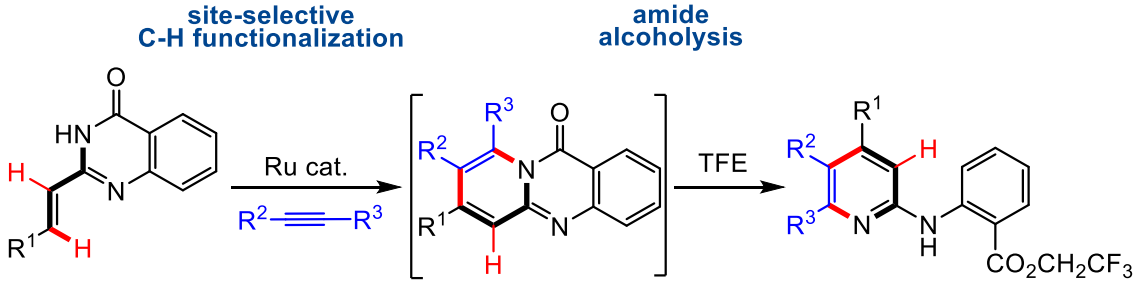

Scheme 5.9: C-H bond functionalization/amide alcoholysis for 2-aminopyridine synthesis

Six-membered nitrogen-containing heterocycles are privileged structures present in many aspects of the physical and biological sciences. They are prevalent in nature, pharmacophores, as well as in supramolecular and organomaterials. The 2-aminopyridyl motif, in particular is an important structural component of pharmaceuticals, agrochemicals, natural products and organic materials.[44–46] As a result, the design and development of general robust methods for the preparation of substituted 2-aminopyridines is highly significant. Classical methods for 2-alkyl/arylaminopyridines rely on the nucleophilic addition and/or aromatic substitution reaction of pyridine derivatives including 2-halopyridines,[47,48] 2-alkoxypyridines,[49] pyridinium,[50] pyridine-*N*-oxides,[51] pyridone,[52] and transition metal-catalyzed aminations[14] (Scheme 5.10). These methods often require multiple synthetic steps for required pyridine precursors, high temperature and overall offer limited functionalized 2-aminopyridines. A general preparation of 2-aminopyridines via the direct construction of the pyridine ring has not been reported.

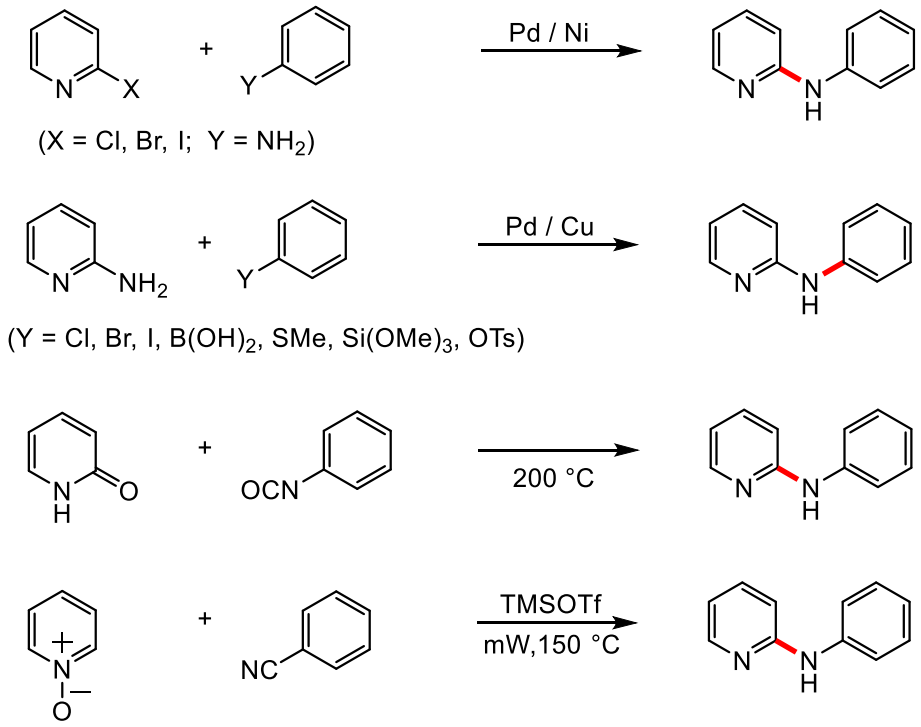

Scheme 5.10: Reported strategies for 2-arylaminopyridine synthesis

To test our hypothesis and evaluate the tandem C-H bond functionalization/amide alcoholysis to access 2-aminopyridines the oxidative alkyne annulation of the diphenylacetylene **5.02** with tautomerizable quinazolinone **5.01a** was investigated as a model reaction. Addition of trifluoroethanol to the optimized reaction conditions of annulation protocol underwent complete conversion yielding desired 2-arylamino pyridine **5.12a** in 66% yield (Scheme 5.11).

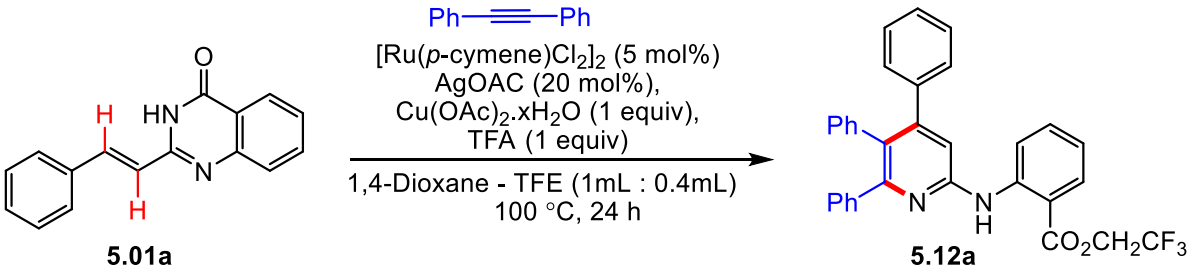

Scheme 5.11: Optimized protocol for *in situ* amide alcoholysis for 2-arylaminopyridine synthesis

5.11. Substrate scope: 2-aminopyridine synthesis

The scope of the tandem annulation/alcoholysis protocol was investigated (Scheme 5.12). A series of 2-styryl quinazolin-4(3*H*)-ones reacted well with alkynes **5.02** to form 2-aminopyridines in moderate to good yields. A wide range of functional groups (-OMe, -NMe_2, -NO_2, -CN, -CF_3, -Cl, -F) were tolerated well validating the robustness of this protocol. Substituent electronics were seemingly not effective in producing 2-aminopyridine derivatives, as both electron donating (**5.12c-e**, Scheme 5.12) or electron withdrawing (**5.12f-j**, Scheme 5.12) produced similar yields. Further, vinyl quinazolinones bearing heteroaromatic groups (furyl **5.12m**, and indolyl **5.12n**) were also reacted smoothly under the optimized conditions. A fully substituted 2-amino-3,4,5,6-functionalized pyridines could also be synthesized using a correspondingly substituted quinazolinone template (**5.12k**) with not much change in the yield. This is important as there are no reports in the literature for the synthesis of fully substituted 2-aminopyridines. Internal alkynes with varied electronics and side chains were also tested and found compatible with the reaction conditions (bisthiophene **5.12o**, -OMe **5.12p**, –Br **5.12q**, and dialkyl **5.12r**). In contrast, terminal alkynes were unreactive for the synthesis of both fused quinazolinones or amino pyridines.

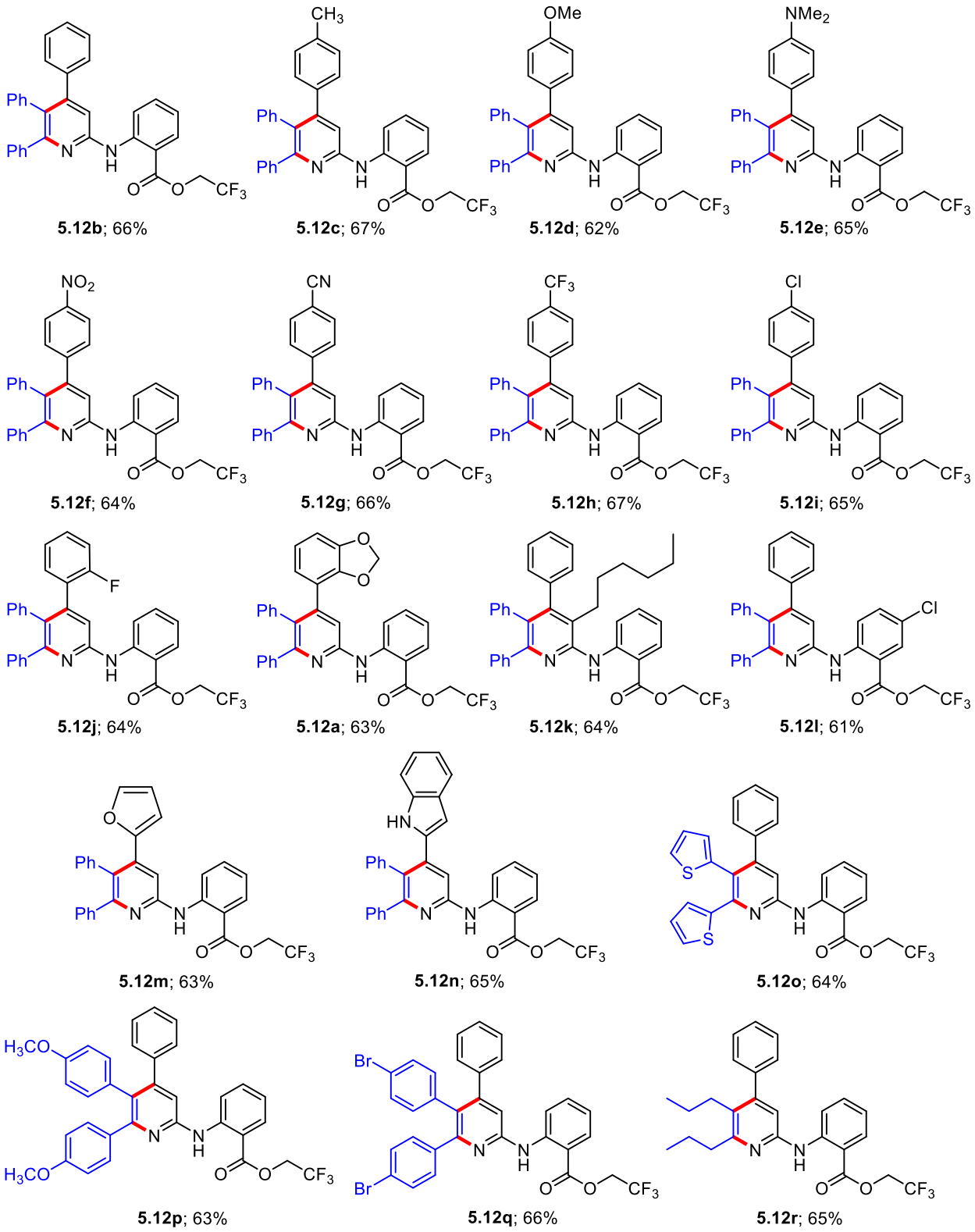

Scheme 5.12: Substrate scope of *in situ* amide alcoholysis *via* C-H functionalization/ annulation

5.12. Conclusion

In conclusion, we reported a novel route to synthesize fused quinazolinone framework via oxidative C-H functionalization/alkyne annulation and synthesis of highly substituted 2-aminopyridines via a tandem oxidative C-H functionalization-annulation followed by amide alcoholysis. Detail mechanistic studies provided insight delineating the origin of the observed chemo- and regioselective C-H/N-H annulation to form pyrido[2,1-b]quinazolin-11-ones.

5.13. Experimental procedures

5.13.1. General information

Unless otherwise noted, all manipulations were carried out under a nitrogen atmosphere using standard Schlenk-line or glovebox techniques. All glassware was oven-dried for at least 1h prior to use. THF, toluene, ether, and hexane were degassed by purging with nitrogen for 45 min and dried with a solvent purification system (MBraun MB-SPS). DMF, dioxane, dimethoxyethane, dichloroethane, methanol, and ethanol were dried over activated 3 Å molecular sieves and degassed by purging with nitrogen. All commercially obtained reagents/solvents were purchased from Alfa Aesar®, Sigma-Aldrich®, Acros®, TCI America®, Mallinckrodt®, and Oakwood® Products, and used as received without further purification. TLC plates were visualized by exposure to ultraviolet light. Organic solutions were concentrated by rotary evaporation at ~10 torr. Flash column chromatography was performed with 32–63 microns silica gel. ^{1}H NMR spectra were obtained on a 400 MHz spectrometer, and chemical shifts were recorded relative to residual protiated solvent. ^{13}C NMR spectra were obtained at 100 MHz, and chemical shifts were recorded to the solvent resonance. Both ^{1}H and ^{13}C NMR chemical shifts were reported in parts per million downfield from tetramethylsilane ($\delta = 0$ ppm). 19F NMR spectra were obtained at 282.4 MHz, and all chemical shifts were reported in parts per million upfield of CF3COOH (δ

= -78.5 ppm). Coupling constants (*J*) are reported in hertz (Hz). Standard abbreviations indicating multiplicity were used as follows: s (singlet), br (broad), d (doublet), t (triplet), q (quartet) and m (multiplet). Data for ^{13}C NMR spectra are reported in terms of chemical shift (δ ppm). High-resolution mass spectra were obtained from a Bruker Daltronics BioTOF HRMS spectrometer.

5.13.2. Representative experimental procedure for synthesis of fused quinazolinones

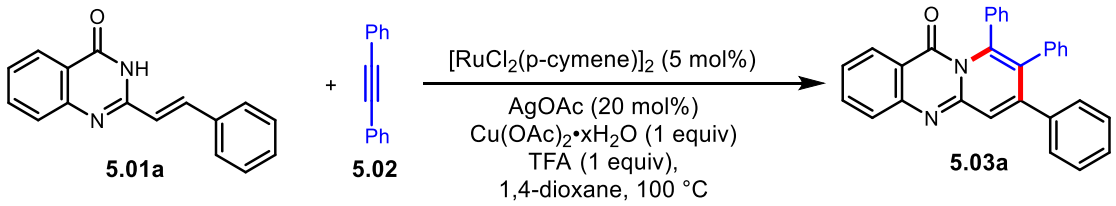

Into a 1 dram scintillation vial equipped with a magnetic stir bar was placed Ru(*p*-cymene)$Cl_2]_2$ (3.67 mg, 0.006 mmol, 5 mol%), AgOAc (4.00 mg, 0.06 mmol, 0.2 equiv), $Cu(OAc)_2.xH_2O$ (21.80 mg, 0.12 mmol, 1 equiv), **5.01a** (26 mg, 0.14 mmol), **5.02** (35 mg, 0.12 mmol, 1 equiv), 0.7 mL of dioxane, and TFA (12 μL, 0.12 mmol 1 equiv). The vial was sealed with a silicone-lined screw cap, transferred out of the glovebox, and stirred at 100°C for 24 hours. The reaction mixture cooled to rt, diluted with MeOH and pass through celite bed to remove the inorganic salts. The filtrate was collected, dried and subjected to column chromatography using silica to get analytically pure **5.03a** (38.71 mg, 76%)**. ^{1}H NMR** (400 MHz, $CDCl_3$) *δ* 8.21 (ddd, *J* = 8.1, 1.5, 0.7 Hz, 1H), 7.85 – 7.75 (m, 2H), 7.53 (s, 1H), 7.39 (ddd, *J* = 8.1, 6.7, 1.5 Hz, 1H), 7.25 – 7.14 (m, 6H), 7.12 – 7.09 (m, 4H), 7.04 – 6.96 (m, 3H), 6.84 – 6.77 (m, 2H); **^{13}C NMR** (100 MHz, $CDCl_3$) *δ* 160.9, 148.8, 148.5, 148.1, 140.5, 137.9, 136.7, 135.5, 134.7, 131.4, 129.2, 128.9, 128.7, 128.0, 127.9, 127.4, 127.3, 127.2, 127.1, 126.7, 126.1, 125.5, 124.9, 118.8; **HRMS** (ESI-TOF) *m/z*: $[M + H]^+$ Calcd for $C_{30}H_{20}N_2O$ 425.1650, Found 425.1647.

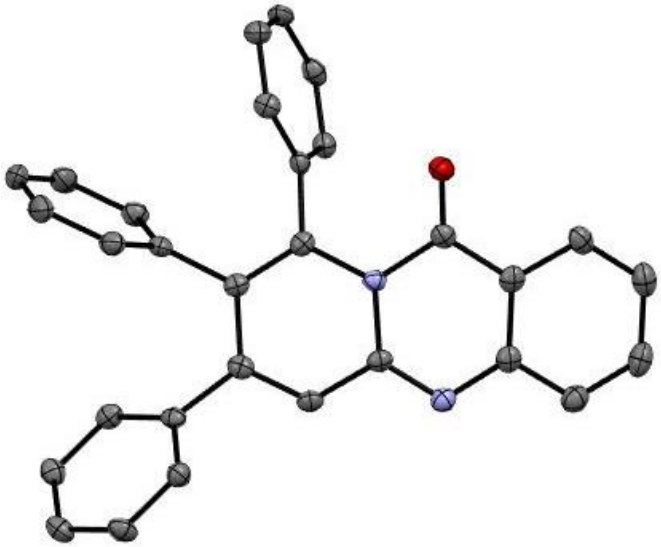

Figure 5.3: ORTEP diagrams of **5.03a** showing 40% probability ellipsoids; all H atoms in compound are omitted for clarity.

5.13.3. Representative experimental procedure for synthesis of 2-aminopyridines

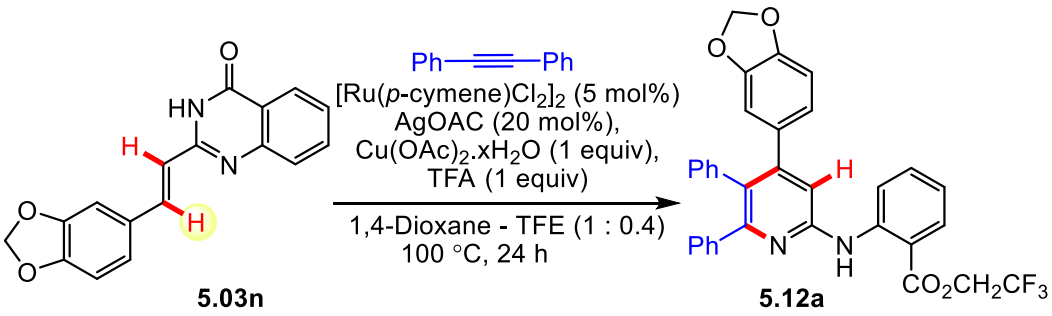

Into a 1 dram scintillation vial equipped with a magnetic stir bar was placed Ru(*p*-cymene)$Cl_2]_2$ (3.67 mg, 0.006 mmol, 5 mol%), AgOAc (4.00 mg, 0.06 mmol, 0.2 equiv), $Cu(OAc)_2.xH_2O$ (21.80 mg, 0.12 mmol, 1 equiv), **5.03n** (26 mg, 0.14 mmol), **5.02a** (35 mg, 0.12 mmol, 1 equiv), 0.7 mL of dioxane, and 0.3 mL of TFE followed by TFA (12 µL, 0.12 mmol 1 equiv). The vial was sealed with a silicone-lined screw cap, transferred out of the glovebox, and stirred at 100°C for 24 hours. The reaction mixture cooled to rt, diluted with MeOH and pass through celite bed to remove the inorganic salts. The filtrate was collected, dried and subjected to column chromatography using silica to get analytically pure **5.12a** (42.9 mg, 63%). **^{1}H NMR** (400

MHz, $CDCl_3$) δ 10.40 (s, 1H), 8.98 (dd, J = 8.8, 1.1 Hz, 1H), 8.10 (dd, J = 8.1, 1.7 Hz, 1H), 7.57 (ddd, J = 8.8, 7.1, 1.7 Hz, 1H), 7.41 – 7.31 (m, 2H), 7.25 – 7.19 (m, 3H), 7.13 – 7.09 (m, 3H), 6.98 – 6.90 (m, 4H), 6.68 (d, J = 8.0 Hz, 1H), 6.62 – 6.56 (m, 2H), 5.94 (s, 2H), 4.74 (q, J = 8.4 Hz, 2H); **^{13}C NMR** (100 MHz, $CDCl_3$) δ 166.8, 156.3, 153.1, 151.5, 147.2, 146.9, 145.5, 140.9, 138.0, 135.5, 133.4, 131.7, 131.4, 130.1, 127.8, 127.7, 127.5, 127.2, 126.4, 124.5 (q, J = 273.4 Hz), 123.1, 119.2, 118.4, 112.4, 111.3, 109.8, 107.9, 101.0, 60.6 (q, J = 36.9 Hz); **^{19}F NMR** (376 MHz, $CDCl_3$) δ -73.49; **HRMS (ESI-TOF):** *m/z* $[M + H]^+$ Calcd for $C_{33}H_{23}F_3N_2O_4$ 569.1688, Found 569.1689.

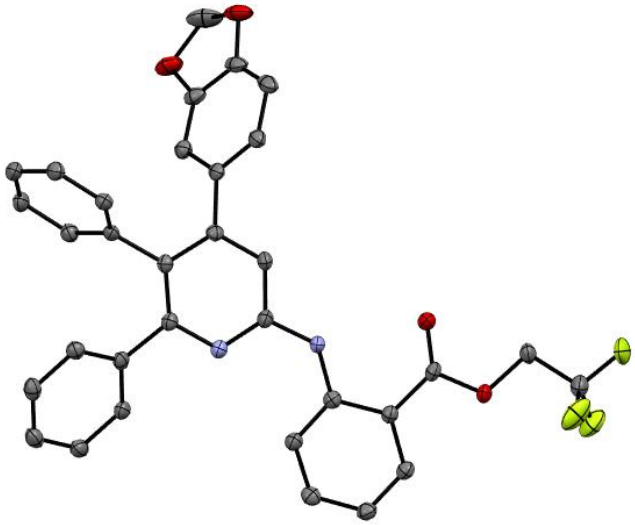

Figure 5.4: ORTEP diagrams of **5.12a** showing 40% probability ellipsoids; all H atoms in compound are omitted for clarity.

5.13.3.1. H/D exchange study

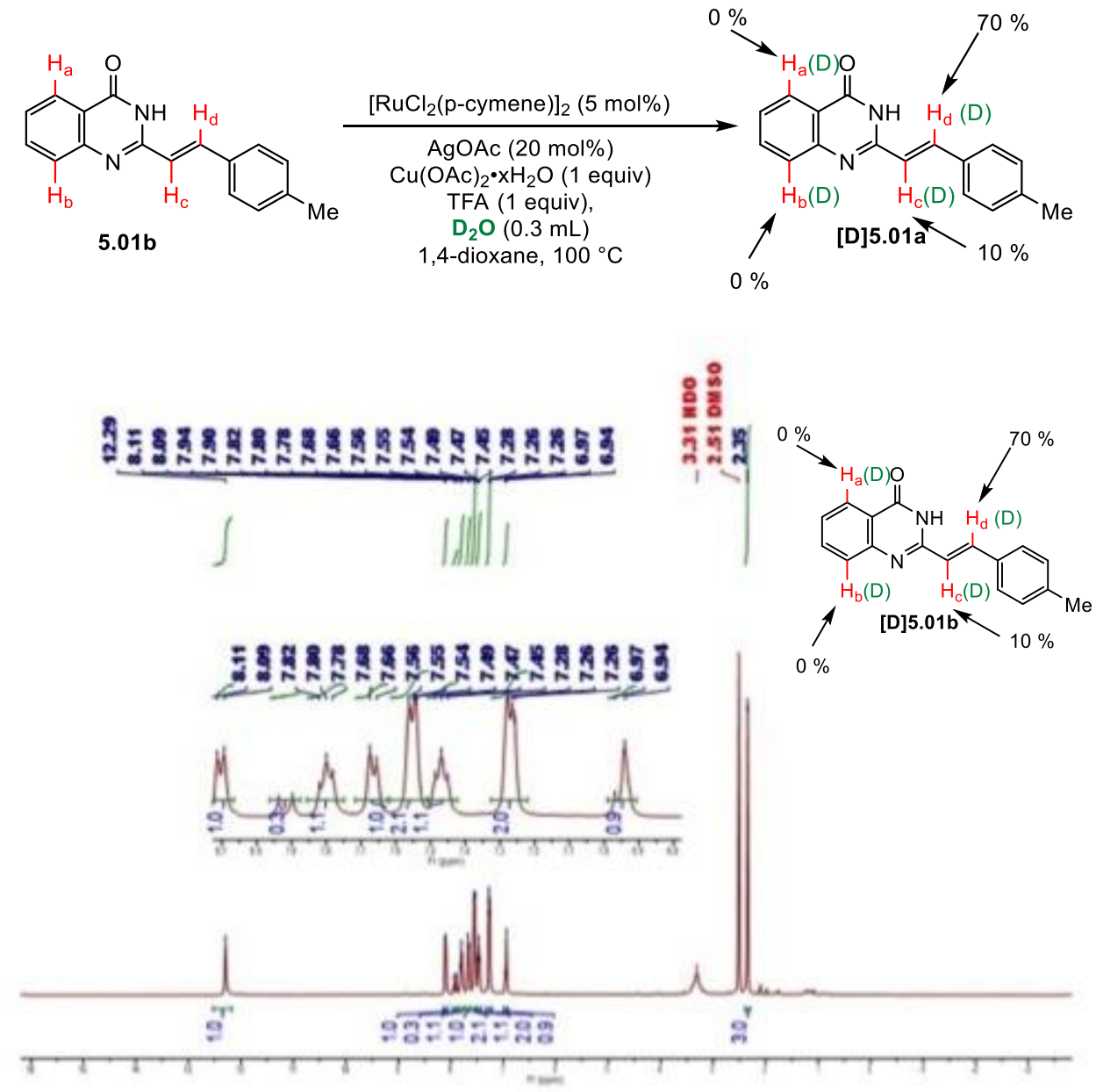

Figure 5.5: ^{1}H-NMR of deuterium scrambling experiment of **5.01a**

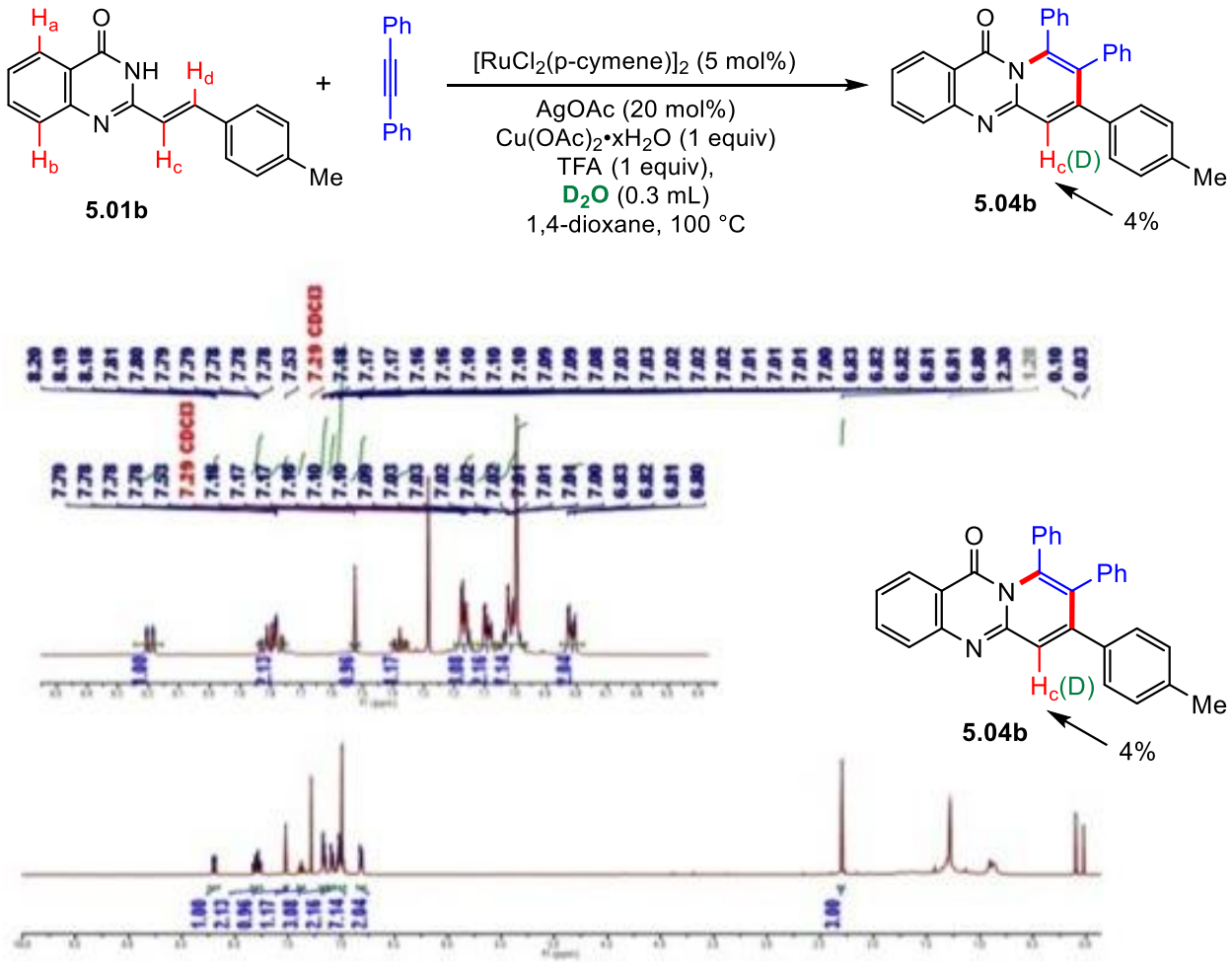

Figure 5.6: ^{1}H-NMR of cyclized product from **5.01b**

Condition for deuteration: Into a 1 dram scintillation vial equipped with a magnetic stir bar was placed Ru(*p*-cymene)$Cl_2]_2$ (3.67 mg, 0.006 mmol, 5 mol%), AgOAc (4.00 mg, 0.06 mmol, 0.2 equiv), $Cu(OAc)_2.xH_2O$ (21.80 mg, 0.12 mmol, 1 equiv), **5.01b** (31.48 mg, 0.12 mmol), 1.0 mL of dioxane, 0.3 mL of D_2O followed by TFA (12 µL, 0.12 mmol 1 equiv). The vial was sealed with a silicone-lined screw cap, transferred out of the glovebox, and stirred at 100°C for 24 hours. The reaction mixture cooled to rt, diluted with MeOH and pass through celite bed to remove the inorganic salts. Deuterium incorporation determined by ^{1}H NMR spectroscopic analysis. The

observed deuteration in absence of alkyne indicated that reversible C–H ruthenation occurred mainly at one vinyl carbon under the reaction conditions. No other C–H functionalizations of **5.01b** was observed in presence of alkyne **5.02** indicating that ruthenium is 'trapped' between amide-H and one of vinylic C-H bond of **5.01b**. This N-Ru-C coordinated ruthenium center is involved in a reversible step, which on the alkyne insertion followed by reductive elimination to annulated products.

5.13.3.2. Kinetic isotopic effect experiment

Preparation of substrate

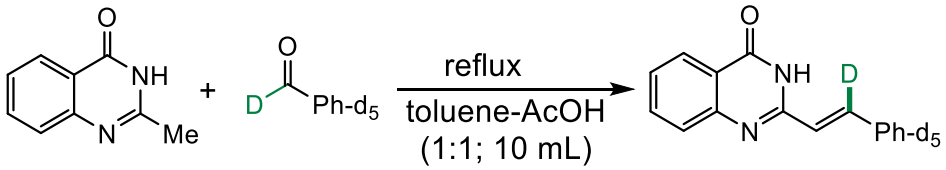

Experimental procedure for the preparation of [D_6]-5.01a: Into a 100 mL round bottom flask, 2-methyl quinazolone (0.80 g, 5 mmol), benzaldehyde-d_6 (0.673 g, 6 mmol, 1.2 equiv), 5 mL of toluene followed by 5 mL of glacial acetic acid was added. The resultant mixture was refluxed for 24 h. The reaction mixture cooled to rt, dried and subjected to column chromatography using silica to get analytically pure **[D_6]-5.01a** (0.912 g, 72%).**^{1}H NMR** (400 MHz, DMSO-d_6) δ 12.34 (s, 1H), 8.12 (dd, J = 7.9, 1.5 Hz, 1H), 7.82 (ddd, J = 8.4, 7.1, 1.6 Hz, 1H), 7.69 (d, J = 8.2 Hz, 1H), 7.49 (ddd, J = 8.0, 7.0, 1.1 Hz, 1H), 7.01 (s, 1H); **HRMS** (ESI-TOF) m/z: $[M + H]^+$ Calcd for $C_{16}H_6D_6N_2O$ 255.1404, Found 255.1408.

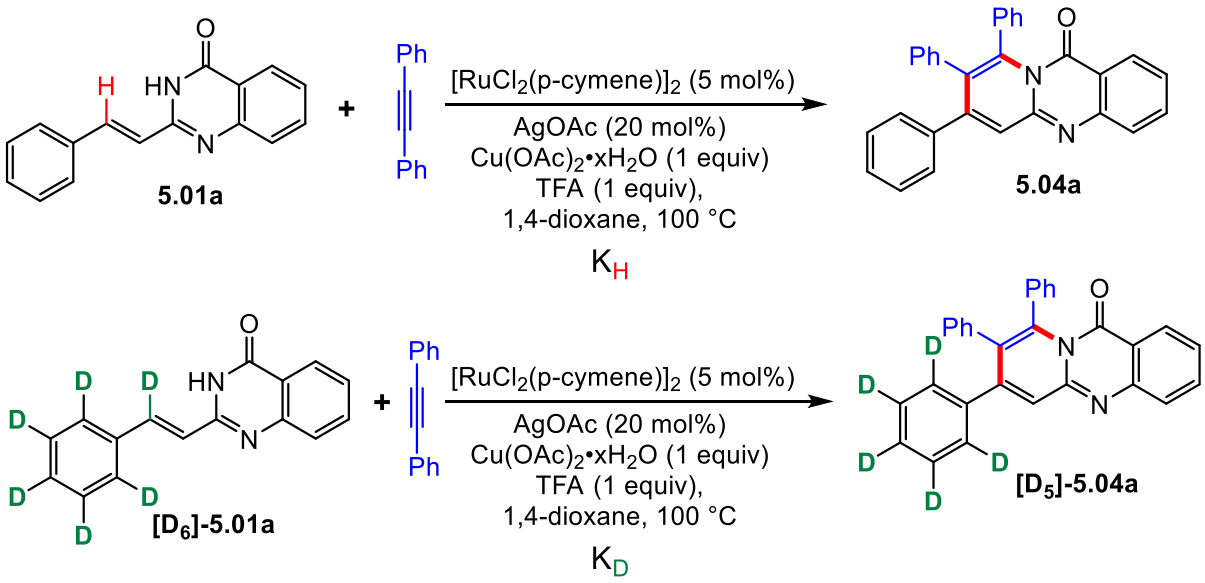

The reactions were prepared according to the general procedure and stopped after 30, 60, 95, and 120 minutes and immediately cooled to room temperature. The reaction mixtures were filtered through a plug of silica to remove unreacted **5.02**. The obtained crude was added triphenylmethane as an internal standard, then concentrated under reduced pressure, and analyzed by ^{1}H-NMR spectroscopy. The obtained yields were plotted as concentration of **4a** vs. time (min). From the data, the initial rates were determined. A significant kinetic isotope effect ($k_H/k_D \approx 3.0$) was observed, suggesting the reversible C–H cleavage to be the rate-determining step.

$k_H = 0.0003$ mmol.mL^{-1}.min^{-1}

$k_D = 0.0001$ mmol.mL^{-1}.min^{-1}

$k_H/k_D = 0.0003/0.0001 = 3$

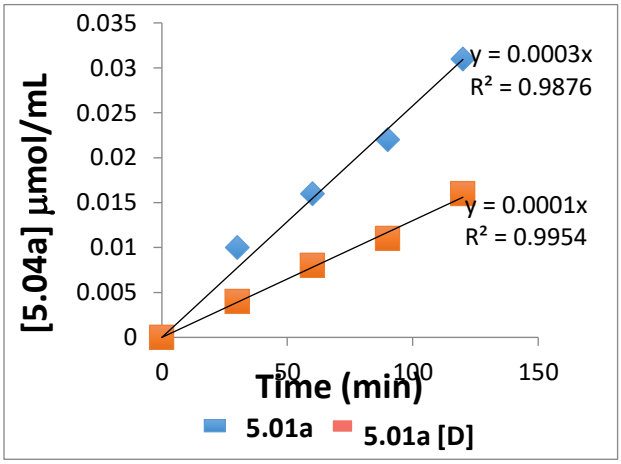

Figure 5.7: KIE studies of **5.01a** and **5.01a [D]**

5.13.3.3. Investigation for the formation larger ring ruthenacycles

Synthesis of 5.05:

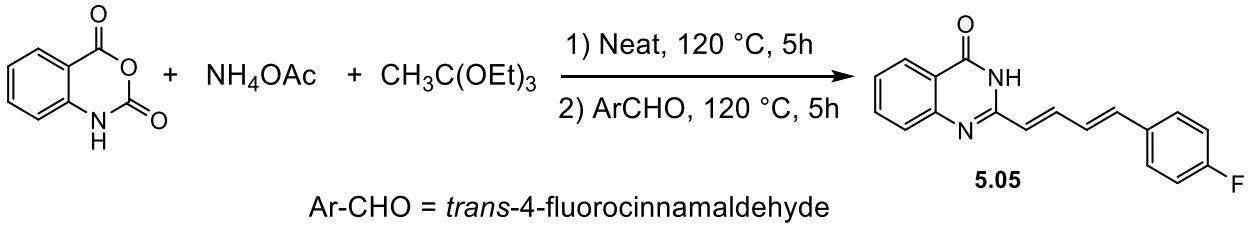

Ar-CHO = *trans*-4-fluorocinnamaldehyde

Experimental procedure: A mixture of isatoic anhydride (0.815 g, 5 mmol), ammonium acetate (0.578 g, 7.5 mmol, 1.5 equiv), and triethyl orthoacetate (1.22 g, 7.5 mmol, 1.5 equiv) were stirred magnetically at 120 °C (oil bath temp) for 5 h followed by addition of *trans*-4-fluorocinnamaldehyde (0.9 g, 6 mmol, 1.2 equiv) and the stirring was continued for another 5 h. The crude reaction mixture was cooled to rt and recrystallized from EtOH to obtain analytically pure 2-[4-(4-fluoro-phenyl)-buta-1,3-dienyl]-3*H*-quinazolin-4-one **5.05** as white solid[1] (1.10 g, 75%). **^{1}H NMR** (400 MHz, DMSO-d_6) δ 12.44 (s, 1H), 8.12 (dd, J = 7.9, 1.5 Hz, 1H), 8.04 (d, J = 16.3 Hz, 1H), 7.86 – 7.74 (m, 2H), 7.71 (dd, J = 8.2, 1.2 Hz, 1H), 7.54 – 7.43 (m, 2H), 7.37 – 7.27 (m, 2H), 7.12 (d, J = 16.3 Hz, 1H); **^{13}C NMR** (100 MHz, DMSO-d_6) δ 162.2, 159.7, 151.6, 149.3, 135.0, 132.1 (d, J = 8 Hz), 131.0, 129.3 (d, J = 3 Hz), 127.7, 126.9, 126.3, 125.6 (d, J = 4 Hz), 124.2 (d, J = 7 Hz), 123.1 (d, J = 11 Hz), 121.7, 116.6 (d, J = 22 Hz); ^{9}F NMR (376 MHz, DMSO-d_6) δ -112.38; **HRMS** (ESI-TOF) *m/z*: $[M + H]^+$ Calcd for $C_{18}H_{13}FN_2O$ 293.1090, Found 293.1090.

Reaction of 5.05 with 5.02:

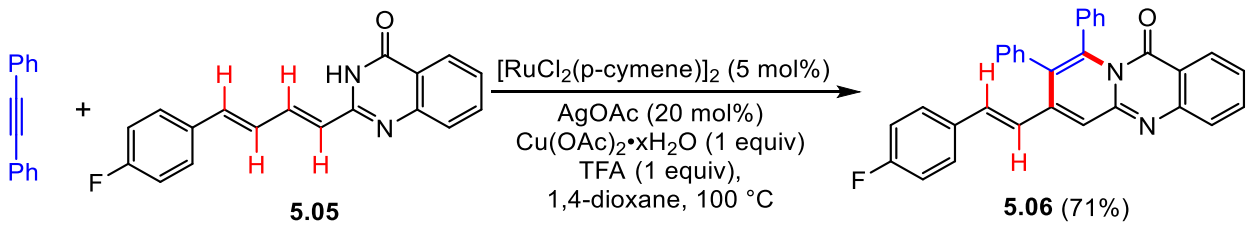

Experimental procedure: Into a 1 dram scintillation vial equipped with a magnetic stir bar was placed Ru(*p*-cymene)$Cl_2]_2$ (3.67 mg, 0.006 mmol, 5 mol%), AgOAc (4.00 mg, 0.06 mmol, 0.2 equiv), $Cu(OAc)_2.xH_2O$ (21.80 mg, 0.12 mmol, 1 equiv), **5.02** (25.66 mg, 0.14 mmol, 1.2 equiv), **5.05** (35.08 mg, 0.12 mmol), and 1.0 mL of dioxane followed by TFA (12 µL, 0.12 mmol 1 equiv). The vial was sealed with a silicone-lined screw cap, transferred out of the glovebox, and stirred at 100°C for 24 hours. The reaction mixture cooled to rt, diluted with MeOH and pass through celite bed to remove the inorganic salts. An aliquot portion (100 µL) of the filtrates was taken out and subjected to GC-MS, the remaining filtrates were dried and subjected to column chromatography. The exclusive formation of 7-[2-(4-fluoro-phenyl)-vinyl]-8,9-diphenyl-pyrido[2,1-b]quinazolin-11-one **5.06**, **(**39.92 mg, 71%) indicates the preferred formation of 5-membered ruthenacycle over higher ring size 6/7-membered ruthenacycles following vinylic trapping of Ru. **7-[2-(4-Fluoro-phenyl)-vinyl]-8,9-diphenyl-pyrido[2,1-b]quinazolin-11-one:** **^{1}H NMR** (400 MHz, $CDCl_3$) δ 8.18 (dd, J = 8.3, 1.4 Hz, 1H), 7.87 – 7.75 (m, 3H), 7.37 (ddd, J = 8.2, 6.4, 1.8 Hz, 2H), 7.32 – 7.20 (m, 8H), 7.17 (dd, J = 5.0, 2.0 Hz, 3H), 7.09 – 6.96 (m, 6H), 6.48 (d, J = 16.1 Hz, 1H); **^{13}C NMR** (100 MHz, $CDCl_3$) δ 163.0 (d, J = 249.2 Hz), 160.7, 149.2, 148.0, 143.7, 140.2, 136.58, 135.1, 134.8, 133.7, 132.4 (d, J = 3.5 Hz), 130.9, 129.2, 128.9 (d, J = 8.1 Hz) 128.4, 128.0, 127.5, 127.4, 127.2, 127.1, 125.9, 124.8, 123.8, 119.7, 118.5, 115.9 (d, J = 21.7 Hz); **^{19}F NMR** (376 MHz, $CDCl_3$) δ -115.72; **HRMS** (ESI-TOF) *m/z*: $[M + H]^+$ Calcd for $C_{32}H_{21}FN_2O$ 469.1716, Found 469.1710.

5.13.3.4. Effect of extended conjugation on the oxidative annulation

Preparation of 5.07:

Experimental procedure: Anthranilamide (0.681 g, 5.0 mmol) and crotonaldehyde (0.42 g, 6 mmol, 1.2 equiv) were dissolved in DMSO (10 mL). Then, the reaction mixture was stirred at 100 ^{o}C in an open flask for 20 h (TLC). The reaction mixture was cooled to rt, diluted with EtOAc and extracted ice-cold water. The collected organic layers were dried and subjected to column chromatography to get analytically pure **5.07** (0.62 g, 67%) as white solid. **^{1}H NMR** (400 MHz, $CDCl_3$) δ 12.10 (s, 3H), 8.31 (ddd, J = 7.9, 1.6, 0.6 Hz, 3H), 7.83 – 7.69 (m, 6H), 7.48 (ddd, J = 8.1, 6.9, 1.4 Hz, 3H), 7.33 – 7.19 (m, 4H), 6.41 (dq, J = 15.9, 1.7 Hz, 3H), 2.09 (dd, J = 6.8, 1.8 Hz, 9H), 0.02 (s, 1H); **^{13}C NMR** (100 MHz, $CDCl_3$) δ 164.2, 150.9, 149.7, 138.5, 134.8, 127.5, 126.3, 126.3, 125.3, 120.7, 18.7; **Mass** (ESI) *m/z*: = 186.1(M^+).

Reaction of 5.07 with 5.02:

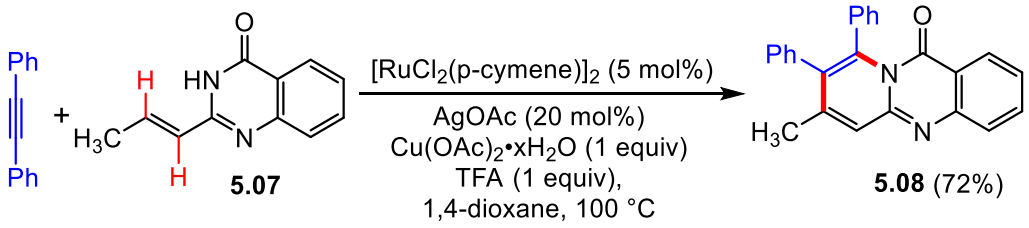

Experimental procedure: Into a 1 dram scintillation vial equipped with a magnetic stir bar was added Ru(*p*-cymene)$Cl_2]_2$ (3.67 mg, 0.006 mmol, 5 mol%), AgOAc (4.00 mg, 0.06 mmol, 0.2 equiv), $Cu(OAc)_2.H_2O$ (21.80 mg, 0.12 mmol, 1 equiv), **5.07** (22.35 mg, 0.12 mmol), **5.02** (25.66 mg, 0.14 mmol, 1.2 equiv), and 1.0 mL of dioxane followed by TFA (12 µL, 0.12 mmol 1 equiv). The vial was sealed with a silicone-lined screw cap, transferred out of the glovebox, and

stirred at 100°C for 24 hours. The reaction mixture cooled to rt, diluted with MeOH and pass through celite bed to remove the inorganic salts. An aliquot portion (100 µL) of the filtrates was taken out and subjected to GC-MS, the remaining filtrates were dried and subjected to column chromatography to obtain 7-methyl-8,9-diphenyl-pyrido[2,1-b]quinazolin-11-one **5.08** (31.31 mg, 72%) exclusively. **^{1}H NMR** (400 MHz, $CDCl_3$) δ 8.19 – 8.16 (m, 1H), 7.84 – 7.71 (m, 2H), 7.41 – 7.32 (m, 2H), 7.26 – 7.18 (m, 3H), 7.18 – 7.11 (m, 3H), 7.06 – 7.00 (m, 2H), 7.00 – 6.93 (m, 2H), 2.08 (d, J = 1.2 Hz, 3H); **^{13}C NMR** (100 MHz, $CDCl_3$) δ 160.9, 148.9, 148.1, 145.4, 139.6, 136.7, 135.9, 134.6, 130.7, 130.3, 128.3, 127.9, 127.4, 127.1, 127.1, 126.0, 124.6, 124.2, 118.5, 21.6; **HRMS** (ESI-TOF) *m/z*: $[M + H]^+$ Calcd for $C_{25}H_{18}N_2O$ 363.1497, Found $C_{25}H_{18}N_2O$ 363.1496.

5.13.3.5. Investigation of the cascade hyroamidation/C-H activation pathway

Treatment of preformed 3.09 under optimized conditions

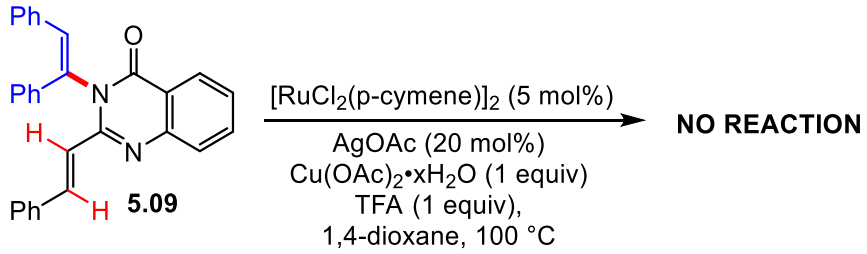

Experimental procedure: Into a 1 dram scintillation vial equipped with a magnetic stir bar was added Ru(*p*-cymene)$Cl_2]_2$ (3.67 mg, 0.006 mmol, 5 mol%), AgOAc (4.00 mg, 0.06 mmol, 0.2 equiv), $Cu(OAc)_2.H_2O$ (21.80 mg, 0.12 mmol, 1 equiv), **5.09** (51.42 mg, 0.12 mmol), and 1.0 mL of dioxane followed by TFA (12 µL, 0.12 mmol 1 equiv). The vial was sealed with a silicone-lined screw cap, transferred out of the glovebox, and stirred at 100°C for 24 hours. The reaction mixture cooled to rt, diluted with MeOH and pass through celite bed to remove the inorganic salts. An aliquot portion (100 µL) of the filtrates was taken out and subjected to GC-MS, the remaining

filtrates were dried and subjected to column chromatography to recover **5.09** quantitatively. **^{1}H NMR** (400 MHz, $CDCl_3$) δ 8.32 (dt, J = 7.9, 1.2 Hz, 1H), 7.92 (d, J = 15.4 Hz, 1H), 7.89 – 7.76 (m, 2H), 7.55 – 7.47 (m, 4H), 7.44 – 7.32 (m, 8H), 7.19 (s, 5H), 7.02 (d, J = 15.4 Hz, 1H); **^{13}C NMR** (100 MHz, $CDCl_3$) δ 161.7, 151.8, 147.9, 140.8, 136.8, 135.4, 134.8, 134.5, 134.1, 129.6, 129.2, 129.1, 129.0, 128.9, 128.5, 128.6, 128.3, 127.8, 127.5, 127.4, 126.6, 125.1, 120.7, 119.3, 29.7; **HRMS** (ESI-TOF) *m/z*: $[M + H]^+$ Calcd for $C_{30}H_{22}N_2O$ 427.1810, Found 427.1808.

5.13.3.6. Investigation of the site of primary metal insertion

(i) Investigation of Amide-NH as primary site of metal insertion

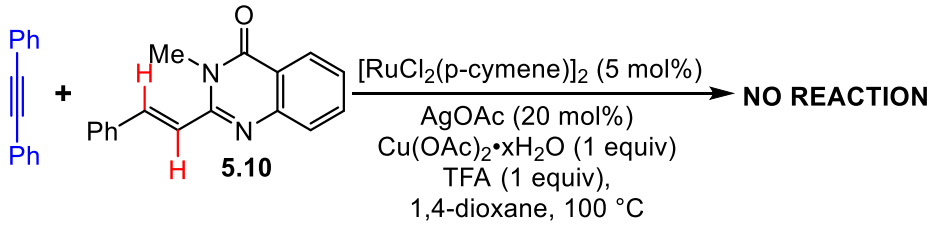

Experimental procedure: Into a 1 dram scintillation vial equipped with a magnetic stir bar was added Ru(*p*-cymene)$Cl_2]_2$ (3.67 mg, 0.006 mmol, 5 mol%), AgOAc (4.00 mg, 0.06 mmol, 0.2 equiv), $Cu(OAc)_2.H_2O$ (21.80 mg, 0.12 mmol, 1 equiv), **5.10** (31.48 mg, 0.12 mmol), **5.02** (25.66 mg, 0.14 mmol, 1.2 equiv), and 1.0 mL of dioxane followed by TFA (12 µL, 0.12 mmol 1 equiv). The vial was sealed with a silicone-lined screw cap, transferred out of the glovebox, and stirred at 100°C for 24 hours. The reaction mixture cooled to rt, diluted with MeOH and pass through celite bed to remove the inorganic salts. An aliquot portion (100 µL) of the filtrates was taken out and subjected to GC-MS, the remaining filtrates were dried and subjected to column chromatography to recover **5.10** quantitatively.

(ii) Investigation of vinylic-H as primary site of metal insertion

Preparation of 5.11

Experimental procedure: Anthranilamide (0.681 g, 5.0 mmol) and *β*-methyl crotonaldehyde (0.50 g, 6 mmol, 1.2 equiv) were dissolved in DMSO (10 mL). Then, the reaction mixture was stirred at 100 ^{o}C in an open flask for 20 h (TLC). The reaction mixture was cooled to rt, diluted with EtOAc and extracted ice-cold water. The collected organic layers were dried and subjected to column chromatography to get analytically pure 2-(2-methyl-propenyl)-3*H*-quinazolin-4-one **5.11** (0.60 g, 60%) as white solid.[2] **^{1}H NMR** (400 MHz, DMSO-d_6) δ 12.01 (s, 1H), 8.08 (dd, J = 7.9, 1.5 Hz, 1H), 7.77 (ddd, J = 8.5, 7.1, 1.6 Hz, 1H), 7.64 – 7.55 (m, 1H), 7.44 (ddd, J = 8.1, 7.1, 1.2 Hz, 1H), 6.11 – 6.01 (m, 1H), 2.32 (d, J = 1.3 Hz, 3H), 1.95 (d, J = 1.4 Hz, 3H); **^{13}C NMR** (100 MHz, DMSO) δ 162.2, 152.2, 150.3, 149.4, 134.7, 127.6, 126.3, 126.1, 121.0, 117.7, 28.2, 21.1; **Mass** (ESI) *m/z*: = 200.1(M^+).

Reaction of 5.11 with 5.02 under optimized condition

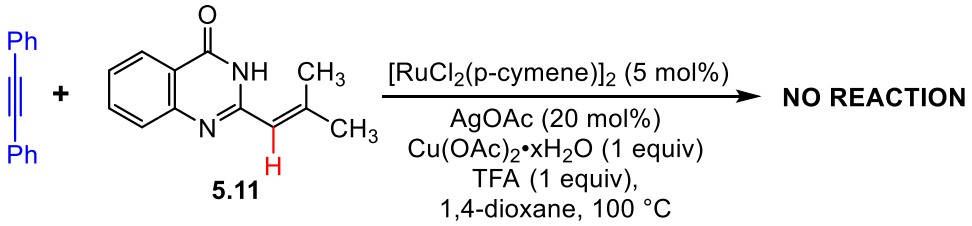

Experimental procedure: Into a 1 dram scintillation vial equipped with a magnetic stir bar was placed Ru(*p*-cymene)$Cl_2]_2$ (3.67 mg, 0.006 mmol, 5 mol%), AgOAc (4.00 mg, 0.06 mmol, 0.2 equiv), $Cu(OAc)_2.H_2O$ (21.80 mg, 0.12 mmol, 1 equiv), **5.02** (25.66 mg, 0.14 mmol, 1.2 equiv), **5.11** (24.03 mg, 0.12 mmol), and 1.0 mL of dioxane followed by TFA (12 µL, 0.12 mmol 1 equiv).

The vial was sealed with a silicone-lined screw cap, transferred out of the glovebox, and stirred at 100°C for 24 hours. The reaction mixture cooled to rt, diluted with EtOAc and pass through celite bed to remove the inorganic salts. An aliquot portion (100 μL) of the filtrates was taken out and subjected to GC-MS, the remaining filtrates were dried and subjected to column chromatography to obtain **5.11** quantitatively.

5.13.3.7. Investigation of regioselective alkyne insertion to ruthenacycle

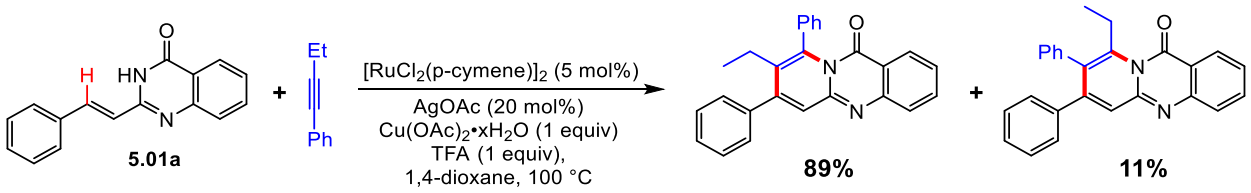

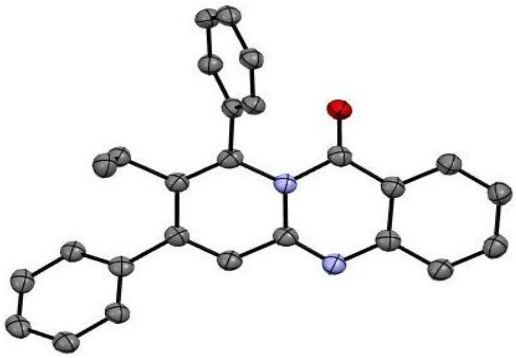

Figure 5.6: ORTEP diagrams showing 40% probability ellipsoids; all H atoms in compound are omitted for clarity

8-Ethyl-7,9-diphenyl-pyrido[2,1-b]quinazolin-11-one: Prepared by following the general procedure for the synthesis of fused quinazolinones to yield **5.04x** as a white solid (71%): **^{1}H NMR** (400 MHz, $CDCl_3$) δ 8.17 (dd, J = 8.1, 1.4 Hz, 1H), 7.82 – 7.72 (m, 2H), 7.51 – 7.42 (m, 8H), 7.41 – 7.32 (m, 4H), 2.40 (q, J = 7.4 Hz, 2H), 0.58 (t, J = 7.4 Hz, 3H); **^{13}C NMR** (100 MHz, $CDCl_3$) δ 160.6, 149.5, 148.4, 148.0, 139.3, 138.2, 136.9, 134.5, 129.0, 128.5, 128.4, 128.3, 128.2, 127.8, 127.7, 127.4, 126.3, 126.0, 124.8, 118.8, 21.8, 14.1; **HRMS** (ESI-TOF) *m/z*: $[M + H]^+$ Calcd for $C_{26}H_{20}N_2O$ 377.1654, Found 377.1652.

5.13.4. Mechanistic pathway for the transformation of annulated quinazolone to 2-amino pyridines

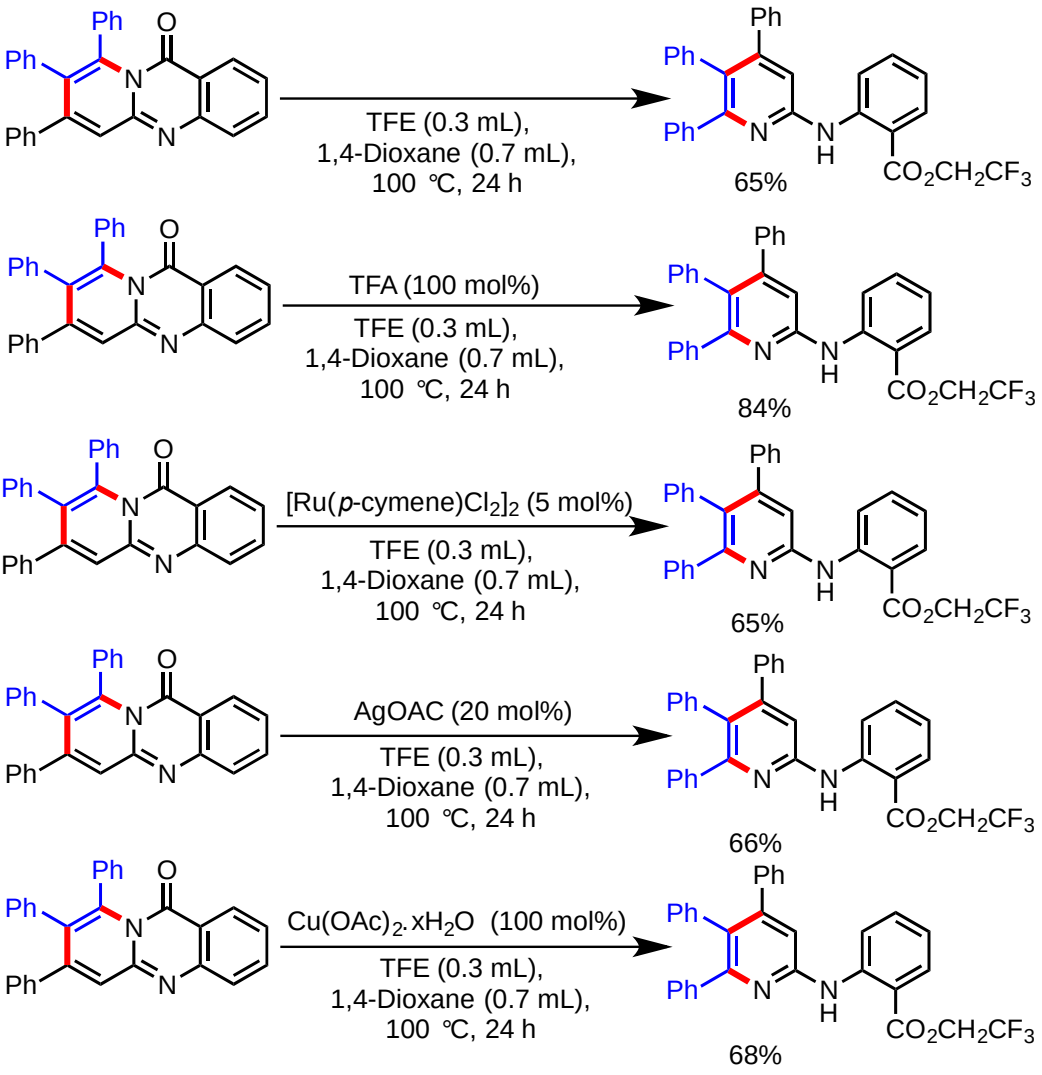

Scheme 5.13: Control studies for the importance of reaction components

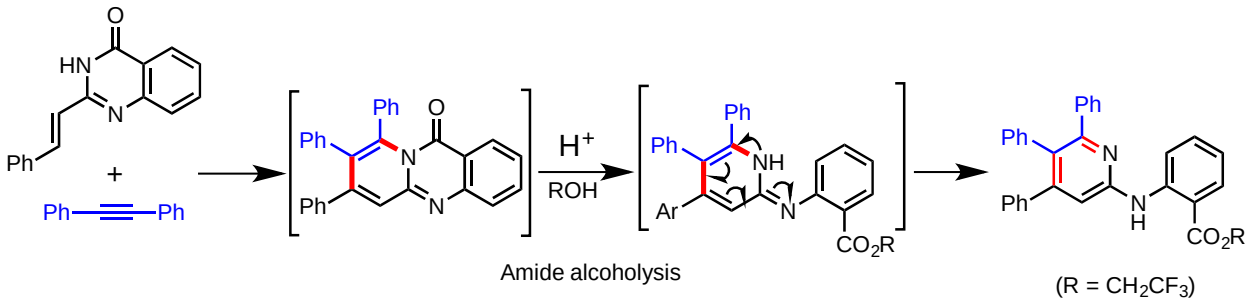

Scheme 5.14: Mechanistic route for alcoholysis of annulated quinazolone to 2-amino pyridines

5.13.5. Use of molecular oxygen (O_2) as terminal oxidant

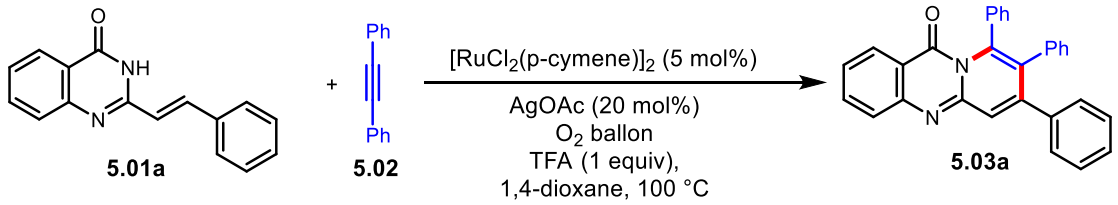

Into a 1 dram scintillation vial equipped with a magnetic stir bar was placed Ru(*p*-cymene)$Cl_2]_2$ (3.67 mg, 0.006 mmol, 5 mol%), AgOAc (4.00 mg, 0.06 mmol, 0.2 equiv), **5.02** (25.66 mg, 0.14 mmol, 1.2 equiv), **5.01a** (29.79 mg, 0.12 mmol), and 0.7 mL of dioxane, TFA (12 µL, 0.12 mmol 1 equiv). The vial was sealed with a silicone-lined screw cap, transferred out of the glovebox, and stirred at 100°C for 24 hours in the presence of oxygen balloon. The reaction mixture cooled to rt, diluted with MeOH and pass through celite bed to remove the inorganic salts. The filtrate was collected, dried and subjected to column chromatography using silica to get analytically pure **5.03a** (62%).

5.13.6. Synthesis of starting materials

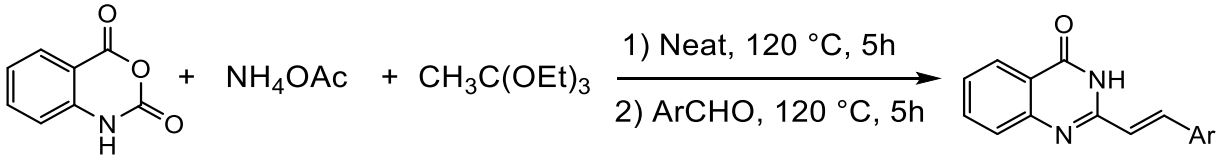

General experimental procedure: A mixture of isatoic anhydride (0.816 g, 5 mmol), ammonium acetate (0.578 g, 7.5 mmol, 1.5 equiv), and triethyl orthoacetate (1.217 g, 7.5 mmol, 1.5 equiv) were stirred magnetically at 120 °C (oil bath temp) for 5 h followed by addition of aldehyde (5 mmol. 1 equiv) and the stirring was continued for another 5 h. The reaction mixture was cooled to rt and recrystallized from EtOH to obtain analytically pure compounds.

2-Styryl-3*H*-quinazolin-4-one (5.01a): ^{1}H NMR (400 MHz, DMSO-d_6) δ 12.34 (s, 1H),

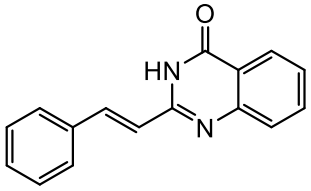

8.12 (dd, J = 7.8, 1.5 Hz, 1H), 7.97 (d, J = 16.2 Hz, 1H), 7.82 (ddd, J = 8.5, 7.1, 1.6 Hz, 1H), 7.68 (ddd, J = 8.1, 5.4, 1.2 Hz, 3H), 7.54 – 7.38 (m, 4H), 7.02 (d, J = 16.2 Hz, 1H); **^{13}C NMR** (100 MHz, DMSO-d_6) δ 162.2, 151.9, 138.7, 135.5, 134.9, 130.2, 129.5, 128.1 127.5, 126.7, 126.3, 121.6, 40.6, 40.4, 40.2, 40.0, 39.8, 39.6, 39.4.

2-(2-*p*-Tolyl-vinyl)-3*H*-quinazolin-4-one (5.01b): ^{1}H NMR (400 MHz, DMSO-d_6) δ

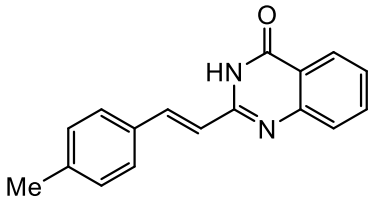

12.27 (s, 1H), 8.11 (dd, J = 8.0, 1.5 Hz, 1H), 7.92 (d, J = 16.1 Hz, 1H), 7.85 – 7.75 (m, 1H), 7.67 (d, J = 8.1 Hz, 1H), 7.55 (d, J = 7.7 Hz, 2H), 7.47 (t, J = 7.5 Hz, 1H), 7.27 (d, J = 7.8 Hz, 2H), 6.95 (d, J = 16.1 Hz, 1H), 2.34 (s, 3H); **^{13}C NMR** (100 MHz, DMSO-d_6) δ 162.3, 152.1, 149.5, 140.1, 138.7, 134.9, 132.7, 130.1, 128.1, 127.5, 126.5, 126.32, 121.5, 120.5, 21.5.

2-[2-(4-Methoxy-phenyl)-vinyl]-3*H*-quinazolin-4-one (5.01c): ^{1}H NMR (400 MHz,

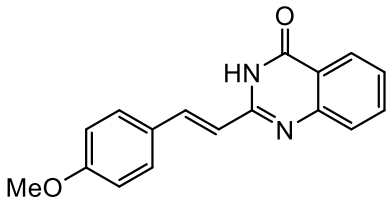

DMSO-d_6) δ 12.25 (s, 1H), 8.16 – 8.04 (m, 1H), 7.91 (d, J = 16.0 Hz, 1H), 7.84 – 7.73 (m, 1H), 7.63 (dd, J = 17.2, 8.2 Hz, 3H), 7.46 (t, J = 7.5 Hz, 1H), 7.02 (d, J = 8.3 Hz, 2H), 6.86 (d, J = 16.1 Hz, 1H), 3.81 (s, 3H); **^{13}C NMR** (100 MHz, DMSO-d_6) δ 162.2, 161.1, 152.2, 149.6, 138.5, 134.9, 129.7, 128.1, 127.5, 126.4, 126.3, 121.4, 118.9, 115.0, 55.8.

2-[2-(4-Dimethylamino-phenyl)-vinyl]-3*H*-quinazolin-4-one (5.01d): ^{1}H NMR (400

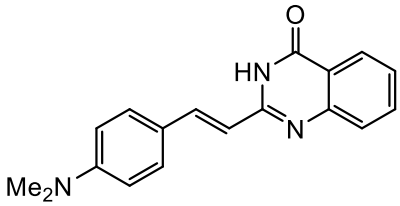

MHz, DMSO-d_6) δ 12.14 (s, 1H), 8.09 (d, J = 7.9 Hz, 1H), 7.87 (d, J = 16.0 Hz, 1H), 7.77 (t, J = 7.8 Hz, 1H), 7.63 (d, J = 8.2 Hz, 1H), 7.49 (d, J = 8.4 Hz, 2H), 7.43 (t, J = 7.6 Hz, 1H), 6.84 –

6.68 (m, 3H), 2.99 (s, 6H); **^{13}C NMR** (100 MHz, DMSO-d_6) δ 162.3, 152.7, 151.8, 149.9, 139.4, 134.8, 129.6, 127.3, 126.3, 125.9, 122.9, 121.2, 115.5, 112.5.

4-[2-(4-Nitro-3,4-dihydro-quinazolin-2-yl)-vinyl]-benzonitrile (5.01e): ^{1}H NMR (400

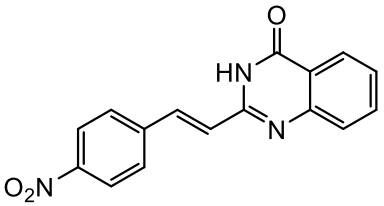

MHz, DMSO-d_6) δ ^{1}H NMR (400 MHz, DMSO-d_6) δ 12.40 (s, 1H), 8.20 – 8.06 (m, 1H), 7.92-7.82 (m, 6H), 7.69 (d, J = 8.1 Hz, 1H), 7.51 (t, J = 7.5 Hz, 1H), 7.15 (d, J = 16.2 Hz, 1H); **^{13}C NMR** (100 MHz, DMSO-d_6) δ 162.3, 151.8, 149.5, 137.4, 135.0, 134.6, 134.6, 129.8, 129.6, 127.5, 126.8, 126.4, 122.4, 121.2.

2-[2-(4-Trifluoromethyl-phenyl)-vinyl]-3*H*-quinazolin-4-one (5.01f): **^{1}H NMR** (400

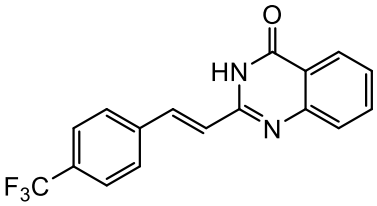

MHz, DMSO-d_6) δ 12.32 (s, 1H), 8.12 (d, J = 7.7 Hz, 1H), 7.99 (t, J = 16.1 Hz, 3H), 7.87 – 7.62 (m, 4H), 7.51 (s, 1H), 7.14 (d, J = 16.4 Hz, 1H); **^{13}C NMR** (100 MHz, DMSO-d_6) δ 162.1, 151.5, 149.3, 136.9, 136.6, 135.0, 131.7, 130.6, 130.3 (q, J = 32.1 Hz), 127.7, 126.9, 126.4, 124.5 (q, J = 3.7 Hz) 124.4 (q, J = 273.4 Hz), 123.7, 121.7; **^{19}F NMR** (376 MHz, DMSO-d_6) δ -61.18; **HRMS** (ESI-TOF) *m/z*: $[M + H]^+$ Calcd for $C_{17}H_{11}F_3N_2O$ 317.0902, Found 317.0902.

4-[2-(4-Oxo-3,4-dihydro-quinazolin-2-yl)-vinyl]-benzonitrile (5.0g): ^{1}H NMR (400

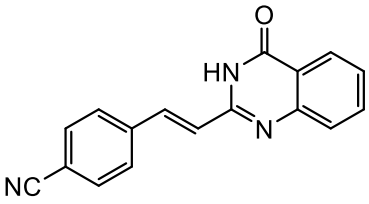

MHz, DMSO-d_6) δ 12.40 (s, 1H), 8.17 – 8.09 (m, 1H), 7.98 (d, J = 16.2 Hz, 1H), 7.91 (d, J = 7.9 Hz, 2H), 7.88 – 7.77 (m, 3H), 7.69 (d, J = 8.2 Hz, 1H), 7.51 (t, J = 7.5 Hz, 1H), 7.15 (d, J = 16.2 Hz, 1H); **^{13}C NMR** (100 MHz, DMSO-d_6) δ 162.1, 151.3, 149.3, 140.0, 136.7, 135.1, 133.4, 128.7, 127.7, 127.1, 126.4, 125.1, 121.7, 119.1, 112.0; **HRMS** (ESI-TOF) *m/z*: $[M + H]^+$ Calcd for $C_{17}H_{11}N_3O$ 274.0980, Found 274.0984.

2-[2-(4-Chloro-phenyl)-vinyl]-3*H*-quinazolin-4-one (5.01h): ^{1}H NMR (400 MHz,

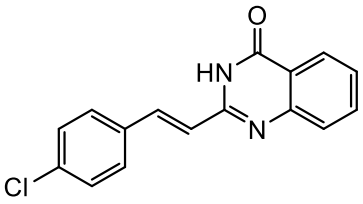

DMSO-d_6) δ 11.36 (s, 1H), 8.12 (d, J = 8.0 Hz, 1H), 7.94 (d, J = 16.2 Hz, 1H), 7.81 (d, J = 7.9 Hz, 1H), 7.69 (dd, J = 7.6, 4.2 Hz, 3H), 7.51 (dd, J = 17.3, 7.8 Hz, 3H), 7.02 (d, J = 16.2 Hz, 1H); **^{13}C NMR** (100 MHz, DMSO-d_6) δ 162.2, 151.8, 149.4, 137.3, 135.0, 134.6, 134.4, 129.7, 129.6, 127.6, 126.8, 126.3, 122.4, 121.6.

6-Chloro-2-styryl-3*H*-quinazolin-4-one (5.01i): ^{1}H NMR (400 MHz, DMSO-d_6) δ 12.51

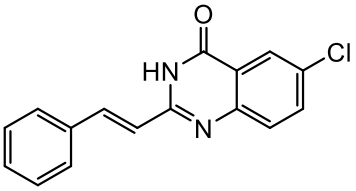

(s, 1H), 8.04 (d, J = 2.5 Hz, 1H), 7.96 (d, J = 16.1 Hz, 1H), 7.89 – 7.78 (m, 1H), 7.68 (dd, J = 12.2, 8.0 Hz, 3H), 7.46 (dt, J = 10.9, 6.5 Hz, 4H), 7.00 (d, J = 16.1 Hz, 1H); **^{13}C NMR** (100 MHz, DMSO-d_6) δ 161.2, 152.4, 148.2, 139.2, 135.3, 135.1, 130.8, 130.4, 129.5, 128.8, 128.2, 125.3, 122.8, 121.2.

2-[2-(2-Fluoro-phenyl)-vinyl]-3*H*-quinazolin-4-one (**5.01j**): **^{1}H NMR** (400 MHz,

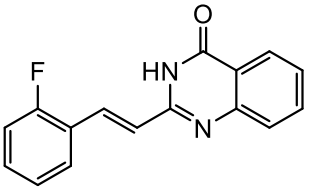

DMSO-d_6) δ 12.44 (s, 1H), 8.12 (dd, J = 7.9, 1.5 Hz, 1H), 8.04 (d, J = 16.3 Hz, 1H), 7.85 – 7.74 (m, 2H), 7.71 (dd, J = 8.2, 1.2 Hz, 1H), 7.53 – 7.44 (m, 2H), 7.37 – 7.28 (m, 2H), 7.12 (d, J = 16.3 Hz, 1H); **^{13}C NMR** (100 MHz, DMSO-d_6) δ 159.3 (d, J = 255.1 Hz), 151.6, 149.3, 135.0, 132.1 (d, J=8.8 Hz), 131.0, 129.3 (d, J = 3.6 Hz), 127.7, 126.9, 126.3, 125.6, 125.7, 124.3(d, J = 6.4 Hz), 123.2 (d, J = 11.5 Hz), 121.7, 116.7 (d, J = 23.0 Hz); **^{19}F NMR** (376 MHz, DMSO-d_6) δ -115.73; HRMS (ESI-TOF) *m/z*: $[M + H]^+$ Calcd for $C_{16}H_{11}FN_2O$ 267.0934, Found 267.0934.

2-(2-Benzo[1,3]dioxol-5-yl-vinyl)-3*H*-quinazolin-4-one (5.01k): ^{1}H NMR (400 MHz, DMSO-d_6) δ 12.23 (s, 1H), 7.91 – 7.75 (m, 2H), 7.65 (d, J = 8.1 Hz, 1H), 7.52 – 7.41 (m, 1H), 7.26 (d, J = 2.2 Hz, 1H), 7.14 (dd, J = 8.0, 1.7 Hz, 1H), 7.00 (t, J = 7.0 Hz, 1H), 6.84 (d, J = 16.1 Hz, 1H), 6.10 (s, 2H); **^{13}C NMR** (100 MHz, DMSO-d_6) δ 162.2, 152.1, 149.6, 149.3, 148.6, 138.5, 135.0, 129.9, 127.5, 126.5, 126.3, 124.2, 121.4, 119.6, 109.2, 106.6, 102.0; HRMS (ESI-TOF) *m/z*: $[M + H]^+$ Calcd for $C_{17}H_{12}N_2O_3$ 293.0926, Found 293.0924.

2-(2-Pyridin-3-yl-vinyl)-3*H*-quinazolin-4-one (5.01l): ^{1}H NMR (400 MHz, DMSO-d_6) δ 12.39 (s, 1H), 8.84 (d, J = 2.3 Hz, 1H), 8.60 (d, J = 4.8 Hz, 1H), 8.17 – 8.07 (m, 2H), 7.98 (d, J = 16.3 Hz, 1H), 7.83 (t, J = 7.8 Hz, 1H), 7.70 (d, J = 8.2 Hz, 1H), 7.55 – 7.46 (m, 2H), 7.13 (d, J = 16.3 Hz, 1H); **^{13}C NMR** (101 MHz, DMSO-d_6) δ 162.2, 151.5, 150.8, 149.7, 149.3, 135.3, 135.0, 134.3, 131.3, 127.7, 126.9, 126.4, 124.6, 123.6, 121.7.

2-(2-Thiophen-2-yl-vinyl)-3*H*-quinazolin-4-one (5.01m): ^{1}H NMR (400 MHz, DMSO-d_6) δ 12.26 (s, 1H), 8.21 – 8.01 (m, 2H), 7.79 (t, J = 7.1 Hz, 1H), 7.74 – 7.59 (m, 2H), 7.46 (dp, J = 9.9, 3.2, 2.4 Hz, 2H), 7.16 (p, J = 3.6, 2.9 Hz, 1H), 6.74 (d, J = 15.8 Hz, 1H); **^{13}C NMR** (100 MHz, DMSO-d_6) δ 162.10, 151.60, 149.49, 140.53, 134.95, 131.88, 131.4, 129.2, 129.0, 127.5, 126.5, 126.3, 121.5, 119.9, 40.6, 40.4, 40.2, 40.0, 39.8, 39.6, 39.3.

2-(2-Furyl-2-yl-vinyl)-3*H*-quinazolin-4-one (5.01n): ^{1}H NMR (400 MHz, DMSO-d_6) δ 12.34 (s, 1H), 8.10 (dd, J = 7.9, 1.6 Hz, 1H), 7.95 – 7.73 (m, 3H), 7.64 (d, J = 8.2 Hz, 1H), 7.46 (t, J = 7.5 Hz, 1H), 6.90 (d, J = 3.4 Hz, 1H), 6.77 (d, J = 15.8 Hz, 1H), 6.65 (dd, J = 3.3, 1.8 Hz, 1H); **^{13}C NMR** (100

MHz, DMSO-d_6) δ 162.2, 151.7, 151.5, 149.5, 145.8, 134.9, 127.5, 126.5, 126.3, 125.9, 121.5, 118.4, 115.1, 113.2.

2-[2-(1H-Indol-3-yl)-vinyl]-3*H*-quinazolin-4-one (5.01o): ^{1}H NMR (400 MHz, DMSO-

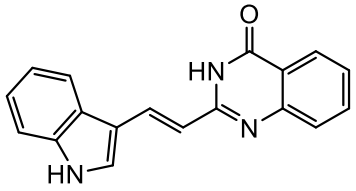

d_6) δ 12.13 (s, 1H), 11.73 (s, 1H), 8.20 (d, J = 16.0 Hz, 1H), 8.09 (dd, J = 8.0, 1.5 Hz, 1H), 8.07 – 7.99 (m, 1H), 7.93 (d, J = 2.7 Hz, 1H), 7.83 – 7.73 (m, 1H), 7.63 (d, J = 8.2 Hz, 1H), 7.55 – 7.47 (m, 1H), 7.41 (t, J = 7.5 Hz, 1H), 7.24 (qd, J = 7.4, 3.6 Hz, 2H), 6.98 (d, J = 16.0 Hz, 1H); **^{13}C NMR** (100 MHz, DMSO-d_6) δ 162.3, 153.3, 150.0, 137.9, 134.8, 133.7, 131.5, 127.1, 126.3, 125.6, 125.3, 122.9, 121.2, 121.1, 120.5, 114.7, 113.2, 112.9.

2-[2-(2,3,4,5,6-Pentfluoro-phenyl)-vinyl]-3*H*-quinazolin-4-one (**5.01p**): **^{1}H NMR** (400

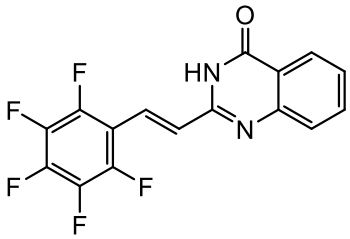

MHz, Pyridine-d_5) δ 13.73 (s, 1H), 8.55 (dd, J = 7.9, 1.6 Hz, 1H), 8.13 (d, J = 16.2 Hz, 1H), 7.95 (d, J = 8.1 Hz, 1H), 7.75 (ddd, J = 8.3, 7.0, 1.6 Hz, 1H), 7.53 – 7.40 (m, 2H); **^{13}C NMR** (100 MHz, DMSO-d_6) δ 162.5, 151.0, 146.7, 144.3, 144.2, 135.0, 129.2, 128.0, 126.8, 126.5, 122.7, 122.5, 122.1, 110.9; **^{19}F NMR** (376 MHz, Pyridine-d_5) δ -141.14, -153.84, -162.54; HRMS (ESI-TOF) *m/z*: $[M + H]^+$ Calcd for $C_{16}H_7F_5N_2O$ 339.0557, Found 339.0558.

Starting materials **5.01q** and **5.01r** were prepared from 2-amino benzamide or its analogous following general procedure given below

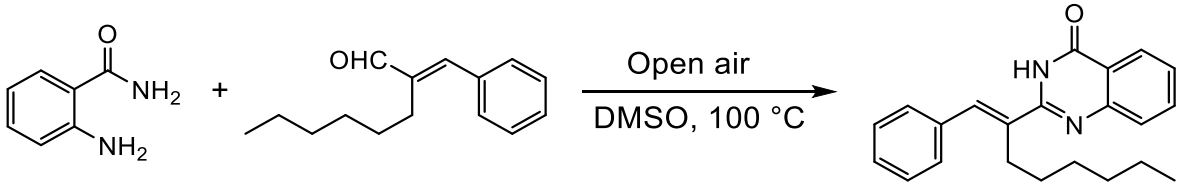

Representative experimental procedure: Anthranilamide (0.681 g, 5.0 mmol) and α-hexylcinnamaldehyde (1.298 g, 6 mmol, 1.2 equiv) were dissolved in DMSO (10 mL). Then, the

reaction mixture was stirred at 100 °C in an open flask for 20 h (TLC). The reaction mixture was cooled to rt, water (100 mL) was added to get the precipitate. The precipitates were collected by filtration and purified by recrystallization (EtOH) to afforded analytically pure **5.01q** (1.097 g, 66%) as white solid, 2-(1-Benzylidene-heptyl)-3H-quinazolin-4-one **(5.01q): ^{1}H NMR** (400 MHz, DMSO-d_6) δ 12.24 (s, 1H), 8.14 (d, J = 8.0 Hz, 1H), 7.82 (t, J = 7.8 Hz, 1H), 7.67 (d, J = 8.2 Hz, 1H), 7.57 – 7.29 (m, 7H), 2.94 – 2.64 (m, 2H), 1.60 – 1.42 (m, 2H), 1.37 – 1.16 (m, 6H), 0.82 (d, J = 6.4 Hz, 3H); **^{13}C NMR** (100 MHz, DMSO-d_6) δ 162.5, 154.9, 149.1, 136.6, 136.4, 134.9, 134.5, 129.3, 129.0, 128.4, 127.9, 126.9, 126.3, 121.5, 31.2, 28.9, 28.6, 27.8, 22.4, 14.3; HRMS (ESI-TOF) *m/z*: $[M + H]^+$ Calcd for $C_{22}H_{24}N_2O$ 333.1967, Found 333.1965.

2-Styryl-3H-thieno[3,2-d]pyrimidin-4-one (5.01r): ^{1}H NMR (400 MHz, DMSO-d_6) δ

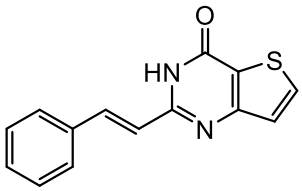

12.65 (s, 1H), 8.20 (d, J = 5.3 Hz, 1H), 7.93 (d, J = 16.0 Hz, 1H), 7.66 (d, J = 7.4 Hz, 2H), 7.44 (dt, J = 16.1, 6.2 Hz, 4H), 7.28 (d, J = 6.5 Hz, 1H), 7.16 (d, J = 16.2 Hz, 1H); **^{13}C NMR** (100 MHz, DMSO-d_6) δ 158.6, 158.5, 153.7, 138.4, 135.7, 135.4, 130.2, 129.5, 128.8, 128.1, 125.6, 121.0, 40.6, 40.4, 40.2, 40.0, 39.8, 39.6, 39.4; **HRMS** (ESI-TOF) *m/z*: $[M + H]^+$ Calcd for $C_{14}H_{12}N_2OS$ 257.0749, Found 257.0747.

5.14. Analytical data of purified compounds

5.14.1. Spectroscopic data of pyrido[2,1-b]quinazolin-11-one derivatives

8,9-Diphenyl-7-p-tolyl-pyrido[2,1-b]quinazolin-11-one: Prepared by general procedure

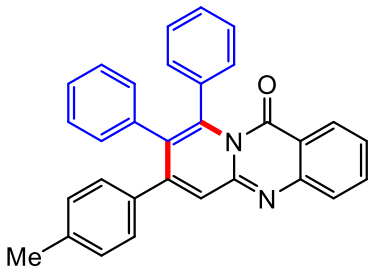

of fused quinazolinone synthesis to yield **5.04b** (75%). **^{1}H NMR** (400 MHz, $CDCl_3$) δ 8.20 (ddd, J = 8.2, 1.5, 0.7 Hz, 1H), 7.86 – 7.73 (m, 2H), 7.52 (s, 1H), 7.38 (ddd, J = 8.1, 6.6, 1.5 Hz, 1H), 7.20 – 7.14 (m, 3H), 7.13 – 7.07 (m, 2H), 7.05 – 6.96 (m, 7H), 6.88 –

6.78 (m, 2H), 2.30 (s, 3H); **^{13}C NMR** (100 MHz, $CDCl_3$) δ 160.9, 148.9, 148.5, 148.2, 140.4, 138.0, 136.7, 135.6, 135.0, 134.7, 131.4, 129.3, 128.9, 128.7, 128.6, 127.4, 127.3, 127.1, 127.0, 126.7, 126.1, 125.3, 124.8, 118.7, 21.2; **HRMS** (ESI-TOF) *m/z*: $[M + H]^+$ Calcd for $C_{31}H_{22}N_2O$ 439.1810, Found 439.1812.

7-(4-Methoxy-phenyl)-8,9-diphenyl-pyrido[2,1-b]quinazolin-11-one: Prepared by general procedure of fused quinazolinone synthesis to yield **5.04c** (72%). **^{1}H NMR** (400 MHz, $CDCl_3$) δ 8.20 (dd, J = 8.1, 1.4 Hz, 1H), 7.85 – 7.73 (m, 2H), 7.51 (s, 1H), 7.37 (ddd, J = 8.3, 6.7, 1.5 Hz, 1H), 7.17 (dd, J = 4.9, 2.1 Hz, 3H), 7.09 (dd, J = 6.5, 3.0 Hz, 2H), 7.06 – 7.00 (m, 5H), 6.86 – 6.79 (m, 2H), 6.76 – 6.68 (m, 2H), 3.77 (s, 3H); **^{13}C NMR** (100 MHz, $CDCl_3$) δ 160.9, 159.4, 149.0, 148.2, 148.1, 140.4, 136.8, 135.7, 134.7, 131.4, 130.3, 130.2, 129.3, 128.7, 127.4, 127.4, 127.1, 127.0, 126.7, 126.1, 125.0, 124.8, 118.7, 113.4, 55.2; **HRMS** (ESI-TOF) *m/z*: $[M + H]^+$ Calcd for $C_{31}H_{22}N_2O_2$ 455.1760, Found 455.1780.

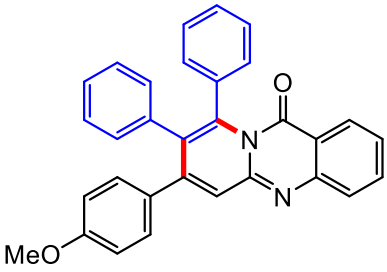

7-(4-Dimethylamino-phenyl)-8,9-diphenyl-pyrido[2,1-b]quinazolin-11-one: Prepared by general procedure of fused quinazolinone synthesis to yield **5.04d** (70%). **^{1}H NMR** (400 MHz, $CDCl_3$) δ 8.18 (ddd, J = 8.1, 1.4, 0.7 Hz, 1H), 7.84 – 7.71 (m, 2H), 7.52 (s, 1H), 7.34 (ddd, J = 8.1, 6.6, 1.5 Hz, 1H), 7.16 (dt, J = 4.4, 2.8 Hz, 3H), 7.12 – 7.07 (m, 2H), 7.07 – 7.02 (m, 3H), 7.01 – 6.95 (m, 2H), 6.92 – 6.82 (m, 2H), 6.55 – 6.46 (m, 2H), 2.94 (s, 6H); **^{13}C NMR** (100 MHz, $CDCl_3$) δ 160.9, 150.0, 149.3, 148.5, 148.4, 140.3, 137.0, 136.1, 134.6, 131.6, 130.2, 129.5, 128.8, 127.4, 127.3, 127.0, 126.9, 126.6, 125.9, 125.1, 124.4, 124.0, 118.5, 111.3, 40.1; **HRMS** (ESI-TOF) *m/z*: $[M + H]^+$ Calcd for $C_{32}H_{25}N_3O$ 468.2076, Found 468.2072.

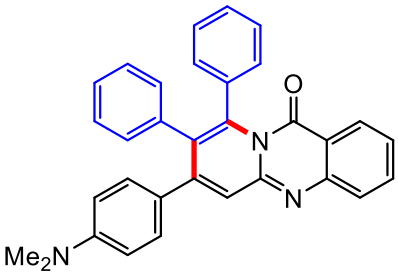

7-(4-Nitro-phenyl)-8,9-diphenyl-pyrido[2,1-b]quinazolin-11-one: Prepared by general procedure of fused quinazolinone synthesis to yield **5.04e** (71%).

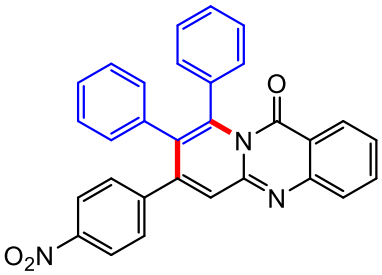

^{1}H NMR (400 MHz, $CDCl_3$) δ 8.21 (dd, J = 8.1, 1.4 Hz, 1H), 8.10 – 8.04 (m, 2H), 7.88 – 7.76 (m, 2H), 7.54 (s, 1H), 7.45-7.41 (m, 1H), 7.32 – 7.26 (m, 3H), 7.24 – 7.15 (m, 3H), 7.14 – 7.07 (m, 2H), 7.07 – 6.98 (m, 3H), 6.83 – 6.76 (m, 2H); **^{13}C NMR** (100 MHz, $CDCl_3$) δ 160.6, 147.8, 147.4, 146.1, 144.5, 141.2, 136.2, 134.9, 134.8, 131.2, 129.8, 128.6, 128.0, 127.7, 127.5, 127.5, 127.3, 127.2, 126.3, 126.2, 125.5, 123.1; **HRMS** (ESI-TOF) *m/z*: $[M + H]^+$ Calcd for $C_{30}H_{19}N_3O_3$ 470.1505, Found 470.1509.

8,9-Diphenyl-7-(4-trifluoromethyl-phenyl)-pyrido[2,1-b]quinazolin-11-one: Prepared by general procedure of fused quinazolinone synthesis to yield **5.04f** (78%).

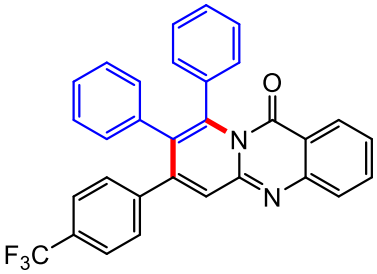

^{1}H NMR (400 MHz, $CDCl_3$) δ 8.24 – 8.18 (m, 1H), 7.84 (ddd, J = 8.3, 6.8, 1.5 Hz, 1H), 7.81 – 7.76 (m, 1H), 7.52 (s, 1H), 7.49 – 7.45 (m, 2H), 7.41 (ddd, J = 8.1, 6.8, 1.4 Hz, 1H), 7.25 – 7.21 (m, 2H), 7.20 – 7.15 (m, 3H), 7.13 – 7.07 (m, 2H), 7.06 – 6.98 (m, 3H), 6.82 – 6.77 (m, 2H); **^{13}C NMR** (100 MHz, $CDCl_3$) δ 160.7, 148.5, 148.0, 146.9, 141.6, 140.9, 136.4, 135.0, 134.8, 131.3, 130.2, 129.9, 129.2, 128.6, 128.4, 127.6, 127.4, 127.4, 127.2, 127.0, 126.2, 126.0, 125.3, 125.2 (q, J = 271.7 Hz), 124.9 (q, J = 3.7 Hz), 118.9; **^{19}F NMR** (376 MHz, $CDCl_3$) δ -62.7; **HRMS** (ESI-TOF) *m/z*: $[M + H]^+$ Calcd for $C_{31}H_{19}F_3N_2O$ 493.1528, Found 493.1536.

4-(11-Oxo-8,9-diphenyl-11H-pyrido[2,1-b]quinazolin-7-yl)-benzonitrile: Prepared by general procedure of fused quinazolinone synthesis to yield **5.04g** (76%). **^{1}H NMR** (400 MHz, $CDCl_3$) δ 8.23 – 8.18 (m, 1H), 7.84 (ddd, J = 8.4, 6.8, 1.5 Hz, 1H), 7.80 – 7.76 (m, 1H), 7.53 – 7.47 (m, 3H), 7.42 (ddd, J = 8.2, 6.9, 1.3 Hz, 1H), 7.24 – 7.16 (m, 5H), 7.12 – 7.07 (m, 2H), 7.07 – 6.99 (m, 3H), 6.81 – 6.75 (m, 2H); **^{13}C NMR** (100 MHz, $CDCl_3$) δ 160.7, 148.3, 147.9, 146.4, 142.6, 141.1, 136.2, 135.0, 134.8, 131.7, 131.2, 129.6, 128.6, 128.0, 127.7, 127.5, 127.2, 127.2, 126.3, 126.1, 125.4, 119.0, 118.3, 111.9; **HRMS** (ESI-TOF) *m/z*: $[M + H]^+$ Calcd for $C_{32}H_{23}N_3O_3$ 482.1869, Found 482.1873.

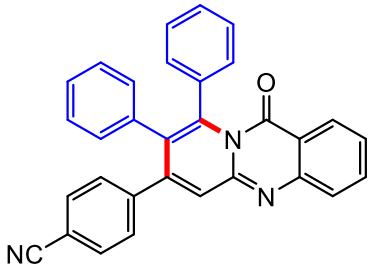

7-(4-Chloro-phenyl)-8,9-diphenyl-pyrido[2,1-b]quinazolin-11-one: Prepared by general procedure of fused quinazolinone synthesis to yield **5.04h** (77%). **^{1}H NMR** (400 MHz, $CDCl_3$) δ 8.21 – 8.19 (m, 1H), 7.85 – 7.81 (m, 1H), 7.79 – 7.76 (m, 1H), 7.50 (s, 1H), 7.42 – 7.38 (m, 1H), 7.19 – 7.17 (m, 5H), 7.11 – 7.01 (m, 7H), 6.82 – 6.77 (m, 2H); **^{13}C NMR** (100 MHz, $CDCl_3$) δ 160.8, 148.6, 148.0, 147.2, 140.7, 136.5, 136.4, 135.2, 134.8, 134.3, 131.3, 130.2, 128.7, 128.7, 128.2, 127.5, 127.4, 127.3, 127.1, 126.9, 126.2, 125.7, 125.1, 118.8; **HRMS** (ESI-TOF) *m/z*: $[M + H]^+$ Calcd for $C_{30}H_{19}ClN_2O$ 459.1264, Found 459.1254.

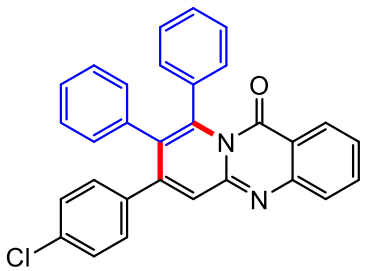

2-Chloro-7,8,9-triphenyl-pyrido[2,1-b]quinazolin-11-one: Prepared by general procedure of fused quinazolinone synthesis to yield **5.04i** (76%). **^{1}H NMR** (400 MHz, $CDCl_3$) δ 8.17 – 8.16 (m, 1H), 7.73 (d, J = 1.8 Hz, 2H), 7.53 (s, 1H), 7.25-7.15 (m, 6H), 7.12-7.08 (m, 4H), 7.04 – 6.97 (m, 3H), 6.84 – 6.77 (m, 2H); **^{13}C NMR** (100 MHz, $CDCl_3$) δ 159.9, 148.9, 146.6, 140.5, 137.8, 136.4, 135.3, 135.2, 131.3, 130.4, 129.6, 128.9, 128.7, 128.1, 127.9,

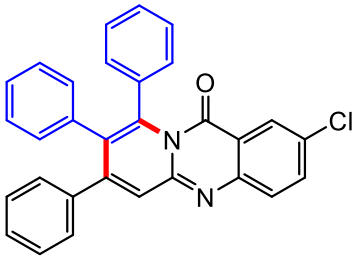

127.9, 127.4, 127.1, 126.8, 126.5, 125.5, 119.5; **HRMS** (ESI-TOF) *m/z*: $[M + H]^+$ Calcd for $C_{30}H_{19}ClN_2O$ 459.1264, Found 459.1260.

8,9-Bis-(4-bromo-phenyl)-7-phenyl-pyrido[2,1-b]quinazolin-11-one: Prepared by general procedure of fused quinazolinone synthesis to yield **5.04j** (78%). **^{1}H NMR** (400 MHz, $CDCl_3$) δ 8.19 (ddd, J = 8.1, 1.6, 0.7 Hz, 1H), 7.86 (ddd, J = 8.3, 6.8, 1.5 Hz, 1H), 7.82 – 7.79 (m, 1H), 7.58 (s, 1H), 7.47 – 7.41 (m, 3H), 7.30 – 7.19 (m, 8H), 7.08 – 7.03 (m, 2H), 6.93 – 6.90 (m, 2H); **^{13}C NMR** (100 MHz, $CDCl_3$) δ 160.7, 148.4, 148.1, 147.9, 139.3, 137.4, 135.3, 135.0, 134.2, 132.8, 130.8, 130.6, 130.1, 128.8, 128.3, 128.3, 128.1, 127.3, 126.2, 126.0, 125.4, 121.7, 121.4, 118.6; **HRMS** (ESI-TOF) *m/z*: $[M + H]^+$ Calcd for $C_{30}H_{18}Br_2N_2O$ 582.9846, Found 582.9850.

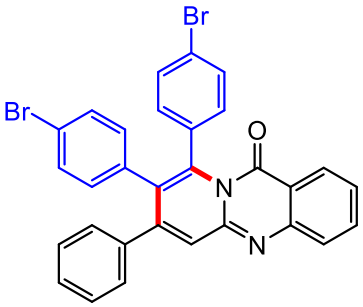

7-Phenyl-8,9-bis-(4-trifluoromethyl-phenyl)-pyrido[2,1-b]quinazolin-11-one: Prepared by general procedure of fused quinazolinone synthesis to yield **5.04k** (77%). **^{1}H NMR** (400 MHz, $CDCl_3$) δ 8.19 (ddd, J = 8.1, 1.6, 0.7 Hz, 1H), 7.86 (ddd, J = 8.3, 6.8, 1.5 Hz, 1H), 7.82 – 7.79 (m, 1H), 7.58 (s, 1H), 7.47 – 7.41 (m, 3H), 7.30 – 7.19 (m, 8H), 7.08 – 7.03 (m, 2H), 6.93 – 6.90 (m, 2H); **^{13}C NMR** (100 MHz, $CDCl_3$) δ 160.6, 148.2, 148.0, 147.6, 140.0, 139.1, 139.0, 137.1, 135.2, 131.6, 129.6, 129.5, 129.3, 129.2, 128.9, 128.8, 128.5, 128.3, 128.2, 127.3, 126.5, 126.4, 125.58, 125.2 (q, J = 273.2 Hz), 125.0 (q, J = 271.4 Hz), 124.51, 124.5 (q, J = 3.74 Hz), 124.3 (q, J = 3.71 Hz), 118.52; **HRMS** (ESI-TOF) *m/z*: $[M + H]^+$ Calcd for $C_{32}H_{18}F_6N_2O$ 561.1401, Found 561.1406.

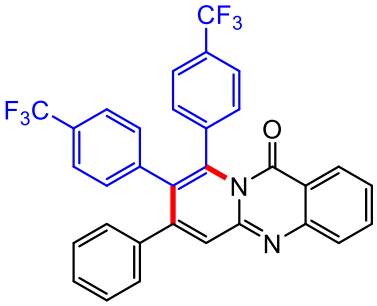

8,9-Bis-(4-methoxy-phenyl)-7-phenyl-pyrido[2,1-b]quinazolin-11-one: Prepared by general procedure of fused quinazolinone synthesis to yield **5.04l** (74%). **^{1}H NMR** (400 MHz, $CDCl_3$) δ 8.22 - 8.19 (m, 1H), 7.84 – 7.74 (m, 2H), 7.49 (s, 1H), 7.40 – 7.36 (m, 1H), 7.26 – 7.18 (m, 3H), 7.13 – 7.06 (m, 2H), 7.03 – 6.96 (m, 2H), 6.76 – 6.67 (m, 4H), 6.59 – 6.51 (m, 2H), 3.78 (s, 3H), 3.70 (s, 3H); **^{13}C NMR** (100 MHz, $CDCl_3$) δ 161.1, 158.4, 158.1, 149.0, 148.9, 148.1, 140.5, 138.2, 134.6, 132.4, 129.9, 129.1, 129.0, 128.9, 127.9, 127.7, 127.4, 126.1, 125.2, 124.8, 118.8, 114.2, 112.9, 112.7, 55.0, 55.0; **HRMS** (ESI-TOF) *m/z*: $[M + H]^+$ Calcd for $C_{32}H_{24}N_2O_3$ 485.1865, Found 485.1870.

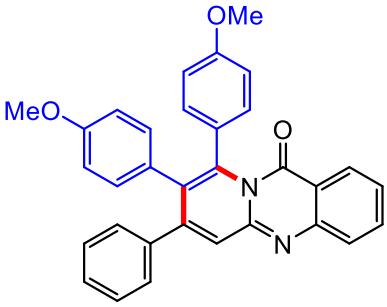

7-(2-Fluoro-phenyl)-8,9-diphenyl-pyrido[2,1-b]quinazolin-11-one: Prepared by general procedure of fused quinazolinone synthesis to yield **5.04m** (72%). **^{1}H NMR** (400 MHz, $CDCl_3$) δ 8.25 – 8.18 (m, 1H), 7.87 – 7.76 (m, 2H), 7.52 (s, 1H), 7.41 (ddd, J = 8.1, 6.6, 1.6 Hz, 1H), 7.19 – 7.15 (m, 3H), 7.14 – 7.08 (m, 3H), 7.03 (dd, J = 7.5, 1.1 Hz, 1H), 6.99 – 6.93 (m, 3H), 6.93 – 6.87 (m, 1H), 6.86 – 6.80 (m, 2H); **^{13}C NMR** (100 MHz, $CDCl_3$) δ 160.9, 158.8 (d, J = 245.2 Hz), 148.2 (d, J = 55.2 Hz), 143.4, 140.3, 136.5, 135.20, 134.7, 130.9, 130.6 (d, J = 2.7 Hz), 130.2 (d, J = 7.9 Hz), 129.7, 128.6, 127.3 (d, J = 13.4 Hz), 127.2, 127.1, 127.1, 126.7, 126.6, 126.2, 125.9 (d, J = 14.5 Hz), 125.2, 123.7 (d, J = 3.9 Hz), 118.9, 115.4 (d, J = 21.0 Hz); **^{19}F NMR** (376 MHz, $CDCl_3$) δ -112.26; **HRMS** (ESI-TOF) *m/z*: $[M + H]^+$ Calcd for $C_{30}H_{19}FN_2O$ 443.1560, Found 443.1564.

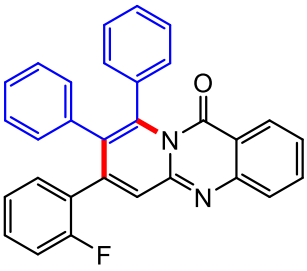

7-Benzo[1,3]dioxol-5-yl-8,9-diphenyl-pyrido[2,1-b]quinazolin-11-one: Prepared by general procedure of fused quinazolinone synthesis to yield **5.04n** (75%). 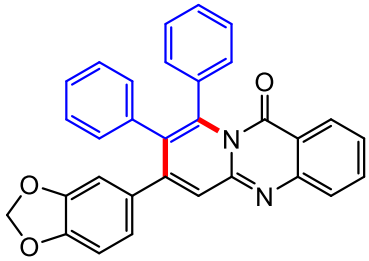

^{1}H NMR (400 MHz, $CDCl_3$) δ 8.21 – 8.18 (m, 1H), 7.85 – 7.74 (m, 2H), 7.50 (s, 1H), 7.40 – 7.36 (m, 1H), 7.19 – 7.15 (m, 3H), 7.11 – 7.00 (m, 5H), 6.86 – 6.80 (m, 2H), 6.69 – 6.60 (m, 2H), 6.54 (d, J = 1.7 Hz, 1H), 5.92 (s, 2H); **^{13}C NMR** (100 MHz, $CDCl_3$) δ 160.8, 148.8, 148.1, 148.1, 147.5, 147.2, 140.5, 136.7, 135.5, 134.7, 131.7, 131.3, 129.2, 128.7, 127.4, 127.2, 127.1, 127.0, 126.8, 126.0, 125.2, 124.9, 123.2, 118.7, 109.4, 107.9, 101.2; **HRMS** (ESI-TOF) *m/z*: $[M + H]^+$ Calcd for $C_{31}H_{20}N_2O_3$ 469.1552, Found 469.1556.

8,9-Diphenyl-7-pyridin-2-yl-pyrido[2,1-b]quinazolin-11-one: Prepared by general procedure of fused quinazolinone synthesis to yield **5.04o** (66%). 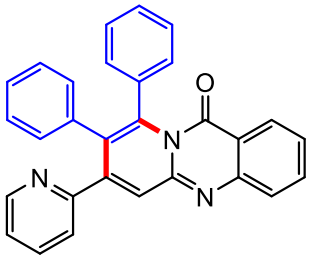

^{1}H NMR (400 MHz, $CDCl_3$) δ 8.51 – 8.43 (m, 2H), 8.21 (dd, J = 8.3, 1.5 Hz, 1H), 7.87 – 7.77 (m, 2H), 7.55 (s, 1H), 7.44-7.39 (m, 1H), 7.35-7.32 (m, 1H), 7.21 – 7.16 (m, 3H), 7.13-7.07 (m, 3H), 7.06 – 6.99 (m, 3H), 6.83-66.80 (m, 2H); **^{13}C NMR** (100 MHz, $CDCl_3$) δ 160.7, 149.2, 149.1, 148.5, 147.9, 144.8, 141.0, 136.3, 136.1, 134.8, 133.9, 131.3, 128.6, 128.5, 127.7, 127.4, 127.4, 127.2, 127.2, 126.2, 126.1, 125.3, 122.6, 118.9; **HRMS** (ESI-TOF) *m/z*: $[M + H]^+$ Calcd for $C_{29}H_{19}N_3O$ 426.1606, Found 426.1609.

8,9-Diphenyl-7-thiophen-2-yl-pyrido[2,1-b]quinazolin-11-one: Prepared by general procedure of fused quinazolinone synthesis to yield **5.04p** (72%). 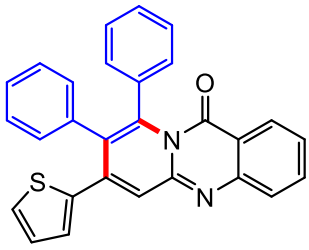

^{1}H NMR (400 MHz, $CDCl_3$) δ 8.21 – 8.15 (m, 1H), 7.85 – 7.75 (m, 3H), 7.40 – 7.36 (m, 1H), 7.30 (d, J = 1.2 Hz, 2H), 7.20 – 7.14 (m, 5H), 7.12 – 7.05 (m, 2H), 7.03 – 6.97 (m, 2H), 6.88 (dd, J = 5.1, 3.7 Hz, 1H), 6.74

(dd, J = 3.8, 1.2 Hz, 1H); **^{13}C NMR** (100 MHz, $CDCl_3$) δ 160.6, 148.7, 148.1, 140.9, 140.8, 139.2, 136.7, 135.4, 134.8, 131.6, 129.2, 128.6, 128.6, 128.1, 127.8, 127.6, 127.5, 127.3, 127.2, 127.0, 126.0, 125.0, 124.0, 118.7; **HRMS** (ESI-TOF) *m/z*: $[M + H]^+$ Calcd for $C_{28}H_{18}N_2OS$ 431.1140, Found 431.1146.

7-Furan-2-yl-8,9-diphenyl-pyrido[2,1-b]quinazolin-11-one: Prepared by general procedure of fused quinazolinone synthesis to yield **5.04q** (76%). **^{1}H NMR** (400 MHz, $CDCl_3$) δ 8.22 – 8.13 (m, 1H), 8.03 (s, 1H), 7.83 – 7.73 (m, 2H), 7.48 (d, J = 1.6 Hz, 1H), 7.38 – 7.32 (m, 1H), 7.27 – 7.22 (m, 3H), 7.18 – 7.13 (m, 3H), 7.10 – 7.06 (m, 4H), 6.21 (dt, J = 3.4, 1.6 Hz, 1H), 5.09 (d, J = 3.5 Hz, 1H); **^{13}C NMR** (100 MHz, $CDCl_3$) δ 160.6, 149.3, 149.1, 148.4, 143.9, 140.9, 136.7, 136.0, 135.4, 134.7, 131.1, 128.6, 128.0, 127.8, 127.4, 127.1, 127.0, 126.2, 126.1, 124.8, 120.5, 118.6, 114.1, 112.2; **HRMS** (ESI-TOF) *m/z*: $[M + H]^+$ Calcd for $C_{28}H_{18}N_2O_2$ 415.1447, Found 415.1442.

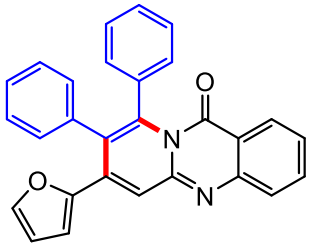

7-(1H-Indol-3-yl)-8,9-diphenyl-pyrido [2,1-b]quinazolin-11-one: Prepared by general procedure of fused quinazolinone synthesis to yield **5.04r** (73%). **^{1}H NMR** (400 MHz, DMSO-d_6) δ 11.37 (s, 1H), 8.01 – 7.94 (m, 1H), 7.92 – 7.81 (m, 2H), 7.72 (d, J = 8.3 Hz, 1H), 7.66 (s, 1H), 7.42 – 7.34 (m, 2H), 7.27 – 6.96 (m, 12H), 6.22 (d, J = 2.8 Hz, 1H); **^{13}C NMR** (100 MHz, DMSO-d_6) δ 160.5, 149.3, 148.6, 142.1, 140.5, 137.4, 136.8, 136.3, 135.1, 131.8, 129.5, 129.3, 127.9, 127.5, 127.1, 127.1, 127.0, 126.3, 126.2, 124.7, 122.6, 122.5, 120.9, 119.4, 118.4, 112.6, 111.5, 100.0; **HRMS** (ESI-TOF) *m/z*: $[M + H]^+$ Calcd for $C_{32}H_{21}N_3O$ 464.1763, Found 464.1769.

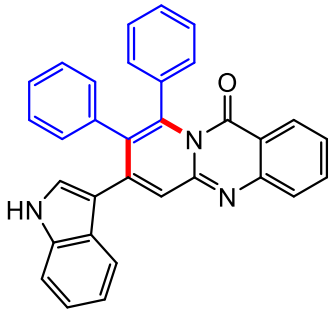

7-Pentafluorophenyl-8,9-diphenyl-pyrido[2,1-b]quinazolin-11-one: Prepared by general procedure of fused quinazolinone synthesis to yield **5.04s** (72%). **^{1}H NMR** (400 MHz, $CDCl_3$) δ 8.22 (dd, J = 8.0, 1.4 Hz, 1H), 7.89 – 7.76 (m, 2H), 7.50 (s, 1H), 7.47 – 7.43 (m, 1H), 7.22 – 7.14 (m, 3H), 7.14 – 7.08 (m, 2H), 7.08 – 7.00 (m, 3H), 6.91 – 6.84 (m, 2H); **^{13}C NMR** (100 MHz, $CDCl_3$) δ 160.7, 147.8, 147.6, 144.6 (m), 142.5, 141.3, 139.9 (d, J = 14 Hz), 138.4 (m), 135.9, 134.9, 135.6, 134.1, 129.8, 128.7, 128.4, 128.3, 127.8, 127.7 (d, J = 23 Hz), 127.4, 127.3, 126.4, 125.8, 119.2, 112.7 (m); **HRMS** (ESI-TOF) *m/z*: $[M + H]^+$ Calcd for $C_{30}H_{15}F_5N_2O$ 515.1183, Found 515.1186.

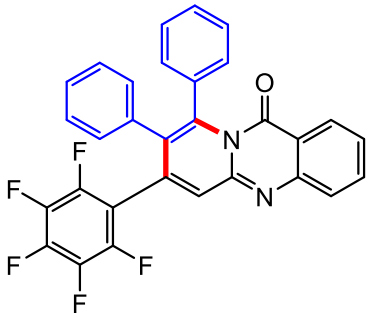

6-Hexyl-7,8,9-triphenyl-pyrido[2,1-b]quinazolin-11-one: Prepared by general procedure of fused quinazolinone synthesis to yield **5.04t** (71%). **^{1}H NMR** (400 MHz, $CDCl_3$) δ 8.21-8.19 (m, 1H), 7.85 – 7.80 (m, 2H), 7.41-7.36 (m, 1H), 7.23 – 7.16 (m, 3H), 7.17-7.11 (m, 3H), 7.07-7.04 (m, 2H), 7.01 – 6.96 (m, 2H), 6.91-6.87 (m, 3H), 6.70 (dd, J = 6.7, 2.9 Hz, 2H), 2.86 – 2.78 (m, 2H), 1.69-1.65 (m, 2H), 1.33 – 1.21 (m, 6H), 0.88 (t, J = 6.8 Hz, 3H); **^{13}C NMR** (100 MHz, $CDCl_3$) δ 161.8, 148.1, 147.9, 145.6, 138.0, 137.0, 136.9, 136.3, 135.7, 134.2, 131.2, 129.6, 128.9, 128.5, 127.7, 127.1, 127.1, 127.0, 126.9, 126.9, 126.1, 124.7, 118.8, 31.2, 29.6, 29.6, 29.2, 22.5, 14.1; **HRMS** (ESI-TOF) *m/z*: $[M + H]^+$ Calcd for $C_{36}H_{32}N_2O$ 509.2593, Found 509.2592.

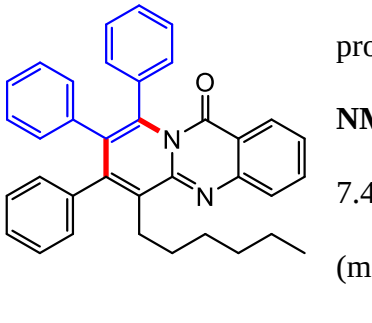

7-Phenyl-8,9-di-thiophen-2-yl-pyrido[2,1-b]quinazolin-11-one: Prepared by general procedure of fused quinazolinone synthesis to yield **5.04u** (70%). **^{1}H NMR** (400 MHz, $CDCl_3$) δ 8.25-8.23 (m, 1H), 7.86-7.75 (m, 2H), 7.50 (s, 1H), 7.44-7.40 (m, 1H), 7.34 (dd, J = 4.1, 2.2 Hz, 1H), 7.31 – 7.25

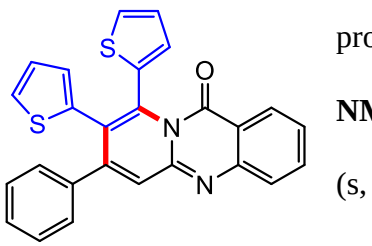

(m, 4H), 7.24 – 7.20 (m, 2H), 7.14 (dd, *J* = 5.1, 1.2 Hz, 1H), 6.94 – 6.89 (m, 2H), 6.77 (dd, *J* = 5.1, 3.5 Hz, 1H), 6.69 (dd, *J* = 3.5, 1.2 Hz, 1H); **^{13}C NMR** (100 MHz, $CDCl_3$) δ 160.7, 148.5, 148.4, 147.8, 137.7, 136.9, 136.0, 135.4, 134.8, 130.8, 129.0, 128.4, 128.3, 128.0, 127.4, 127.2, 126.8, 126.2, 126.1, 126.0, 125.9, 125.3, 124.6, 118.9; **HRMS** (ESI-TOF) *m/z*: $[M + H]^+$ Calcd for $C_{26}H_{16}S_2N_2O$ 437.0782, Found 437.0784.

7-Phenyl-8,9-dipropyl-pyrido[2,1-b]quinazolin-11-one: Prepared by general procedure of fused quinazolinone synthesis to yield **5.04v** (65%).**^{1}H NMR** (400 MHz, $CDCl_3$) δ 8.36 (dd, *J* = 8.2, 1.5 Hz, 1H), 7.78 (ddd, *J* = 8.4, 6.9, 1.6 Hz, 1H), 7.70 (dt, *J* = 8.3, 0.9 Hz, 1H), 7.49 – 7.39 (m, 4H), 7.39 – 7.34 (m, 2H), 7.19 (s, 1H), 3.37 – 3.25 (m, 2H), 2.59 – 2.49 (m, 2H), 1.75 – 1.67 (m, 2H), 1.39 – 1.32 (m, 2H), 1.02 (t, *J* = 7.3 Hz, 3H), 0.77 (t, *J* = 7.3 Hz, 3H); **^{13}C NMR** (100 MHz, $CDCl_3$) δ 162.3, 149.9, 148.9, 147.9, 142.7, 138.8, 134.4, 128.4, 128.2, 128.2, 127.1, 126.3, 125.8, 124.6, 124.5, 118.7, 32.3, 30.8, 23.6, 23.3, 14.3, 14.2; **HRMS** (ESI-TOF) *m/z*: $[M + H]^+$ Calcd for $C_{24}H_{24}N_2O$ 357.1967, Found 357.1967.

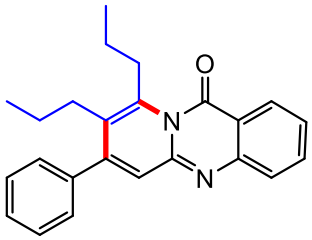

6,7,8-Triphenyl-1-thia-4,8a-diaza-cyclopenta[b]naphthalen-9-one: Prepared by general procedure of fused quinazolinone synthesis to yield **5.04w** (72%). **^{1}H NMR** (400 MHz, $CDCl_3$) δ 7.86 (d, *J* = 5.3 Hz, 1H), 7.67 (s, 1H), 7.39 (d, *J* = 5.3 Hz, 1H), 7.26 – 7.20 (m, 3H), 7.19 – 7.15 (m, 3H), 7.14 – 7.10 (m, 4H), 7.03 – 6.96 (m, 3H), 6.85 – 6.79 (m, 2H); ^{13}C NMR (100 MHz, $CDCl_3$) δ 157.0, 156.4, 150.4, 148.4, 140.8, 137.9, 136.7, 136.2, 135.5, 131.4, 130.3, 129.0, 128.8, 128.1, 127.9, 127.3, 127.2, 126.9, 126.7, 125.6, 124.4, 118.1; **HRMS** (ESI-TOF) *m/z*: $[M + H]^+$ Calcd for $C_{28}H_{18}N_2OS$ 431.1218, Found 431.1218.

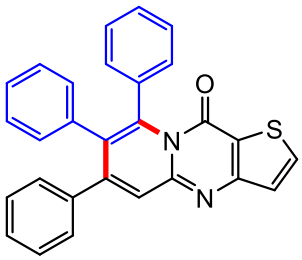

5.14.2. Spectroscopic data of 2-aminopyridine derivatives

2-(4,5,6-Triphenyl-pyridin-2-ylamino)-benzoic acid 2,2,2-trifluoro-ethyl ester:

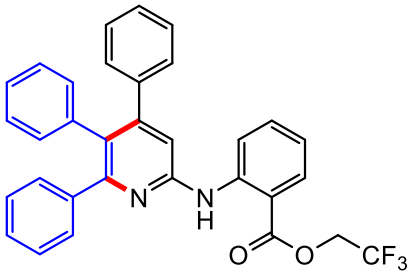

Prepared by general procedure of 2-aminopyridine synthesis to yield **5.12 b** (66%). **^{1}H NMR** (400 MHz, $CDCl_3$) δ 10.42 (s, 1H), 9.00 (d, J = 8.7 Hz, 1H), 8.10 (d, J = 8.1 Hz, 1H), 7.57 (dd, J = 8.8, 6.9 Hz, 1H), 7.40 – 7.34 (m, 2H), 7.27 – 7.19 (m, 6H), 7.14 – 7.04 (m, 5H), 6.93 (ddd, J = 23.7, 5.2, 2.9 Hz, 4H), 4.74 (td, J = 8.4, 1.6 Hz, 2H); ^{13}C NMR (101 MHz, $CDCl_3$) δ 166.8, 156.2, 153.1, 151.9, 145.5, 140.9, 139.6, 137.9, 135.5, 131.7, 131.4, 130.1, 129.2, 127.8, 127.7, 127.6, 127.5, 127.32, 127.27, 126.3, 123.1 q, J = 278.7 Hz), 121.7, 119.2, 118.4, 112.4, 111.3, 60.6 (q, J = 34.5 Hz); **^{9}F NMR** (376 MHz, $CDCl_3$) δ -73.50; HRMS (ESI-TOF) *m/z*: $[M + H]^+$ Calcd for $C_{32}H_{23}F_3N_2O_2$ 525.1790, Found 525.1794.

2-(5,6-Diphenyl-4-p-tolyl-pyridin-2-ylamino)-benzoic acid 2,2,2-trifluoro-ethyl ester:

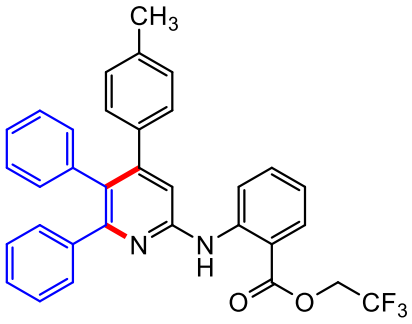

Prepared by general procedure of 2-aminopyridine synthesis to yield **5.12c** (67%). **^{1}H NMR** (400 MHz, $CDCl_3$) δ 10.41 (s, 1H), 8.99 (dd, J = 8.6, 1.1 Hz, 1H), 8.11 (dd, J = 8.1, 1.7 Hz, 1H), 7.57 (ddd, J = 8.8, 7.2, 1.7 Hz, 1H), 7.43 – 7.33 (m, 2H), 7.27 – 7.19 (m, 3H), 7.13 – 6.99 (m, 7H), 6.98 – 6.90 (m, 4H), 4.74 (q, J = 8.4 Hz, 2H), 2.33 (s, 3H); **^{13}C NMR** (101 MHz, $CDCl_3$) δ 166.8, 156.2, 153.1, 151.9, 145.6, 141.0, 138.2, 137.1, 136.6, 135.5, 131.8, 131.4, 130.1, 129.1, 128.6, 127.8, 127.7, 127.5, 127.3, 127.2, 126.2, 124.5 (q, J = 279.6 Hz), 121.7, 119.2, 118.4, 112.5, 111.2, 60.6 (q, J = 36.4 Hz), 21.2; **^{9}F NMR** (376 MHz, $CDCl_3$) δ -73.48; HRMS (ESI-TOF) *m/z*: $[M + H]^+$ Calcd for $C_{33}H_{25}F_3N_2O_2$ 539.1946, Found 555. 539.1949.

2-[4-(4-Methoxy-phenyl)-5,6-diphenyl-pyridin-2-ylamino]-benzoic acid 2,2,2-trifluoro-ethyl ester:

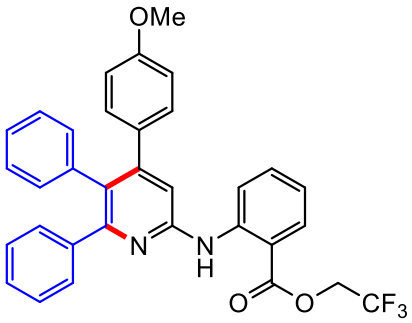

Prepared by general procedure of 2-aminopyridine synthesis to yield **5.12d** (62%). **^{1}H NMR** (400 MHz, $CDCl_3$) δ 10.38 (s, 1H), 8.97 (dd, J = 8.8, 1.1 Hz, 1H), 8.10 (dd, J = 8.1, 1.7 Hz, 1H), 7.58 – 7.54 (m, 1H), 7.38 – 7.32 (m, 2H), 7.24 – 7.19 (m, 3H), 7.11 – 7.07 (m, 3H), 7.05 – 7.01 (m, 2H), 6.97 – 6.88 (m, 4H), 6.78 – 6.72 (m, 2H), 4.73 (q, J = 8.4 Hz, 2H), 3.79 (s, 3H); **^{13}C NMR** (100 MHz, $CDCl_3$) δ 166.8, 158.9, 156.2, 153.1, 151.5, 145.6, 141.0, 138.2, 135.5, 131.9, 131.8, 131.4, 130.5, 130.1, 127.8, 127.7, 127.5, 127.2, 126.2 (q, J = 275.2 Hz), 119.2, 118.3, 113.3, 112.4, 111.2, 100.0, 60.7 (q, J = 37.2 Hz), 55.2; **^{9}F NMR** (376 MHz, $CDCl_3$) δ -73.50; HRMS (ESI-TOF) *m/z*: $[M + H]^+$ Calcd for $C_{33}H_{25}F_3N_2O_3$ 555.1896, Found 555.1892.

2-[4-(4-Dimethylamino-phenyl)-5,6-diphenyl-pyridin-2-ylamino]-benzoic acid 2,2,2-trifluoro-ethyl ester:

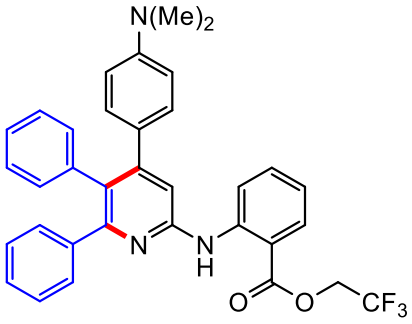

Prepared by general procedure of 2-aminopyridine synthesis to yield **5.12e** (65%). **^{1}H NMR** (400 MHz, $CDCl_3$) δ 10.35 (s, 1H), 8.94 (d, J = 8.7 Hz, 1H), 8.09 (dd, J = 8.1, 1.7 Hz, 1H), 7.55 (ddd, J = 8.8, 7.1, 1.7 Hz, 1H), 7.34 (dddd, J = 6.7, 4.3, 3.5, 1.1 Hz, 2H), 7.24 – 7.19 (m, 3H), 7.13 – 7.08 (m, 3H), 6.99 (s, 1H), 6.98 – 6.92 (m, 5H), 6.56 (d, J = 8.7 Hz, 2H), 4.73 (q, J = 8.4 Hz, 2H), 2.95 (s, 6H); **^{13}C NMR** (100 MHz, $CDCl_3$) δ 166.7, 156.2, 153.1, 151.9, 149.6, 145.7, 141.2, 138.5, 135.4, 131.9, 131.3, 130.2, 130.0, 127.7, 127.7, 127.4, 127.1, 126.1, 123.1 (q, J = 278.5 Hz), 119.01, 118.28, 112.33, 111.58, 111.14, 60.5 (q, J = 35.3 Hz), 40.3; **^{9}F NMR** (376 MHz, $CDCl_3$) δ -73.49; HRMS (ESI-TOF) *m/z*: $[M + H]^+$ Calcd for $C_{34}H_{28}F_3N_3O_2$ 568.2212, Found 568.2215.

2-[4-(4-Nitro-phenyl)-5,6-diphenyl-pyridin-2-ylamino]-benzoic acid 2,2,2-trifluoro-ethyl ester: 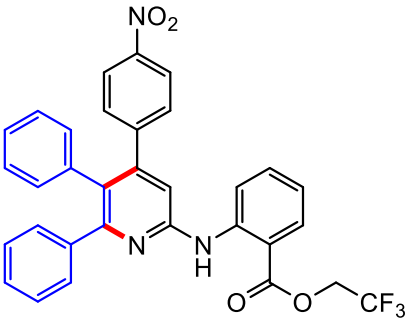

Prepared by general procedure of 2-aminopyridine synthesis to yield **5.12f** (64%). **^{1}H NMR** (400 MHz, $CDCl_3$) δ 10.52, 10.51, 9.05, 9.05, 9.03, 9.03, 8.14, 8.14, 8.12, 8.12, 8.10, 8.09, 8.08, 8.07, 8.07, 7.61, 7.61, 7.59, 7.59, 7.59, 7.57, 7.57, 7.40, 7.39, 7.38, 7.38, 7.37, 7.29, 7.29, 7.28, 7.27, 7.27, 7.26, 7.26, 7.25, 7.14, 7.12, 7.11, 7.09, 7.08, 7.07, 7.01, 6.99, 6.97, 6.91, 6.89, 6.89, 6.88, 6.87, 4.78, 4.75, 4.73, 4.71; **^{13}C NMR** (100 MHz, $CDCl_3$) δ 166.9, 156.6, 153.3, 149.6, 147.0, 146.5, 145.2, 140.3, 137.2, 135.6, 131.6, 131.4, 130.1, 130.0, 128.1, 127.6, 127.1, 126.8, 124.5 (q, J = 274.7 Hz), 123.1, 121.7, 119.7, 118.6, 111.8, 111.5, 60.6 (q, J = 37.4 Hz); **^{9}F NMR** (376 MHz, $CDCl_3$) δ -73.46; HRMS (ESI-TOF) *m/z*: $[M + H]^+$ Calcd for $C_{32}H_{22}F_3N_3O_4$ 570.1641, 570.1647.

2-[4-(4-Cyano-phenyl)-5,6-diphenyl-pyridin-2-ylamino]-benzoic acid 2,2,2-trifluoro-ethyl ester: 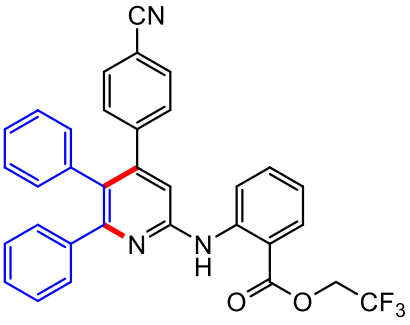

Prepared by general procedure of 2-aminopyridine synthesis to yield **5.12g** (66%). **^{1}H NMR** (400 MHz, $CDCl_3$) δ 10.49 (s, 1H), 9.01 (dd, J = 8.6, 1.1 Hz, 1H), 8.12 (dd, J = 8.1, 1.7 Hz, 1H), 7.58 (ddd, J = 8.8, 7.2, 1.7 Hz, 1H), 7.55 – 7.48 (m, 2H), 7.42 – 7.32 (m, 2H), 7.27 – 7.19 (m, 5H), 7.16 – 7.05 (m, 3H), 6.98 (ddd, J = 8.2, 7.1, 1.2 Hz, 1H), 6.91 – 6.83 (m, 3H), 4.74 (q, J = 8.4 Hz, 2H); **^{13}C NMR** (100 MHz, $CDCl_3$) δ 166.9, 156.6, 153.3, 149.9, 145.2, 144.5, 140.4, 137.2, 135.6, 131.7, 131.6, 131.4, 130.0, 129.9, 127.9, 127.6, 127.6, 127.1 (q, J = 278.5 Hz), 126.7, 124.4, 121.7, 119.6, 118.6, 118.5, 111.8, 111.5, 111.2, 99.9, 60.6 (q, J = 37.4 Hz); **^{9}F NMR** (376 MHz, $CDCl_3$) δ -73.49; HRMS (ESI-TOF) *m/z*: $[M + H]^+$ Calcd for $C_{33}H_{22}F_3N_3O_2$ 550.1743, Found 550.1747.

2-[5,6-Diphenyl-4-(4-trifluoromethyl-phenyl)-pyridin-2-ylamino]-benzoic acid 2,2,2-trifluoro-ethyl ester: 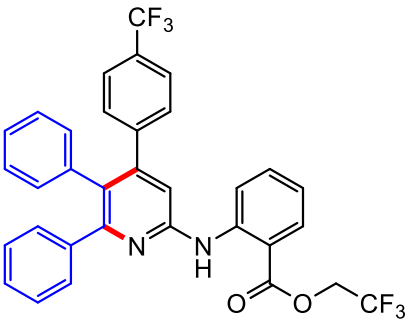 Prepared by general procedure of 2-aminopyridine synthesis to yield **5.12h** (65%). **^{1}H NMR** (400 MHz, $CDCl_3$) δ 10.47 (s, 1H), 9.01 (d, J = 8.7 Hz, 1H), 8.12 (dd, J = 8.1, 1.7 Hz, 1H), 7.61 – 7.55 (m, 1H), 7.49 (d, J = 8.0 Hz, 2H), 7.42 – 7.35 (m, 2H), 7.24 (dd, J = 7.5, 2.2 Hz, 5H), 7.10 (ddt, J = 9.1, 7.8, 4.8 Hz, 3H), 7.01 – 6.95 (m, 1H), 6.92 (s, 1H), 6.89 (dt, J = 6.3, 1.7 Hz, 2H), 4.74 (q, J = 8.4 Hz, 2H); **^{13}C NMR** (100 MHz, $CDCl_3$) δ 166.8, 156.5, 153.2, 150.5, 145.3, 140.6, 137.4, 135.5, 131.6, 131.4, 130.0, 129.5, 129.3, 127.9, 127.6, 127.5, 127.4, 126.6, 124.0 (q, J = 271.8 Hz), 124.8 (q, J = 3.8 Hz), 123.1 (q, J = 276.8 Hz), 119.5, 118.5, 112.1, 111.4, 60.59 (q, J = 35.4 Hz); **^{9}F NMR** (376 MHz, $CDCl_3$) δ -82.58, -73.51; HRMS (ESI-TOF) *m/z*: $[M + H]^+$ Calcd for $C_{33}H_{22}F_6N_2O_2$ 593.1664, Found 593.1668.

2-[4-(4-Chloro-phenyl)-5,6-diphenyl-pyridin-2-ylamino]-benzoic acid 2,2,2-trifluoro-ethyl ester: 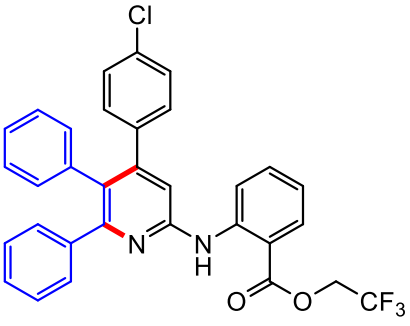 Prepared by general procedure of 2-aminopyridine synthesis to yield **5.12i** (65%)**. ^{1}H NMR** (400 MHz, $CDCl_3$) δ 10.43 (s, 1H), 8.99 (dd, J = 8.8, 1.1 Hz, 1H), 8.11 (dd, J = 8.1, 1.7 Hz, 1H), 7.57 (ddd, J = 8.9, 7.2, 1.7 Hz, 1H), 7.40 – 7.32 (m, 2H), 7.27 – 7.17 (m, 5H), 7.16 – 7.01 (m, 5H), 6.96 (ddd, J = 8.1, 7.1, 1.1 Hz, 1H), 6.93 – 6.86 (m, 3H), 4.74 (q, J = 8.4 Hz, 2H); **^{13}C NMR** (100 MHz, $CDCl_3$) δ 166.8, 156.4, 153.2, 150.6, 145.4, 140.7, 138.1, 137.7, 135.5, 133.6, 131.7, 131.4, 130.5, 130.0, 128.1, 127.8, 127.5, 127.5, 127.4, 126.48, 124.46 (q, J = 277.7 Hz), 121.7, 119.4, 118.4, 112.2, 111.3, 60.6 (q, J = 36.4 Hz); **^{9}F NMR** (376 MHz, $CDCl_3$) δ -73.50; HRMS (ESI-TOF) *m/z*: $[M + H]^+$ Calcd for $C_{32}H_{22}ClF_3N_2O_2$ 559.1401, Found 559.1406.

2-[4-(2-Fluoro-phenyl)-5,6-diphenyl-pyridin-2-ylamino]-benzoic acid 2,2,2-trifluoro-ethyl ester: 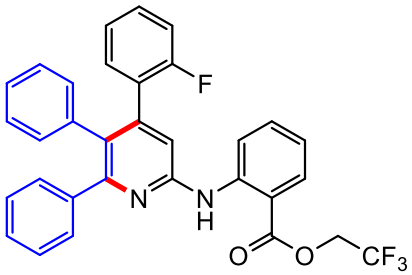

Prepared by general procedure of 2-aminopyridine synthesis to yield **5.12j** (64%). **^{1}H NMR** (400 MHz, $CDCl_3$) δ 10.47 (s, 1H), 9.04 (dd, J = 8.7, 1.1 Hz, 1H), 8.14 (dd, J = 8.1, 1.7 Hz, 1H), 7.59 (ddd, J = 8.8, 7.1, 1.7 Hz, 1H), 7.48 – 7.41 (m, 2H), 7.26 (qd, J = 4.6, 4.2, 2.7 Hz, 4H), 7.14 – 6.95 (m, 10H), 4.75 (q, J = 8.4 Hz, 2H); **^{13}C NMR** (100 MHz, $CDCl_3$) δ 166.8, 160.4, 157.9, 158.0, 152.9, 146.5, 145.5, 140.7, 137.8, 135.5, 131.4, 131.2 (t, J = 3.2 Hz), 130.1, 129.6 (d, J = 7.8 Hz), 128.7, 127.5 (t, J = 4.7 Hz), 127.3, 126.4, 123.2 (d, J = 278.2 Hz), 123.7 (d, J = 3.4 Hz), 119.4, 118.4, 115.5, 115.3, 112.8, 111.4, 60.5 (q, J = 36.8 Hz); **^{9}F NMR** (376 MHz, $CDCl_3$) δ -73.43, 113.8 (hp, J = 2.7 Hz); HRMS (ESI-TOF) *m/z*: $[M + H]^+$ Calcd for $C_{32}H_{22}F_4N_2O_2$ 543.1696, Found 543.1699.

2-(3-Hexyl-4,5,6-triphenyl-pyridin-2-ylamino)-benzoic acid 2,2,2-trifluoro-ethyl ester: 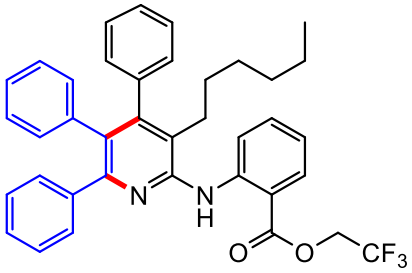

Prepared by general procedure of 2-aminopyridine synthesis to yield **5.12k** (64%). **^{1}H NMR** (400 MHz, $CDCl_3$) δ 10.63 (s, 1H), 9.28 (dd, J = 8.7, 1.1 Hz, 1H), 8.14 (dd, J = 8.1, 1.7 Hz, 1H), 7.59 (ddd, J = 8.8, 7.1, 1.8 Hz, 1H), 7.47 – 7.33 (m, 2H), 7.32 – 7.13 (m, 6H), 7.15 – 6.94 (m, 6H), 6.87 (ddd, J = 5.5, 2.9, 1.6 Hz, 2H), 4.74 (q, J = 8.4 Hz, 2H), 2.71 – 2.48 (m, 2H), 1.60 (qd, J = 8.2, 6.5, 3.7 Hz, 2H), 1.36 – 1.16 (m, 6H), 0.86 (t, J = 6.9 Hz, 3H); **^{13}C NMR** (101 MHz, $CDCl_3$) δ 167.0, 152.2, 151.6, 151.4, 146.0, 141.0, 138.9, 138.8, 135.4, 131.6, 131.2, 130.1, 129.4, 128.8, 127.6, 127.5, 127.3, 127.0, 126.7, 125.8, 123.1, 122.4 (q, J = 276.3 Hz), 118.9, 118.8, 111.2, 61.05 (q, J = 35.7 Hz), 31.2, 29.4, 28.8, 28.5, 22.4, 14.0; **^{9}F NMR** (376 MHz, $CDCl_3$) δ -73.52; HRMS (ESI-TOF) *m/z*: $[M + H]^+$ Calcd for $C_{38}H_{35}F_3N_2O_2$ 609.2729, Found 609.2734.

5-Chloro-2-(4,5,6-triphenyl-pyridin-2-ylamino)-benzoic acid 2,2,2-trifluoro-ethyl ester: 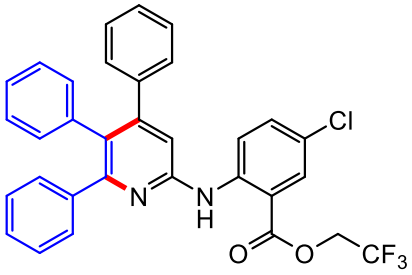 Prepared by general procedure of 2-aminopyridine synthesis to yield **5.12l** (61%)**. ^{1}H NMR** (400 MHz, $CDCl_3$) δ 10.42 (s, 1H), 9.11 (d, J = 9.3 Hz, 1H), 8.05 (d, J = 2.6 Hz, 1H), 7.52 (dd, J = 9.2, 2.6 Hz, 1H), 7.39 – 7.34 (m, 2H), 7.27 – 7.22 (m, 6H), 7.14 – 7.07 (m, 5H), 6.95 – 6.89 (m, 3H), 4.74 (q, J = 8.3 Hz, 2H); **^{13}C NMR** (100 MHz, $CDCl_3$) δ 165.9, 156.1, 152.7, 152.1, 144.2, 140.8, 139.5, 137.8, 135.4, 131.7, 130.4, 130.0, 129.2, 128.1, 127.9, 127.7, 127.6, 127.42, 127.39, 126.38, 124.3 (q, J = 275.3 Hz), 123.9, 121.6, 120.1, 118.8, 112.6, 112.1, 60.7 (q, J = 37.4 Hz); **^{9}F NMR** (376 MHz, $CDCl_3$) δ -73.39; HRMS (ESI-TOF) *m/z*: $[M + H]^+$ Calcd for $C_{32}H_{22}ClF_3N_2O_2$ 559.1401, Found 559.1405.

2-(4-Furan-2-yl-5,6-diphenyl-pyridin-2-ylamino)-benzoic acid 2,2,2-trifluoro-ethyl ester: 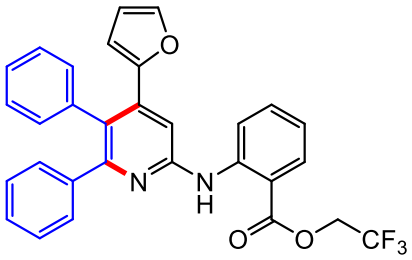 Prepared by general procedure of 2-aminopyridine synthesis to yield **5.12m** (63%). **^{1}H NMR** (400 MHz, $CDCl_3$) δ 10.46 (s, 1H), 8.97 (dd, J = 8.7, 1.1 Hz, 1H), 8.12 (dd, J = 8.1, 1.7 Hz, 1H), 7.56 (ddd, J = 8.8, 7.2, 1.7 Hz, 1H), 7.49 – 7.42 (m, 2H), 7.40 – 7.30 (m, 5H), 7.26 – 7.19 (m, 3H), 7.20 – 7.14 (m, 2H), 6.95 (ddd, J = 8.1, 7.1, 1.1 Hz, 1H), 6.24 (dd, J = 3.5, 1.8 Hz, 1H), 5.43 – 5.18 (m, 1H), 4.77 (q, J = 8.4 Hz, 2H); **^{13}C NMR** (100 MHz, $CDCl_3$) δ 166.8, 156.5, 153.7, 150.5, 145.6, 142.5, 140.7, 139.5, 138.6, 135.5, 131.4, 131.1, 129.9, 128.5, 127.4, 127.37, 127.2, 125.1, 124.5 (q, J = 276.7 Hz), 121.8, 119.2, 118.3, 112.4, 111.8, 111.2, 107.6, 99.9, 60.6 (q, J = 36.4 Hz); **^{9}F NMR** (376 MHz, $CDCl_3$) δ -73.46; HRMS (ESI-TOF) *m/z*: $[M + H]^+$ Calcd for $C_{30}H_{21}F_3N_2O_3$ 515.1583, Found 515.1589.

2-[4-(1H-Indol-3-yl)-5,6-diphenyl-pyridin-2-ylamino]-benzoic acid 2,2,2-trifluoro-ethyl ester: 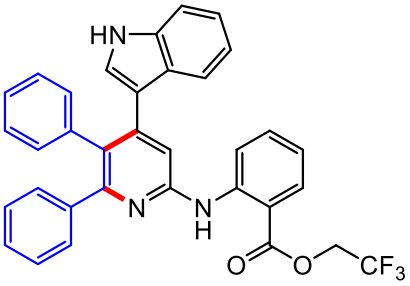

Prepared by general procedure of 2-aminopyridine synthesis to yield **5.12n** as a white solid (65%). **^{1}H NMR** (400 MHz, $CDCl_3$) δ 10.37 (s, 1H), 8.96 (d, J = 8.7 Hz, 1H), 8.18 – 8.00 (m, 2H), 7.85 (d, J = 7.6 Hz, 1H), 7.57 (ddd, J = 8.9, 7.1, 1.7 Hz, 1H), 7.38 (td, J = 6.1, 5.7, 2.2 Hz, 3H), 7.34 – 7.18 (m, 6H), 7.17 – 7.06 (m, 3H), 7.06 – 6.98 (m, 2H), 6.95 (t, J = 7.6 Hz, 1H), 6.40 (d, J = 2.6 Hz, 1H), 4.73 (q, J = 8.4 Hz, 2H); **^{13}C NMR** (100 MHz, $CDCl_3$) δ 166.7, 156.5, 153.2, 145.7, 145.1, 141.2, 139.0, 135.6, 135.4, 131.7, 131.4, 130.0, 128.0, 127.8, 127.5, 127.1, 126.4, 125.2, 124.5 (q, J = 275.3 Hz), 122.4, 121.8, 120.6, 119.6, 119.1, 118.3, 114.3, 112.2, 111.3, 60.5 (q, J = 37.4 Hz); **^{9}F NMR** (376 MHz, $CDCl_3$) δ -73.49; HRMS (ESI-TOF) *m/z*: $[M + H]^+$ Calcd for $C_{34}H_{24}F_3N_3O_2$ 564.1899, Found 564.1902.

2-(4-Phenyl-5,6-di-thiophen-2-yl-pyridin-2-ylamino)-benzoic acid 2,2,2-trifluoro-ethyl ester: 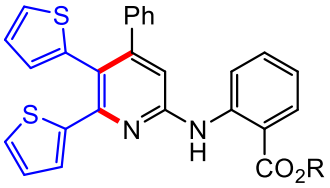

Prepared by general procedure of 2-aminopyridine synthesis to yield **5.12o** as a white solid (64%). **^{1}H NMR** (400 MHz, $CDCl_3$) δ 10.48 (s, 1H), 9.18 – 9.11 (m, 1H), 8.13 (dd, J = 8.1, 1.8 Hz, 1H), 7.70 (ddd, J = 8.8, 7.1, 1.8 Hz, 1H), 7.37 – 7.19 (m, 8H), 7.07 – 6.94 (m, 2H), 6.92 – 6.76 (m, 3H), 6.55 (dd, J = 3.7, 1.1 Hz, 1H), 4.73 (q, J = 8.4 Hz, 2H); **^{13}C NMR** (101 MHz, $CDCl_3$) δ 166.9, 153.9, 153.1, 150.0, 145.1, 144.9, 139.1, 138.8, 135.5, 131.3, 129.4, 128.6, 127.7, 127.7, 127.6, 127.1, 127.0, 124.5 (q, J = 278.2 Hz), 121.7, 119.7, 119.1, 117.8, 111.7, 111.5, 60.6 (q, J = 36.4 Hz); **^{9}F NMR** (376 MHz, $CDCl_3$) δ -73.49; HRMS (ESI-TOF) *m/z*: $[M + H]^+$ Calcd for $C_{28}H_{19}F_3N_2O_2S_2$ 537.0919, Found 537.0922.

2-[5,6-Bis-(4-methoxy-phenyl)-4-phenyl-pyridin-2-ylamino]-benzoic acid 2,2,2-trifluoro-ethyl ester: 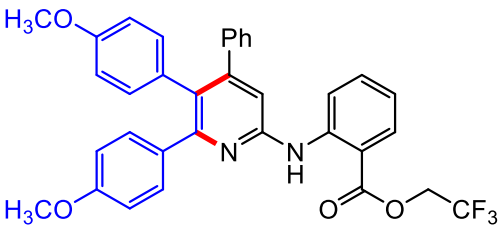

Prepared by general procedure of 2-aminopyridine synthesis to yield **5.12p** as a white solid (63%). **^{1}H NMR** (400 MHz, $CDCl_3$) δ 10.38 (s, 1H), 8.99 (d, J = 8.7 Hz, 1H), 8.10 (dd, J = 8.1, 1.7 Hz, 1H), 7.61 – 7.54 (m, 1H), 7.38 – 7.31 (m, 2H), 7.24 (q, J = 2.7 Hz, 3H), 7.12 (dd, J = 6.7, 3.0 Hz, 2H), 6.98 – 6.92 (m, 1H), 6.85 – 6.75 (m, 4H), 6.68 – 6.61 (m, 2H), 4.73 (q, J = 8.4 Hz, 2H), 3.81 (s, 3H), 3.75 (s, 3H); **^{13}C NMR** (101 MHz, $CDCl_3$) δ 166.8, 158.8, 157.9, 155.8, 152.8, 152.1, 145.7, 139.9, 135.4, 133.5, 132.7, 131.4, 131.3, 130.4, 129.2, 127.8, 127.2, 127.0, 123.1 (q, J = 274.4 Hz), 119.1, 118.3, 113.3, 113.0, 112.1, 111.2, 60.3 (q, J = 36.5 Hz), 55.2, 55.1; **^{9}F NMR** (376 MHz, $CDCl_3$) δ -73.49; HRMS (ESI-TOF) *m/z*: $[M + H]^+$ Calcd for $C_{34}H_{27}F_3N_2O_4$ 585.2001, Found 585.2007.

2-[5,6-Bis-(4-bromo-phenyl)-4-phenyl-pyridin-2-ylamino]-benzoic acid 2,2,2-trifluoro-ethyl ester: 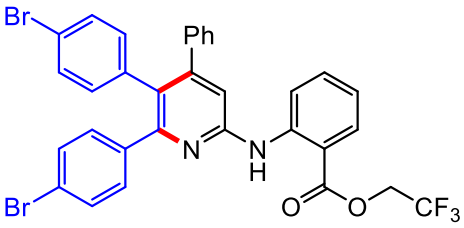

Prepared by general procedure of 2-aminopyridine synthesis to yield **5.12q** as a white solid (66%). **^{1}H NMR** (400 MHz, $CDCl_3$) δ ^{1}H NMR (400 MHz, Chloroform-*d*) δ 10.46 (s, 1H), 8.94 (dd, J = 8.7, 1.2 Hz, 1H), 8.11 (dd, J = 8.1, 1.7 Hz, 1H), 7.57 (ddd, J = 8.8, 7.2, 1.8 Hz, 1H), 7.42 – 7.36 (m, 2H), 7.29 – 7.21 (m, 7H), 7.08 (dd, J = 7.6, 1.9 Hz, 2H), 6.98 (ddd, J = 8.1, 7.2, 1.2 Hz, 1H), 6.94 (s, 1H), 6.76 (d, J = 8.4 Hz, 2H), 4.73 (q, J = 8.4 Hz, 2H); **^{13}C NMR** (101 MHz, $CDCl_3$) δ 154.8, 153.4, 152.0, 145.2, 139.5, 139.0, 136.7, 135.5, 133.2, 131.7, 131.4, 131.1, 130.9, 129.1, 128.1, 127.6, 126.2, 123.2 60.6 (q, J = 277.3 Hz), 121.9, 121.7, 120.8, 119.6, 118.4, 112.7, 111.5, 60.3 (q, J =

36.9 Hz); **^{9}F NMR** (376 MHz, $CDCl_3$) δ -73.49; HRMS (ESI-TOF) *m/z*: $[M + H]^+$ Calcd for $C_{32}H_{21}Br_2F_3N_2O_2$ 682.9982, Found 682.9981.

2-(4-Phenyl-5,6-dipropyl-pyridin-2-ylamino)-benzoic acid 2,2,2-trifluoro-ethyl ester:

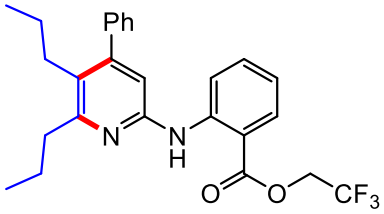

Prepared by general procedure of 2-aminopyridine synthesis to yield **5.12r** as a white solid (65%) **^{1}H NMR** (400 MHz, $CDCl_3$) δ 10.15 (s, 1H), 8.85 (d, *J* = 8.7 Hz, 1H), 8.08 (dd, *J* = 8.1, 1.7 Hz, 1H), 7.56 (ddd, *J* = 8.8, 7.1, 1.8 Hz, 1H), 7.50 – 7.40 (m, 3H), 7.37 – 7.30 (m, 2H), 6.91 (ddd, *J* = 8.0, 6.8, 1.1 Hz, 1H), 6.64 (s, 1H), 4.71 (d, *J* = 8.4 Hz, 2H), 2.90 – 2.83 (m, 2H), 2.58 – 2.49 (m, 2H), 2.01 – 1.91 (m, 2H), 1.47 – 1.39 (m, 2H), 1.13 (t, *J* = 7.3 Hz, 3H), 0.83 (t, *J* = 7.3 Hz, 3H); **^{13}C NMR** (101 MHz, $CDCl_3$) δ 166.7, 158.9, 152.2, 151.3, 146.1, 140.5, 135.2, 131.3, 128.5, 128.1, 127.5, 126.4, 123.2 (q, *J* = 277.5 Hz), 118.5, 117.8, 111.4, 110.7, 60.4 (q, *J* = 36.4 Hz), 36.9, 30.4, 24.3, 22.7, 14.4, 14.3**; ^{9}F NMR** (376 MHz, $CDCl_3$) δ -73.54; HRMS (ESI-TOF) *m/z*: $[M + H]^+$ Calcd for $C_{26}H_{27}F_3N_2O_2$ 456.2103, Found 456.2107

5.15. References

(1) Wang, S.; Fang, K.; Dong, G.; Chen, S.; Liu, N.; Miao, Z.; Yao, J.; Li, J.; Zhang, W.; Sheng, C. Scaffold Diversity Inspired by the Natural Product Evodiamine: Discovery of Highly Potent and Multitargeting Antitumor Agents. *J. Med. Chem.* **2015**, *58* (16), 6678–6696.

(2) Cagir, A.; Jones, S. H.; Gao, R.; Eisenhauer, B. M.; Hecht, S. M. Luotonin A. A Naturally Occurring Human DNA Topoisomerase I Poison. *J. Am. Chem. Soc.* **2003**, *125* (45), 13628–13629.

(3) Nathubhai, A.; Wood, P. J.; Lloyd, M. D.; Thompson, A. S.; Threadgill, M. D. Design and Discovery of 2-Arylquinazolin-4-Ones as Potent and Selective Inhibitors of Tankyrases. *ACS Med. Chem. Lett.* **2013**, *4* (12), 1173–1177.

(4) Bouley, R.; Kumarasiri, M.; Peng, Z.; Otero, L. H.; Song, W.; Suckow, M. A.; Schroeder, V. A.; Wolter, W. R.; Lastochkin, E.; Antunes, N. T.; et al. Discovery of Antibiotic (E)-3-(3-Carboxyphenyl)-2-(4-Cyanostyryl)Quinazolin-4(3 H)-One. *J. Am. Chem. Soc.* **2015**, *137* (5), 1738–1741.

(5) Takaya, Y.; Tasaka, H.; Chiba, T.; Uwai, K.; Tanitsu, M. A.; Kim, H. S.; Wataya, Y.; Miura, M.; Takeshita, M.; Oshima, Y. New Type of Febrifugine Analogues, Bearing a Quinolizidine Moiety, Show Potent Antimalarial Activity against Plasmodium Malaria Parasite. *J. Med. Chem.* **1999**, *42* (16), 3163–3166.

(6) Malamas, M. S.; Millen, J. Quinazolineacetic Acids and Related Analogs as Aldose Reductase Inhibitors. *J. Med. Chem.* **1991**, *34* (4), 1492–1503.

(7) Peet, N. P.; Baugh, L. E.; Sunder, S.; Lewis, J. E.; Matthews, E. H.; Olberding, E. L.; Shah, D. N. 3-(LH-Tetrazol-5-Yl)-4(3H)-Quinazolinone Sodium Salt (MDL 427): A New Antiallergic Agent. *J. Med. Chem.* **1986**, *29* (11), 2403–2409.

(8) Corbett, J. W.; Ko, S. S.; Rodgers, J. D.; Gearhart, L. A.; Magnus, N. A.; Bacheler, L. T.; Diamond, S.; Jeffrey, S.; Klabe, R. M.; Cordova, B. C.; et al. Inhibition of Clinically Relevant Mutant Variants of HIV-1 by Quinazolinone Non-Nucleoside Reverse Transcriptase Inhibitors. *J. Med. Chem.* **2000**, *43* (10), 2019–2030.

(9) Wolfe, J. F.; Rathman, T. L.; Sleevi, M. C.; Campbell, J. A.; Greenwood, T. D. Synthesis and Anticonvulsant Activity of Some New 2-Substituted 3-Aryl-4(3H)-Quinazolinones. *J. Med. Chem.* **1990**, *33* (1), 161–166.

(10) Liverton, N. J.; Armstrong, D. J.; Claremon, D. A.; Remy, D. C.; Baldvin, J. J.; Lynch, R. J.; Zhang, G.; Gould, R. J. Nonpeptide Glycoprotein IIb/IIIa Inhibitors: Substituted Quinazolinediones and Quinazolinones as Potent Fibrinogen Receptor Antagonists. *Bioorg. Med. Chem. Lett.* **1998**, *8* (5), 483–486.

(11) Schwender, C. F.; Sunday, B. R.; Herzig, D. J. 11-Oxo-11H-Pyrido[2,1-b]Quinazoline-8-Carboxylic Acid, an Orally Active Antiallergy Agent. *J. Med. Chem.* **1979**, *22* (1), 114–116.

(12) Maity, A.; Mondal, S.; Paira, R.; Hazra, A.; Naskar, S.; Sahu, K. B.; Saha, P.; Banerjee, S.; Mondal, N. B. A Novel Approach for the One-Pot Synthesis of Linear and Angular Fused Quinazolinones. *Tetrahedron Lett.* **2011**, *52* (23), 3033–3037.

(13) Watanabe, M.; Sato, T.; Inomata, H.; Smith, R. L.; Arai, K.; Kruse, A.; Dinjus, E. Chemical Reactions of C(1) Compounds in near-Critical and Supercritical Water. *Chem. Rev.* **2004**, *104* (12), 5803–5821.

(14) Park, Y.; Kim, Y.; Chang, S. Transition Metal-Catalyzed C–H Amination: Scope, Mechanism, and Applications. *Chem. Rev.* **2017**, *117* (13), 9247–9301.

(15) Sambiagio, C.; Schönbauer, D.; Blieck, R.; Dao-Huy, T.; Pototschnig, G.; Schaaf, P.; Wiesinger, T.; Zia, M. F.; Wencel-Delord, J.; Besset, T.; et al. A Comprehensive Overview of Directing Groups Applied in Metal-Catalysed C–H Functionalisation Chemistry. *Chem. Soc. Rev.* **2018**, *47* (17), 6603–6743.

(16) Lyons, T. W.; Sanford, M. S. Palladium-Catalyzed Ligand-Directed C−H Functionalization Reactions. *Chem. Rev.* **2010**, *110* (2), 1147–1169.

(17) Ackermann, L. Carboxylate-Assisted Ruthenium-Catalyzed Alkyne Annulations by C-H/Het-H Bond Functionalizations. *Acc. Chem. Res.* **2014**, *47* (2), 281–295.

(18) Kakiuchi, F.; Murai, S. Catalytic C−H/Olefin Coupling. *Acc. Chem. Res.* **2002**, *35* (10), 826–834.

(19) Ritleng, V.; Sirlin, C.; Pfeffer, M. Ru-, Rh-, and Pd-Catalyzed C−C Bond Formation Involving C−H Activation and Addition on Unsaturated Substrates: Reactions and Mechanistic Aspects. *Chem. Rev.* **2002**, *102* (5), 1731–1770.

(20) Ackermann, L.; Lygin, A. V.; Hofmann, N. Ruthenium-Catalyzed Oxidative Annulation by Cleavage of C-H/N-H Bonds. *Angew. Chem. Int. Ed.* **2011**, *50* (28), 6379–6382.

(21) Li, B.; Feng, H.; Wang, N.; Ma, J.; Song, H.; Xu, S.; Wang, B. Ruthenium-Catalyzed Oxidative Coupling/Cyclization of Isoquinolones with Alkynes through C-H/N-H Activation: Mechanism Study and Synthesis of Dibenzo[a,g]Quinolizin-8-One Derivatives. *Chem - Eur. J.* **2012,** *18* (40), 12873–12879.

(22) Piou, T.; Rovis, T. Rh(III)-Catalyzed Cyclopropanation Initiated by C–H Activation: Ligand Development Enables a Diastereoselective [2 + 1] Annulation of N-Enoxyphthalimides and Alkenes. *J. Am. Chem. Soc.* **2014**, *136* (32), 11292–11295.

(23) Shi, Z.; Koester, D. C.; Boultadakis-Arapinis, M.; Glorius, F. Rh(III)-Catalyzed Synthesis of Multisubstituted Isoquinoline and Pyridine N -Oxides from Oximes and Diazo Compounds. *J. Am. Chem. Soc.* **2013**, *135* (33), 12204–12207.

(24) Kujawa, S.; Best, D.; Burns, D. J.; Lam, H. W. Synthesis of Spirocyclic Enones by Rhodium-Catalyzed Dearomatizing Oxidative Annulation of 2-Alkenylphenols with Alkynes and Enynes. *Chem. - A Eur. J.* **2014**, *20* (28), 8599–8602.

(25) Seoane, A.; Casanova, N.; Quiñones, N.; Mascareñas, J. L.; Gulías, M. Straightforward Assembly of Benzoxepines by Means of a Rhodium(III)-Catalyzed C–H Functionalization of o -Vinylphenols. *J. Am. Chem. Soc.* **2014**, *136* (3), 834–837.

(26) Zhao, M.-N.; Ren, Z.-H.; Wang, Y.-Y.; Guan, Z.-H. Pd-Catalyzed Oxidative Coupling of Enamides and Alkynes for Synthesis of Substituted Pyrroles. *Org. Lett.* **2014**, *16* (2), 608–611.

(27) Su, Y.; Zhao, M.; Han, K.; Song, G.; Li, X. Synthesis of 2-Pyridones and Iminoesters via Rh(III)-Catalyzed Oxidative Coupling between Acrylamides and Alkynes. *Org. Lett.* **2010**, *12* (23), 5462–5465.

(28) Parthasarathy, K.; Jeganmohan, M.; Cheng, C.-H. Rhodium-Catalyzed One-Pot Synthesis of Substituted Pyridine Derivatives from α,β-Unsaturated Ketoximes and Alkynes. *Org. Lett.* **2008**, *10* (2), 325–328.

(29) Colby, D. A.; Bergman, R. G.; Ellman, J. A. Stereoselective Alkylation of α,β-Unsaturated Imines via C−H Bond Activation. *J. Am. Chem. Soc.* **2006**, *128* (17), 5604–5605.

(30) Colby, D. A.; Bergman, R. G.; Ellman, J. A. Synthesis of Dihydropyridines and Pyridines from Imines and Alkynes via C−H Activation. *J. Am. Chem. Soc.* **2008**, *130* (11), 3645–3651.

(31) Kumar, D.; Vemula, S. R.; Cook, G. R. Highly Chemo- and Regioselective Allylic Substitution with Tautomerizable Heteroarenes. *Green Chem.* **2015**, *17* (8), 4300–4306.

(32) Kumar, D.; Vemula, S. R.; Cook, G. R. Merging C-H Bond Functionalization with Amide Alcoholysis: En Route to 2-Aminopyridines. *ACS Catal.* **2016**, *6* (6).

(33) Vemula, S. R.; Kumar, D.; Cook, G. R. Palladium-Catalyzed Allylic Amidation with N-Heterocycles via Sp^3 C-H Oxidation. *ACS Catal.* **2016**, *6* (8).

(34) Vemula, S. R.; Kumar, D.; Cook, G. R. Bismuth-Catalyzed Synthesis of 2-Substituted Quinazolinones. *Tetrahedron Lett.* **2018**, *59* (42), 3801–3805.

(35) Ryabov, A. D. Mechanisms of Intramolecular Activation of Carbon-Hydrogen Bonds in Transition-Metal Complexes. *Chem. Rev.* **1990**, *90* (2), 403–424.

(36) Li, B.; Darcel, C.; Dixneuf, P. H. Ruthenium(II)-Catalysed Functionalisation of C□H Bonds via a Six-Membered Cyclometallate: Monoarylation of Aryl 2-Pyridyl Ketones. *ChemCatChem* **2014**, *6* (1), 127–130.

(37) Ackermann, L.; Lygin, A. V. Cationic Ruthenium(II) Catalysts for Oxidative C–H/N–H Bond Functionalizations of Anilines with Removable Directing Group: Synthesis of Indoles in Water. *Org. Lett.* **2012**, *14* (3), 764–767.

(38) Simmons, E. M.; Hartwig, J. F. On the Interpretation of Deuterium Kinetic Isotope Effects in C□H Bond Functionalizations by Transition-Metal Complexes. *Angew. Chemie Int. Ed.* **2012**, *51* (13), 3066–3072.

(39) Ackermann, L. Carboxylate-Assisted Transition-Metal-Catalyzed C−H Bond Functionalizations: Mechanism and Scope. *Chem. Rev.* **2011**, *111* (3), 1315–1345.

(40) Fujiwara, Y.; Dixon, J. A.; O'Hara, F.; Funder, E. D.; Dixon, D. D.; Rodriguez, R. A.; Baxter, R. D.; Herlé, B.; Sach, N.; Collins, M. R.; et al. Practical and Innate Carbon–hydrogen Functionalization of Heterocycles. *Nature* **2012**, *492* (7427), 95–99.

(41) Brückl, T.; Baxter, R. D.; Ishihara, Y.; Baran, P. S. Innate and Guided C–H Functionalization Logic. *Acc. Chem. Res.* **2012**, *45* (6), 826–839.

(42) Manoharan, R.; Jeganmohan, M. Ruthenium-Catalyzed Cyclization of N-Carbamoyl Indolines with Alkynes: An Efficient Route to Pyrroloquinolinones. *Org. Biomol. Chem.* **2015**, *13* (35), 9276–9284.

(43) Warratz, S.; Kornhaaß, C.; Cajaraville, A.; Niepötter, B.; Stalke, D.; Ackermann, L. Ruthenium(II)-Catalyzed C-H Activation/Alkyne Annulation by Weak Coordination with O2 as the Sole Oxidant. *Angew. Chemie Int. Ed.* **2015**, *54* (18), 5513–5517.

(44) Varela, J. A.; Saá, C. Construction of Pyridine Rings by Metal-Mediated [2 + 2 + 2] Cycloaddition †. *Chem. Rev.* **2003**, *103* (9), 3787–3802.

(45) Heller, B.; Hapke, M. The Fascinating Construction of Pyridine Ring Systems by Transition Metal-Catalysed [2 + 2 + 2] Cycloaddition Reactions. *Chem. Soc. Rev.* **2007**, *36* (7), 1085.

(46) Hill, M. D. Recent Strategies for the Synthesis of Pyridine Derivatives. *Chem. - A Eur. J.* **2010**, *16* (40), 12052–12062.

(47) Pasumansky, L.; Hernández, A. R.; Gamsey, S.; Goralski, C. T.; Singaram, B. Synthesis of Aminopyridines from 2-Fluoropyridine and Lithium Amides. *Tetrahedron Lett.* **2004**, *45* (34), 6417–6420.

(48) Thomas, S.; Roberts, S.; Pasumansky, L.; Gamsey, S.; Singaram, B. Aminoborohydrides 15. The First Mild and Efficient Method for Generating 2-(Dialkylamino)-Pyridines from 2-Fluoropyridine. *Org. Lett.* **2003**, *5* (21), 3867–3870.

(49) Quintela, J. M.; Peinador, C.; Veiga, M. C.; Botana, L. M.; Alfonso, A.; Riguera, R. Synthesis, Antihistaminic and Cytotoxic Activity of Pyridothieno- and Pyridodithienotriazines. *Eur. J. Med. Chem.* **1998**, *33* (11), 887–897.

(50) Poola, B.; Choung, W.; Nantz, M. H. A Mild, Catalyst-Free Synthesis of 2-Aminopyridines. *Tetrahedron* **2008**, *64* (48), 10798–10801.

(51) Vamos, M.; Cosford, N. D. P. 2-Aminopyridines via Reaction of Pyridine N -Oxides and Activated Isocyanides. *J. Org. Chem.* **2014**, *79* (5), 2274–2280.